Dynamics and Control of Retention and Formation on a Paper Machine using a Microparticulate Retention Aid System

Byoung-Uk Cho
Department of Chemical Engineering
McGill University, Montreal

May 2005

A thesis submitted to McGill University
in partial fulfillment of the requirements of the degree of
Doctor of Philosophy

Your file Votre référence
ISBN: 978-0-494-21633-0
Our file Notre référence
ISBN: 978-0-494-21633-0

To my dear parents

Abstract

Control strategies for retention and formation processes are developed in order to stabilize the wet end operation and to reduce variations in the machine direction properties of paper without deteriorating formation of paper. The papermaking process using a microparticulate retention aid system is focused.

The main factors affecting retention and formation were investigated with a CPAM (cationic polyacrylamide)/bentonite retention aid system and on a Fourdrinier pilot paper machine. The deposition efficiency model and the bridging strength model were developed to express the effects of the dosages of microparticulate retention aids on retention and paper formation, respectively. Effects of the pulp mass flow and the filler addition on first-pass retention and formation are also discussed.

Dynamic models of a retention process of a paper machine were developed from first-principles (mass balances). To describe the wet end chemistry effect, first-pass retention was included into the model as a parameter dependent on operating conditions. In addition, it was attempted to simulate dynamics of formation by developing an empirical model of formation and coupled with the dynamic models for the retention process. Transfer functions were derived from the models. It was found that the two major factors affecting the dynamics of the retention process are the first-pass retention of solids and the parameters related to the white water

circulation such as the volume of the wire pit and the residence time at the wire pit.

Several control strategies were studied through simulation. The study showed that controlling the pulp mass and the filler mass in paper instead of basis weight and paper ash content can reduce the interactions without using decouplers. To reduce the variations in formation, the headbox pulp consistency control and the ratio control of a microparticle flow to a polymer flow are suggested. The problem concerning the set-points of white water consistency during grade changes was solved. Multivariable control of basis weight, ash content, white water consistency and headbox pulp consistency is also discussed.

Résumé

Des stratégies de contrôle pour les procédés de rétention et de formation sont développées pour stabiliser l'opération de la partie humide et réduire les variations dans le sens machine des propriétés du papier sans détérioation de la formation. L'accent est mis sur un procédé de fabrication du papier basé sur un système d'agent de rétention microparticulaire.

Les principaux facteurs affectant la rétention et la formation ont été étudiés avec un système d'agent de rétention basé sur le CPAM (polyacrylamide cationique)/bentonite et avec une machine à papier pilote de type Fourdrinier. Des modèles d'efficacité de déposition et de force de pontage ont été développés pour exprimer l'effet des dosages d'agents de rétention microparticulaires sur la rétention et la formation du papier respectivement. Les effets des débits massiques de pâte et de charge sur la rétention première-passe sont aussi discutés.

Des modèles dynamiques du procédé de rétention d'une machine à papier ont été développés à partir de principes fondamentaux de bilans de matière. Afin de décrire l'effet de la chimie de la partie humide, la rétention première-passe a été inclue dans le modèle comme un paramètre variant en fonction des conditions d'opération. De plus, la simulation de la dynamique de formation a été essayée en développant un modèle empirique de la formation couplé avec les modèles dynamiques du procédé de rétention. Des fonctions de transfert ont été déterminées à partir des modèles.

Il a été observé que les deux facteurs majeurs affectant la dynamique du procédé de rétention sont la rétention première-passe des solides et des paramètres reliés à la recirculation de l'eau blanche comme le volume de la fosse sous toile et du temps de séjour à la fosse sous toile.

Une sélection de stratégies de contrôle ont été étudiées par simulation. Ces études ont montré que le contrôle de la masse de pâte et de charge dans le papier au lieu du grammage et du contenu en cendres du papier peuvent réduire les interactions sans utiliser de découpleurs. Afin de réduire les variations de la formation, il est suggéré de contrôler la consistance de la pâte dans la caisse d'arrivée et le rapport du débit de microparticules sur le débit de polymère. Les problèmes reliés au choix des points de consigne de la consistance de l'eau blanche durant les changements de grade sont résolus. Le contrôle multivariable du grammage, de contenu en cendres, de la consistance de l'eau blanche et de la consistance de la pâte dans la caisse d'arrivée est aussi discuté.

Foreword

The present author chooses the manuscript-based thesis option according to the Guidelines for Thesis Preparation given by the Faculty of Graduate Studies and Research. The article reads as follows:

As an alternative to the traditional thesis format, the dissertation can consist of a collection of papers of which the student is an author or co-author. These papers must have a cohesive, unitary character making them a report of a single program of research. The structure for the manuscript-based thesis must conform to the following:

1. *Candidates have the option of including, as part of the thesis, the text of one or more papers submitted, or to be submitted, for publication, or the clearly-duplicated text (not the reprints) of one or more published papers. These texts must conform to the "Guidelines for Thesis Preparation" with respect to font size, line spacing and margin sizes and must be bound together as an integral part of the thesis. (Reprints of published papers can be included in the appendices at the end of the thesis.)*

2. *The thesis must be more than a collection of manuscripts. All components must be integrated into a cohesive unit with a logical progression from one chapter to the next. In order to ensure that the thesis has continuity, connecting texts that provide logical bridges preceding and following each manuscript are mandatory.*

3. *The thesis must conform to all other requirements of the "Guidelines for Thesis Preparation" in addition to the manuscripts.*
   The thesis must include the following:

   (a) *a table of content;*

   (b) *a brief abstract in both English and French;*

   (c) *an introduction which clearly states the rational and objectives of the research;*

(d) a comprehensive review of the literature (in addition to that covered in the introduction to each paper);

(e) a final conclusion and summary;

(f) a thorough bibliography ;

(g) Appendix containing an ethics certificate in the case of research involving human or animal subjects, microorganisms, living cells, other biohazards and/or radioactive material.

4. *As manuscripts for publication are frequently very concise documents, where appropriate, additional material must be provided (e.g., in appendices) in sufficient detail to allow a clear and precise judgement to be made of the importance and originality of the research reported in the thesis.*

5. *In general, when co-authored papers are included in a thesis the candidate must have made a substantial contribution to all papers included in the thesis. In addition, the candidate is required to make an explicit statement in the thesis as to who contributed to such work and to what extent. This statement should appear in a single section entitled "Contributions of Authors" as a preface to the thesis. The supervisor must attest to the accuracy of this statement at the doctoral oral defence. Since the task of the examiners is made more difficult in these cases, it is in the candidate's interest to clearly specify the responsibilities of all the authors of the co-authored papers.*

6. *When previously published copyright material is presented in a thesis, the candidate must include signed waivers from the publishers and submit these to the Graduate and Postdoctoral Studies Office with the final deposition, if not submitted previously. The candidate must also include signed waivers from any co-authors of unpublished manuscripts.*

7. *Irrespective of the internal and external examiners reports, if the oral defence committee feels that the thesis has major omissions with regard to the above guidelines, the candidate may be required to resubmit an amended version of the thesis. See the "Guidelines for Doctoral Oral Examinations," which can be obtained from the web (http://www.mcgill.ca/fgsr), Graduate Secretaries of departments or from the Graduate and Postdoctoral Studies Office, James Administration Building, Room 400, 398-3990, ext. 00711 or 094220.*

8. *In no case can a co-author of any component of such a thesis serve as an external examiner for that thesis.*

This thesis consists of seven chapters. Chapter 1 describes the motivation and methodology of this research project. Chapter 2 presents the field of research pertaining to the present work and introduces previous results on research relating to the subject of this thesis. Chapters 3, 4, 5, and 6 present the principal results and research conducted. Chapter 7 gives an overview of the work and presents the claimed contributions.

The followings are the manuscripts written by the author, which are used in the preparation of this thesis.

Chapter 3 is based on
Byoung-Uk Cho, Gil Garnier, Jean Paradis and Michel Perrier, "Filler retention with a PAM/bentonite retention system: effect of collision efficiency", *Nordic Pulp and Paper Research Journal*, 16(3), pp. 188-194, 2001.

Chapter 4 is based on
Byoung-Uk Cho, Gil Garnier, Theo G.M. van de Ven and Michel Perrier, "Parameters affecting Formation of a Papermaking System using CPAM/Bentonite retention aids System", *5th International Paper and Coating Chemistry Symposium 2003*, Montreal, Canada, June 16-19, pp. 193-200, 2003.

Chapter 5 is based on
Byoung-Uk Cho, Gil Garnier, Jean Paradis and Michel Perrier, "The process dynamics of filler retention in paper using a CPAM/bentonite retention aid system", *Canadian Journal of Chemical Engineering*, 79(6), pp. 923-930, 2001.

Byoung-Uk Cho, Gil Garnier, and Michel Perrier, "Dynamic modeling of retention and formation processes" *Control Systems 2002*, Stockholm, Sweden, June 3-5, pp. 200-204, 2002.

Contributions of Authors

Contents of Chapters 3 to 5 of the present thesis are adopted or revised from the papers that have been published or submitted for publication in scientific journals under the normal supervision of my research supervisors, Dr. Michel Perrier, Dr. Gil Garnier and Dr. Theo G. M. van de Ven, who are also co-authors.

In Chapters 3 and 5, Mr. Jean Paradis, who is a co-author of the corresponding papers, helped organize the pilot paper machine trials and operated the paper machine.

All the experimental and theoretical work and the writing of the papers have been done by the author of this thesis.

Acknowledgements

This research could not been accomplished without the assistance and contributions of many people. I would like to express my gratitude to all those who have contributed in the various ways to this work, and especially to:

Dr. Michel Perrier, my main research supervisor, for his guidance, advices and suggestions, kindness and generosity throughout the course of this work. I also appreciate for his patience and for the translation of the abstract of this thesis.

Dr. Gil Garnier, my supervisor, for his guidance, constant encouragement and enthusiasm for the project and for showing me how one can be a fundamental scientist and an engineer.

Dr. Theo G. M. van de Ven, for being a faithful adviser and then becoming my supervisor after Dr. Garnier's leave from McGill. His inspiring discussions, questions and suggestions are also much appreciated.

Dr. Sylvain Coulombe for being my supervisor in Dept. of Chemical Engineering and for the involvement in the submission of this thesis.

Mr. Jean Paradis at CSPP, CEGEP in Trois-Rivières, for helping me with organizing the experiments at CSPP and for operating the pilot paper machine.

Drs. Bob Alince and Jurek Petlicki for precious questions and advices. Mr. Louis Godbout for helping me take SEM pictures.

NCE on Mechanical pulp network (NSERC) and McGill for financial support.

My friends at McGill Pulp and Paper Research Centre and at École Polytechnique for the great time I spent. I especially thank to Nancy Harnois for helping me with organizing the experiments at CSPP and for questions and discussions. I learned much from you.

My Korean friends, who I have met in Montreal, for the time we have spent together.

Most of all, I would like to express my thanks to my parents for their unlimited love and support. I also thank to my lovely sisters, Eun-Hee, Eun-Jyoung, Eun-Sook, for their love and constant encouragement.

Contents

List of Figures

List of Tables

Chapter 1

Introduction

1.1 Motivation

Current trends in the papermaking industry involve many process transformations. These consist of increased machine speed, stronger drainage profiles (twin wire machine), higher contaminant concentration (white water system closure), shocks in pH (conversion from acid to alkaline papermaking), higher filler content and increased content of recycled pulp and mechanical pulp [1, 2]. The use of a twin wire machine and increased machine speed make it more difficult to achieve high first-pass retention. The use of secondary furnishes and mechanical pulp greatly increases the contaminants, especially anionic ones, which render most of the cationic additives ineffective. Also, increased level of white water system closure causes the buildup of contaminants in the system. These trends affect most of the physicochemical phenomena involved in the wet end and make it more difficult to stabilize the papermaking process. At the same time, the market requests higher paper quality at lower cost.

Optimization and control of a papermaking process provide a key solution to improve paper quality and production efficiency at the same time. Especially, the control of the wet end of a paper machine has received much attention due to

the profound effect on product quality and process efficiency. Variations in the wet end variables such as the first-pass retention of solids (mainly, fibres, fines and fillers), consistency, and fibre flocculation directly result in variations in the final product properties such as basis weight, ash content, formation and caliper of paper. Controlling the wet end of a paper machine can improve paper quality and process efficiency and also eliminate the long delay in control action between the wet end and the dry end by removing the disturbances created in the wet end before it reaches the dry end.

Controlling the wet end of a papermaking process has always been problematic. This can be explained by two reasons. First, the wet end process is so complicated that physical and chemical phenomena are not fully understood and modelled. Second, there had been no appropriate sensors for measuring the variables that we want to control. Thus, there are difficulties in deciding what to measure and what and how to control. As a result, there is no comprehensive control strategy for the wet end process.

In recent years, several on-line sensors for the wet end have been developed, making it possible to measure some of the variables that should be controlled: for example, total consistency and filler consistency in the headbox and in the wire pit, drainage, cationic demand, zeta potential, conductivity and pH [3, 4]. Several control strategies for the wet end have been suggested and tested. The strategy controlling the white water total consistency by retention aids has been commercialized [5, 6] and in some cases it was integrated with the existing basis weight and ash content control loops [7–9]. Control of headbox fibre and filler consistencies was also suggested [10, 11]. Use of model predictive control (MPC) for the wet end and the dry end has been suggested [9, 12–15]. In addition, pH and cationic demand control have been suggested and applied [16].

However, no satisfying control strategy concerning formation has been suggested yet. Formation and first-pass retention are competitive processes in papermaking. When only first-pass retention is considered, formation might be out of control. In addition, most of the wet end control strategies utilize a single polymer retention system due to its simplicity. In reality, the use of multicomponent retention system has been increasing. Concerning microparticulate retention aids, some fundamental questions have not been clearly answered yet. In case of the white water consistency control system employing a single polymer retention system, the flow rate of polymer solution is manipulated based on the white water total consistency measurements. However, it is not clear how to manipulate polymer and microparticle flows, when a microparticulate retention aid system is used. Any satisfying model to relate the dosages of polymer and microparticles to retention and formation does not exist yet. Moreover, most of the existing wet end control strategies utilize a black box approach to model and to control the wet end of papermaking. Although several control strategies suggested to integrate wet end and dry end, no robust strategy is available for simultaneously controlling retention and formation processes. In addition, dry basis weight and ash content control configuration have been used for decades without questioning the efficiency of the control structure. The challenge is to control the machine direction properties of paper without deteriorating formation of paper.

1.2 Thesis objective

The objective of this research project is to develop control strategies for the wet end of a papermaking process utilizing a microparticulate retention aid system, focusing on retention and formation processes. Focus is on the following issues:

1. To elucidate the effects of the process parameters on first-pass retention and formation;

2. To obtain an understanding of the dynamic behaviour of solid concentrations in the wet end and in paper and to develop mathematical models from first-principles;

3. To investigate the control strategies to stabilize and optimize both the retention and the formation processes at the same time.

1.3 Methodology

As a first step in developing a comprehensive control strategy for the wet end of a papermaking process, this research project focused on controlling the machine direction variation of the mass of solid materials in paper and the spatial distribution of the solids in paper. The first-pass retention of solids (mainly fibre, fines and filler) is a key factor affecting the former and fibre flocculation mainly influences the later. This research project followed three major steps:

1. The process parameters affecting retention and formation were investigated using a pilot paper machine (Fourdrinier) and a microparticulate retention aid system. Among the numerous variables affecting retention and formation, we first focused on the main three process variables: thick stock flow, filler flow, and the dosages of retention aids. To elucidate the relationship between the dosages of retention aids and filler retention and paper formation, mathematical models (the deposition efficiency model and the bridging strength model) were developed.

2. To study the dynamic behaviour of headbox and white water consistencies,

basis weight, paper ash content and formation, mathematical models were developed. A challenge is to include the effect of wet end chemistry into the dynamic models. A simple approach is used. Empirical models for filler retention and paper formation were formulated from experimental data and combined with dynamic models developed from first principles (mass balances of fibre, fines and fillers). The nonlinear models were solved and the dynamics of concentrations of solids and paper formation were simulated using MATLAB/SIMULINK.

3. Several control configurations were developed and tested using the nonlinear models. The primary control objective of the wet end is to control basis weight and ash content, without deteriorating formation. The performance of several control schemes was evaluated through simulation with regard to set-point tracking and disturbance rejection.

1.4 Scope of the thesis

In Chapter 2, the background and the review of the research results pertaining to the present work are described.

Chapter 3 discusses the parameters affecting first-pass retention. The deposition efficiency model is developed based on interactions between two different sized particles and the effects of the dosages of polymer and microparticles on filler retention are explained using the model. The effects of thick stock flow and filler flow on filler retention are also discussed.

Chapter 4 discusses the parameters affecting paper formation. To relate the dosages of retention aids (polymer and microparticles) to formation, the bridging

strength model is developed based on interactions between a single fibre and neighbouring fibres in a fibre floc, taking into account the surface coverage of retention aids on the fibre surface. The effects of the headbox pulp consistency and the headbox filler concentration are also discussed.

Chapter 5 presents the models describing the dynamics of the concentration of solids (fibres, fines and fillers) in the wet end and in paper and the paper formation. The main factors affecting the dynamics of the retention and formation processes are also discussed.

Chapter 6 presents the design and evaluation of the control system for the retention and the formation processes. Conclusions of this research and contributions to knowledge are given in Chapter 7.

Chapter 2

Review of the wet end process

2.1 Introduction

This chapter provides information on a general papermaking process, the on-line sensors for the wet end control and the current control practices. In the next Section, a general description of a papermaking process is presented with the pilot paper machine at the CEGEP, Trois-Rivières, used for this study. Then parameters in the wet end are discussed in Section 2.2.2. Definitions of retention and formation processes and the variables affecting them are presented in Sections 2.2.3 and 2.2.4. A general overview of a microparticulate retention aid system is given in Section 2.2.5. During the last decades, a number of sensors for on-line measurements of wet end variables have been developed. These are described in Section 2.3. Modelling of the dynamics of the wet end process are discussed in Section 2.4. Finally, the current practice of wet end control is discussed in Section 2.5 focusing on the control of retention.

2.2 Description of the wet end process

2.2.1 Papermaking process

The experiments for this research project were performed on the pilot paper machine at the Centre Spécialisé en Pâtes et Papiers (CSPP), CEGEP de Trois-Rivières. The pilot paper machine is illustrated in Figure 2.1. It is a Fourdrinier paper machine, 76 cm wide, operating typically at a velocity of 40 m/min (with maximum speed of 90 m/min). Pulp from a high consistency pulper is refined using a conical refiner, stored in stock chests and sent to a machine chest. Thick stock (with a consistency of about 2.6 %) from the machine chest is diluted to less than 1 % consistency by recirculated white water from the wire pit. Mineral fillers, such as precipitated calcium carbonate (PCC) are normally added at this point (at the fan pump). The stock is further delivered to centrifugal cleaners and a pressure screen to remove contaminants and then to a headbox. The headbox of the pilot machine is of the open type. The function of a headbox is to take the stock delivered by the fan pump, to transform the pipeline flow into an even, rectangular discharge equal in width to a paper machine and to deliver a uniform amount of stock onto an endless, finely woven belt (wire) at uniform velocity in the machine direction. The drainage is achieved by 18 table rolls, 4 vacuum boxes and a couch roll. The drained water from the wire section is collected at the wire pit to be reused to dilute the thick stock. This is termed the short circulation of white water. By the end of the wire, the wet web reaches a solids content of about 15 to 20 %. The web solids content is further increased to a solids content of 40 to 45 % by a mechanical compression of the web between two press rolls. The wet web from the press section passes through a series of rotating steam-heated cylinders (10 cylinders in the pilot paper machine) where water is evaporated and a calender section before

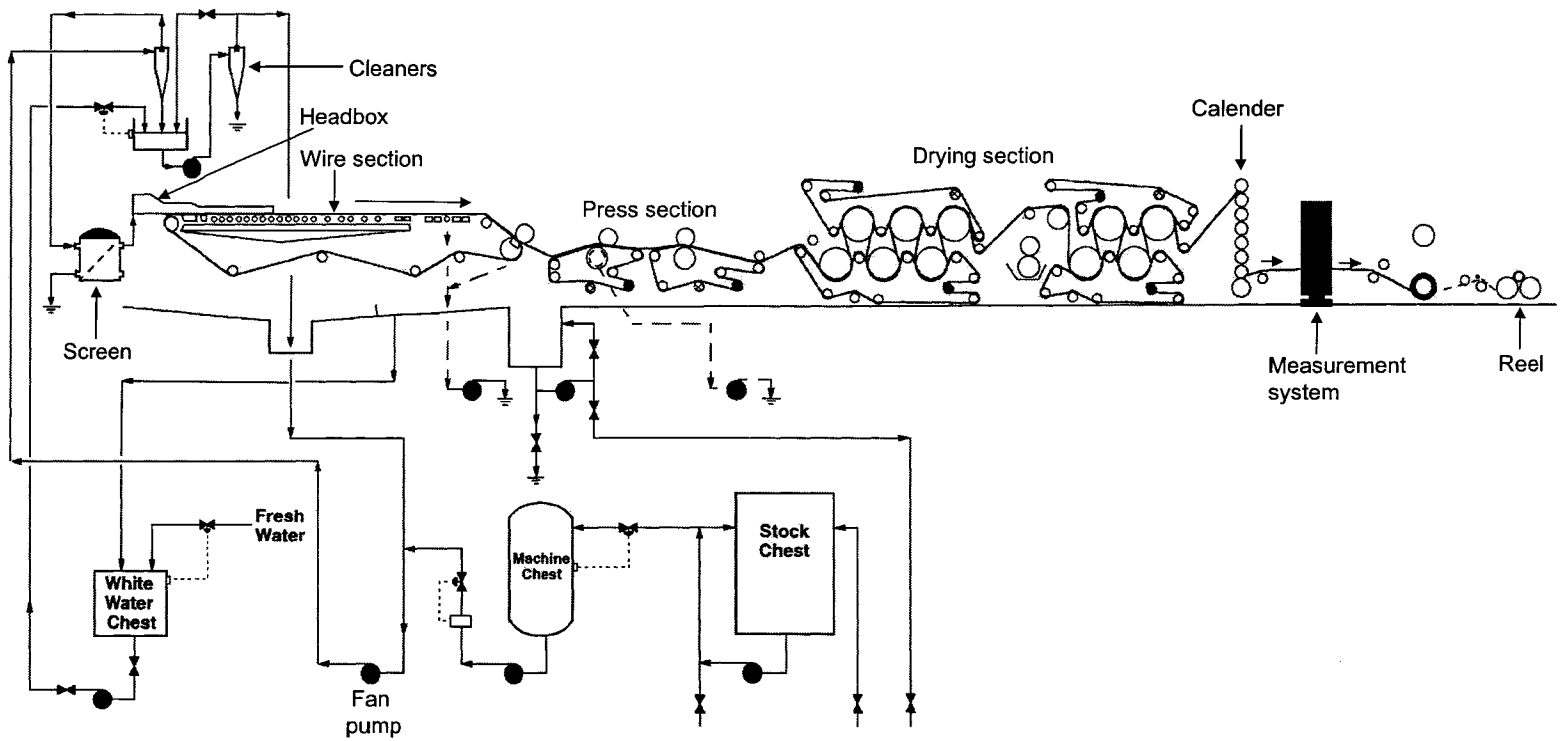

Figure 2.1. Pilot paper machine (Fourdrinier) at the Centre Spécialisé en Pâtes et Papiers (CSPP), CEGEP de Trois-Rivières

being placed on reels. Water which is not used for short circulation dilution of thick stock is sent to dilution points further back in the process for consistency control at various points: this is called the long circulation of white water.

2.2.2 Parameters in the wet end

Optimizing the wet end starts with identifying the variables that are important for the performance on a paper machine and developing an understanding of the interactions between the variables. Figure 2.2 shows a classification of the wet end parameters. The five categories are: practical variables, disturbances, molecular and colloidal interactions, process consequences, and product consequences, as understood in industry [2, 17].

Practical variables are those parameters that papermakers can directly control. These include the type of pulp, filler, and chemical additives, the addition points of chemical additives, the refining degree, the consistency and the flow rate of pulp stock and filler slurry, pH, temperature, concentration and flow rate of chemical additives, machine speed, and machine design. Factors such as machine design and machine speed tend to be fixed. Disturbances are the noise factors upon which the papermaker has less or no control. These include upsets initiated by breaks, grade changes, variations in fresh materials and broke, machine wear, and seasonal water and temperature changes. Molecular and colloidal interactions include complicated physical and chemical processes, such as adsorption, desorption, coagulation, decoagulation, flocculation and deflocculation of fibres, fines, fillers and chemical additives. The interactions between these variables are fundamental to the papermaking process. Process and product factors are the most direct consequences of the molecular and colloidal interactions. Process consequences include first-pass retention, drainage, system cleanliness, effluent, and runnability. Product

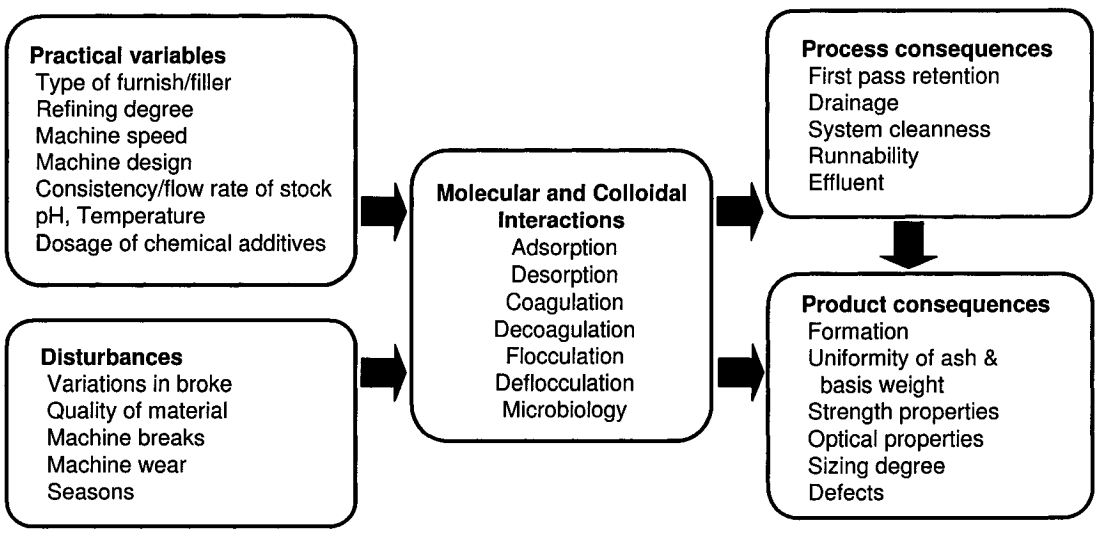

Figure 2.2. Parameters in the wet end of a papermaking process. [2, 17]

consequences include basis weight, ash content, formation, porosity, caliper, sizing degree, strength properties and optical properties. These process and product factors are the consequences of everything that goes on in the wet end and provide further means of measuring the stability of the wet end process.

The papermaker's primary interest is to improve production efficiency and product quality. Among the process and product consequences, first-pass retention and formation are particulary important for these demands. In addition, the practical variables and disturbances represent the sources of the wet end variability. Controlling these factors makes it possible to control the variability in the wet end chemistry process and hence the process and the product consequences.

2.2.3 First-pass retention

First-pass retention (R) simply results from a mass balance on the wire section. It is defined as the ratio of the mass of solid materials entering the wire section to that of solid materials retained in the web, leaving the wire section. It can be mathematically defined as:

$$R\ (\%) = \frac{F_{web}C_{web}}{F_{hb}C_{hb}} \times 100 \tag{2.1}$$

where F represents the flow rate of each stream (L/min), C is consistency (g/L), the subscript "*hb*" means headbox stock and "*web*" is the wet web leaving the wire section. The consistency is used with g/L in this thesis contrary to the TAPPI [18] and PAPTAC [19] definition, in which it is defined as a mass fraction: the oven-dry weight of suspended matter per 100 g of stock. This is justified on the basis of the control literatures [5,6,10,11,13,16,20–22]. In practice, the first-pass retention is calculated from the headbox stock consistency and the white water consistency

measurements:

$$R\,(\%) = \frac{F_{hb}C_{hb} - F_{ww}C_{ww}}{F_{hb}C_{hb}} \times 100 = \left(1 - K_{ww:hb}\frac{C_{ww}}{C_{hb}}\right) \times 100 \tag{2.2}$$

where $K_{ww:hb} = F_{ww}/F_{hb}$ and the subscript "ww" represents white water. If the flow rate of the white water from the wire (F_{ww}) is known, the value of $K_{ww:hb}$ can be calculated. Otherwise, it is normally assumed to be $F_{ww} \approx F_{hb}$ (i.e., $K_{ww:hb} = 1$) since $F_{ww} \gg F_{web}$.

The first-pass retention R is a direct measure of the efficiency of a wire section to capture fibres, fines, and fillers to form a wet web. It therefore affects the system cleanliness. Fines and fillers which are not retained enter the white water system and circulate in the wet end system. First-pass retention also has a strong relationship with drainage. Drainage and retention are conventionally considered to be opposed [23]: the more fines and fillers are retained, the more capillaries are filled, and the drainage through the web is reduced. If drainage is speeded up by increasing turbulence and shear forces on the wire section, retention is hampered. Most of all, any variation in the first-pass retention of solids (fibre, fines and filler) directly influences the white water consistency, the headbox consistency and the ash content and the basis weight of paper.

Two possible mechanisms of fines and filler retention are traditionally considered to be filtration-based and deposition-based retention [24]. Theoretical study by van de Ven [25] showed that, for particles smaller than 10 μm in diameter, filtration by the forming web during drainage on a Fourdrinier is rather low, usually less than 5 %. For particles with a diameter in the range of 10~50 μm, the deposition increases from a few to 100 %. Hence, primary filler particles (0.1~10 μm) and the small fines ($<$ 10 μm) are usually considered to be too small for mechanical entrapment [25,26]. Solberg and Wågberg showed that fillers with a mean particle

size of 0.6 and 0.8 μm are predominantly retained in the web by depositing on fibre surface during papermaking [27].

Even though it is likely that filtration-based retention plays a minor role, there are some experimental evidences of filtration-based retention [24]. If fines are large enough (> 10 μm) and if filler particles are aggregated more than a certain size, filtration-based retention can occur.

2.2.4 Formation

Formation is the degree of uniformity of spatial distribution of fibres, fines, and fillers in paper. Several ways exist to measure and to mathematically define formation [28]. One of the easiest definition to present the meaning of formation is the formation number. It is mathematically defined in a dimensionless form, based on local variations in actual basis weight:

$$F_A = \frac{\sigma(W_A)}{\overline{W}} \tag{2.3}$$

where the subscript "A" is the size of the measuring area, $\sigma(W_A)$ the standard deviation of local basis weight W_A, and $\overline{W}$ the average basis weight of the sheet. A uniform sheet, therefore, has a low formation number. Since the basis weight of a sample affects the standard deviation of the basis weight, it is normalized to compare formation of samples having different basis weight. Normalized standard deviation is based on the assumption that material in paper is distributed according to a Poisson distribution:

$$F_n = \frac{\sigma(W_A)}{\sqrt{\overline{W}}} \tag{2.4}$$

where F_n is the normalized standard deviation of basis weight ($\sqrt{\text{g}}/\text{m}$).

Formation is a critical property for the quality of the product. Poor formation will lead poor paper properties. High variations in the spatial distribution of

solid components (i.e., poor formation) will cause weak paper strength, poor optical properties and high variations in surface roughness and microstructure, which will consequently result in poor printability. In general, formation shows a trend opposite to first-pass retention: paper formation is adversely affected when first-pass retention is improved [29]. Thus, the challenge is *to improve first-pass retention without deteriorating formation.*

The main factor affecting formation is fibre flocculation [30]. Basis weight [28, 31,32] and ash content of paper [33] also influence formation. Mason [34] recognized that fibre flocculation occurred primarily from mechanical interaction between fibres and defined a "critical concentration" at which fibres are likely to collide in rotation. This concept was extended to the "crowding number", the number of fibres in the volume swept out by the length of a single fibre [35]. Increasing fibre concentration and fibre length increases the number of contacts between fibres and hence the tendency of fibres to flocculate. When chemical flocculants are used to improve the first-pass retention, they also influence fibre flocculation [30].

Formation can be improved by increasing the shear in the headbox and in the wire section: for instance, by adjusting dewatering elements or the jet-to-wire speed difference. High shear disrupts fibre flocs. Nordström and Norman [36] showed that a high headbox nozzle contraction ratio reduces fibre flocculation in the jet. According to Swerin and Ödberg [30], formation can be improved at a constant retention level by increasing the wire tension during blade forming at low and moderate dosages of retention aids.

2.2.5 Microparticulate retention aid system

Since fines and filler are one to two orders of magnitude smaller than fibre, the retention by filtration in the wet web is very limited [27]. Increased retention can

be obtained by depositing fine materials on fibre surface, that can be promoted by using retention aids (mostly water soluble high molecular weight polymers).

The major trends in papermaking industry such as system closure and increased shear in the wire section force the papermaking industry to adopt novel retention strategies. One of such strategies is the use of microparticulate retention aids, in which microparticles (colloidal silica, bentonite or aluminum hydroxide) are used with a cationic polyelectrolyte (cationic polyacrylamide or cationic starch) [30, 37–39]. The claimed advantages of these systems compared to single polymeric retention aids are numerous [30, 37, 40, 41]: 1) higher fines and filler retention; 2) improved formation; 3) improved drainage; and 4) better performance under high circuit closure condition. In this research project, a Hydrocol system consisting of cationic polyacrylamide (CPAM) and bentonite is chosen. In this system, polymer is typically added first to pulp suspension and microparticles are added subsequently. The polymer adsorbs onto fibre, fines and fillers and then aggregates are formed. The flocculated suspension passes through several operations involving high shear (e.g., pressure screen) for the flocs to be broken up. The microparticles are normally added after the point of highest shear to induce a reflocculation of the suspension. The polymer adsorbed on both the fibre and the filler or the fines provides anchoring spots for microparticles [42]. Then the microparticle acts as a bridge agent between adsorbed polymer layers for heteroflocculation of fibre and fines or filler and for homoflocculation of fibres or of fines and fillers. It is also believed that bentonite provides a stronger link than a simple polymer bridge [42–44].

2.3 On-line sensors for the wet end control

Until the beginning of 1980s, pH, thick stock consistency and additive flow rates were the only three variables which are measured on-line routinely [45]. Since then, various on-line sensors have been developed and some of them are being used for controlling wet end chemistry [4, 46].

2.3.1 Consistency measurements

A breakthrough in the wet end control was the development of the on-line first-pass retention measurement system. It measures total solids and filler consistencies at the headbox and in the wire pit [20, 47]. Then total solids retention and filler retention are calculated using the equation 2.2. The consistencies are measured by optical methods. The measurement principle is based on the fact that wood fibres and fillers used in papermaking have different polarisability values: pulp fibres, with their partly crystalline structure, depolarize light. By measuring differential reactions of light in various forms, sensor signals are obtained pertinent to the filler/fibre sample. The obtained measurement signals are applied in various calculation models, to yield the total solids and filler consistencies of the sample. More detailed information on the retention monitoring systems can be found elsewhere [4, 20, 47].

For a consistency above 1 %, the most commonly employed sensors utilize principle that the shear force exerted by the flowing stock suspension is directly related to its consistency [45]. Applications of an optical consistency sensor for pulp slurries as high as 7 % consistency have been reported [45]. Also, thick stock ash content can be measured using a low consistency ash measurement system with a dilution unit [10]. Recently a microwave-based total consistency transmitter has been introduced [48]. It is based on the determination of microwave transit time and can

measure consistency from 0 % to 70 %. Applications to the thick stock consistency control has been reported [48,49].

2.3.2 Chemical environment measurements

pH is fundamental to most papermaking chemistry phenomena [45, 50]. It has been measured on-line in many paper mills. It is measured by immersing an active or measuring electrode and a reference electrode into a solution. The measuring electrode produces an electrical potential based on the activity of the hydrogen ion and the reference electrode serves as a source of constant voltage against which the output of the measuring electrode is compared. pH sensors require regular maintenance to keep the stock from clogging and coating the pH electrode.

Conductivity measurement is the determination of the solution's ability to conduct electric current [50]. It indicates the amount of electrolytic contaminants around water. It is therefore a measure of system cleanness and can also indicate the presence of non-organic carryover from pulp mill operations.

An on-line zeta potential instrument has been developed based on streaming potential method, which involve forming a pulp pad, pumping white water through the pad and measuring the electrical charge of streaming potential across the pad [51].

On-line cationic demand measurements provide the amount of anions in a system. The principle underlying commercial cationic demand measurement systems is either a photometric back titration [52] or a potentiometric titration [53, 54]. The photometric back titration method involves adding an abundant quantity of cationization reagent to a sample, titrating back to anionic side with an anionic titration solution and measuring iso-electric point based on a color change of the sample solution. The charge of the original sample is calculated from the amount

of anionic solution needed to change the color of the solution. In the potentiometric cationic demand measurement, a cationic polyelectrolyte (cationic standard reagent) is added to the sample until charge equalization is attained. The equalization point measurement is based on potential difference between two different electrodes. From the amount of cationic standard reagent consumed, the cationic demand is calculated.

An on-line measuring system to determine soluble anions such as chloride, sulfate and acetate and cations such as potassium, calcium, sodium, magnesium and aluminium has been developed based on capillary electrophoresis and tested in paper and board mills [55]. Also an on-line analyzer utilizing conductivity and UV absorbance sensors to measure total dissolved solids, organic dissolved solids and inorganic dissolved solids was developed [56] and had been tested [57].

Recently, commercial systems offer on-line measurements of several wet end chemistry variables in one analyzer system (paper machine wet end analyzers). The Kajaani RMi and Kajaani CATi measure total and ash consistencies, cationic demand, pH, conductivity, turbidity and temperature [16]. The WIC (wet end information centre) system from ABB provides information on pH, conductivity, turbidity, temperature, cationic demand, aluminium, silicate, calcium, dissolved organic carbon (DOC) and alkalinity [52].

2.3.3 Basis weight, ash content and formation measurements

The predominant measurement principle used to determine the basis weight of paper is beta ray transmission [50, 58]. Beta rays are radiated from a radioactive source and absorbed by the paper. Unabsorbed beta rays enter an ionization chamber and create a small current output. This current is converted to a voltage or

digital signals for use. The relative amount of beta rays transmitted through the sheet is an inverse function of its mass (basis weight).

The measurement of ash content is used as an indication of the filler content of paper. On-line ash content sensors are based on the principle of selective absorption of radiation passing through the paper sheet [50, 58]. They are quite similar to basis weight sensors, having a source and an ionization chamber detector mounted on opposite side of the sheet. Radioactive sources that have been used are X-ray and the gamma emitter Fe-55.

Nearly all commercial on-line formation sensors employ optical method. They utilize transmitted light and in some cases reflected light as well as beta ray and X-ray. Some examples of the sources used for commercial on-line sensors are He-Ne laser, a tungsten halogen lamp, a white light source and a laser diode [59]. The formation is then mainly quantified in two ways: variance or formation spectrum [28, 58]. The first provides a systematic equivalent of the subjective look-through test, traditionally used by many papermakers. Light transmission is measured over a small area (1 mm diameter) representing local basis weight and compared with the transmission through a concentric larger (30 mm diameter) surrounding area. Formation number or formation index is calculated from the difference between the two optical densities. The second sensor design measures light transmission through the sheet to determine floc size and intensity. Floc size spectrum is provided in the range of $2 \sim 32$ mm. Recently, a method measuring formation in the forming zone has been developed [60]. The method used light that is transmitted through the pulp suspension and wire(s). The light passed though pulp suspension and wire(s) is captured by a digital color camera. Then the image is processed to provide the formation spectrum.

2.4 Modelling of the dynamics of the wet end

After developing an understanding of a papermaking process and the process variables needed to be optimized, a dynamic model has to be developed to describe the state of output variables, such as white water fines and filler consistencies, basis weight and paper ash content, in terms of the input variables, such as thick stock flow rate and the dosage of retention aids. For the retention process, a sound dynamic model predicting the concentration of fibres, fines, and fillers in a paper machine is required.

Two types of modelling techniques can be used: 1) experimental modelling or black box method, and 2) theoretical modelling [61]. The black box method simply consists of creating perturbations with input variables and recording output variables. A process model for the system is then obtained by directly correlating the input and the output data. Several researchers have used black box approaches to model and to control the dynamics of the retention process. Piirto and Koivo [62] used an ARX (AutoRegressive with eXternal input) model for retention modelling (input: retention aid flow rate; output: retention). Rantala et al. [63,64] employed a multivariable ARX model for retention modelling. The input variables were alum, retention aid (polymer), filler, refining degree, furnish (birch/pine) and the output variable was retention. An ARX model has the form of:

$$\sum_{i=0}^{l} a_i y(t-i) = \sum_{j=1}^{m} \sum_{k=1}^{n} b_{jk} u_j(t-k) + e(t) \tag{2.5}$$

where y is retention, u_j is the inputs, e is the modelling error and a_i and b_{jk} are constants. It was reported that total retention is described by a first order dynamic system and filler retention by a second order. Isaksson et al. [65] utilized a 2×2 transfer function matrix, each element of which consists of a first order plus time delay model, to study the paper machine machine direction (MD) control (input

$u(s)$: dry basis weight and ash content; output $y(s)$: thick stock valve and filler valve):

$$y(s) = \frac{K}{\tau s + 1} e^{-T_d} u(s) \tag{2.6}$$

where K is a process gain, τ a time constant and T_d a time delay. Makkonen et al. [66] used the same input and output variables as Isaksson et al. [65] but they utilized second order transfer function models instead of first order plus time delay models, each element of which consists of a sum of two first order transfer functions with different time constants. Piipponen and Ritala [67] used a short-circulation model shown in Figure 2.3. The model can be expressed with two first order blocks and gains dependent on retention. This model structure was also employed by Kosonen et al. [8].

An alternative consists of deriving a model from first-principles. Using the mathematical modelling approach, the basics of the steady state and the dynamic simulation of the wet end of paper machines has already been established for decades. Beecher [68] created a dynamic model, focusing on the short circulation loop of a Fourdrinier, that consists of mass balances of pulp and water. St. Jacques [69] expanded this dynamic model by including the thick stock dilution recycle, the long circulation loop, and several control strategies. Miyanishi et al. [70] developed steady-state and dynamic simulation models based on mass balances of pulp and filler and studied the distribution of pulp and filler in a paper machine during grade changes. Bussière et al. [71] modelled the operation of a Quebec newsprint mill looking specifically at its broke and white water system using PAPMOD, a steady state simulator with critical dynamic equations to study the dynamic aspects. Orccotoma et al. [72, 73] developed a model representing a white water network and studied the effect of web breaks on the wet end dynamic behavior and

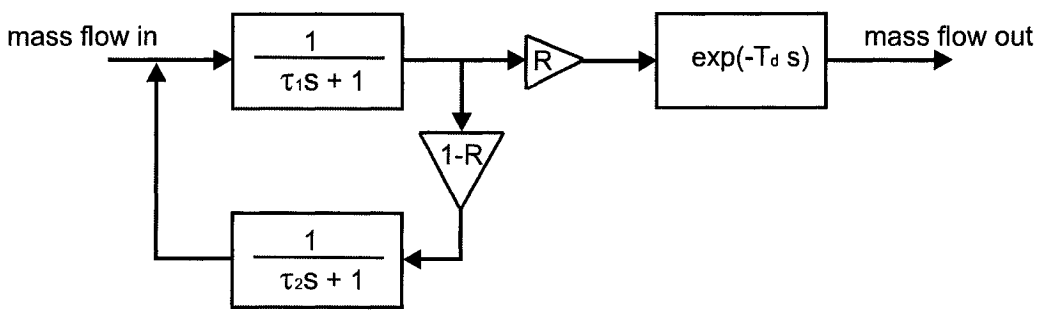

Figure 2.3. Short circulation model. R represents retention, τ_1 and τ_2 are time constants and T_d is the time delay.

the dynamics of fines concentration in the wet end.

A challenge in modelling the wet end of a paper machine using a mass balance technique has been in including the effects of wet end chemistry on the dynamics of the wet end and of paper properties. Shirt [74,75] included polymer adsorption, flocculation and drainage into the model. The polymer adsorption was calculated with Langmuir kinetics [76]

$$\frac{d\theta}{dt} = k_{att}(n_0 - \theta)(1 - \theta) - k_{det}\theta \tag{2.7}$$

where,

- θ is the fractional polymer coverage of particle surface (fibre, fines and filler),
- $n_0 = c_0/\Gamma_{max}$, c_0 being the concentration of polymers and Γ_{max} the maximum amount that can adsorb,
- k_{att} and k_{det} are the attachment and the detachment rate constants, respectively.

The flocculation between components (long fibre, fibre fines, filler and flocs) induced by a dual polymeric retention aid system was calculated by the following equation [74,75]:

$$\frac{dC_{ij}}{dt} = k^{ij} C_i C_j \theta_i^- \theta_j^+ \left(\frac{V_i V_j}{V_i + V_j}\right) \tag{2.8}$$

where,

- k^{ij} = flocculation rate constant for collisions between components i and j,
  $= k_0^{ij} r^i r^j$, r^i and r^j being empirical rate constants for each components,
- C_{ij} = consistency of flocs formed from components i and j,

- C_i, C_j = consistencies of components i and j,
- V_i, V_j = volumes of individual component particles i and j,
- θ_i^- = fractional coverage of component i by anionic polymer,
- θ_j^+ = fractional coverage of component j by cationic polymer.

Then it was assumed that the particles are retained in the web due to mechanical entrapment. The fixed retentions for various particles were assumed: 100 % for flocs (composed of lone fibre, fines and filler), 90 % for long fibres and 2 % for fibre fines and for fillers. The $\theta_i^-\theta_j^+$ term was used to express the effect of the dosages of retention aids on flocculation. The major drawback of the expression is on the assumption that the high molecular anionic polymer adsorbed onto particle i with coverage θ_i^- interacts with the cationic polymer covered sites on particle j with coverage θ_j^+. The generally accepted mechanism of a dual polymer system is that low molecular weight, high charge density cationic polymer adsorbs on particles, providing anchor spots for anionic polymer, and then high molecular weight, low charge density anionic polymer bridges between the cationic polymer covered sites [2]. Hauge and Lie [77] pointed out that Shirt's approach requires to solve many differential equations. For a simpler solution, Hauge and Lie [77] developed a model for the concentration of flocculated component i that can be either filler particles or fines in pipelines:

$$\frac{\partial C_{floc,i}}{\partial t} = -\nu \frac{\partial C_{floc,i}}{\partial x} + \frac{1}{\rho} C_{fibre}(k_{i,ret} C_{ret} C_{non-floc,i} + k_{i,fibre}). \tag{2.9}$$

where

- $C_{floc,i}$: the concentration of flocculated component i
- ν : the velocity of the mass inside the pipeline

- x : the variable corresponding to the direction along the pipeline
- $C_{non-floc,i}$: the concentration of non-flocculated component
- $k_{i,ret}$ and $k_{i,fibre}$: flocculation constants
- C_{ret} and C_{fibre} : concentrations of retention aids and fibres

Then, they assumed that only flocculated components are retained on the wire by mechanical entrapment. The major drawback of this approach is on the major assumption: the main retention mechanism is the mechanical entrapment of fines and filler. Retention of fines and filler by depositing on fibre surface was ignored.

2.5 Current control practices

2.5.1 White water consistency control

The on-line control of white water consistency was suggested and tested in a pilot paper machine by Rantala et al. in the beginning of 1990s [11, 63, 64]. The idea of the strategy is to bring under control the white water consistency by manipulating the flow rate of retention aids through which retention and the whole wet end are stabilized. Several studies confirmed that white water consistency control stabilizes the wet end [5, 6, 11, 21, 41, 78–80]. It improves paper machine stability and runnability, reduces variations in white water and headbox consistencies, basis weight, moisture and thickness and reduces the cost for retention aids.

In the control system, the white water total and filler consistencies are mostly measured at the channel from the white water tray to the wire pit [6, 11, 41, 78]. In some cases, they are sampled at the overflow stream from the wire pit [5, 21]. Then the white water total consistency is controlled by manipulating the flow rates of retention aids: i.e., the dosages of retention aids.

When a single polymer retention system is used, the application is simple: the flow rate of a polymer solution is manipulated based on the white water total consistency measurement [5–7, 10, 62, 78, 79, 81]. For simplicity, most of researches utilized a single polymer retention aid system. However, the use of a microparticulate retention aid system has been increasing. When a microparticulate retention aid system or a dual polymer system is used, several possibilities exist to choose the manipulated variables.

Only a few studies dealt with microparticulate retention aids. Bernier and Begin [41] used microparticulate retention aids consisting of a cationic polymer and bentonite. They regulated the flow rate of polymer solution based on white water consistency measurement, keeping the microparticle flow constant. Rantala et al. [11] utilized a Compozil retention system consisting of cationic starch and colloidal silica and they used both chemical components in identical ratio to control white water total consistency. Renaud and Olsson [5] used anionic nanoparticles to control white water total consistency and polyacrylamide (PAM) to control the amount of fines in the white water. In addition, a few papers using a dual polymer system were published. Tomney et al. [82] utilized a strategy in which white water consistency is controlled by both polymers: flocculant (a high molecular weight anionic polymer) and coagulant (a low molecular weight high charge cationic polymer). The ratio of coagulant to flocculant was also controlled. Proulx and Renaud [21] proposed to use the flow of flocculant as a manipulated variable for the white water consistency, and the flow of coagulant for the dewatering capability of the headbox furnish. However, it is not clearly understood which strategy would be the optimal control structure when microparticulate retention aids are used and when both retention and formation are of concern.

The determination of the set-point of white water consistency has caused some

problems. Generally, the white water consistency measured by putting the controller in manual mode is chosen as a set-point. This would work well when a paper machine produces a single grade of paper. However, different white water consistency values might be needed for different grades when several grades of paper are produced in a paper machine. Hence, Laurikkala et al. [10] tried to install an automatic set-point determination algorithm for grade changes. It collects pairs of basis weight and white water consistency values and then the set-points of the white water consistency are calculated as a function of the basis weight of paper. On the other hand, Proulx and Renaud [21] tried to keep a constant white water consistency during grade changes by regulating retention aids to eliminate any disturbances caused by variations in white water consistency. They implemented a percent-applied polymer dosage calculation to automatically adjust the ratio between the retention aid dosage and the production rate (calculated from headbox consistency and flow rate). But, Kessler et al. [78] disagreed. They initially used the control algorithm similar to Proulx and Renaud [21]. In this control system, if there is a change in stock flow, the polymer flow changes, even before a change was measured by the white water consistency sensor. They argued that this system is ineffective as a grade changes to lower basis weight. Since the production rate is reduced, the flow rate of polymer is initially reduced. The combined effects of reduced retention due to lower basis weight and reduced polymer dosage increases the white water consistency and correspondingly the polymer flow. Thus they returned back to a simple control in which a deviation from the white water consistency set-point causes a change in the retention aid flow.

2.5.2 Integrated approaches

The white water consistency control has a limitation in terms of the magnitude of disturbances it can handle [6]. For instance, really large disturbances in filler or thick stock consistency cannot be dampened enough by the white water consistency control loop. These disturbances can be handled by a basis weight or an ash content control loop, which creates long delay. They should instead be dealt with on the thick stock side before the furnish reaches the basis weight valve. Rantala et al. [11] suggested the idea of controlling the headbox stock consistency by regulating the feeds of fresh filler and fresh pulp, together with the white water consistency control. In this control scheme, measurements at the dry end only provide set-points for the headbox consistencies. Laurikkala et al. [10] suggested a more sophisticated control strategy in which several control loops exist. The control strategy is illustrated in Figure 2.4. Together with the white water total consistency control, the headbox total consistency is controlled to reduce the time delay in controlling consistency disturbances in the headbox. The headbox ash consistency controller is connected in cascade between the paper ash content controller and the filler flow controller. Thick stock total consistency is feedforward controlled to keep the thick stock flow proportional to the set-point of thick stock volume flow and thus to enable the basis weight controller to control fibre flow. Thick stock ash content is also measured and controlled by feedforward and feedback controllers. A more complete strategy has been proposed by Rantala et al. [81], although they did not implement it, as a whole, on a paper machine. The proposed control system includes feedforward control of thick stock consistency, control of white water total consistency, breaktime headbox ash consistency control, feedforward control of thick stock ash content, wire pit pH control and cationic demand control. The main pH control is done in the stock

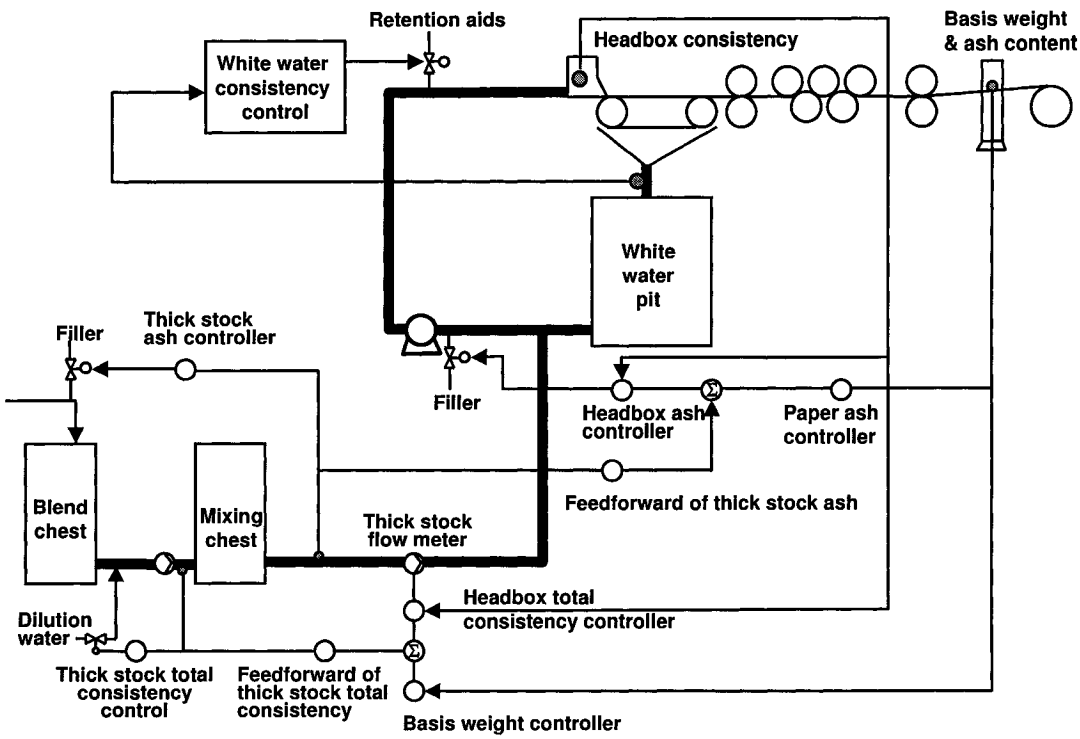

Figure 2.4. A simplified schematic of the control strategies suggested by Laurikkala et al. [10]

preparation. Adding a pH meter in the short circulation loop stabilizes the pH value to its set-point. The cationic demand of white water in the short circulation loop is measured to adjust the flow rate of the coagulant.

Lang et al. [7] pointed out that, when a number of separate control loops are used, optimal tuning of each separate loop will probably not result in optimal performance of the process as a whole: there will be interactions between separate loops. This problem can be resolved by integrating the separate loops into a single multivariable control approach. Due to the advantage of naturally handling multivariable problems, model predictive control (MPC) has been used to control the wet end of papermaking [7–9, 14, 15]. Lang et al. [7] implemented multivariable MPC into three paper machines. The first paper machine used a 2×2 multivariable controller, using paper ash and white water consistency to manipulate fresh filler flow and retention aid. During breaks and immediately afterward, the control is switched to the headbox ash consistency signal rather than the signal from the scanner at the dry end. The second paper machine included the basis weight and the moisture content of paper as the controlled variables as well as paper ash content and retention. In a third paper machine, paper ash, broke ash and retention were integrated into the multivariable controller. Kosonen et al. [8, 14] and Hauge et al. [9] also used multivariable MPC approach. Kosonen et al. chose oven dry weight (kg/s), paper ash (kg/s), headbox ash consistency (g/L) and white water consistency (g/L) as controlled variables and thick stock, filler and retention aids flow rate as manipulated variables while Hauge et al. chose basis weight, paper ash content and the white water total consistency in a wire tray as controlled variables.

2.5.3 Optimization of paper formation

Even though formation of paper is a critical property, very few groups have investigated the on-line control of formation. Blanco et al. [83] suggested that formation can be optimized by controlling fibre flocculation on the wire section by mechanical action. They developed a prototype flocculation control system. The degree of flocculation is measured by on-line sensors before the headbox, in the headbox, or in the slice, and in the wire. Based on the difference between the derived flocculation set-point and the actual flocculation state as measured by the sensors, the actuator is adjusted on the wire section (feedforward and feedback control). Different mechanical actuators have been tried: perforated rolls, sonic rolls, and sonic shakers. The actuators placed under the forming wire generate shear forces to break-up flocs and to avoid the reflocculation process. However, no results about the performance of mechanical actuators have been reported to date. Moreover, in general, dewatering elements in the wire section are previously adjusted, and considered to be fixed factors. Recently, Yue et al. [84] tried to control formation by polymer flow rate, but variations in retention caused by varying polymer flow were not considered.

Chapter 3

Parameters affecting Retention

3.1 Introduction

Retention of solid components (mainly fines and fillers) is a key factor affecting the machine direction variations in paper properties. It directly affects white water and headbox consistencies and consequently the basis weight and the ash content of paper. The main papermaking process variables affecting the retention of fines and filler are the flow rates and the consistencies of retention aids, thick stock and filler slurry. Variations in chemical environmental such as pH, conductivity and cationic demand can also influence the fines and filler retention. In this study, we first focused on the three main variables: the dosages of retention aids, the thick stock flow and the filler flow.

In a retention control system, the white water total consistency is controlled by manipulating the flow rates of retention aids. Indeed, the independent variable controlled is the surface coverage of retention aids on the furnish (fibre, fines and filler). Flocculation and deposition, governing the first-pass retention and hence the white water consistency, are influenced by the surface coverage of retention aids onto the furnish. A robust model describing retention in terms of the surface coverage of retention aids is thus needed.

Models based on the collision efficiency factor can relate the surface coverage of retention aids on a particle to their colloidal behavior (coagulation, adsorption). The collision efficiency is defined as the fraction of particle collisions that lead to adhesion of particles, i.e. to bridging [85–88]. Swerin et al. [89] extended the model for a microparticulate retention aid system. A shortcoming of the approach is that the model considered flocculation of mono-dispersed particles. In papermaking, the furnish consists of fibres, fines, and fillers. Fines and fillers are one to two orders of magnitude smaller than fibre and are retained in the sheet mainly by the deposition on the fibre surface [27]. Hence, the collision or flocculation between a larger particle (fibre) and a smaller particle (fibre fines and filler) has to be considered. Another important phenomenon neglected in the model is the polymer transfer during heteroflocculation. Fines and fillers which are not retained enter the white water system and circulate in the wet end system. There is enough time for fines and fillers to collide and flocculate each other in the short circulation loop. The co-flocculated fines or fillers can be retained in the sheet by either depositing on fibre surface or being mechanically entrapped if the size of aggregates is large enough. The Swerin et al.'s model [89] can be used to express the co-flocculation efficiency for fines and fillers.

The objectives of this chapter are two-fold: 1) to elucidate the effect of the papermaking parameters on the first-pass retention of filler; and 2) to modify the collision efficiency model for two different sized particles (fibre and filler) and for polymer transfer.

The deposition efficiency model relating the dosages of polymer and microparticle to first-pass retention and the characteristic times for the collision of particles are presented in Section 3.2. The experimental section follows in Section 3.3. The

results of changes in filler retention are presented as a function of dosages of retention aids, filler concentration and pulp mass flow rate in Section 3.4. The main parameters affecting filler retention and the implication for wet end control are discussed in Section 3.5.

3.2 Theory

3.2.1 Deposition efficiency

The bridging theory of flocculation is based on the assumption that the flocculation rate (F) is proportional to the product of the particle collision frequency and the fraction of collisions (E) that gives bridging [90, 91]. Under turbulent conditions, the collision frequency (F) is proportional to the square of the number of particles (N_0). Therefore,

$$F = KEN_0^2 \tag{3.1}$$

where K is a constant. The collision efficiency factor (E) is given by:

$$E = 2\theta(1-\theta) \tag{3.2}$$

where θ represents the surface coverage of polymer on particles.

Several attempts have been made to extend the original bridging model in terms of collision efficiency factors [85–88]. Swerin et al. [89] extended the model for a microparticulate retention aid system. The extended model describes the flocculation efficiency in terms of the surface coverage of mono-dispersed particles by low molecular weight polymer, by high molecular weight polymer and by a third component (microparticles) which interacts with adsorbed high molecular weight

cationic polymer. The overall flocculation efficiency is:

$$E = 2\theta^2\mu(1-\mu) + 2\theta(1-\mu)(1-\theta) + a[1 - e^{b\theta/(1-\phi)}] \tag{3.3}$$

where μ is the surface coverage of microparticles onto the sites on the particle surfaces which carry adsorbed polymer, ϕ represents the surface coverage of low molecular weight non-bridging polymer and a and b are constants [89]. The first term describes the interactions by microparticles, the second term is for interactions by polymer and the third term provides the effect of the conformation of the adsorbed polymer layer.

A major shortcoming of this model is that the model is based on collisions between equal sized particles. Fines and filler particles are one to two orders of magnitude smaller than fibres. When retention aids are used, fines and filler particles are mostly retained in the forming web by depositing on fibre surface [27]. In addition, the co-flocculated fines or fillers (flocculated in the short circulation loop) can be retained in the sheet by depositing on fibre surface if the size of aggregates is not big enough to be filtrated by the forming web. Hence, the model has to be modified for the interactions between two different sized particles.

Another important phenomenon is the polymer transfer during heteroflocculation. Polymer transfer between two surfaces can occur during the detachment of particles from fibres [92, 93]. During the break-up of the bond, cleavage of polymer chains can also happen [92]. This creates a transferred and a depleted polymer layer, on the originally bare and polymer-covered surfaces, respectively [94]. The bridging ability of these layers is different from the fresh polymer layer. The degree of deposition of fines covered by a transferred layer onto fibres is very low, but high onto bentonite-covered fibres. Bare fines can deposit on polymer sites (depleted layer) on fibres with or without addition of bentonite [93]. For this study, the

surface coverage of a low molecular weight cationic polymer was neglected since only a high molecular weight polymer was used. The effect of conformation of the adsorbed polymer layer was also neglected. Instead, polymer transfer from fibre to filler was included.

When a microparticulate retention aid system is used, the surfaces of a fibre and a filler or fines can be originally divided into: 1) bare or naked surfaces (n); 2) polymer covered surfaces (p); and 3) bentonite covered sites on the polymer covered surfaces (m). Also polymer transfer from fibre to filler creates a depleted polymer layer ($p_{i,D}$) on the fibre surface and a transferred polymer layer ($p_{j,T}$) on the filler or the fines surface (the subscript i is for the bigger particle (fibre) and j for the smaller particle (fines or filler)). Hence, the polymer covered sites on fibre, fines and filler consist of two parts: fresh polymer covered surface ($p_{i,F}$ and $p_{j,F}$) and depleted or transferred polymer surface. Microparticles can deposit on the fresh polymer covered surface, the depleted polymer layer and the transferred polymer layer, creating $m_{i,F}$, $m_{j,F}$, $m_{i,D}$ and $m_{j,T}$. Since each particle can have five different sites, twenty five interactions can be considered between fibre and filler or fines. Each interaction may have a different bond strength. Then the deposition efficiency is defined as a sum of each interaction:

$$\begin{aligned} E_{dep} &= a_1(n_i : n_j) + a_2(n_i : p_{j,F}) + a_3(n_i : p_{j,T}) + a_4(n_i : m_{j,F}) + a_5(n_i : m_{j,T}) \\ &+ a_6(p_{i,F} : n_j) + a_7(p_{i,F} : p_{j,F}) + a_8(p_{i,F} : p_{j,T}) + a_9(p_{i,F} : m_{j,F}) \\ &+ a_{10}(p_{i,F} : m_{j,T}) + a_{11}(p_{i,D} : n_j) + a_{12}(p_{i,D} : p_{j,F}) + a_{13}(p_{i,D} : p_{j,T}) \\ &+ a_{14}(p_{i,D} : m_{j,F}) + a_{15}(p_{i,D} : m_{j,T}) + a_{16}(m_{i,F} : n_j) + a_{17}(m_{i,F} : p_{j,F}) \\ &+ a_{18}(m_{i,F} : p_{j,T}) + a_{19}(m_{i,F} : m_{j,F}) + a_{20}(m_{i,F} : m_{j,T}) + a_{21}(m_{i,D} : n_j) \\ &+ a_{22}(m_{i,D} : p_{j,F}) + a_{23}(m_{i,D} : p_{j,T}) + a_{24}(m_{i,D} : m_{j,F}) + a_{25}(m_{i,D} : m_{j,T}) \end{aligned} \tag{3.4}$$

where a_k $(k = 1 \ldots 25)$ are the weighting factors of each possible interaction, which are related to the bond strength. Let us define that the surface coverage of fresh polymer and depleted polymer on fibre as $\theta_{i,F}$ and $\theta_{i,D}$, that of fresh polymer and transferred polymer on fines or filler as $\theta_{j,F}$ and $\theta_{j,T}$, the surface coverage of microparticles on the fresh polymer and the depleted polymer covered fibres as $\mu_{i,F}$ and $\mu_{i,D}$, and that on the fresh polymer and the depleted polymer covered fines or filler particles as $\mu_{j,F}$ and $\mu_{j,T}$, respectively. Then, the following relations hold:

- the fraction of the bare surface on fibre surfaces $(n_i) = 1 - \theta_{i,F} - \theta_{i,D}$
- the fraction of the bare surface on filler surfaces $(n_j) = 1 - \theta_{j,F} - \theta_{j,T}$
- the fraction of fresh polymer covered surface without microparticles on fibre $(p_{i,F}) = \theta_{i,F}(1 - \mu_{i,F})$
- the fraction of fresh polymer covered surface without microparticles on filler $(p_{j,F}) = \theta_{j,F}(1 - \mu_{j,F})$
- the fraction of depleted polymer covered surface without microparticles on fibre $(p_{i,D}) = \theta_{i,D}(1 - \mu_{i,D})$
- the fraction of transferred polymer covered surface without microparticles on filler $(p_{j,T}) = \theta_{j,T}(1 - \mu_{j,T})$
- the fraction of microparticle covered sites deposited on fresh polymer on fibre $(m_{i,F}) = \mu_{i,F}\theta_{i,F}$
- the fraction of microparticle covered sites deposited on fresh polymer on filler $(m_{j,F}) = \mu_{j,F}\theta_{j,F}$
- the fraction of microparticles on the depleted polymer covered sites on fibre $(m_{i,D}) = \mu_{i,D}\theta_{i,D}$

- the fraction of microparticles on the transferred polymer covered sites on filler $(m_{j,T}) = \mu_{j,T}\theta_{j,T}$

Assuming that the probability of having interactions between each site is proportional to the fraction of each site, the equation 3.4 becomes:

$$\begin{aligned}
E_{dep} &= a_1(1-\theta_{i,F}-\theta_{i,D})(1-\theta_{j,F}-\theta_{j,T}) + a_2(1-\theta_{i,F}-\theta_{i,D})\theta_{j,F}(1-\mu_{j,F}) \\
&+ a_3(1-\theta_{i,F}-\theta_{i,D})\theta_{j,T}(1-\mu_{j,T}) + a_4(1-\theta_{i,F}-\theta_{i,D})\mu_{j,F}\theta_{j,F} \\
&+ a_5(1-\theta_{i,F}-\theta_{i,D})\mu_{j,T}\theta_{j,T} + a_6\theta_{i,F}(1-\mu_{i,F})(1-\theta_{j,F}-\theta_{j,T}) \\
&+ a_7\theta_{i,F}(1-\mu_{i,F})\theta_{j,F}(1-\mu_{j,F}) + a_8\theta_{i,F}(1-\mu_{i,F})\theta_{j,T}(1-\mu_{j,T}) \\
&+ a_9\theta_{i,F}(1-\mu_{i,F})\mu_{j,F}\theta_{j,F} + a_{10}\theta_{i,F}(1-\mu_{i,F})\mu_{j,T}\theta_{j,T} \\
&+ a_{11}\theta_{i,D}(1-\mu_{i,D})(1-\theta_{j,F}-\theta_{j,T}) + a_{12}\theta_{i,D}(1-\mu_{i,D})\theta_{j,F}(1-\mu_{j,F}) \\
&+ a_{13}\theta_{i,D}(1-\mu_{i,D})\theta_{j,T}(1-\mu_{j,T}) + a_{14}\theta_{i,D}(1-\mu_{i,D})\mu_{j,F}\theta_{j,F} \\
&+ a_{15}\theta_{i,D}(1-\mu_{i,D})\mu_{j,T}\theta_{j,T} + a_{16}\mu_{i,F}\theta_{i,F}(1-\theta_{j,F}-\theta_{j,T}) \\
&+ a_{17}\mu_{i,F}\theta_{i,F}\theta_{j,F}(1-\mu_{j,F}) + a_{18}\mu_{i,F}\theta_{i,F}\theta_{j,T}(1-\mu_{j,T}) \\
&+ a_{19}\mu_{i,F}\theta_{i,F}\mu_{j,F}\theta_{j,F} + a_{20}\mu_{i,F}\theta_{i,F}\mu_{j,T}\theta_{j,T} \\
&+ a_{21}\mu_{i,D}\theta_{i,D}(1-\theta_{j,F}-\theta_{j,T}) + a_{22}\mu_{i,D}\theta_{i,D}\theta_{j,F}(1-\mu_{j,F}) \\
&+ a_{23}\mu_{i,D}\theta_{i,D}\theta_{j,T}(1-\mu_{j,T}) + a_{24}\mu_{i,D}\theta_{i,D}\mu_{j,F}\theta_{j,F} + a_{25}\mu_{i,D}\theta_{i,D}\mu_{j,T}\theta_{j,T}
\end{aligned} \tag{3.5}$$

Let us set the weighting factor for the strongest interaction to one and that of the weakest one to zero ($0 \leq a_k \leq 1$). To simplify this model, the followings are assumed:

- The interactions between the polymer covered surfaces ($p_{i,F} : p_{j,F}$, $p_{i,F} : p_{j,T}$, $p_{i,D} : p_{j,F}$ and $p_{i,D} : p_{j,T}$), between the microparticle covered surfaces ($m_{i,F} : m_{j,F}$, $m_{i,F} : m_{j,T}$, $m_{i,D} : m_{j,F}$ and $m_{i,D} : m_{j,T}$), and between the microparticle

covered surface and the bare surface ($n_i : m_{j,F}$, $n_i : m_{j,T}$, $m_{i,F} : n_j$ and $m_{i,D} : n_j$) are so weak due to electrostatic repulsion that the interactions can be negligible ($a_4 = a_5 = a_7 = a_8 = a_{12} = a_{13} = a_{16} = a_{19} = a_{20} = a_{21} = a_{24} = a_{25} = 0$) [30, 94, 95].

- Microparticles deposit uniformly on the fresh polymer covered sites and on the depleted polymer layer on fibre surfaces, $\mu_i = \mu_{i,F} = \mu_{i,D}$
- Microparticles deposit uniformly on the fresh polymer covered sites and on the transferred polymer layer on filler surfaces, $\mu_j = \mu_{j,F} = \mu_{j,T}$.
- Deposition of microparticles on filler and fines surfaces is so slow that the interactions by microparticle deposited on fines and filler can be neglected ($a_9 = a_{10} = a_{14} = a_{15} = 0$) (see Table 3.1).
- The interactions between microparticle covered sites and polymer covered sites form the strongest bond, $a_{17} = a_{18} = a_{22} = a_{23} = 1$ [94].

In addition, let us define the relative bond strength of the interaction between bare fibre and bare filler surfaces compared to that of the microparticle bridging as γ_{inh}, i.e., $\gamma_{inh} = a_1$, and the relative bond strength of the polymer bridging to the microparticle bridging as γ_{pol}, $\gamma_{pol} = a_2 = a_3 = a_6 = a_{11}$. Then the equation 3.5 reduces to:

$$\begin{aligned} E_{dep} &= \gamma_{inh}(1-\theta_{i,F}-\theta_{i,D})(1-\theta_{j,F}-\theta_{j,T}) \\ &+ \gamma_{pol}(1-\theta_{i,F}-\theta_{i,D})(\theta_{j,F}+\theta_{j,T})(1-\mu_j) \\ &+ \gamma_{pol}(\theta_{i,F}+\theta_{i,D})(1-\mu_i)(1-\theta_{j,F}-\theta_{j,T}) \\ &+ \mu_i(\theta_{i,F}+\theta_{i,D})(\theta_{j,F}+\theta_{j,T})(1-\mu_j) \end{aligned} \tag{3.6}$$

The first part of the equation 3.6 expresses the inherent interaction between the bare fibre surface and the bare filler surface; the second and the third parts are for the polymer bridging; and the fourth part represents the microparticle bridging.

3.2.2 Characteristic times

Collisions between particles can be induced either by shear (orthokinetic) or by diffusion (perikinetic). In a simple shear flow of gradient G, the rate constant for a collision process between two spherical particles of radii a_i and a_j is, according to Smoluchowski [96]:

$$k_o = \frac{4}{3} G(a_i + a_j)^3 \tag{3.7}$$

For diffusion induced collisions, the rate constant is:

$$k_p = \frac{2kT}{3\eta} \frac{(a_i + a_j)^2}{a_i a_j} \tag{3.8}$$

where kT is the thermal energy and η the viscosity of the medium. The characteristic time of initial adsorption or deposition of particle i on particle j can be estimated from:

$$\tau_{att}^{ij} = \frac{1}{k_{o,p} N_j n_0^{ij}} \tag{3.9}$$

N_j is the number of particle j and n_0^{ij} the dimensionless initial concentration of particle i relative to particle j [76].

3.3 Experimental

Experiments were performed on a pilot paper machine (Centre Spécialisé en Pâtes et Papiers, CEGEP in Trois-Rivières) shown in Figure 2.1. Two types of furnishes

were used: softwood bleached kraft pulp (SwBKP); and a mixture of hardwood bleached kraft pulps (HwBKP) and SwBKP (70:30), refined to a freeness of 360 mL CSF. The pH of the furnish was adjusted to 7.5 by adding sodium hydroxide to the stock chests. Precipitated calcium carbonate, PCC, (30 % slurry, Albacar HO) was mixed with pulp at the blend chest (17 % filler content in thick stock) for SwBKP. For a mixture of HwBKP and SwBKP, the PCC slurry was diluted to 10 % and injected at the fan pump. A microparticulate retention aid system consisting of a cationic poly(acrylamide)(CPAM) and bentonite was used. CPAM (Allied colloids, Percol 292) of high molecular weight (~5 x 10^6) and with a degree of substitution of 25 % was used as received. CPAM was diluted to a concentration of 1.5 g/L. A commercial bentonite (Hydrocol O, Allied Colloids) was also used as received. The bentonite was dispersed at a concentration of 3 g/L. The CPAM solution was injected at the inlet of the pressure screen and the bentonite solution was added at the screen outlet.

To investigate the effects of process parameters on filler retention, step changes were applied to the CPAM flow rate, the bentonite flow rate, the filler slurry flow rate, and the thick stock flow rate. Only one variable was changed at a time. Samples were taken from the headbox and the wire pit when the system reached a steady state, and the filler retention (R_{filler}) was calculated with the equation 2.2, assuming that the constant $K_{ww:hb}$ is one:

$$R_{filler} = 1 - \frac{C_{ww}}{C_{hb}} . \tag{3.10}$$

3.4 Results

The CPAM and the bentonite dosages on pulp were varied by manipulating the flow rates of each solutions to change the surface coverage of the retention aids on

the furnish. Figures 3.1 and 3.2 represent the influence of CPAM and bentonite concentration on filler retention, respectively. To test the effect of CPAM and bentonite concentration, the thick stock flow kept constant (headbox pulp consistency was 0.5 % and thick stock filler content was 17 %). There was no additional filler added. The SwBKP furnish showed higher filler retention. When the dosage of CPAM was increased at a bentonite dosage of 3 mg/g (HwBKP + SwBKP), the filler retention linearly increased. In case of SwBKP, the filler retention initially increased with CPAM and then leveled-off after 5 mg/g of CPAM at a lower bentonite dosage (1 mg/g), while it slightly increased at a higher bentonite dosage (5 mg/g). From the natural values of 25 % for a mixture of HwBKP and SwBKP and 28 % for a SwBKP furnish, the filler retention increased to 92 % at a bentonite dosage of 3 mg/g (HwBKP + SwBKP) and 89 % at bentonite 1 mg/g and 95 % at bentonite 0.5 mg/g (SwBKP). SEM pictures representing the effect of CPAM dosage on filler flocculation are shown in Figures 3.3 and 3.4. At a low CPAM concentration (0.1 mg/g), filler particles form smaller flocs well distributed in the sheet, while at a high CPAM dosage (1.4 mg/g), the filler particles aggregate into larger flocs.

The effect of bentonite on the filler retention is less significant than CPAM (Figure 3.2). Filler retention varied from 68 to 43 % for a mixture of HwBKP and SwBKP and from 76 to 88 % at CPAM 0.35 mg/g (SwBKP) and from 87 to 95 % at CPAM 0.5 and 0.85 mg/g (SwBKP). For a fixed CPAM concentration of 0.35 mg/g (HwBKP + SwBKP), the filler retention decreased as a function of bentonite dosage. Arguably, a maximum in the filler retention is expected at the bentonite concentration of around 1 mg/g, as shown with the dotted line in Figure 3.2. This maximum is corroborated by Swerin et al.'s experiment [89], and it also corresponds to the maximum in floc size [44]. For a SwBKP furnish and at

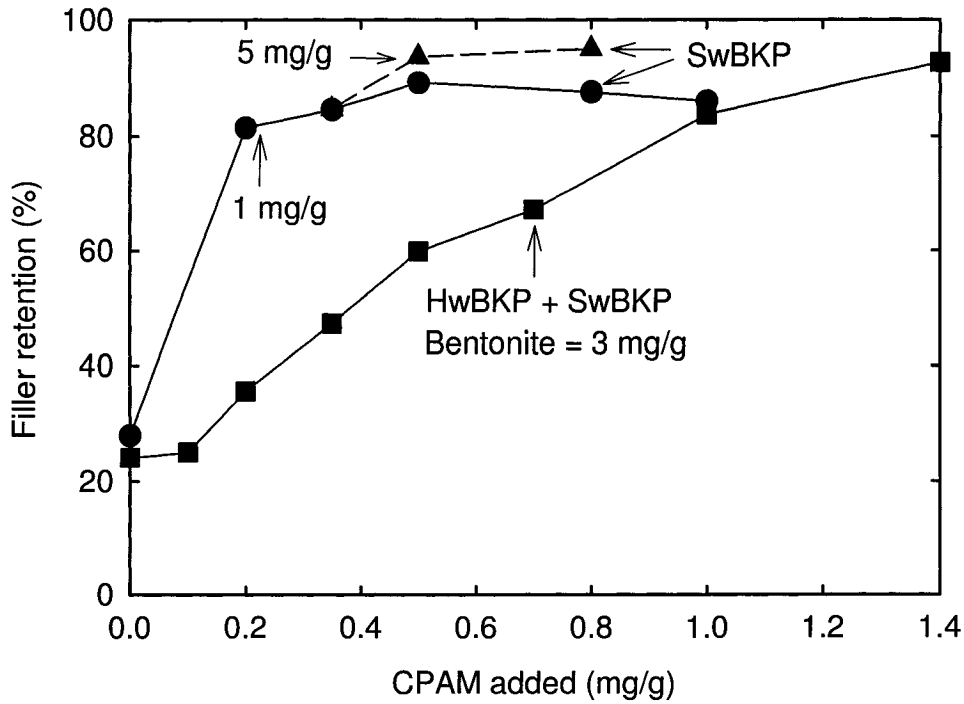

Figure 3.1. Effect of the CPAM dosage on the filler retention for various bentonite dosages shown in the figure for two different furnishes. The filler concentration = 0.2 g/g pulp for a SwBKP furnish and 0.144 g/g pulp for a mixture of HwBKP and SwBKP.

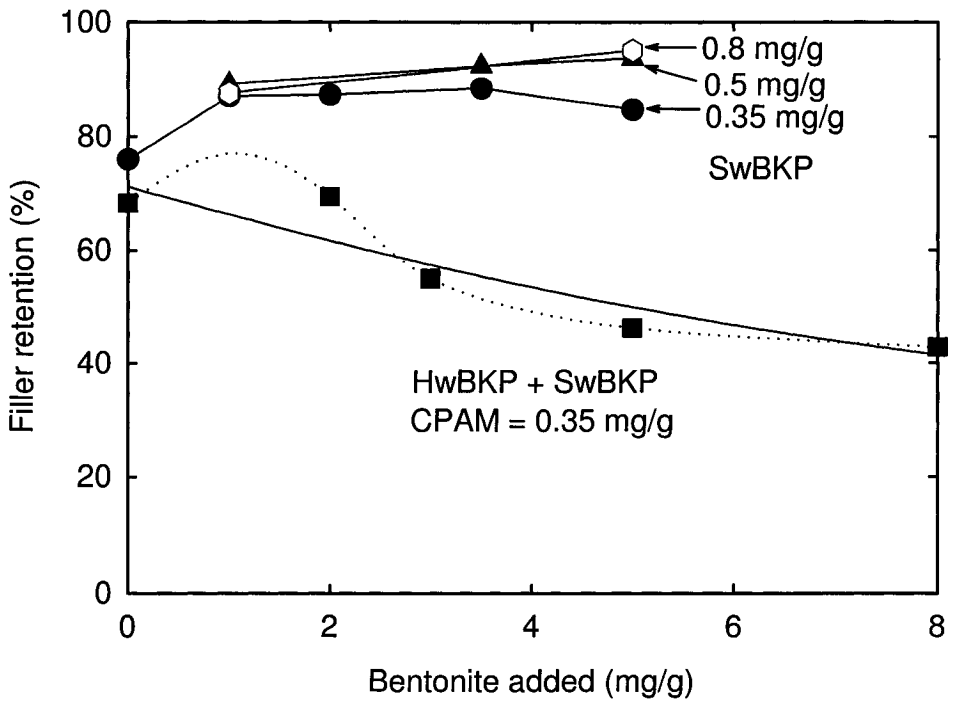

Figure 3.2. Effect of the bentonite dosage on the filler retention for various CPAM dosages shown in the figure for two different furnishes. The filler concentration = 0.2 g/g pulp for a SwBKP furnish and 0.144 g/g pulp for a mixture of HwBKP and SwBKP.

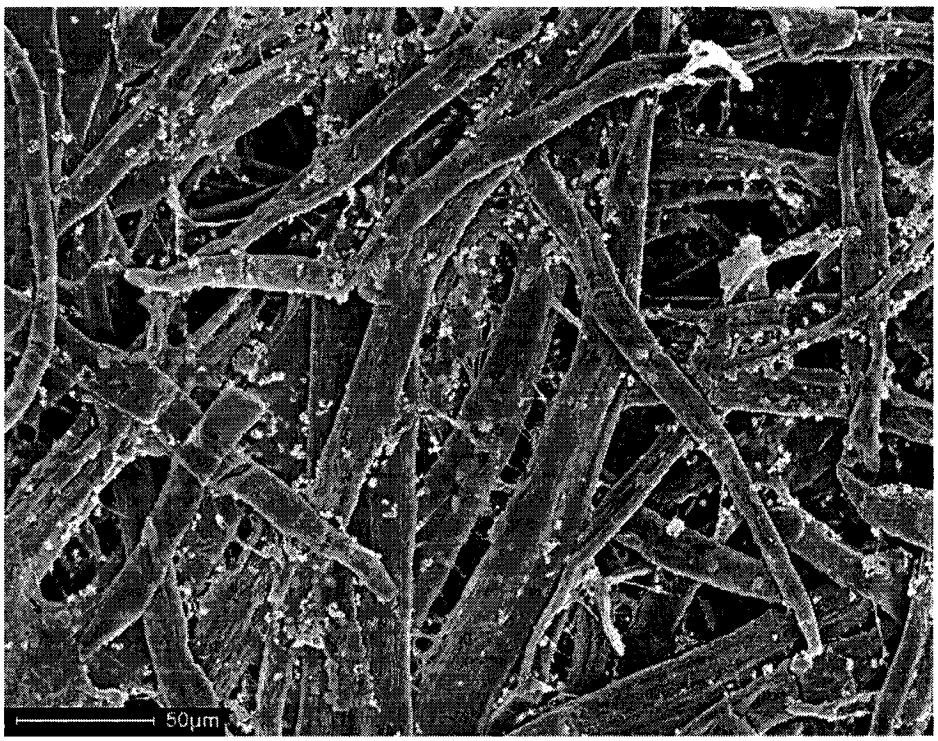

Figure 3.3. SEM picture representing the effect of the CPAM dosage on the flocculation of filler particles. The CPAM dosage was 0.1 mg/g

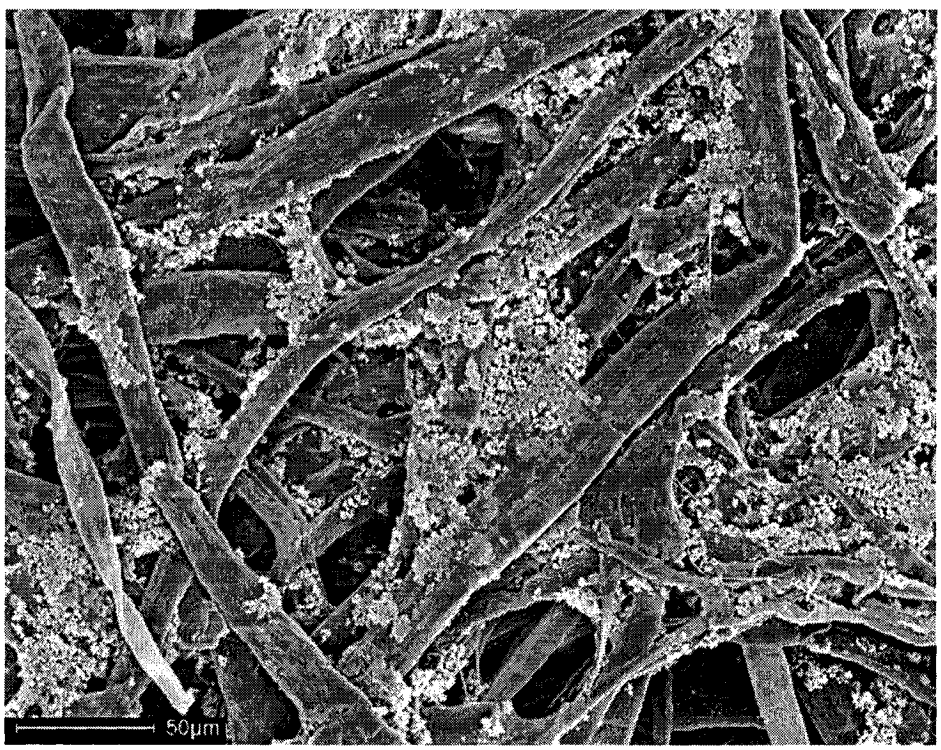

Figure 3.4. SEM picture representing the effect of the CPAM dosage on the flocculation of filler particles. The CPAM dosage was 1.4 mg/g

a CPAM concentration of 0.35 mg/g, the filler retention initially increased with bentonite and leveled-off (Figure 3.2). At higher CPAM dosages (0.5 mg/g and 0.8 mg/g), the filler retention slightly increased with bentonite.

The filler retention slowly decreased as a linear function of the filler concentration for both furnishes (Figure 3.5). The mass flow rate of thick stock pulp was varied with the thick stock flow rate, keeping the flow rate at the headbox constant. Increasing the pulp mass flow rate slightly increased filler retention (Figure 3.6). For a mixture of HwBKP and SwBKP, the flow rate of filler slurry kept constant during the change of the thick stock flow rate. As a result, the filler fraction on pulp also varies. In case of SwBKP, the ratio between pulp and filler kept constant since we mixed filler into thick stock. When the thick stock mass flow rate was increased, the corresponding basis weights were 50, 76, and 102 g/m^2 (HwBKP + SwBKP) and 51, 59 and 67 g/m^2 (SwBKP), respectively. Concerning a mixture of HwBKP and SwBKP, filler retention only slightly increased as the pulp mass flow was more than doubled: the filler retention changed from 42 to 51 %. For a SwBKP furnish, all three of them were around 86 %. This magnitude of retention increase is not significant compared to the effect of CPAM and bentonite.

By comparing changes in filler retention, it is clear that the CPAM dosage is the most important variable affecting the filler retention, followed by the bentonite dosage. Filler concentration, pulp mass flow and headbox pulp consistency are secondary variables of the filler retention.

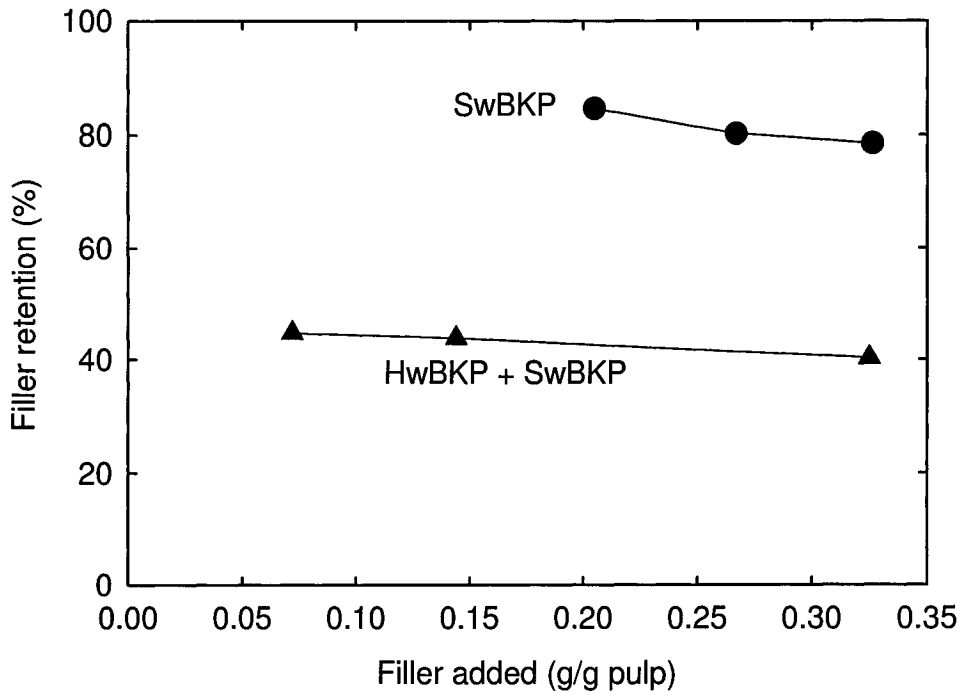

Figure 3.5. Effect of the filler concentration on the filler retention for two different furnishes. For a SwBKP furnish, CPAM dosage = 0.35 mg/g and bentonite dosage = 1 mg/g, and for a mixture of HwBKP and SwBKP, CPAM dosage = 0.35 mg/g and bentonite dosage = 3 mg/g.

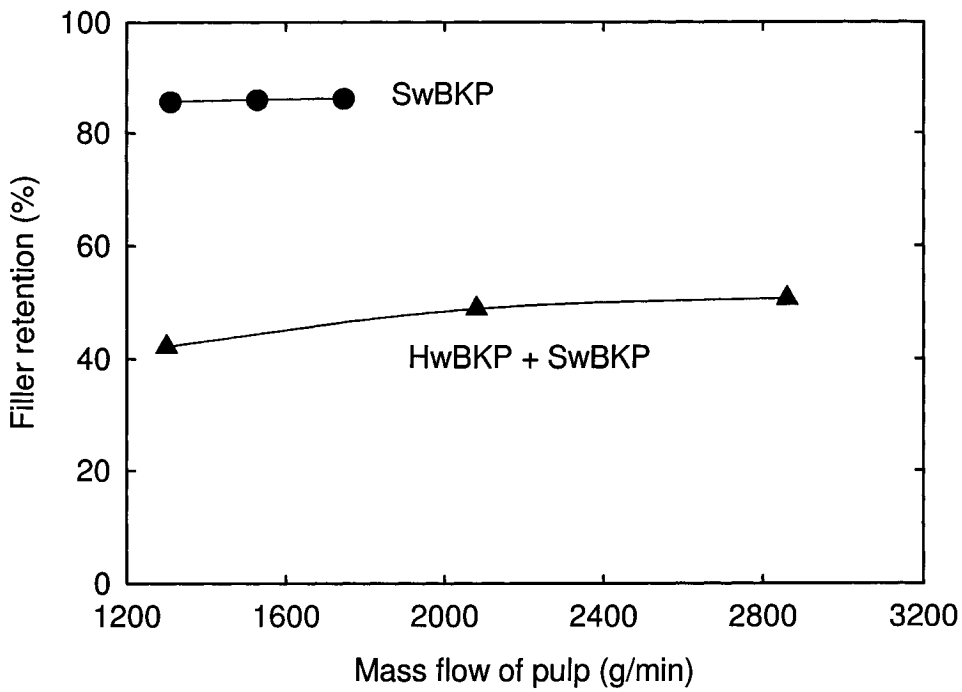

Figure 3.6. Effect of the thick stock pulp mass flow rate on the filler retention for two different furnishes. For a SwBKP furnish, CPAM dosage = 0.35 mg/g and bentonite dosage = 1 mg/g, and for a mixture of HwBKP and SwBKP, CPAM dosage = 0.35 mg/g and bentonite dosage = 3 mg/g.

3.5 Discussion

3.5.1 Characteristic times

CPAM was injected at the inlet of the pressure screen and bentonite at its outlet. The residence time at the pressure screen was of 45 seconds and that between the outlet of the screen and the forming board was about 5 seconds. The characteristic times for adsorption or deposition between particles were calculated using the equation 3.9. The following was assumed for the calculation: for fibres, a length of 2 mm, a diameter of 30 μm, a fibre wall thickness of 5 μm, density of 1.5 g/m^3, and concentration of 5.16 kg/m^3; for PCC, a diameter of 0.5 μm, density of 2.7 g/m^3, and concentration of 1.26 kg/m^3; for CPAM, a radius of gyration of 50 nm and concentration of 0.002 kg/m^3; and, for bentonite, the effective radius of 62 nm and concentration of 0.016 kg/m^3. The maximum shear rate at the pressure screen was estimated to be 2000 s^{-1} and that at the pipeline and flow distributor was 400 s^{-1} [97].

The characteristic times calculated are summarized in Table 3.1. The adsorption of polymers and the deposition of fillers on fibre surfaces were the fastest processes, followed by filler-filler collision. The adsorption of bentonite on fibres at the pipeline had a time scale of the same order as the residence time. When bentonite is added before polymer, there is a sequential adsorption of polymer and bentonite onto the fibres. Bentonite deposition on fillers at the pipeline is not likely to happen. The association of polymer and microparticles in solution is less favored with fibres and fillers present.

Table 3.1. Calculated characteristic time scales for deposition or adsorption between particles (equations 3.7 and 3.9). * Collision induced by diffusion (equations 3.8 and 3.9).

Type of interactions	Characteristic time at the pressure screen (sec)	Characteristic time at the pipeline (sec)
Fibre-Polymer	0.1	
Fibre-Filler	0.2	
Filler-Filler	0.4	
Filler-Polymer	3.9	
Fibre-Bentonite	0.8	3.9
Filler-Bentonite	25.1	125
*Bentonite-Polymer	340	1104

3.5.2 Effect of deposition efficiency

When the dosages of retention aids are changed, the surface coverage of polymer and bentonite on fibres and fillers are varied and consequently the filler retention. Hence, the effect of the dosages of retention aids on the filler retention can be analyzed in terms of the deposition efficiency. The surface coverage of polymer and microparticles can be calculated with the equations in Table 3.2. For the calculation, we assumed that: 1) deposition of bentonite on fillers is very slow: surface coverage of bentonite on fillers is zero ($\mu_j = 0$); and 2) adsorption of polymer on fibres is faster than on fillers. Thus, as long as all fibres are not covered with polymer, no polymer adsorbs on fillers (if $\theta_i \leq 1$, $\theta_j = 0$). Only excess polymer can adsorb on fillers (if $A_{pol}M_{pol} > A_{fibre}M_{fibre}$, $\theta_j > 0$). In addition, the degree of polymer transfer tr is defined as:

$$\text{Degree of polymer transfer}(tr) = \frac{\text{polymer transfered to fines and fillers [g]}}{\text{original polymer adsorbed on fibres [g]}} \quad (3.11)$$

The following values were used for the calculation: the specific surface area of fibre = 1 m^2/g, fines = 8 m^2/g and PCC = 11 m^2/g and the maximum coverage by CPAM = 1 mg/m^2.

Swerin et al. [89] considered that $\gamma_{inh} = 0$ and $\gamma_{pol} = 1$. The calculated results for various degree of polymer transfer (tr) at 3 mg/g of bentonite with $\gamma_{inh} = 0$ and $\gamma_{pol} = 1$ are shown in Figure 3.7. Without polymer transfer ($tr = 0$), the calculated deposition efficiency is zero for CPAM dosages less than 1 mg/g. This is because at these dosages all polymer sites on fibres is covered with bentonite plates ($\mu_i = 1$) and that the bare fillers could not deposit on these sites. Assuming single plates of bentonite, about 2.5 mg is required to cover 1 m^2 of fibre. At CPAM concentration of 1 mg/g, the fibre surface is fully covered with polymer. Any additional polymer will adsorb on fillers. These polymer sites on fillers can bridge with the bentonite

Table 3.2. Equations to calculate the surface coverage of polymer and microparticle on fibre and filler. A_{pol} and A_{mp}: maximum coverage of polymer and microparticles [m^2/g]. A_{fibre} and A_{filler}: surface area of fibre and filler [m^2/g]. M_{pol}, M_{mp}, M_{fibre} and M_{filler}: mass of polymer, microparticles, fibre and filler [g]. tr: the degree of polymer transfer.

when $A_{pol}M_{pol} < A_{fibre}M_{fibre}$	when $A_{pol}M_{pol} \geq A_{fibre}M_{fibre}$
$\theta_i = \frac{A_{pol}M_{pol}}{A_{fibre}M_{fibre}}$	$\theta_i = 1$
$\theta_{i,D} = tr \cdot \theta_i$	$\theta_{i,D} = tr \cdot \theta_i$
$\theta_{i,F} = (1 - tr) \cdot \theta_i$	$\theta_{i,F} = (1 - tr) \cdot \theta_i$
if $tr \cdot A_{pol}M_{pol} \leq A_{filler}M_{filler}$	if $[(1 + tr)A_{pol}M_{pol} - A_{fibre}M_{fibre}] \leq A_{filler}M_{filler}$
$\theta_{j,F} = 0$	$\theta_{j,F} = \frac{A_{pol}M_{pol} - A_{fibre}M_{fibre}}{A_{filler}M_{filler}}$
$\theta_{j,T} = \frac{tr \cdot A_{pol}M_{pol}}{A_{filler}M_{filler}}$	$\theta_{j,T} = \frac{tr \cdot A_{fibre}M_{fibre}}{A_{filler}M_{filler}}$
$\theta_j = \theta_{j,F} + \theta_{j,T}$	$\theta_j = \theta_{j,F} + \theta_{j,T}$
if $tr \cdot A_{pol}M_{pol} > A_{filler}M_{filler}$	if $[(1 + tr)A_{pol}M_{pol} - A_{fibre}M_{fibre}] > A_{filler}M_{filler}$ and if $tr \cdot A_{pol}M_{pol} < A_{filler}M_{filler}$
$\theta_{j,F} = 0$	$\theta_{j,T} = \frac{tr \cdot A_{fibre}M_{fibre}}{A_{filler}M_{filler}}$ and $\theta_{j,F} = 1 - \theta_{j,T}$
$\theta_{j,T} = 1$	if $[(1 + tr)A_{pol}M_{pol} - A_{fibre}M_{fibre}] > A_{filler}M_{filler}$ and if $tr \cdot A_{pol}M_{pol} \geq A_{filler}M_{filler}$
	$\theta_{j,T} = 1$ and $\theta_{j,F} = 0$
if $A_{mp}M_{mp} \geq A_{pol}M_{pol}$	if $A_{mp}M_{mp} \geq A_{fibre}M_{fibre}$
$\mu_i = 1$ and $\mu_j = 0$	$\mu_i = 1$ and $\mu_j = 0$
if $A_{mp}M_{mp} < A_{pol}M_{pol}$	if $A_{mp}M_{mp} < A_{fibre}M_{fibre}$
$\mu_i = \frac{A_{mp}M_{mp}}{A_{pol}M_{pol}}$ and $\mu_j = 0$	$\mu_i = \frac{A_{mp}M_{mp}}{A_{fibre}M_{fibre}}$ and $\mu_j = 0$

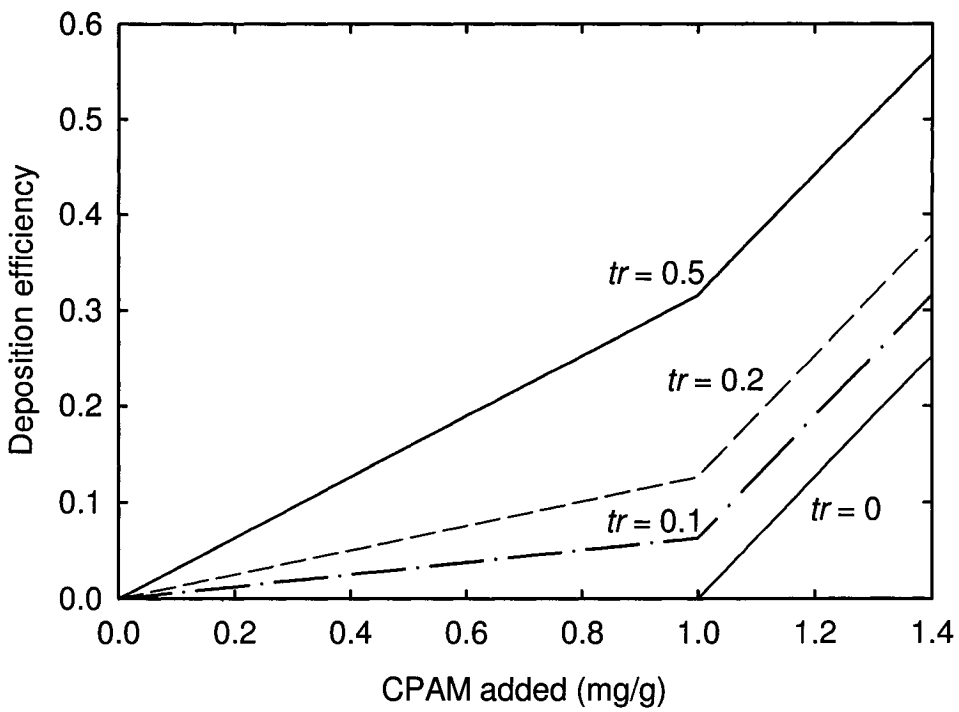

Figure 3.7. Effect of the degree of polymer transfer on the deposition efficiency. Bentonite dosage = 3 mg/g, the maximum coverage by bentonite = 2.5 mg/m^2, $\gamma_{inh} = 0$ and $\gamma_{pol} = 1$.

covered sites on fibres, resulting in an increased deposition efficiency.

However, experiments showed that the filler retention increased even at CPAM concentrations lower than 1 mg/g (Figure 3.1). Two explanations are possible: 1) the maximum coverage of bentonite was lower than the estimated value (2.5 mg/m^2); 2) polymer transfer occurred. If bentonite is not fully delaminated, the surface coverage of bentonite would be lower than estimated. According to Vanerek [98], bentonite in papermaking condition is not fully delaminated: it exists in 4$\sim$6 stacks of montmorillonite plates. In addition, the deposition of bentonite on fibre surface is a relatively slow process (Table 3.1). The characteristic time of a collision between fibre and bentonite is about 4 seconds in the pipeline. Even though the characteristic time is slightly smaller than the residence time, there might not be enough time for bentonite particles to cover the whole fibre surface. If the maximum coverage of bentonite is lower than estimated, its surface coverage on fibres will decrease ($\mu_i < 1$), allowing bentonite-free polymer sites on fibres, which could interact with bare filler surfaces. When CPAM concentration is increased, the bentonite-free polymer sites on fibre increases, resulting in an increase in deposition efficiency and filler retention.

The transferred polymer on the filler surface could interact with the bentonite sites on the fibre surface. The higher the polymer concentration, the higher is the quantity of polymer transferred onto fillers (increase in $\theta_{j,T}$). Figure 3.7 shows that, as polymer transfer occurs ($tr > 0$), the deposition efficiency increases with polymer concentration, even at CPAM dosages lower than 1 mg/g. Tanaka et al. [99] reported that, at a polymer addition of 0.1 %, half of the polymer adsorbed on pulp was transferred to polystyrene latex particles within 1$\sim$2 min. For the rest of the discussion, it was assumed that $tr = 0.5$

Figure 3.8 shows the effect of γ_{inh} on the deposition efficiency at a bentonite

dosage of 3 mg/g. 5 stacks of montmorillonite plates were assumed for the calculation. The value of γ_{inh} determines the deposition efficiency at a polymer dosage of 0 mg/g: the higher γ_{inh}, the higher the deposition efficiency at a CPAM dosage of 0 mg/g. Fillers can deposit without retention aids even though the degree of deposition is very low. The experimental results confirm this: more than 20 % of filler was retained at a CPAM dosage of 0 mg/g (Figure 3.1). This observation corroborates that $\gamma_{inh} > 0$. For the rest of the discussion, the value of γ_{inh} used was 0.05.

Figure 3.9 shows the effect of γ_{pol} on the deposition efficiency at a bentonite dosage of 3 mg/g. The value of γ_{pol} determines the maximum value of deposition efficiency: the higher γ_{pol}, the higher the maximum. When $0.1 \leq \gamma_{pol} < 0.5$, the model gives similar trends as the experimental results. This confirms that the interaction by a polymer bridge is stronger than the interaction between bare fibre and bare filler surfaces. Also, Asselman and Garnier's finding [94] supports that a microparticle bridging provides stronger bond than a polymer bridging. The exact value of γ_{pol} is not known, but it is clear that $\gamma_{inh} < \gamma_{pol} < 1$. For the rest of the discussion, it was assumed that $\gamma_{pol} = 0.2$

It was assumed that at a polymer dosage higher than 1 mg/g, the excess polymer will adsorb on filler surfaces. As the surface coverage of polymer on fillers increases ($\theta_{j,F}$ and $\theta_{j,T}$), the flocculation efficiency between filler particles also increases, improving co-flocculation between fillers. Retention of filler aggregates would also increase. SEM analysis of papers (Figures 3.3 and 3.4) confirms this hypothesis. At low CPAM concentrations, filler particles form smaller flocs well distributed in the sheet, while at high CPAM dosages the filler particles aggregate into larger flocs.

The increase in the filler retention with CPAM for a SwBKP furnish is caused by the increase in the deposition efficiency (compare Figures 3.1 and 3.10). For

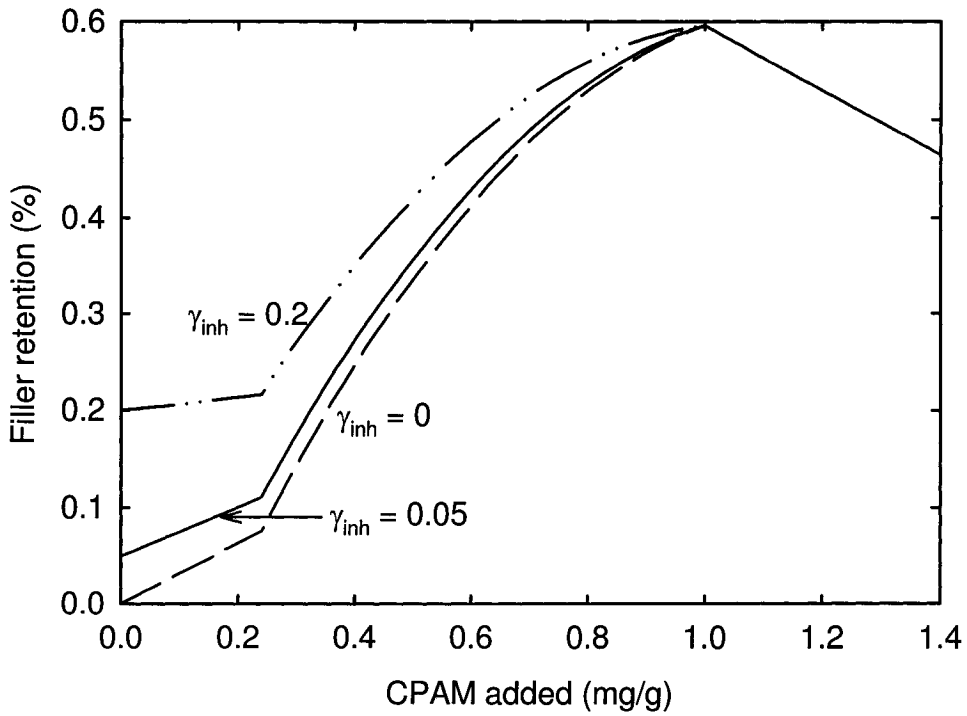

Figure 3.8. Effect of the relative bond strength γ_{inh} (between naked surfaces) on the deposition efficiency. Bentonite dosage = 3 mg/g, γ_{pol} = 1, $tr = 0.5$ and the maximum coverage by bentonite = 12.5 mg/m^2.

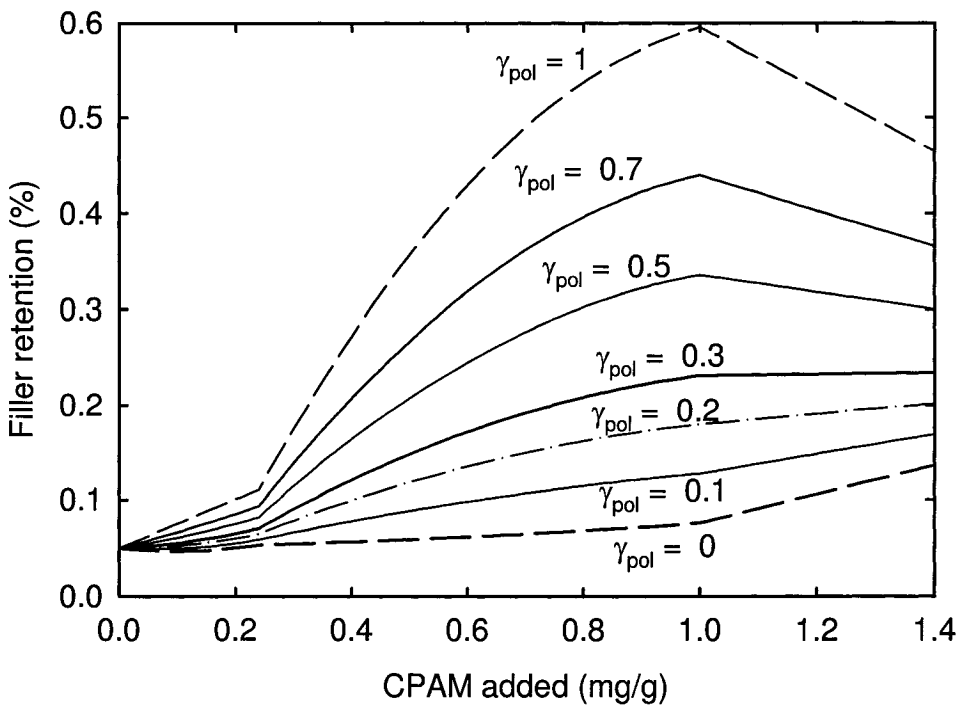

Figure 3.9. Effect of the relative bond strength γ_{pol} (for polymer bridging) on the deposition efficiency. Bentonite dosage = 3 mg/g, the maximum coverage by bentonite = 12.5 mg/m^2, $\gamma_{inh} = 0.05$, and $tr = 0.5$.

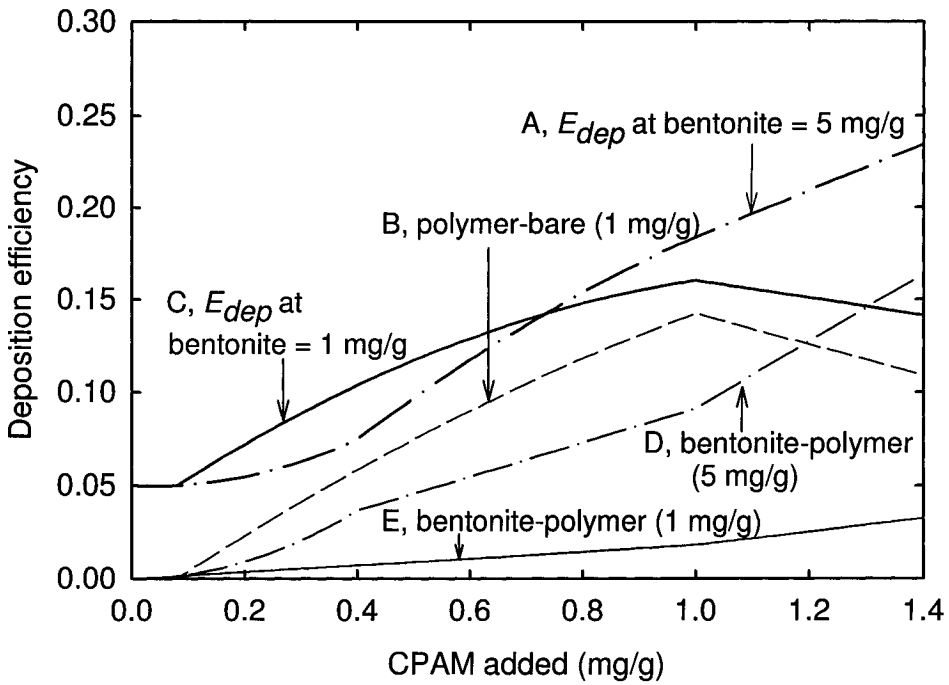

Figure 3.10. Effect of the CPAM dosage on the deposition efficiency for two bentonite dosages. $\gamma_{inh} = 0.05$, $\gamma_{pol} = 0.2$, $tr = 0.5$ and the maximum coverage by bentonite = 12.5 mg/m^2.

a CPAM dosage of 0.08 mg/g, assuming all CPAM adsorbs onto the fibres, the bentonite dosage to just cover all the polymer is 1 mg/g. Hence, at a bentonite dosage of 1 mg/g, the possibility of having interactions between the bentonite covered fibre surface and the polymer covered filler surface is much lower than that between the polymer covered fibre surface and the naked filler surface (compare curves B and E in Figure 3.10). The increase in the deposition efficiency with CPAM dosage is mainly due to the increase in the polymer bridging. For CPAM dosages lower than 0.7 mg/g, the deposition efficiency at a bentonite dosage of 5 mg/g is lower than that at 1 mg/g (compare curves A and C in Figure 3.10). For a CPAM dosage of 0.4 mg/g, assuming all CPAM adsorbs onto the fibres, the bentonite dosage to just cover all the polymer is 5 mg/g. At CPAM dosages lower than 0.4 mg/g, all polymer covered sites on fibre are coated with bentonite. The major interaction is the interaction between the bentonite covered fibre surface and the transferred polymer covered filler surface, which is lower than the interaction by the polymer bridging at a bentonite dosage of 1 mg/g (compare curves B and D in Figure 3.10). With increasing CPAM dosages, the microparticle bridging plays major role in increasing the deposition efficiency. The interaction between the polymer covered fibre surface and the bare filler surface increases as well after a CPAM dosage of 0.4 mg/g. These increased interactions provide higher deposition efficiency at a bentonite dosage of 5 mg/g than that at 1 mg/g after a CPAM dosage of 0.7 mg/g.

For a mixture of HwBKP and SwBKP and at a CPAM dosage of 0.35 mg/g, the deposition efficiency initially decreases with increasing bentonite dosages and then levels-off after 4.4 mg/g (Figure 3.11). The surface coverages of polymer on fibre ($\theta_i = 0.35$) and on filler ($\theta_{j,T} = 0.11$) are constant. For a CPAM dosage of 0.35 mg/g, assuming all polymer adsorbs onto fibres, the bentonite dosage to

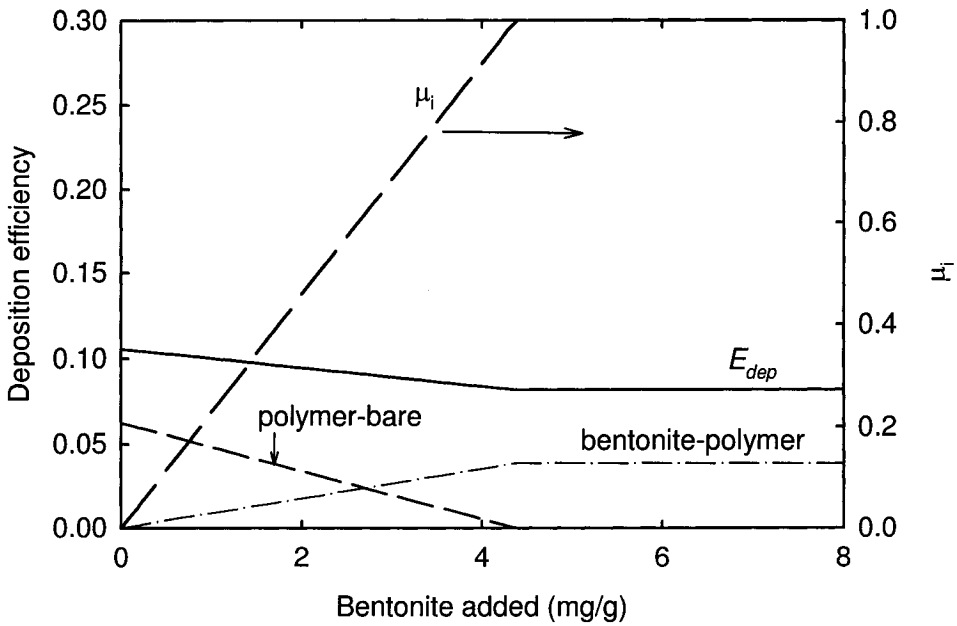

Figure 3.11. Effect of the bentonite dosage on the deposition efficiency. CPAM = 0.35 mg/g, the maximum coverage by bentonite = 12.5 mg/m^2 and filler added = 0.144 g/g pulp.

cover all the polymer is 4.4 mg/g. With increasing bentonite dosages from 0 to 4.4 mg/g, the interaction between the polymer covered fibre surface and the bare filler surface decreases due to the decreasing polymer covered surface without bentonite ($\theta_i(1 - \mu_i)$) while the interaction between the microparticle covered fibre surface and the transferred polymer covered filler surface increases (Figure 3.11). The initial decrease is due to the decrease in the polymer bridging. Filler retention must decrease with increasing bentonite dosage if the filler retention is assumed to vary linearly with the deposition efficiency. This goes against the results of Swerin et al. [89], wherein filler retention initially increased as a function of bentonite concentration, until a maximum was reached in the range of 1.5 to 2 mg/g, and then the filler retention decreased.

Figure 3.12 shows the effect of bentonite dosages on the deposition efficiency for a SwBKP furnish. The deposition efficiency decreases with increasing bentonite dosage at CPAM concentrations of 0.35 mg/g and 0.5 mg/g due to the decreased polymer bridging. The microparticle bridging increases with increasing bentonite dosage, but the increase is smaller than the decrease in the polymer bridging. The deposition efficiency slightly increases at a CPAM dosage of 0.8 mg/g due to the microparticle bridging. The decrease in the deposition efficiency at CPAM dosages of 0.35 mg/g and 0.5 mg/g does not agree with the experimental results (compare Figures 3.2 and 3.12). The possible explanations are:

1. The polymer coverage on fibre is higher than the calculated. At higher polymer coverage on fibre and filler (1 mg/g and 1.2 mg/g), the deposition efficiency increases with increasing bentonite dosage (Figure 3.12).

2. The microparticle bridging plays major role in the deposition of filler. At all polymer dosages, the probability of having microparticle bridging increases

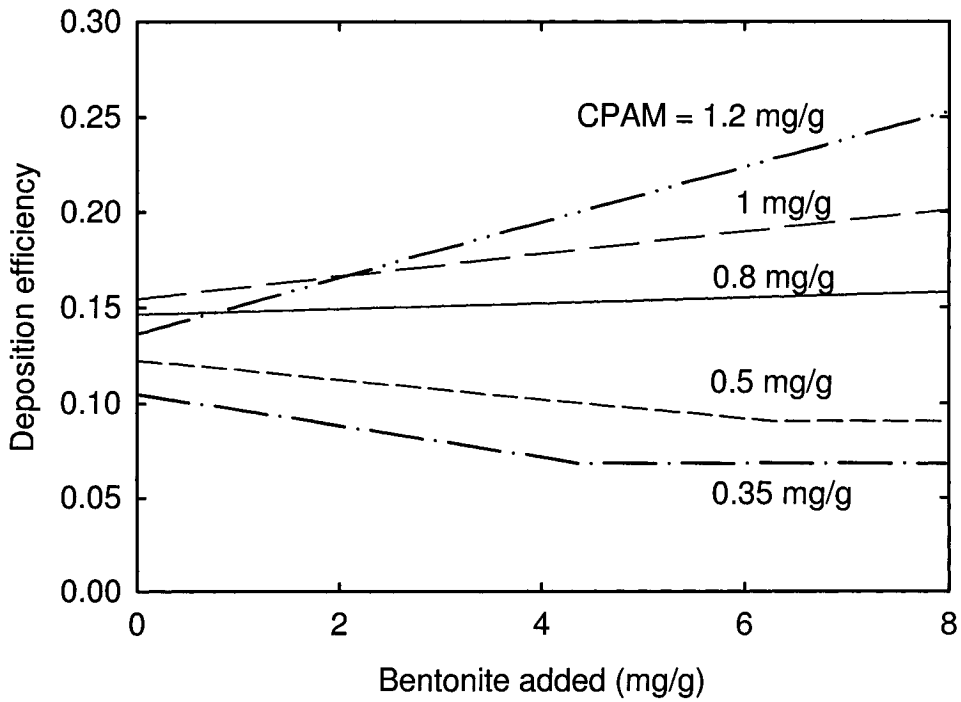

Figure 3.12. Effect of the bentonite dosage on the deposition efficiency for various CPAM dosages shown in the figure. The maximum coverage by bentonite = 12.5 mg/m^2 and filler added = 0.2 g/g pulp.

with increasing bentonite dosage, which could result in the increase in the deposition efficiency.

3.5.3 Effect of PCC concentration

PCC concentration did not have a significant effect on filler retention (Figure 3.5). Increasing filler concentration from 0.05 to 3.5 g/g pulp slightly decreased the deposition efficiency between fibres and fillers (Figure 3.13). However, the magnitude of the change in the deposition efficiency was not significant compared to that by CPAM. The slight decrease in the deposition efficiency with increasing filler concentration is due to the fast kinetics of polymer adsorption on fibre surfaces and polymer transfer from the fibre surface onto the filler surface. The CPAM dosage for this experiment was 0.35 mg/g. Since the amount of CPAM is insufficient to cover the whole fibre surface, the polymer predominantly adsorbs on fibres; basically no polymer adsorbs on filler ($\theta_i = 0.35$ and $\theta_{j,F} = 0$). The polymer coverage on fibres θ_i is not affected by changing the PCC concentration. At the same time, increasing the PCC concentration increases the surface area of fillers. Assuming that the degree of polymer transfer remained the same, the surface coverage of transferred polymer on fillers ($\theta_{j,T}$) decreases with increasing PCC concentration (Figure 3.13), which leads to a slight decrease in the interaction between the bentonite covered sites on fibre and the transferred polymer covered sites on filler and that between the bare fibre surface and the transferred polymer covered sites on filler surface. In addition, increasing filler concentration can lead more collisions between fibres and fillers and consequently more polymer can be transferred onto filler surface. Thus, the changes in the deposition efficiency could be smaller than shown in Figure 3.13.

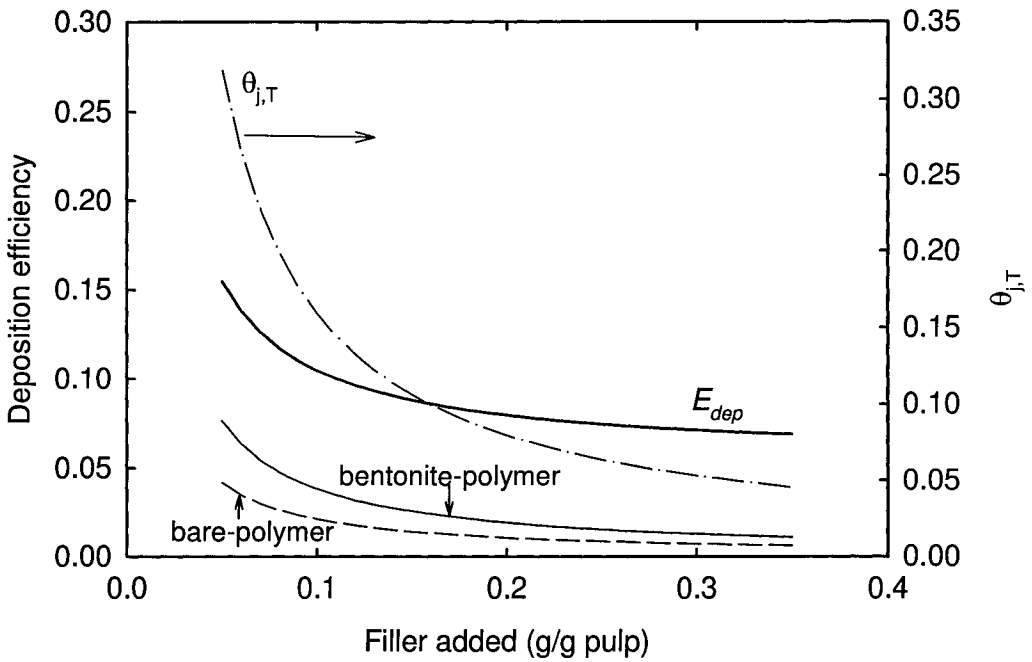

Figure 3.13. Effect of the filler concentration on the deposition efficiency. CPAM = 0.35 mg/g, bentonite = 3 mg/g and $tr = 0.5$.

3.5.4 Effect of pulp mass flow

Increasing the pulp mass flow rate slightly decreases the deposition efficiency (Figure 3.14), while the filler retention is increased (Figure 3.6). When the pulp mass flow rate increased keeping the mass flow rate of the filler slurry and the retention aids constant (HwBKP+SwBKP), the surface coverage of polymer (θ_i) is decreased while the surface coverage of bentonite on the polymer covered fibre surface and the surface coverage of the transferred polymer on filler remained unchanged. The decreased surface coverage of polymer on fibre reduces the interactions between the polymer covered sites on fibre and the bare filler surface and between the bentonite covered sites on fibre and the transferred polymer covered site on filler and consequently decreases the deposition efficiency. When the pulp mass flow rate is increased keeping the filler concentration (g filler/g pulp) constant (for a SwBKP furnish), the surface coverage of polymer on fibre (θ_i) and that of the transferred polymer on filler ($\theta_{j,T}$) decreases, resulting in the decrease in the deposition efficiency.

Two possibilities exist to explain the increase of the filler retention: the increased pulp mass flow has to increase either the mechanical entrapment of fillers by the forming web or the deposition of fillers onto fibre surface. For filler particles to be entrapped by the forming web, the pore size of the forming web has to be smaller than the size of the particles. In addition, the increased pulp mass flow has to have an influence on the pore size to affect the mechanical entrapment of filler. According to van de Ven [25], the average pore size ($\bar{r}$) of the forming web is related to the fibre radius (R):

$$\bar{r} = \frac{\epsilon}{1-\epsilon} R \tag{3.12}$$

where ϵ is the void fraction. Consequently, we can rule out this hypothesis.

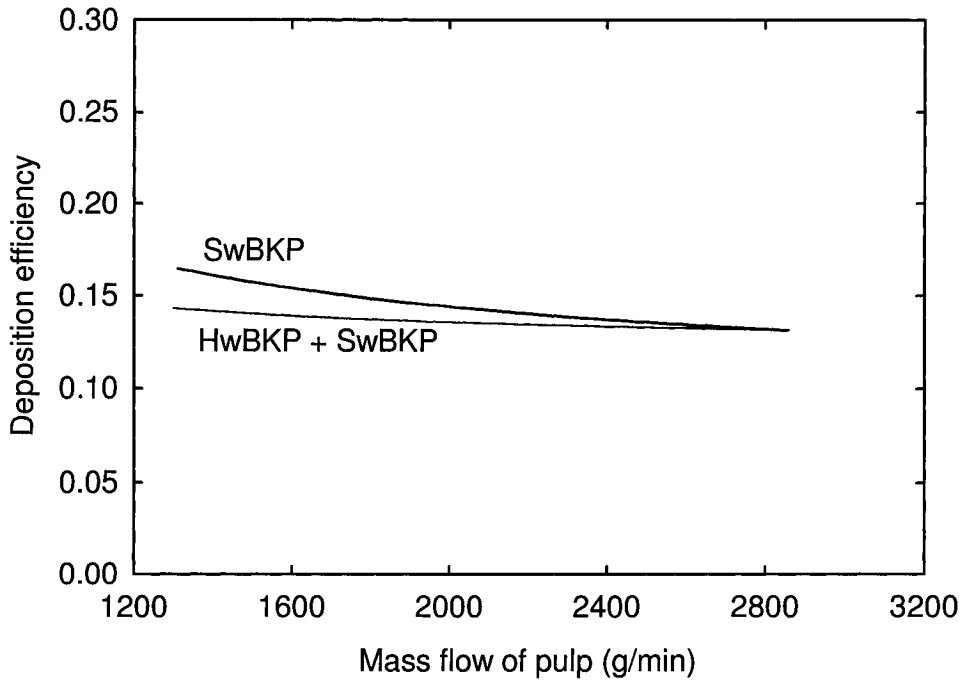

Figure 3.14. Effect of the thick stock pulp mass flow rate on the deposition efficiency for two furnishes. For a mixture of HwBKP and SwBKP, CPAM = 0.35 mg/g, bentonite = 3 mg/g and for a SwBKP furnish, CPAM = 0.35 mg/g, bentonite = 1 mg/g.

Deposition of fines or filler particles on fibre surfaces can occur at the pipe line, in the headbox and on the wire. Deposition of fines or filler particles during drainage improves with increasing pulp consistency by [25]:

$$\frac{n_o - n}{n_o} \simeq \frac{\mathrm{k\ T\ R\ L}\ n_f\ \mathrm{d}\ \overline{\mathrm{Sh_f}}}{6\ \eta\ \epsilon\ \mathrm{v}\quad a^2} \tag{3.13}$$

where n and n_o are the number concentration of filler in white water and in pulp suspension (m^{-3}), k is Boltzmann's constant (J/°K), T represents absolute temperature (°K), L is fibre length (m), n_f is the number concentration of fibres in pulp suspension, d is the distance up to dryline (m), η is viscosity of suspending medium (Pa·s), v is the machine speed (m/s), a is the radius of filler or fines particles (m), $\overline{\mathrm{Sh_f}}$ is the Sherwood number averaged over the whole fibre surface (dimensionless deposition rate per unit length of fibre). When the thick stock flow rate is increased keeping the headbox flow rate constant, the number concentration of fibres in pulp suspension is increased, resulting in an improved filler retention.

The increased fibre concentration can also lead to the improved deposition of filler or fines particles in the pipeline and in the headbox. The collision frequency (in turbulent flow) can be calculated with [100]:

$$N_{12} = 1.294(a_1 + a_2)^3(\varepsilon/\nu)^{(1/2)} n_1 n_2 \tag{3.14}$$

where N_{12} represents the collision frequency between species 1 and 2 ($\mathrm{m}^{-3}\cdot\mathrm{s}^{-1}$), a_1, a_2 the particle radii (m), ε the energy dissipation per unit mass per unit time ($\mathrm{m}^2/\mathrm{s}^3$), the kinematic viscosity (m^2/s) and n_1, n_2 the number concentrations (m^{-3}); $(\varepsilon/\nu)^{(1/2)}$ represents the average shear rate. The number of collision is proportional to the number of fibre and filler (for a given furnish and shear). The collision frequency between fibres and fillers increases with increasing the concentration of fibre in the furnish, which increases the chances for filler particles to deposit on fibre surface.

3.5.5 Implications for the retention control

Filler retention is strongly influenced by the deposition efficiency. According to the equation 3.6, the deposition efficiency is a function of the surface coverage of fibres by polymer ($\theta_{i,F}$ and $\theta_{i,D}$), the surface coverage of fillers by fresh polymer ($\theta_{j,F}$) and by transferred polymer ($\theta_{j,T}$), and the surface coverage of microparticles on the polymer adsorbed fibre surface (μ_i). Due to its fast kinetics, the polymer injected into the furnish preferentially adsorbs on the fibre surface. Polymer transfer then occurs by filler deposition and detachment. Generally, 1 mg/g of polymer is considered to form a monolayer on the fibre surface. In paper mills, less than 0.5 mg/g of polymer is normally applied: the surface coverage of filler by fresh polymer ($\theta_{j,F}$) can be considered as zero. In addition, it is difficult to measure and to control the amount of the transferred polymer onto filler surface ($\theta_{j,T}$). The surface coverage of fillers by transferred polymer ($\theta_{j,T}$) is a function of the surface coverage of fibres by polymer (θ_i). Consequently, manipulating the surface coverage of fibre by polymer (θ_i) and the surface coverage of microparticles on the polymer adsorbed on the fibre surface (μ_i) is the best strategy to control deposition efficiency and consequently filler retention. The most important variables affecting the deposition efficiency and consequently the filler retention are the concentration of CPAM, followed by the dosage of bentonite.

The fibre concentration and the initial filler concentration did not affect the filler retention significantly. Thus, monitoring only the first-pass retention of filler has a limitation. When disturbances take place in the thick stock flow or in the filler flow, the variations in the first-pass retention might not be detected due to the small magnitude of the variations, while it will create large variations in the white water total and filler consistencies as well as in the headbox total and filler consistencies.

This implies that the headbox consistency and the white water consistency must be monitored and controlled separately.

3.6 Chapter summary

A deposition efficiency model relating filler retention to the dosages of retention aids was developed. The model includes the effect of bimodal particles and the polymer transfer from fibre to filler. The increase in the deposition efficiency leads to the increase in the filler retention. The most predominant variables affecting deposition efficiency/filler retention are the dosage of CPAM, followed by the concentration of bentonite. The fast kinetics of polymer adsorption onto fibres and polymer transfer, caused by filler deposition/detachment, govern the deposition efficiency and the filler retention. The pulp mass flow and the filler addition are secondary variables. Consequently, the surface coverage of fibre by polymer (θ_i) and that by microparticles (μ_i) are the two independent input variables to control filler retention.

Chapter 4

Parameters affecting Formation

4.1 Introduction

During a control of the retention process, formation is also affected by the control actions. The challenge is to control the retention process without deteriorating formation. We first need to understand the effect of process variables on formation and subsequently need to develop model to predict formation as a function of those variables. Several researchers have investigated the factors affecting formation. The main factor affecting formation is fibre flocculation [30]. Basis weight [28, 31, 32] and ash content of paper [33] also influence formation.

When chemical flocculants are used to improve the first-pass retention of fines and fillers, the increased retention often results in an impaired formation since retention aids also induce fibre flocculation [30]. Retention aids increase the bond strength at the fibre-fibre contact points [101]. Using microparticles provides a higher fibre network strength than using polymer alone [101,102]. Swerin et al. [89]

developed a model for the flocculation efficiency, which takes into account the surface coverage of polymer and microparticle on the fibre surface, based on interactions between two equal sized particles. However, the effect of the interaction between bare fibre surfaces and the differences in the bond strength of each interaction were not included in the model. Another shortcoming is that the model is based on two fibre collisions. However, fibre flocculation proceeds by mechanical entrapment and not by two fibres joining a doublet.

The objective of this chapter is to elucidate the effect of process parameters on formation using a pilot paper machine and a microparticulate retention aid system. The working hypotheses were that the main factors affecting formation is the fibre floc strength and that the floc strength is influenced by two main factors: 1) a number of contacts between fibres in the headbox; and 2) the bond strength at each contact. The variables of interest were: headbox pulp consistency, headbox filler concentration, CPAM dosage and bentonite dosage. The effects of basis weight and ash content of paper on formation were also investigated. The effect of shear was not included in this study because the shear of the pilot paper machine is quite low compared to an industrial paper machine due to an open headbox and a low machine speed of less than 90 m/min.

The bridging strength model relating dosages of polymer and microparticles to fibre flocculation and paper formation is presented in Section 4.2. The experimental section follows in Section 4.3. The results of changes in paper formation are presented as a function of dosages of retention aids, headbox pulp consistency and paper ash content in Section 4.4. The main parameters affecting formation and the implications for wet end control are discussed in Section 4.5.

4.2 Bridging strength

Chemical flocculants, consisting of a cationic polymer and a microparticle, provide sticky sites on fibre surfaces and hence increase the bond strength at the fibre-fibre contacts [101]. When the dosages of retention aids are varied, the surface coverage of polymer and microparticles will be changed and hence the area of sticky sites on fibre surface will vary as well. The more sticky sites exist, the higher the bridging strength between fibres, which would lead to higher degree of fibre flocculation and hence a poor formation.

The degree of flocculation is determined by how easily a single fibre can be entrapped inside a floc and how easily a fibre can escape from a floc. Hence, the interactions between a single fibre (A) and the neighbouring fibres (B) in a fibre network are considered. When a microparticulate retention aid system is used, fibre surfaces in a floc can be divided into three parts: 1) bare or naked surfaces (n); 2) polymer covered surfaces (p); and 3) bentonite covered surfaces on polymer covered surfaces (m). It was assumed that bentonite deposits only on polymer covered sites, not on the naked fibre surface. Nine possible interactions then exist between a single fibre, A, and neighbouring fibres in a floc, B. Each interaction has a different bond strength. Hence the overall bridging strength, S_b, can be defined as:

$$S_b = a_1(n_A : n_B) + a_2(n_A : p_B) + a_3(n_A : m_B) + a_4(p_A : n_B) + a_5(p_A : p_B) + a_6(p_A : m_B) + a_7(m_A : n_B) + a_8(m_A : p_B) + a_9(m_A : m_B) \quad (4.1)$$

where a_k ($k = 1 \ldots 9$) are the weighting factors of each possible interactions, which are related to the bond strength. Let us set the weighting factor for the strongest interaction to one and that of the weakest to zero ($0 \leq a_k \leq 1$). Also, let us define that the surface coverage of polymer on a single fibre is θ_A, that on the neighbouring

fibres θ_B, the surface coverage of microparticles on the polymer covered sites on a single fibre μ_A and that on the neighbouring fibres μ_B. To simplify the model, the follows were assumed:

- The interactions between the polymer covered surfaces $(p : p)$, between the bentonite covered surfaces $(m : m)$ and between the bentonite covered surface and the naked fibre surface $(m : n)$ are so weak due to electrostatic repulsion that the interactions can be negligible $(a_3 = a_5 = a_7 = a_9 = 0)$ [30, 94, 103];
- The interaction between a polymer covered site and a bentonite covered site forms the strongest bond $(a_6 = a_8 = 1)$ [94];
- Polymer molecules uniformly deposit on a fibre and the neighbouring fibres in a floc. Then, $\theta_i = \theta_A = \theta_B$; and
- Microparticles randomly deposit on the polymer covered sites $(\mu_i = \mu_A = \mu_B)$.

Let us define α_{inh} as the relative bond strength of the interaction between the naked surfaces compared to that of the microparticle bridge, i.e. $\alpha_{inh} = a_1$, and α_{pol} as the relative bond strength of the polymer bridge to the microparticle bridge, i.e. $\alpha_{pol} = a_2 = a_4$. The fraction of naked sites can be expressed as $(1-\theta_i)$; the polymer covered sites without bentonite $\theta_i(1-\mu_i)$; and the fraction of the bentonite covered sites $\theta_i\mu_i$. Assuming that the probability of having interactions between each site is proportional to the area or fraction of each site, the equation (4.1) becomes:

$$S_b = \alpha_{inh}(1-\theta_i)^2 + 2\,\alpha_{pol}\theta_i(1-\theta_i)(1-\mu_i) + 2\,\theta_i^2\mu_i(1-\mu_i) \tag{4.2}$$

The first part of the equation 4.2 expresses the inherent interaction between naked fibre surfaces; the second part is for the polymer bridging; and third part is for the microparticle bridging.

4.3 Experimental

Experiments were performed on a pilot paper machine (Centre Spécialisé en Pâtes et Papiers, CEGEP in Trois-Rivières). The materials used and the injection points of each materials are presented in Chapter 3

To investigate the effect of process parameters on formation, step changes were applied to the flow rates of the thick stock, the recirculating white water, the filler suspension, and the CPAM and bentonite solutions. Only one variable was changed at a time. The formation index of paper was measured by an on-line sensor (ABB) at the dry end. When the system reached steady state, data were sampled and averaged. In the ABB formation sensor, the formation index is expressed in terms of ROD (relative optical density), which is the root mean square (RMS) value of the instantaneous difference in the optical densities from two different measurement sizes: 30 mm and 1 mm in diameter. A higher ROD value indicates poorer formation.

4.4 Results

Bump test perturbations were created in the wet end of the pilot paper machine and the formation index (ROD) was measured. The variables of interests were: (i) the CPAM dosage (ii) the bentonite dosage, (iii) the basis weight of paper, (iv) the headbox pulp consistency and (v) the ash content of paper.

Figures 4.1 and 4.2 show the influence of CPAM and bentonite dosages on the formation index (ROD). To test the effect of CPAM and bentonite concentration, the thick stock flow kept constant (headbox pulp consistency was 0.5 % and thick stock filler content was 17 %). There was no additional filler added. At a bentonite

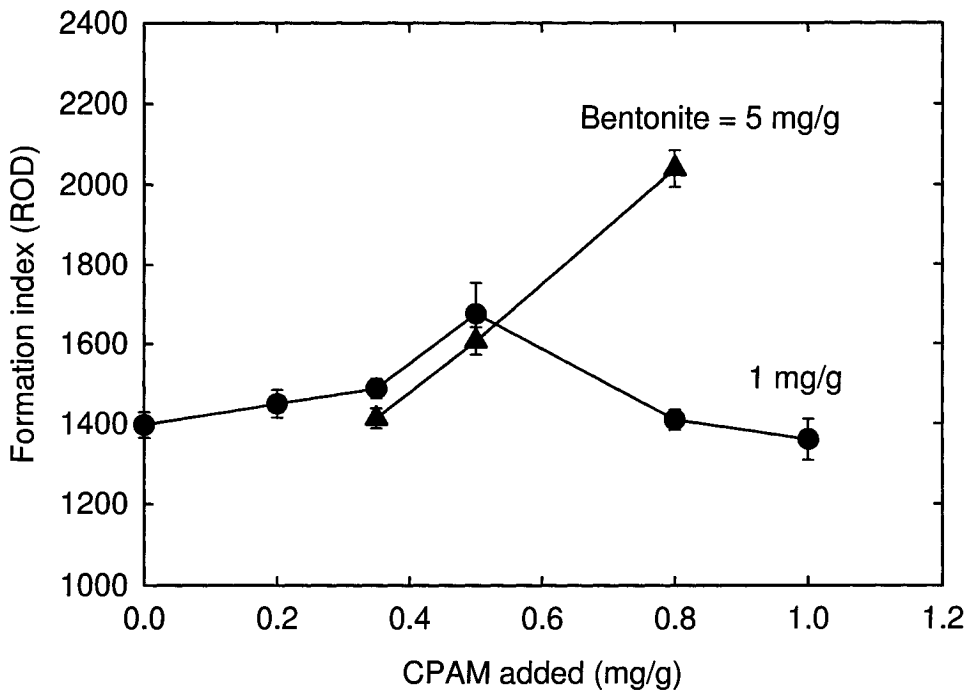

Figure 4.1. Effect of the CPAM dosage on formation for two bentonite dosages shown in the figure.

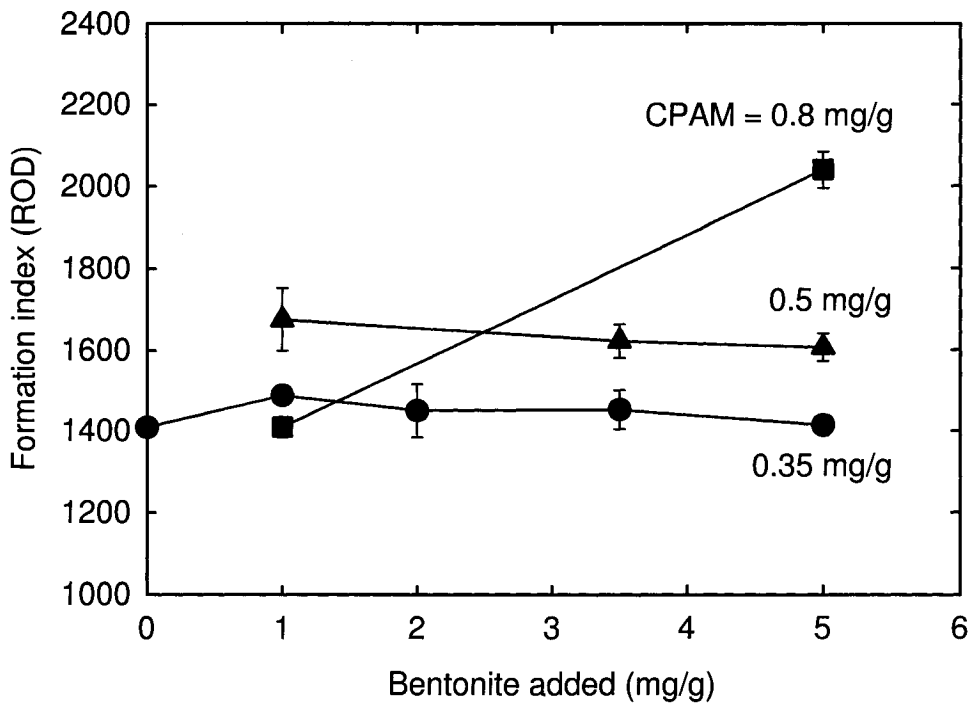

Figure 4.2. Effect of the bentonite dosage on formation for various CPAM dosages shown in the figure.

dosage of 1 mg/g, the formation index initially increased (i.e. formation become poorer) with CPAM and then passed through a maximum at around 0.5 mg/g. At a higher bentonite dosage (5 mg/g), the formation index kept increasing with CPAM, even at 0.8 mg/g of CPAM. The effect of bentonite on formation is less significant than CPAM (Figure 4.2), except at 0.8 mg/g of CPAM. At a CPAM dosage of 0.35 mg/g, the formation index (ROD) initially increased with increasing bentonite concentration and then slightly decreased after 1 mg/g of bentonite. At a CPAM dosage of 0.5 mg/g, the formation index also slightly decreased with bentonite. However, the formation index significantly increased with increasing bentonite dosage at CPAM 0.8 mg/g.

Figure 4.3 shows the effect of the basis weight and the headbox pulp consistency on formation. The numbers in brackets are the basis weight (g/m^2) and the ash content (%) of paper, respectively. The basis weight of paper was manipulated by varying the thick stock flow rate (lines A and C in Figure 4.3). As a result, the headbox pulp consistency was varied at the same time. The formation index slightly increased when the basis weight increased. Also, formation deteriorated when the headbox pulp consistency was increased. The effect of headbox pulp consistency was clearly shown when the white water flow rate was manipulated (line B). When the white water flow rate was decreased while keeping thick stock flow constant, the headbox pulp consistency was increased whereas the basis weight and the ash content of the paper remained unchanged. In this case, the formation index drastically increased with increasing the headbox pulp consistency. Furthermore, increasing the ash content of paper improved the formation (Figure 4.4). The ash content was increased by adding more filler at the fan pump. On the contrary, the formation index increased when ash content was increased by retention aids, keeping the headbox filler concentration constant (Figure 4.5). The mixture of HwBKP and

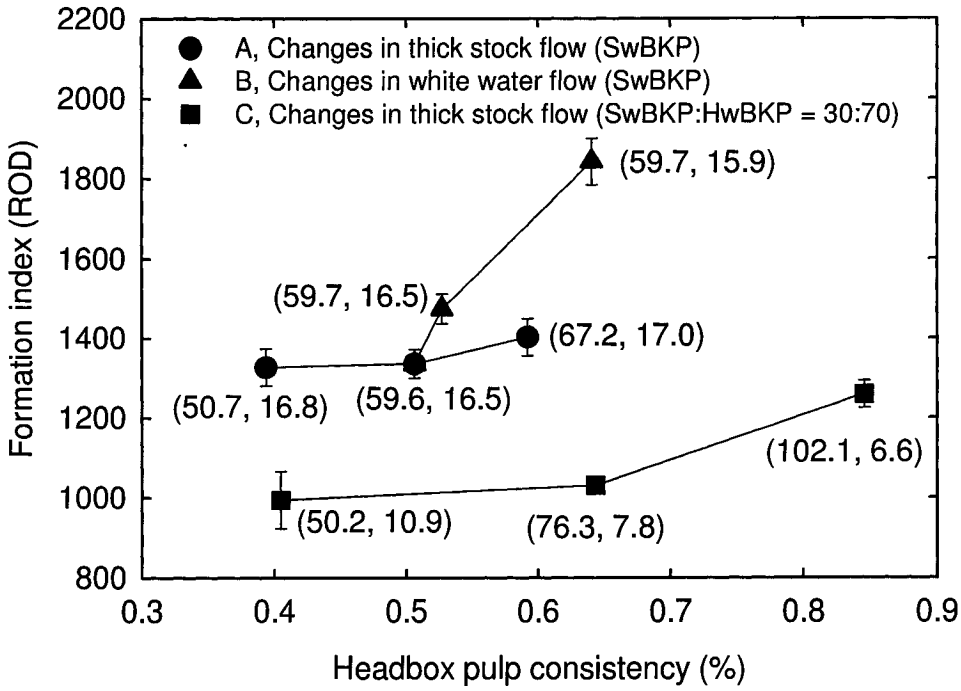

Figure 4.3. Effect of basis weight and fibre consistency on formation caused by a change in the thick stock and the white water flow rates. The number in brackets are basis weight (g/m^2) and ash content(%), respectively.

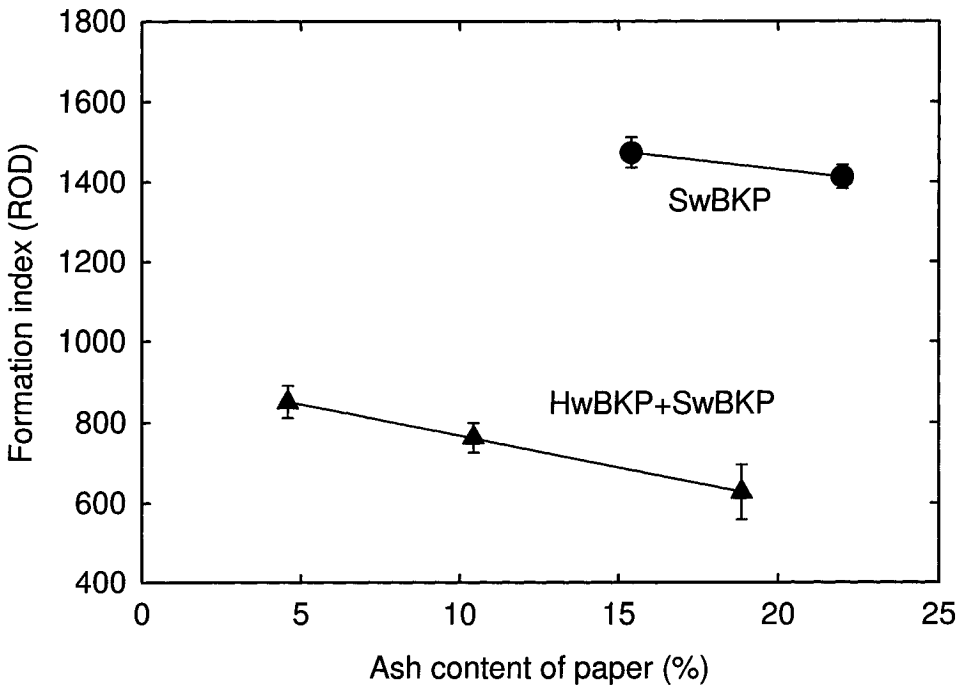

Figure 4.4. Effect of the ash content of paper on formation for two different furnishes. Ash content was varied by varying the filler concentration in the headbox.

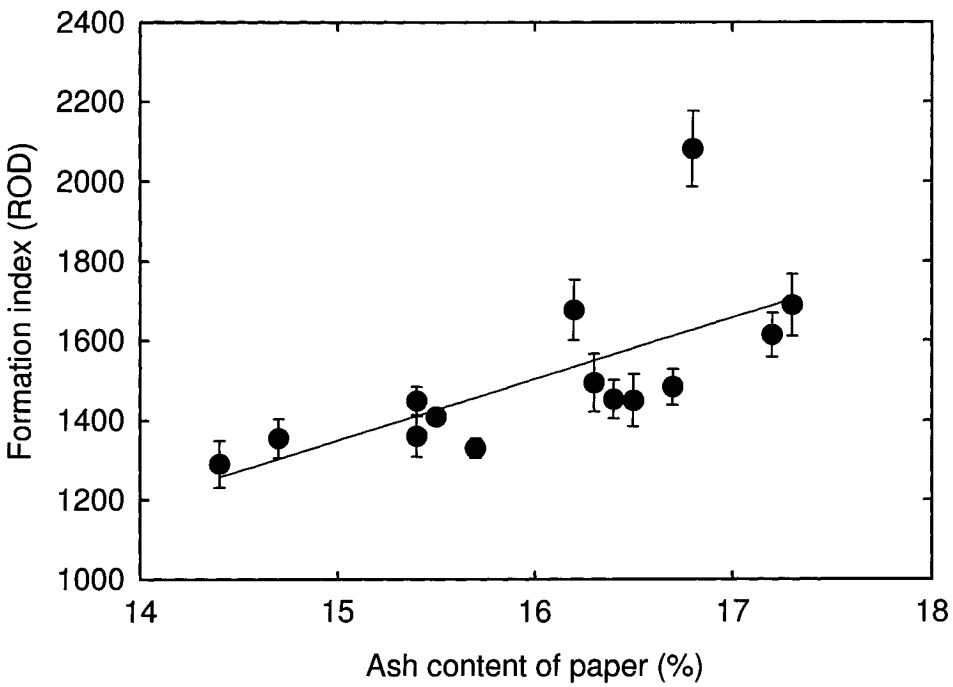

Figure 4.5. Effect of the ash content of paper on formation. Ash content was varied by retention aids, keeping the headbox filler concentration constant.

SwBKP showed better formation than 100 % softwood pulp furnish (Figures 4.3 and 4.4). The major difference between the two furnishes is the mean fibre length: 1.10 mm for a mixture of HwBKP and SwBKP and 1.88 mm for 100 % SwBKP (length weighted mean fibre length, measured by the Kajaani tester). Clearly the fibre length is the dominant variable affecting formation, followed by the headbox pulp consistency, the dosages of retention aids and the ash content of paper.

4.5 Discussion

4.5.1 Effect of bridging strength

Retention aids provide sticky sites on fibre surfaces, which could affect fibre flocculation and then formation. When the dosages of retention aids are changed, the surface coverage of polymer and bentonite are varied and hence the area of sticky sites on the fibres. Hence, the effect of the dosages of retention aids on formation can be analyzed in terms of the bridging strength. To calculate the bridging strength, the following values were used: the specific surface area of fibre = 1 m^2/g and the maximum coverage by CPAM = 1 mg/m^2 and bentonite = 12.5 mg/m^2 (5 stacks of montmorillonite plates were assumed [98]).

If $\alpha_{inh} = 0$ and $\alpha_{pol} = 1$ (i.e., the bond strength of microparticle bridge and that of polymer bridge are same), the equation 4.2 becomes same as the model by Swerin et al. [89]. The calculated results using Swerin's model at 1 mg/g of bentonite are shown in Figure 4.6 ($\alpha_{inh} = 0$). The results show that the bridging strength is zero for CPAM dosages less than 0.08 mg/g; this is because at these dosages all CPAM is covered by bentonite. It can be seen that the bridging strength passes through a maximum around 0.55 mg/g of CPAM and the bridging strength at 1 mg/g is

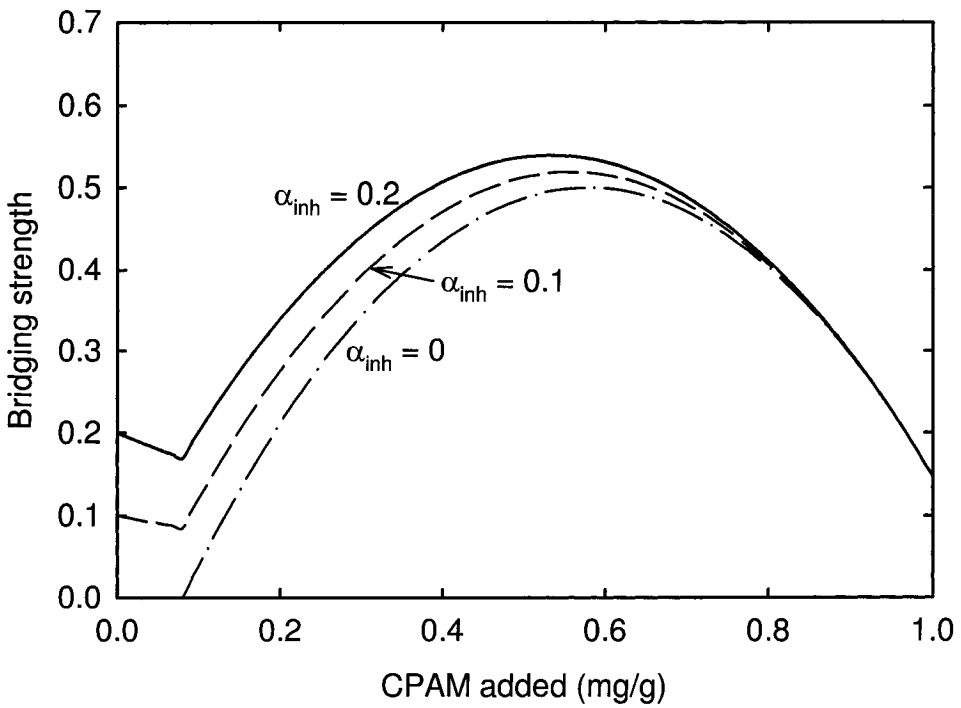

Figure 4.6. Effect of the relative bond strength α_{inh} (between naked fibre surfaces) on the bridging strength. Bentonite dosage = 1 mg/g and $\alpha_{pol} = 1$.

higher than that at 0 mg/g. However, experiments showed that the formation index at 0 mg/g is slightly higher than at 1 mg/g of CPAM (Figure 4.1, Bentonite 1mg/g). We know that fibres can flocculate without a flocculant due to mechanical entanglement. Klingenberg et al. [104, 105] found that friction between naked fibre surfaces is an essential element in mechanical entanglement of fibres and that polyelectrolytes cause strong steric repulsion at high surface coverage, prohibiting fibre flocculation. Also Swerin et al. [106] showed that the average floc diameter at high polymer dosage is smaller than that without polymer. These observations suggest that the interaction between naked fibre surfaces should not be ignored ($\alpha_{inh} \neq 0$). When $\alpha_{inh} > 0$, trends in the bridging strength (Figure 4.6) become similar to those seen in experiments (Figure 4.1, bentonite 1 mg/g): the bridging strength at a CPAM dosage of 0 mg/g has a similar value as that at 1 mg/g. For the rest of the discussion, the value of α_{inh} used was 0.2.

Figure 4.7 shows the effect of α_{pol} on the bridging strength at a bentonite dosage of 1 mg/g. The value of α_{pol} determines the maximum value of the bridging strength: the higher α_{pol}, the higher the maximum. When $\alpha_{pol} < \alpha_{inh}$ (i.e. $\alpha_{pol} < 0.2$), the bridging strength at a CPAM dosage of 0.5 mg/g is less than that at 0 mg/g, which is different from what we have seen in experiments (compare Figures 4.1 and 4.7). When $0.3 \leq \alpha_{pol} \leq 1$, the model gives similar trends as the experimental results: a maximum around CPAM 0.5 mg/g. This confirms that the interaction by a polymer bridge is stronger that between naked fibre surfaces (i.e., $\alpha_{pol} > \alpha_{inh}$). Swerin et al. [101, 106] showed that the maximum value of the flocculation index for fibres by CPAM-bentonite retention aids is about twice as high than that by CPAM alone, when the CPAM dosage was increased. This can be understood if microparticle bridging provides a stronger bond than polymer bridging. The exact value of α_{pol} is not known, but it is clear that $\alpha_{inh} < \alpha_{pol} < 1$. For the

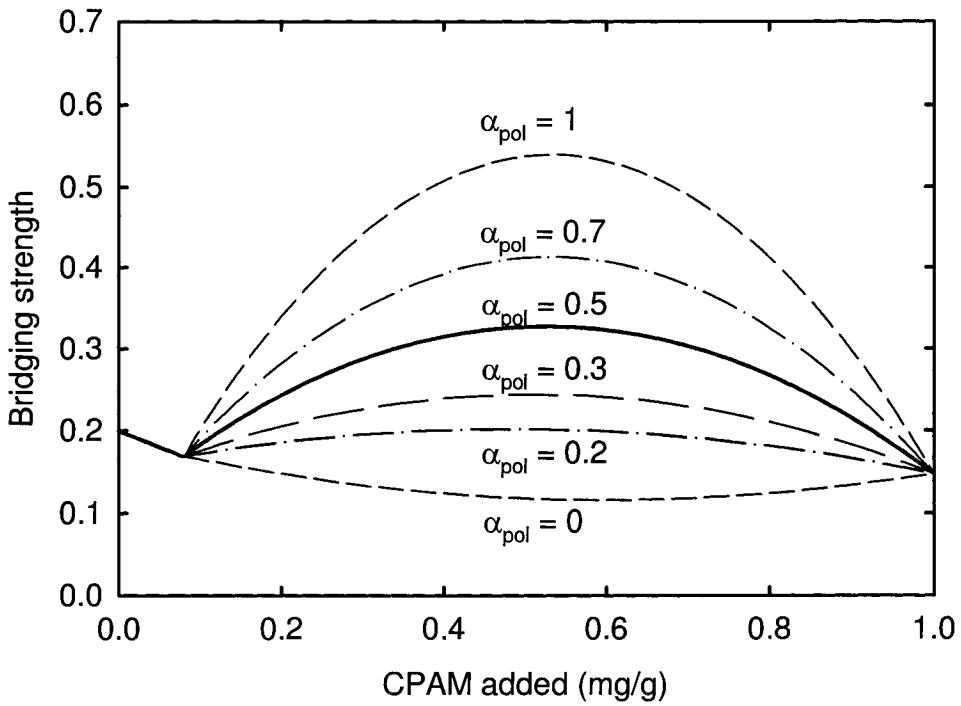

Figure 4.7. Effect of the relative bond strength α_{pol} (for polymer bridging) on the bridging strength. Bentonite dosage = 1 mg/g and α_{inh} = 0.2.

rest of the discussion, it was assumed that $\alpha_{pol} = 0.5$.

For a CPAM dosage of 0.08 mg/g, assuming all CPAM adsorbs onto the fibres, the bentonite dosage to just cover all the polymer covered sites is 1 mg/g. Thus the initial decrease in the bridging strength in Figures 4.6 and 4.7, when the CPAM dosage is less than 0.08 mg/g, is due to the decrease in the interaction between naked fibre surfaces. When the CPAM dosage increased further, the polymer covered sites without bentonite $\theta_i(1 - \mu_i)$ increase, resulting in the increase in the interaction between polymer covered sites and microparticle particle covered sites. The bridging strength due to polymer bridging passes though a maximum at a CPAM dosage of 0.55 mg/g. After 0.55 mg/g of CPAM, the fractional area of the naked surface $(1 - \theta_i)$ decreases, providing more interactions between polymer covered surfaces $(\theta_i : \theta_i)$, which are very weak. This results in the decrease in the bridging strength (Figure 4.7) and as a result the formation index (Figure 4.1).

With a higher dosage of bentonite (5 mg/g), the bridging strength keeps increasing even at high polymer dosages (Figure 4.8), which results in a deterioration of the formation (Figure 4.1). For a CPAM dosage of 0.4 mg/g, assuming all CPAM adsorbs onto the fibres, the bentonite dosage to just cover all the polymer is 5 mg/g. When the polymer dosage increases over 0.4 mg/g, the polymer covered sites without bentonite $\theta_i(1 - \mu_i)$ increase. Consequently, the interaction between naked surfaces continuously decreases; the bridging strength due to polymer bridging passes through a maximum at 0.7 mg/g of CPAM; more polymer covered sites interact with bentonite covered sites, resulting in an increase in the bridging strength (Figure 4.8).

Figure 4.9 shows the effect of bentonite on the bridging strength. For the calculation, it was assumed that $\alpha_{inh} = 0.2$ and $\alpha_{pol} = 0.5$. At CPAM dosages of 0.35 and 0.5 mg/g, the bridging strength decreases with an increase in the bentonite

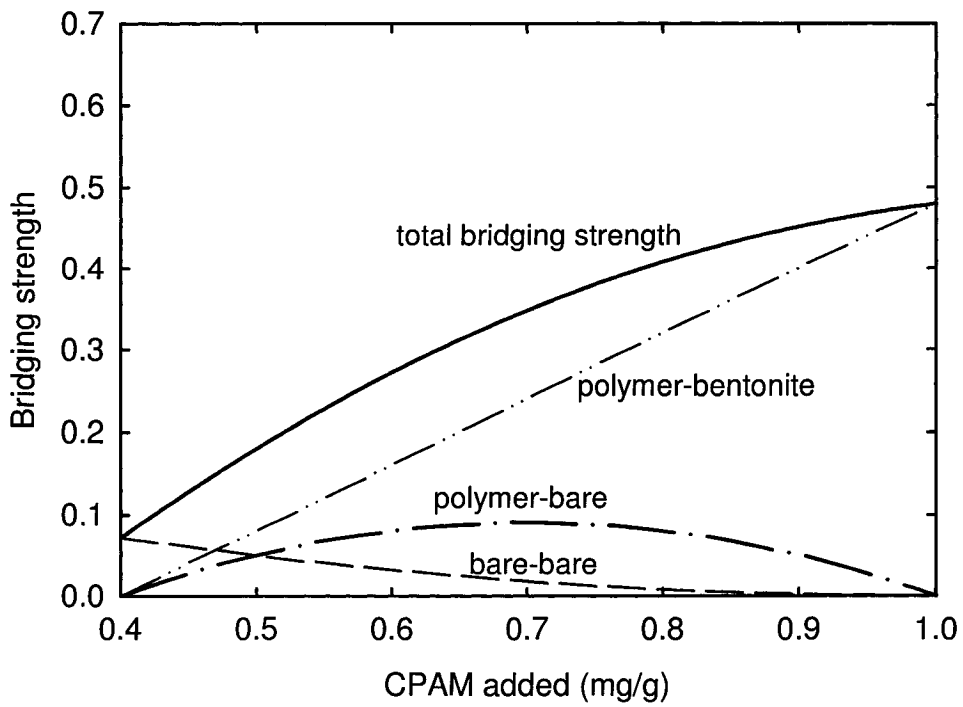

Figure 4.8. Effect of the CPAM dosage on the bridging strength. Bentonite dosage = 5 mg/g, $\alpha_{inh} = 0.2$ and $\alpha_{pol} = 0.5$.

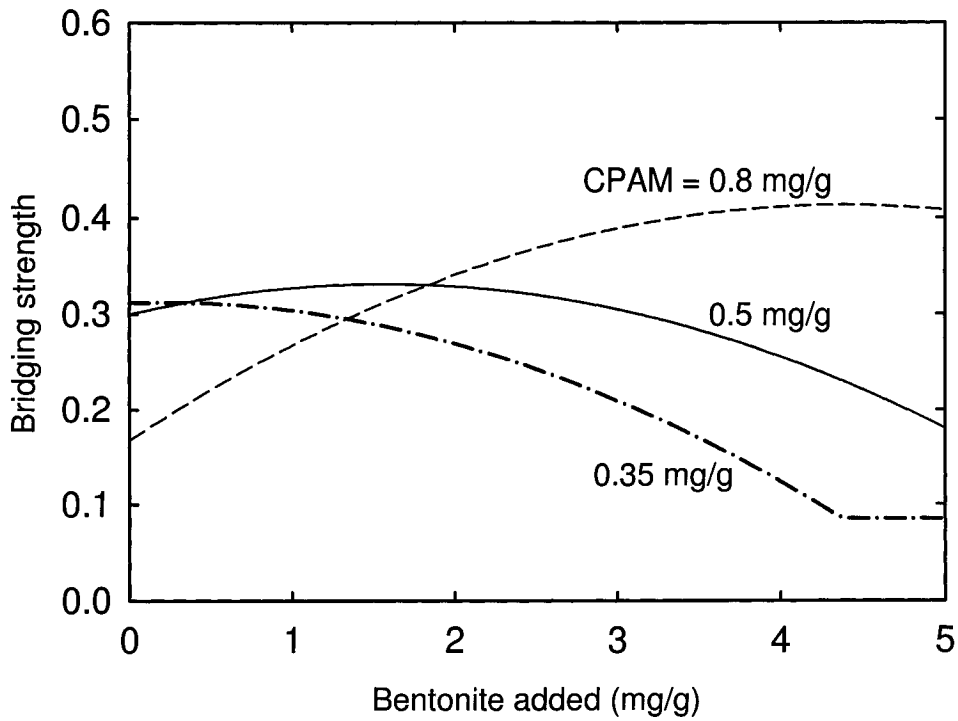

Figure 4.9. Effect of the bentonite dosage on the bridging strength for various CPAM dosages indicated in the figure. $\alpha_{inh} = 0.2$ and $\alpha_{pol} = 0.5$.

dosage. This is mainly due to the decrease in the interaction between naked fibre surfaces and polymer covered sites. Since the CPAM dosage remained constant, the surface coverage of polymer (θ_i) and the fractional area of the naked fibre surface ($1-\theta_i$) remained unchanged: the fraction of the naked surface is 0.65 at 0.35 mg/g of CPAM and 0.5 at 0.5 mg/g. Increasing the bentonite dosage decreases the bentonite-free polymer sites on fibres ($\theta_i(1-\mu_i)$), thus decreasing the interactions by polymer bridging. The bridging strength due to microparticle bridging passes through a maximum at a bentonite dosage of 2.25 mg/g (CPAM 0.35 mg/g) and at 3 mg/g (CPAM 0.5 mg/g). However, the interaction by bentonite bridging plays a minor role at 0.35 mg/g CPAM since more than half of the fibre surface is naked. The higher value of the bridging strength at a CPAM dosage of 0.5 mg/g than at 0.35 mg/g is due to higher microparticle bridging. At a CPAM dosage of 0.8 mg/g, most of the fibres are covered with polymer ($\theta_i = 0.8$). When the bentonite dosage is increased, the probability of having interactions between polymer covered sites and naked surfaces slightly decrease while there is a significant increase in interactions between polymer covered sites and bentonite covered sites, which contribute to the increase in the bridging strength. At a bentonite dosage of 5 mg/g, the surface coverage of bentonite on polymer covered sites is 0.5 ($\mu_i = 0.5$), which provides a maximum interaction by bentonite bridging. The simulated data of the bridging strength show the same trend as experiments (Figure 4.2): the formation index slightly decreased at CPAM 0.35 mg/g and 0.5 mg/g and increased at CPAM 0.8 mg/g.

The above discussion clearly shows that the effect of retention aids on formation can be explained with the bridging strength model. An increase in the bridging strength provides a higher fibre floc strength, resulting in impaired formation. Also, when microparticles cover all of polymer covered fibre surfaces (i.e. $\mu_i = 1$), the

bridging strength is minimized at a given polymer dosage.

4.5.2 Effect of basis weight and headbox pulp consistency

Two opposite arguments exist for the effect of basis weight on formation. According to Norman [28], increased basis weight leads to improved formation due to the smoothing effect of increased dewatering in low-resistance areas. Nordström and Norman [36] showed that formation improved with increasing basis weight in the low basis weight range ($30 \sim 45$ g/m^2) in twin wire roll forming. Sampson et al. [107] pointed out that the smoothing phenomenon exists and that for a given crowding number formation improves with increasing basis weight while formation deteriorates with increasing crowding number at a given basis weight ($0.5 \leq N_{crowd} \leq 25$ and $5 \leq$ basis weight ≤ 60). On the contrary, Winters et al. [32] showed that an increase in basis weight as a result of increasing the headbox pulp consistency deteriorates formation and that the formation index of the sheets made from stocks at the same concentration remained constant from 40 to 120 g/m^2. Our results showed that increasing the basis weight deteriorated formation (Figure 4.3). The basis weight was varied by manipulating the thick stock flow rate, keeping the headbox stock flow rate constant. Hence an increase in basis weight accompanied an increase in the thick stock pulp consistency. From our results, it is difficult to conclude which argument is right. However, from a control perspective, the set point of basis weight is decided for a given grade. Typically, the basis weight is controlled by manipulating the thick stock flow valve. The variation in thick stock flow normally results in the variation of headbox pulp consistency. Hence, for the purpose of formation control, we need to focus on the headbox pulp consistency.

When the headbox pulp consistency is increased by the thick stock flow from

0.39 to 0.59 % (SwBKP) and from 0.4 to 0.85 % (HwBKP+SwBKP), the bridging strength is slightly decreased from 0.31 to 0.29 (SwBKP) and from 0.29 to 0.20 (HwBKP+SwBKP), while the formation index was increased (Figure 4.3). Increasing fibre consistency leads to more fibre-fibre contact points and thus a higher flocculation tendency [108]. Also increasing the fibre length decreases the mass uniformity by increasing the number of fibre contacts and the floc size [109]. The effect of both variables can be expressed in terms of the crowding number, which is defined as the number of fibres in a spherical volume of diameter equal to the mean fibre length [35, 107]:

$$N_{crowd} = \frac{2}{3} C_v \left(\frac{L}{d}\right)^2 = \frac{\pi}{6} C_m \frac{L^2}{\delta} \tag{4.3}$$

where C_v stands for the volume concentration of fibres, C_m the mass concentration of fibres, L fibre length, d mean fibre diameter and δ fibre coarseness. To calculate the crowding number, the following values were used: for a mixture of HwBKP and SwBKP, length weighted average length (L) = 1.10 mm and coarseness (δ) = 0.117 mg/m; and, for SwBKP, L = 1.88 mm and δ = 0.149 mg/m. Data in Figure 4.3 were used to calculate the crowding number. Figure 4.10 clearly shows that an increase in crowding number leads to an increase in the formation index. A larger crowding number means that more contacts between fibres are present in a given volume. The effect of the decreased bridging strength was not noticeable due to the small changes relative to the changes in contact number.

4.5.3 Effect of the filler content of paper and headbox filler concentration

An improvement of formation by an increase in the ash content of paper (Figure 4.4) can be explained by two possible reasons. First, it is generally believed that, when

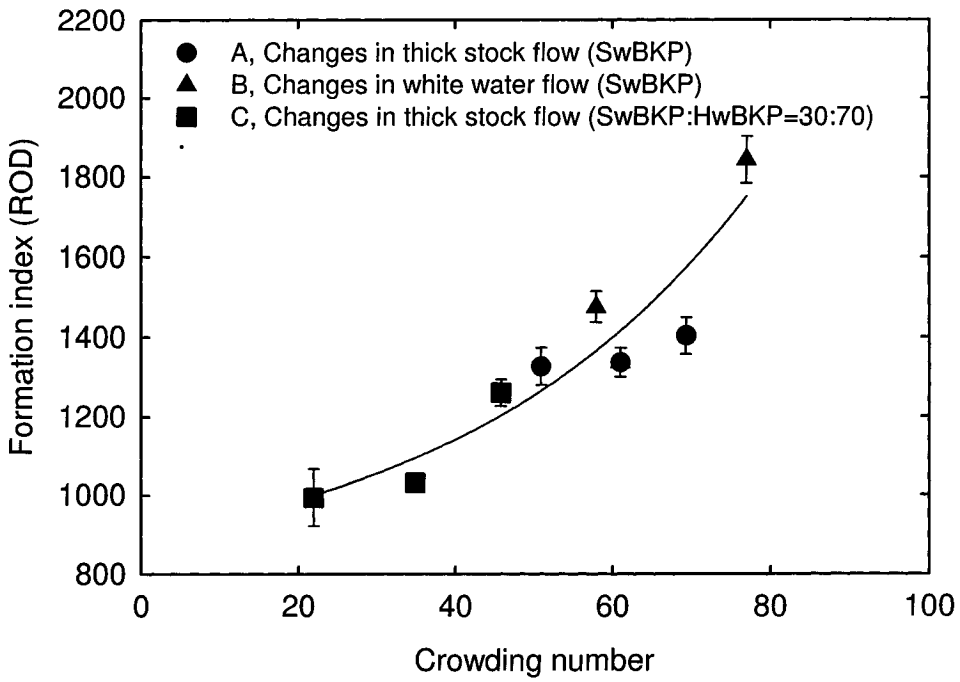

Figure 4.10. Effect of the crowding number on formation.

the ash content of paper increases, filler particles can fill the voids in the fibre network, thus reducing the variation in the local basis weight [33]. Second, fillers in the fibre suspension decrease the fibre floc strength.

The first hypothesis is possibly true if filler is retained in the paper by mechanical entrapment in the fibre network. When retention aids are used, fillers are mostly retained in paper by the adsorption on the fibre surface [27], only when first-pass retention is high; otherwise, they can flocculate in the short circulation loop. It was shown that two formation spectra for a fine paper before and after extraction of 40 % filler pigment ($CaCO_3$) by HCl were practically identical [28]. This result suggests that the filler distribution in paper increases the variation in basis weight at approximately the same rate as the mean basis weight. In addition, the opposite effect was found when the ash content of paper was varied by retention aids, keeping the headbox filler concentration constant. Formation was deteriorated with increasing the ash content of paper (Figure 4.5). This is because retention aids increase the fibre floc strength as well as the filler retention. This result suggests that the increase in fibre flocculation has a more dominant influence on formation than the increased filler content of paper.

Swerin et al. explained that the decrease in fibre flocculation by filler is due to the competitive adsorption of CPAM on fibre and filler [102]. The more filler is present, the more polymer can adsorb on the filler surface. However, from the kinetic aspect, this is less likely. When polymer is added to a mixture of fibre and filler at high shear, most of the polymer will end up on the fibre surface due to faster collisions between fibre and polymer than between filler and polymer [76, 110].

Another possibility to consider is the polymer transfer from fibre to filler particles. Polymer transfer between two surfaces can occur during the deposition and the detachment of particles on fibre [92, 93]. During the break-up of the bond,

cleavage of polymer chains can also happen [111]. This creates transferred and depleted polymer layers on the originally bare and polymer covered surfaces, respectively [112]. The bridging ability of these layers is different from that of a fresh polymer layer. It was shown that the detachment rate of fines on depleted polymer layers with or without bentonite is higher than that of the fresh polymer layer [94]. This can be understood if a depleted polymer layer provides a weaker bond than the fresh polymer layer. The more filler added, the more depleted polymer layers are expected to exist. This could lead to a smaller bridging strength and thus a weaker fibre floc strength, resulting in improved formation.

4.5.4 Implications for the wet end control

The number of contacts between fibres in the wet end, which can be represented as the crowding number, is mainly influenced by the headbox fibre consistency and fibre dimension. The fibre dimension is affected by the type of pulp and refining degree, which can be considered as fixed factors. Hence, concerning formation control, we need to focus on keeping the headbox fibre consistency constant. The main factors affecting the bridging strength are the surface coverage of polymer on fibre surface and that of bentonite on the polymer covered fibre surfaces. When all of the polymer covered sites are covered with bentonite (i.e., $\mu_i = 1$), a minimum fibre flocculation can be obtained at a given polymer dosage, resulting in a best formation. Also, concerning formation control, we need to turn our attention to headbox filler concentration instead of the ash content of paper (filler fraction to fibre). Since filler affects fibre flocculation by transferring polymer from fibre surface, the concentration of fillers without (or less) polymer covered surface is more important than polymer coated fillers, which come from the recirculating white

water. The target filler addition (g/g of fibre) can be decided from the set points of the ash content of paper and the filler retention.

4.6 Chapter summary

Two main parameters in the wet end affecting formation are the number of contacts between fibres and the bond strength at the contacts, which influence the fibre floc strength (the overall bridging strength). To relate the dosages of retention aids to the fibre floc strength, the bridging strength model was developed based on interactions between a single fibre and neighbouring fibres in a fibre network. The bridging strength model, which is a function of the surface coverage of polymer and microparticles on fibre and relative bond strength of each interactions, explains the influence of the dosages of retention aids on formation fairly well. Based on this model, minimum fibre flocculation and best formation, for a given polymer dosage, can be achieved when bentonite covers all of the polymer covered sites on the fibre surface. The increased contact number between fibres provides stronger fibre floc strength and impairs formation. The crowding number, which is affected by fibre concentration and fibre dimensions, can be used to express the effect of the number of contacts between fibres. Filler concentration in the wet end is a more dominant factor than the filler content of paper. It is likely that increasing the filler concentration in the wet end increases polymer transfer from fibre to filler particles and leads to weaker fibre flocs, resulting in improved formation. The transfer of polymer from fibre to fillers is expected to also affect the filler retention, studied in Chapter 3.

Chapter 5

Dynamics of the Retention and Formation Processes

5.1 Introduction

Due to the complexity of the wet end process, black box approaches have been mostly used to model and to control the dynamics of a retention process [62–65,67]. The difficulty in modelling with first-principles has been to include the effects of wet end chemistry on the dynamics of solid concentrations in the wet end and the basis weight and the ash content of paper. Moreover, the dynamic modelling of formation has not been attempted yet.

The objectives of this chapter are to model and to elucidate the dynamics of the retention process and the formation of paper. The study was carried on in three steps. First, the models describing the dynamics of solid concentrations were developed from mass balances. The partition of the process colloid materials (filler and fines) was described in terms of first-pass retention to include the effects of wet end chemistry. An empirical approach was used to describe the first-pass retention and the formation of paper as a function of process variables. Second, the dynamics of headbox consistency, white water consistency, basis weight, ash content of paper

and formation were measured on a Fourdrinier pilot machine, by creating a series of bump type perturbations. The variables of interests include the polymer flow, the microparticle flow, the thick stock flow and the filler concentrations. Third, transfer functions describing the dynamics of concentrations of solids in the wet end and in paper were developed to elucidate which variables are the major factors affecting the dynamics of the retention process.

The details of the dynamic models describing the concentrations of solids in the wet end and in paper and the formation of paper are presented in Section 5.2. Experimental procedure follows in Section 5.3. The models were solved with MATLAB/SIMULINK and the experimental data are compared with the simulated data in Section 5.4. The main factors affecting the dynamics of the wet end of papermaking and implications for the wet end control are discussed in Section 5.5.

5.2 Dynamic modelling

5.2.1 Modelling of retention process

The mass balance technique was used to model the dynamics of material distribution in a paper machine. The paper machine was simplified, as shown in Figure 5.1, to highlight the short circulation loop of white water [113, 114]. The couch pit, savealls, machine chests, a screen and cleaners were omitted. The model is a three-fractional model, that handles fibre, fines and filler consistency. In the headbox and the white water tank, the mixing is assumed to be ideal, i.e. there is the same consistency everywhere in the volume.

Thick stock was assumed to consist of fibre, fines and filler. The consistences of

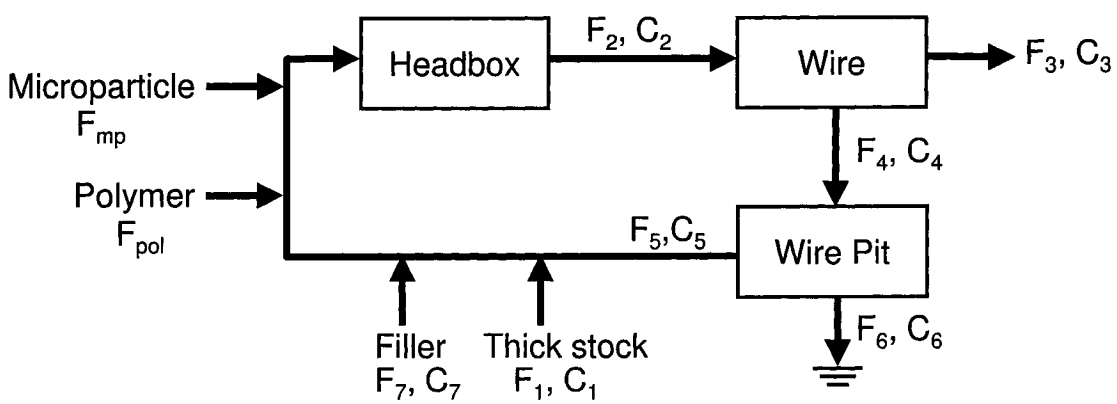

Figure 5.1. Block diagram for the wet end of a paper machine.

each solids are:

$$C_{1,filler} = C_{1,total}\phi_{1,filler}, \tag{5.1}$$

$$C_{1,fines} = C_{1,total}(1-\phi_{1,filler})\phi_{fines}, \tag{5.2}$$

$$C_{1,fibre} = C_{1,total}(1-\phi_{1,filler})(1-\phi_{fines}) , \tag{5.3}$$

where $C_{1,total}$ is the thick stock total consistency (g/L), $C_{1,i}$ (i = fines, filler and fibre) is the concentration of fines, filler and fibre in the thick stock, $\phi_{1,filler}$ is the filler fraction in the thick stock and ϕ_{fines} the fines fraction in the thick stock pulp. The dynamics of the headbox consistencies $C_{2,i}$ can be obtained from the mass balances around the headbox:

$$\frac{dC_{2,fibre}}{dt} = \frac{1}{V_{hb}}(F_1C_{1,fibre} + F_5C_{5,fibre}) - \frac{F_2}{V_{hb}}C_{2,fibre}, \tag{5.4}$$

$$\frac{dC_{2,fines}}{dt} = \frac{1}{V_{hb}}(F_1C_{1,fines} + F_5C_{5,fines}) - \frac{F_2}{V_{hb}}C_{2,fines}, \tag{5.5}$$

$$\frac{dC_{2,filler}}{dt} = \frac{1}{V_{hb}}(F_1C_{1,filler} + F_7C_{7,filler} + F_5C_{5,filler}) - \frac{F_2}{V_{hb}}C_{2,filler}, \tag{5.6}$$

where V_{hb} is the volume of the headbox (L) and F_j (j = 1, 2, 5 and 7) is the flow rate of each stream (L/min). The headbox total consistency (g/L) is then calculated with:

$$C_{2,total} = C_{2,fines} + C_{2,filler} + C_{2,fibre} \tag{5.7}$$

and the headbox ash content is:

$$C_{2,ash}(\%) = \frac{C_{2,filler} \times 100}{(C_{2,fines} + C_{2,filler} + C_{2,fibre})} . \tag{5.8}$$

The flow rate at the headbox (F_2) is controlled by the valve located just before the headbox. Hence, the flow rate of the recirculating white water is determined from the headbox flow rate and the flow rate of other input stream such as the thick stock flow and the filler flow:

$$F_5 = F_2 - (F_1 + F_7 + F_{pol} + F_{mp}) . \tag{5.9}$$

From the mass balance on the wire, the first-pass retention of solid materials R_i (i = fines, filler and fibre) is defined as the ratio of the mass of the solids in the wet web leaving the wire section to that in the stock entering the wire section (i.e., in the headbox):

$$R_i = \frac{F_3 C_{3,i}}{F_2 C_{2,i}} \tag{5.10}$$

where F_3 represents the flow rate of the wet web leaving wire section and F_2 is the flow rate of the stock entering the wire section from the headbox. Since $F_2 = F_4 + F_3$ and $F_4 \gg F_3$, we could assume that $F_4 = F_2$. Then, the consistencies of white water ($C_{4,i}$) from the white water tray under the wire to the wire pit can be calculated with:

$$C_{4,fibre} = (1 - R_{fibre}) C_{2,fibre} \frac{F_2}{F_4} = (1 - R_{fibre}) C_{2,fibre}, \tag{5.11}$$

$$C_{4,fines} = (1 - R_{fines}) C_{2,fines}, \tag{5.12}$$

$$C_{4,filler} = (1 - R_{filler}) C_{2,filler}. \tag{5.13}$$

The white water total consistency is then given by:

$$C_{4,total} = C_{4,fines} + C_{4,filler} + C_{4,fibre} \tag{5.14}$$

and the white water ash content by:

$$C_{4,ash}(\%) = \frac{C_{4,filler} \times 100}{(C_{4,fines} + C_{4,filler} + C_{4,fibre})}. \tag{5.15}$$

The dynamics of the recirculating white water consistency $C_{5,i}$ are obtained from

the mass balances around the wire pit:

$$\frac{dC_{5,fibre}}{dt} = \frac{F_4 C_{4,fibre}}{V_{wp}} - \frac{F_5 C_{5,fibre} + F_6 C_{6,fibre}}{V_{wp}}$$
$$= \frac{F_4 C_{4,fibre}}{V_{wp}} - \frac{F_4}{V_{wp}} C_{5,fibre} \quad (5.16)$$

$$\frac{dC_{5,fines}}{dt} = \frac{F_4 C_{4,fines}}{V_{wp}} - \frac{F_4}{V_{wp}} C_{5,fines} \quad (5.17)$$

$$\frac{dC_{5,filler}}{dt} = \frac{F_4 C_{4,filler}}{V_{wp}} - \frac{F_4}{V_{wp}} C_{5,filler} \quad (5.18)$$

where V_{wp} is the volume of the wire pit and F_4 is the flow rate of the white water from the white water tray to the wire pit. Assuming ideal mixing, $C_{5,i} = C_{6,i}$.

The mass flow rate of solid materials leaving the wire section can be calculated with:

$$F_3 C_{3,i} = R_i F_2 C_{2,i} \quad (i = \text{fines, filler and fibre}) \; . \quad (5.19)$$

The ash content of the web (Ash) leaving wire section is:

$$Ash(\%) = \frac{F_3 C_{3,filler} \times 100}{F_3 (C_{3,fibre} + C_{3,fines} + C_{3,filler})} \; . \quad (5.20)$$

Assuming that there is not any loss of solids at the press and the drying sections, this can be used to represent the ash content of paper. The basis weight of paper (BW) is:

$$BW(\text{g/m}^2) = \frac{F_3 (C_{3,fibre} + C_{3,fines} + C_{3,filler})}{ms \cdot W \cdot r_s} \quad (5.21)$$

where ms stands for the machine speed (m/min), W is the width of dry sheet after calendering (m) and r_s is the shrinkage rate of the wet web, which is defined as:

$$r_s = \frac{\text{width of dry sheet after calendering [m]}}{\text{width of wet web before pressing [m]}} \; . \quad (5.22)$$

It should be noted that the first-pass retention of solids (R_i) was included in equations (5.11), (5.12), (5.13) and (5.19). First-pass retention is significantly affected by wet end chemistry factors such as the type and the dosage of retention

aids, pH, cationic demand and conductivity. Hence, implementing the first-pass retention of solids into the dynamic models makes it possible to include the wet end chemistry effects on the dynamics of the output variables such as the white water consistency and the ash content of paper. The expression for first-pass retention can be developed by two approaches: a first-principles model and an empirical model. At this point no reliable theoretical model exists to predict first-pass retention from operating conditions. Thus, a simple, yet accurate way is still to perform a series of experiments and to obtain an empirical model for the first-pass retention. In this study, filler retention was measured and the empirical model was developed by nonlinear regression, which is expressed as a function of the mass flow rate of pulp, CPAM and bentonite and filler addition:

$$\begin{aligned} R_{filler} &= a_1 M_{pulp} + b_1 C_{filler} + c_1 M_{pol}^2 + c_2 M_{pol} + d_1 M_{mp}^2 + d_2 M_{mp} \\ &+ g_1 M_{pulp} M_{pol} + g_2 M_{pulp} M_{mp} + g_3 C_{filler} M_{pol} + g_4 M_{pol} M_{mp} + e \end{aligned} \tag{5.23}$$

where M_{pulp} is the mass flow rate of pulp in the thick stock (g/min), C_{filler} the filler addition (g of filler/g of pulp), M_{pol} the mass flow of polymer (g/min), M_{mp} the mass flow of microparticle (g/min), and a_1, b_1, c_i, d_i, g_i and e are constants. Each values are scaled to be in the range between 0 to 1. Figure 5.2 compares the predicted data and the experimental results of the filler retention. The predicted data showed a relatively good agreement with the experimental data ($R^2 = 0.84$). Since industrial paper machines are operated in a narrow operating constraints, this simple approach can be a feasible solution to include the wet end chemistry effects.

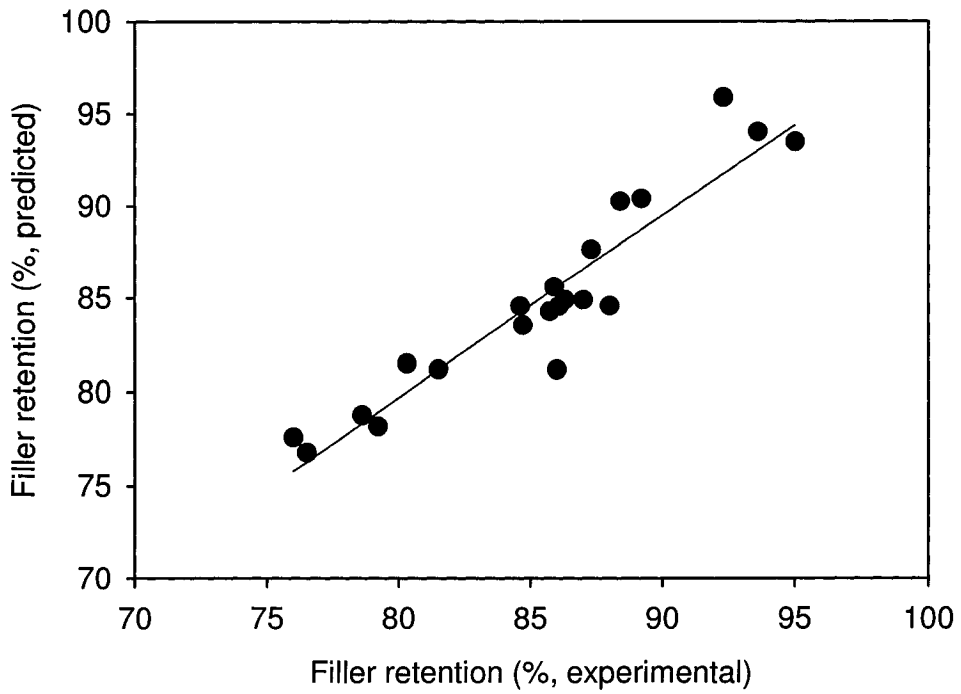

Figure 5.2. Comparison of the predicted and the experimental filler retention ($R^2 = 0.84$).

5.2.2 Modelling of formation

In Chapter 4, it was shown that formation of paper is mainly influenced by the crowding number (N_{crowd}), the bridging strength (S_b) and the filler concentration in the wet end, assuming that the type of furnish and retention aids are chosen before papermaking, that the basis weight and the ash content of paper are decided for a given grade and that the shear in the headbox and on the wire section are optimized for a given grade and for a given paper machine [115]. Thus, formation can be modeled as a function of those parameters. An empirical model was developed to predict formation index (ROD) [114]:

$$FI(\text{ROD}) = a_1 S_b^2 + a_2 S_b + b_1 e^{b_2 N_{crowd}} + c\, C_{filler} + d S_b N_{crowd} + e \qquad (5.24)$$

where a_i, b_i, c, d and e (i = 1 and 2) are constants. Crowding number N_{crowd} is obtained from the equation 4.3 and the fibre consistency C_m is calculated with the equation 5.4. The bridging strength is obtained with the equation 4.2. The equations for the calculation of the surface coverage of polymer and microparticle were shown in Table 3.1. The filler addition can be obtained from:

$$C_{filler} = \frac{M_{1,filler} + M_{7,filler}}{M_{1,pulp}} \qquad (5.25)$$

where $M_{1,filler}$ represents the mass flow rate of filler in the thick stock, $M_{7,filler}$ the mass flow rate of filler slurry and $M_{1,pulp}$ the mass flow rate of pulp in the thick stock. Figure 5.3 shows the comparison of the predicted and the experimental data. The predicted data showed decent agreement with the experimental data ($R^2 = 0.75$).

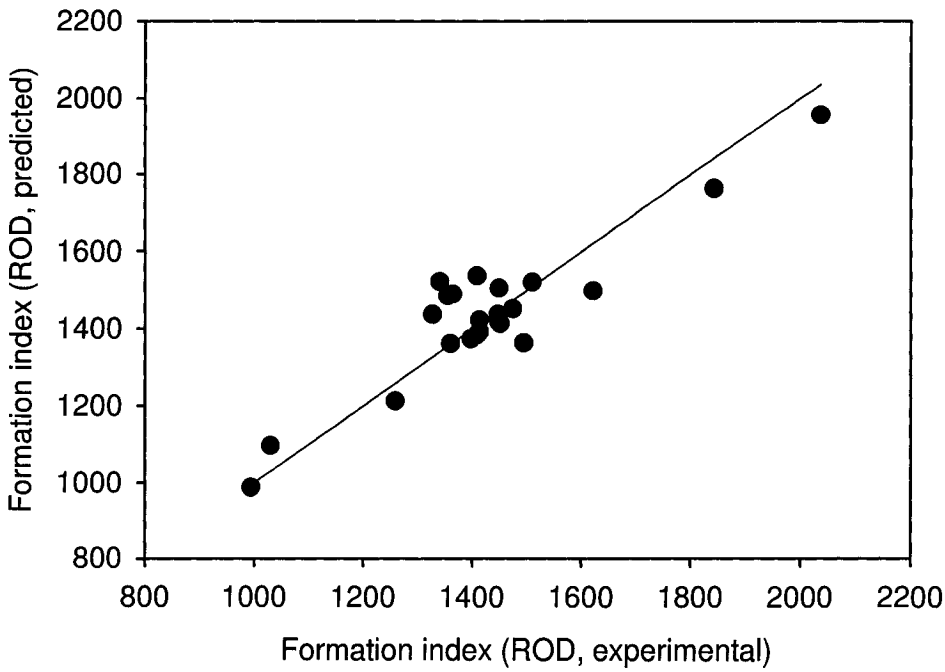

Figure 5.3. Comparison of the predicted and the experimental formation index ($R^2 = 0.75$).

5.3 Experimental

Experiments were performed on a pilot paper machine (Centre Spécialisé en Pâtes et Papiers, CEGEP in Trois-Rivières). The materials used and the injection points of each materials are presented in Chapter 3

To investigate the effect of the process variables on the dynamics of the wet end, step changes were applied to the CPAM dosage, the bentonite dosage, the fibre concentration, the initial filler concentration and the headbox flow rate. Only one variable was changed at a time.

For the experiments with a mixture of HwBKP and SwBKP, the dynamics of paper ash content were measured by an on-line sensor (ABB) after calendering. For the experiments with a SwBKP furnish, the dynamics of basis weight, ash content and formation were measured by on-line sensors (ABB) after calendering and headbox total and filler consistencies and white water total and filler consistencies were followed by Kajaani RMi sensors. The white water consistency sensor takes samples from the white water tray. Typically, basis weight is automatically controlled by regulating the thick stock valve located after the machine chest, and moisture content by steam pressure of driers. The control system of the pilot paper machine is ACCURAY 1190-ABB. However, in our experiments, the basis weight control loop was turned off.

5.4 Simulation

The dynamics of the wet end and the dry end were simulated by solving the nonlinear models presented in Section 5.2 using the MATLAB/SIMULINK software. The SIMULINK model is presented in Appendix A. For the simulation, the first-pass

retention of fibres was assumed to be unchanged by the perturbations: the value of 0.97 was used. Also, it was assumed that the first-pass retention of fines and fillers are identical ($R_{fines} = R_{filler}$).

Figure 5.4 shows the dynamics of the ash content of paper influenced by the polymer dosage, the bentonite dosage and the filler addition for a mixture of Hw-BKP and SwBKP. When the dosage of CPAM was increased, the ash content of paper increased (Figure 5.4-(A)). The changes in bentonite dosage showed inverse responses in the ash content of paper (Figure 5.4-(B)). When the bentonite dosage was step-changed from 3 to 0 mg/g, the ash content initially decreased for a short period and then it started increasing to reach a higher steady state. The opposite trend was observed when the bentonite dosage was step-changed from 0 to 3 mg/g. When the filler addition increased, the ash content initially increased rapidly and then slowed down, and *vice versa* (Figure 5.4-(C)). Changing the filler concentration did not affect the filler retention significantly (Chapter 3). Hence, the changes in the ash content are due to the filler concentration. The simulated results were compared to the experimental data (Figures 5.4-(A)and (C)). The simulation represents the experiments reasonably well. The inverse dynamics of the ash content due to the changes in the bentonite dosage were unable to reproduce.

Figure 5.5 shows the effect of retention aids on the dynamics of the headbox and the white water total consistency and the basis weight, the ash content and the formation of paper for a SwBKP furnish. The changes in the white water consistency and the ash content of paper were due to the changes in the filler retention. When the first-pass retention of filler decreased, the white water consistency was increased and the ash content and the basis weight of paper decreased, and *vice versa*. The magnitude of variations of the recirculated white water consistency is relatively smaller than the magnitude of noises of headbox consistency. Hence,

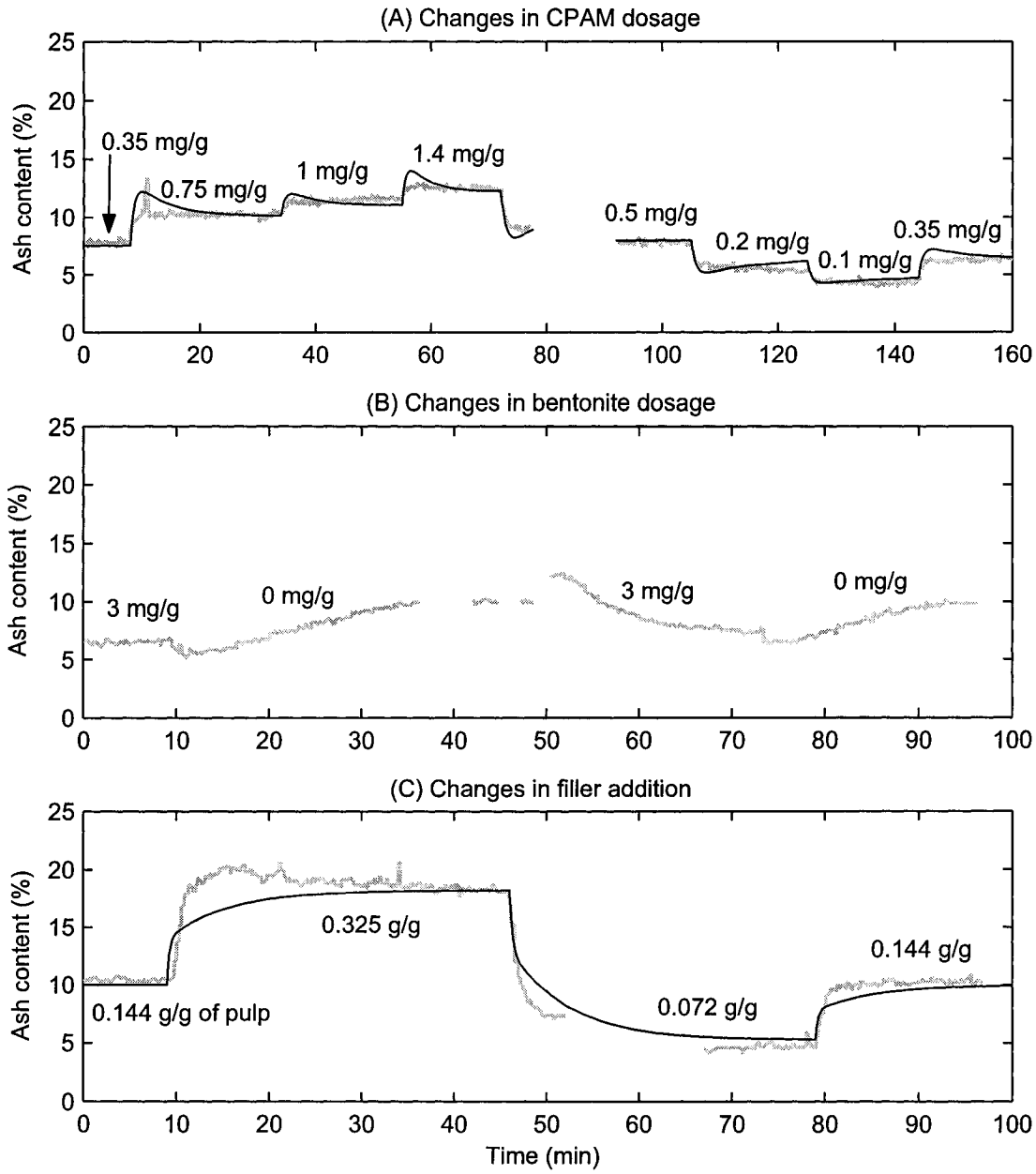

Figure 5.4. Effect of the polymer dosage, the bentonite dosage and the filler addition on the dynamics of the paper ash content. The black line represents the simulated data and the gray line, the experimental data. Furnish = a mixture of HwBKP and SwBKP

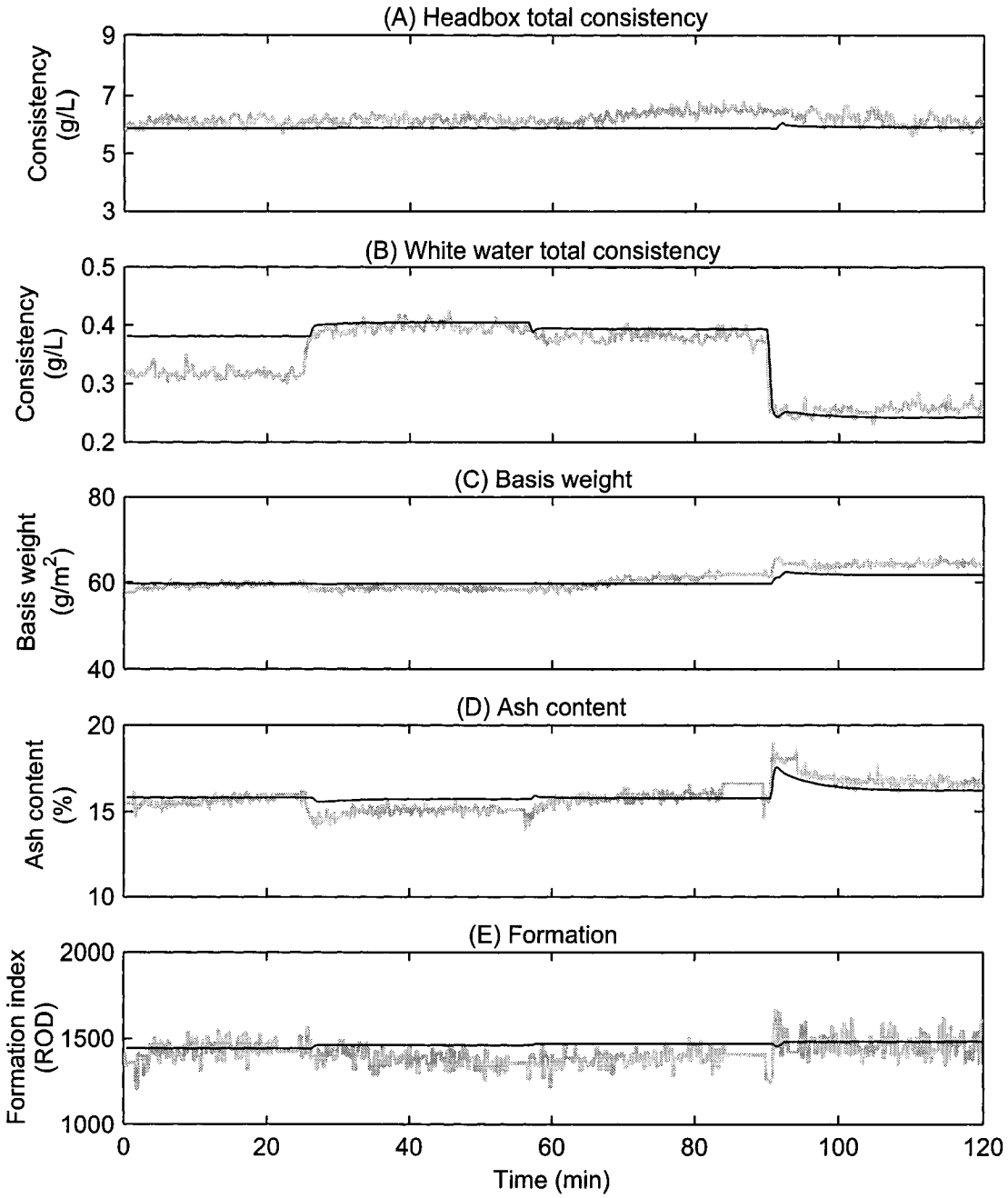

Figure 5.5. Effect of dosages of retention aids on the dynamics of a paper machine for a SwBKP furnish. At 0 min, CPAM = 0.2 mg/g and bentonite = 1 mg/g; at 25 min, CPAM = 0.2 mg/g and bentonite = 0 mg/g; at 56 min, CPAM = 0.35 mg/g and bentonite = 0 mg/g; at 89 min, CPAM = 0.35 mg/g and bentonite = 2 mg/g. The black line represents the simulated data and the gray line, the experimental data.

small variations in the headbox total consistency was observed. The changes in formation was caused by the changes in the bridging strength.

Figure 5.6 shows the effect of thick stock flow rate. When the thick stock flow rate was decreased, the headbox consistency decreased and hence the white water consistency and the basis weight of paper were decreased, and *vice versa.* Filler was mixed with pulp at the blend chest: i.e., the mass ratio of filler to pulp kept constant. Also, the variations in filler retention due to the changes in the mass flow rate of pulp were very small (Chapter 3). Hence, the ash content of paper was observed to be almost constant. The changes in formation is due to the changes in the crowding number.

The effect of the filler addition (g/g of pulp) on the dynamics of a paper machine is shown in Figure 5.7. When the filler addition increased, the headbox total consistency, the white water total consistency, the basis weight and the ash content were increased and *vice versa.* When filler addition decreased at 54 min, formation index slightly increased.

Figure 5.8 shows the effect of the white water flow rate F_5 on the dynamics of a paper machine. The recirculated white water flow rate was manipulated by changing the headbox flow valve (F_2). When the headbox flow rate was decreased at $t = 25$ min, keeping the thick stock flow F_1 constant, the recirculated white water flow F_5 decreased. This resulted in the increase of the headbox total consistency and the white water total consistency. Because of the sudden decrease of the headbox valve opening, the basis weight dropped sharply and recovered to its original value. The filler addition was kept constant for this set of experiments, which resulted in constant ash content. The changes in formation of paper are due to the changes in headbox fibre consistency, which affects the crowding number (Chapter 4). Some discrepancies are found in Figures 5.5, 5.6, 5.7 and 5.8, but the experimental data

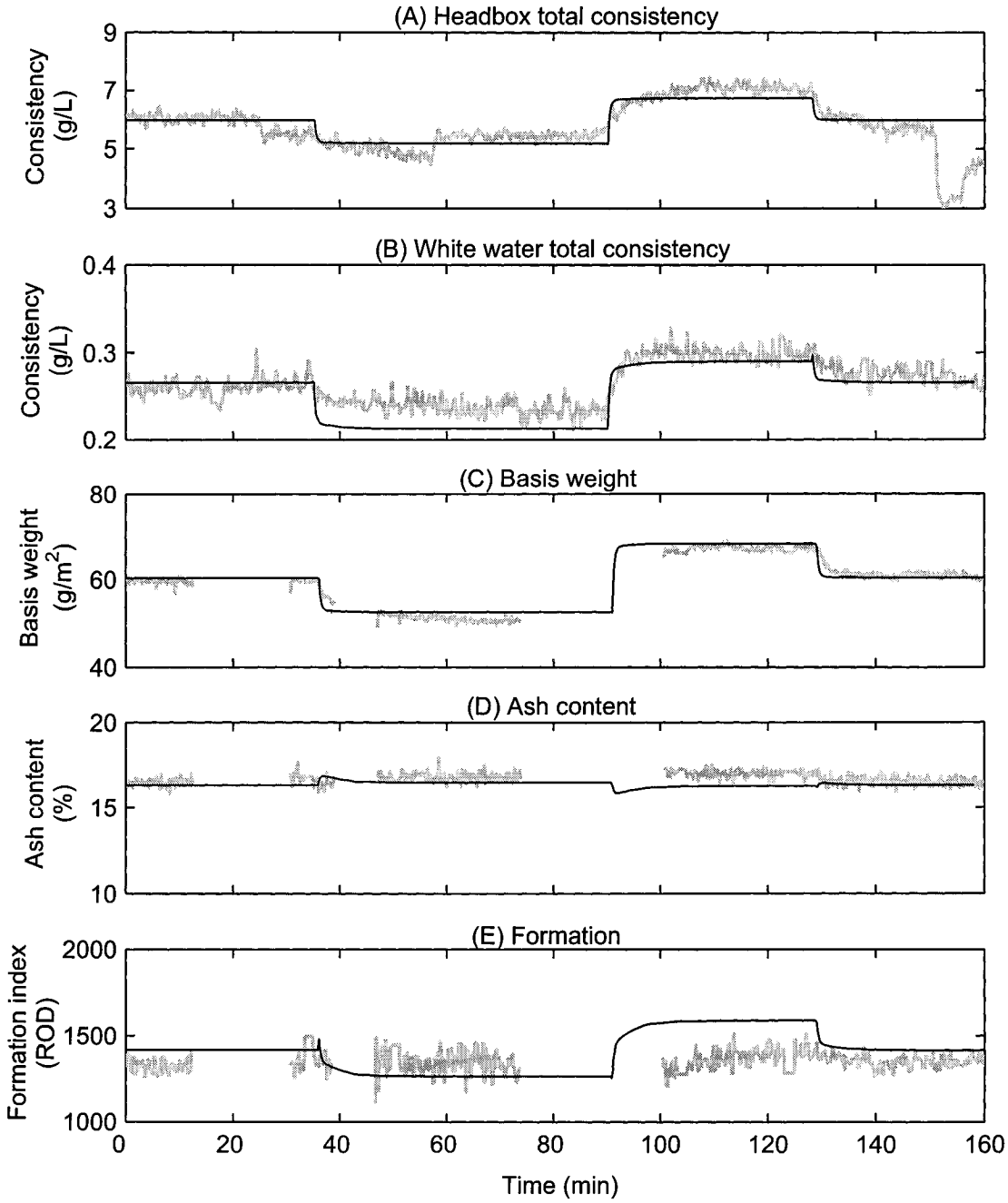

Figure 5.6. Effect of the thick stock mass flow rate on the dynamics of a paper machine for a SwBKP furnish. At 0 min, M_1 = 1840 g/min; at 35 min, M_1 = 1580 g/min; at 90 min, M_1 = 2100 g/min; and at 128 min, M_1 = 1840 g/min. The black line represents the simulated data and the gray line, the experimental data.

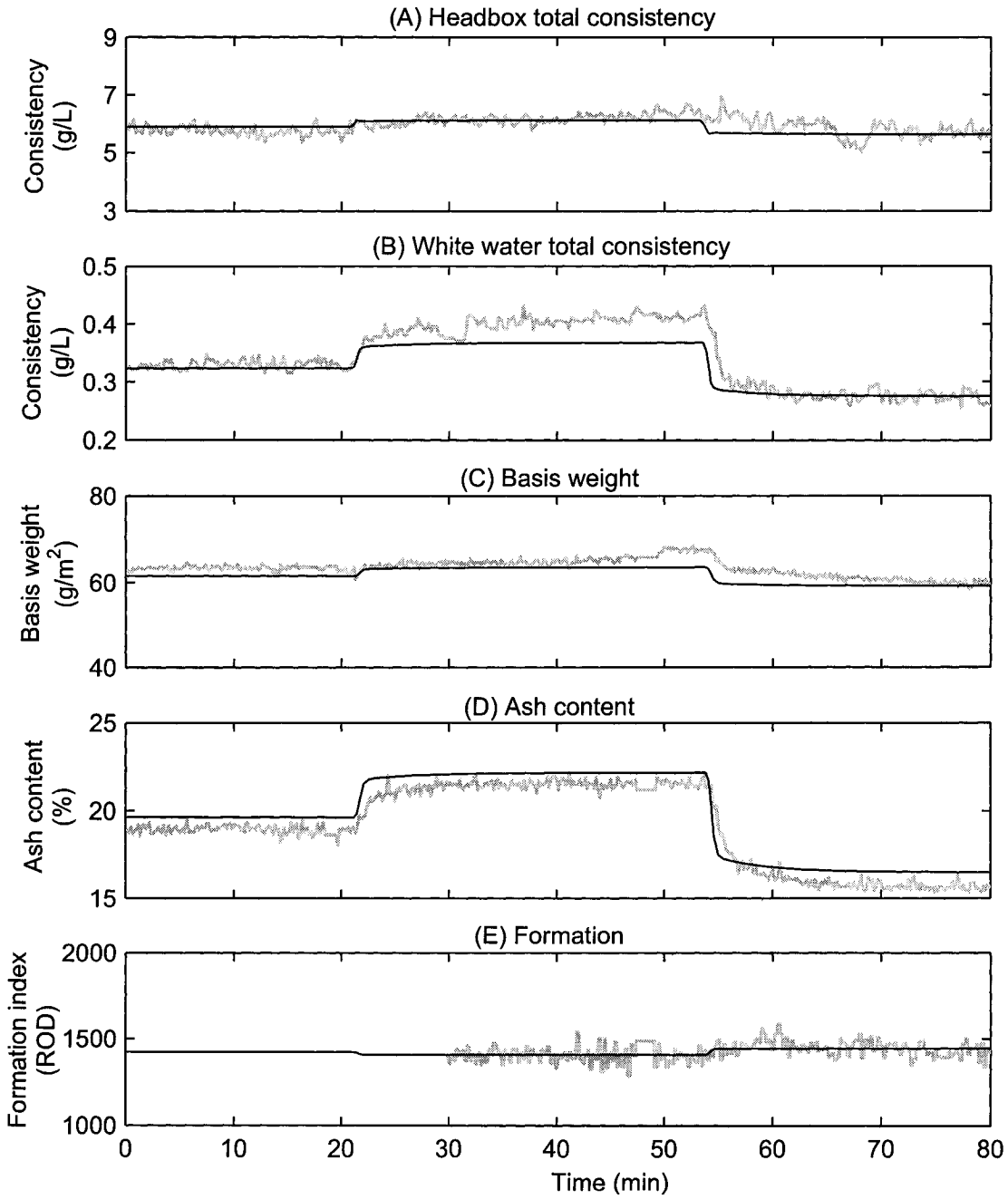

Figure 5.7. Effect of the filler addition on the dynamics of a paper machine for a SwBKP furnish. At 0 min, $C_{filler} = 0.25$ g/g; at 19 min, $C_{filler} = 0.30$ g/g; and at 54 min, $C_{filler} = 0.20$ g/g. The black line represents the simulated data and the gray line, the experimental data.

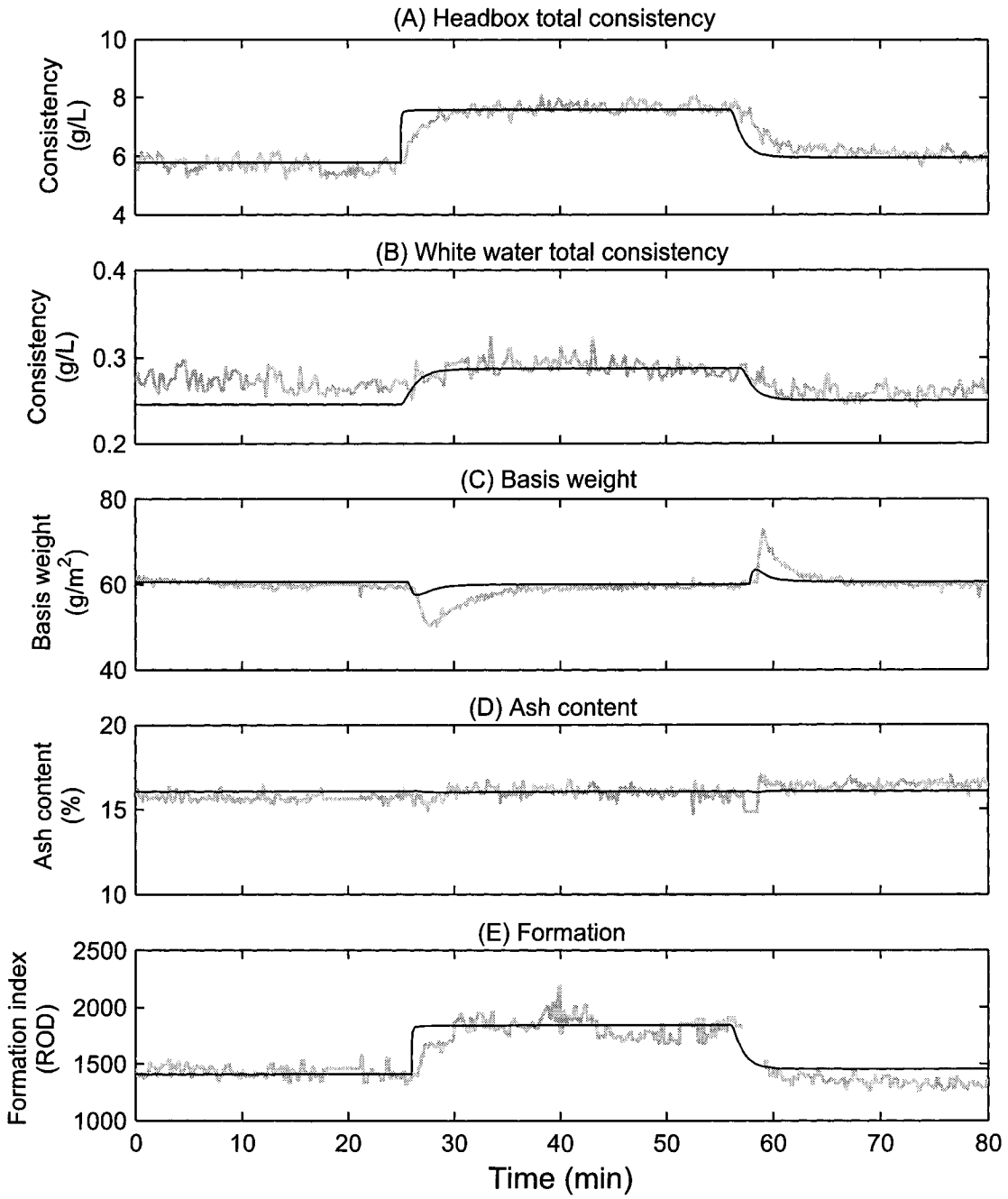

Figure 5.8. Effect of white water flow rate on the dynamics of a paper machine for a SwBKP furnish. At 0 min, headbox flow rate $F_2 = 340$ L/min; at 25 min, F_2 changed to 245 L/min; at 57 min, $F_2 = 320$ L/min. The black line represents the simulated data and the gray line, the experimental data.

and model predictions show relatively good agreement.

5.5 Discussion

5.5.1 Dynamics of the wet end

Analyzing transfer functions provides insight into the main factors affecting the dynamics of a paper machine. Transfer functions relating the input variables to the output variables can be obtained mathematically by solving equations presented in Section 5.2.

Table 5.1 shows the transfer functions relating the headbox consistency, the white water consistency, the basis weight and the ash content to the dosage of a retention aid. The first-pass retention of fines and fillers was assumed to be a second order polynomial of the form: $R = au^2 + bu + c$, where, a, b and c are constants, and u is the dosage of retention aid (CPAM or bentonite). The derivation of the transfer functions is shown in Appendix B. The white water consistency (C_4), the basis weight (BW) and the ash content (Ash) show second order systems with two zeros. The precess gains are influenced by the headbox consistency at a steady state ($C_{2,s}$), the flow rate at the headbox (F_2) and of the recirculated white water (F_5), and the first-pass retention of solids (R). The time constants are a function of the volume of the headbox (V_{hb}) and the white water pit (V_{wp}), the flow rate of the recirculated white water (F_5) and the overflowed white water (F_6) and the first-pass retention. The steady state values of the mass flow of total solids and filler ($F_3C_{3,total,s}$ and $F_3C_{3,filler,s}$) affect the process gain and the time constants of the ash content. The headbox consistency shows the second order system (no zero), which is a slower process than the white water consistency. This also agrees

Table 5.1. Transfer functions for the headbox consistency (C_2), the white water consistency (C_4) and the basis weight (BW) and the ash content (Ash) of paper. Input variable is the dosage of retention aids (u). It was assumed that $R = au^2 + bu + c$

output	transfer functions
C_2	$C_2(s) = \dfrac{-\frac{(2au_s+b)F_5C_{2,s}}{F_2-(1-R_s)F_5}}{\frac{F_2}{F_2-(1-R_s)F_5}(\frac{V_{hb}}{F_2})(\frac{V_{wp}}{F_5+F_6})s^2+\frac{F_2}{F_2-(1-R_s)F_5}(\frac{V_{hb}}{F_2}+\frac{V_{wp}}{F_5+F_6})s+1}\ U(s)$
C_4	$C_4(s) = \dfrac{-\frac{(2au_s+b)F_2C_{2,s}}{F_2-(1-R_s)F_5}(\frac{V_{hb}}{F_2}s+1)(\frac{V_{wp}}{F_5+F_6}s+1)}{\frac{F_2}{F_2-(1-R_s)F_5}(\frac{V_{hb}}{F_2})(\frac{V_{wp}}{F_5+F_6})s^2+\frac{F_2}{F_2-(1-R_s)F_5}(\frac{V_{hb}}{F_2}+\frac{V_{wp}}{F_5+F_6})s+1}\ U(s)$
BW	$BW(s) = \dfrac{\frac{(2au_s+b)(F_2C_{2,s})(F_2-F_5)}{ms\cdot W\cdot\tau_s[F_2-(1-R_s)F_5]}\left[\frac{F_2}{(F_2-F_5)}(\frac{V_{hb}}{F_2})(\frac{V_{wp}}{F_5+F_6})s^2+\frac{F_2}{(F_2-F_5)}(\frac{V_{hb}}{F_2}+\frac{V_{wp}}{F_5+F_6})s+1\right]}{\frac{F_2}{F_2-(1-R_s)F_5}(\frac{V_{hb}}{F_2})(\frac{V_{wp}}{F_5+F_6})s^2+\frac{F_2}{F_2-(1-R_s)F_5}(\frac{V_{hb}}{F_2}+\frac{V_{wp}}{F_5+F_6})s+1}\ U(s)$
Ash	$Ash(s) = \dfrac{K_{ash}(\xi_1 s+1)(\xi_2 s+1)}{(\tau_1 s+1)(\tau_2 s+1)}\ U(s)$ $K_{ash} = \dfrac{(2au_{s,filler}+b)(F_2C_{2,filler,s})(F_3C_{3s,total})(F_2-F_5)[F_2-(1-R_{s,total})F_5]-(2au_{total,s}+b)(F_2C_{2,s,total})(F_3C_{3s,filler})(F_2-F_5)[F_2-(1-R_{s,filler})F_5]}{(F_3C_{3s,total})^2[F_2-(1-R_{s,filler})F_5][F_2-(1-R_{s,total})F_5]}$ $\xi_1 = \dfrac{F_2}{F_2-F_5}\left(\dfrac{V_{wp}}{F_5+F_6}\right)$ $\xi_2 = \dfrac{F_2\left[(2au_{filler,s}+b)(F_2C_{2,filler,s})(F_3C_{3,total,s})-(2au_{total,s}+b)(F_2C_{2,total,s})(F_3C_{3,filler,s})\right]}{(2au_{filler,s}+b)(F_2C_{2,filler,s})(F_3C_{3,total,s})[F_2-(1-R_{total,s})F_5]-(2au_{total,s}+b)(F_2C_{2,total,s})(F_3C_{3,filler,s})[F_2-(1-R_{filler,s})F_5]}\left(\dfrac{V_{wp}}{F_5+F_6}\right)$ $\tau_1 = \dfrac{F_2}{F_2-(1-R_{filler,s})F_5}\left(\dfrac{V_{wp}}{F_5+F_6}\right),\ \tau_2 = \dfrac{F_2}{F_2-(1-R_{total,s})F_5}\left(\dfrac{V_{wp}}{F_5+F_6}\right)$

with the experimental results. When the first-pass retention of fillers increased by increasing a CPAM dosage or by varying a bentonite dosage (Figures 5.4-(A) and 5.5), the instantaneous increase in the first-pass retention caused a rapid increase in the ash content of paper and a sudden decrease in the white water concentration (C_4) in the stream separated from the wire. The small amount of polymer and bentonite does not affect the headbox consistency. The recirculating white water consistency (C_5, wire pit) decreased slowly to reach a new steady state. Since the recirculated white water consistency, used to dilute the thick stock, decreased slowly, the headbox consistency decreased slowly as well. Consequently, the ash content in the sheet also decreased slowly to reach a new steady state. Certainly, the first-pass retention of solids and the circulation of the white water play a major role in the dynamics of a paper machine. The main factors related to the circulation of white water are the volume of the wire pit (V_{wp}) and the residence time at the wire pit (F_5 and F_6). During changes in the retention aids, the flow rates of the headbox stock and the volumes of the headbox and the wire pit do not change. Hence these can be considered as fixed parameters for a given grade and for a given paper machine.

The inverse response by bentonite (Figure 5.4-(B)) can be explained by the excess bentonite. The CPAM dosage for this experiments was 0.35 mg/g. Assuming that all CPAM adsorbs onto fibres and that bentonite exists in 3 stacks of plates in the wet end, which have less stacks of bentonite plates than the assumed in Chapters 3 and 4, the bentonite dosage to just cover all the polymer is 2.63 mg/g. 3 mg/g of bentonite was more than needed to cover the polymer-coated fibres. When the bentonite dosage is positively step-changed from 0 to 3 mg/g (Figure 5.4-(B)), the added bentonite immediately worked as a bridging agent and improved flocculation of fibres and fillers, resulting in a sudden increase in the measured filler

content in paper. The excess bentonite did not remain in the web and entered the white water pit with the separated white water from the wire. The concentration of bentonite in the white water slowly increased to reach a new steady state. The bentonite platelets in the circulated white water could scavenge the CPAM molecules, reducing the efficiency of the cationic polymer. Another explanation is that the recirculated bentonite platelets were adsorbed on the polymer-covered fibre surface followed by adsorption of polymer molecules on top of the bentonite platelets, and formed polymer-bentonite complexes. The bare filler particles could then deposit on the complexes. Asselman and Garnier [94] showed that the bridge by polymer-bentonite-polymer could be weaker than that by only polymer depending on the order of polymer adsorption. When polymer is first adsorbed on bentonite, the resulting bond strength is much weaker due to a flatter conformation caused by the high surface charge of bentonite. This leads to an increase in the detachment rate and hence a decrease in the filler retention. The higher the level of recirculated bentonite, the higher the tendency of CPAM and bentonite to complex into the weakest bond configuration. As a result, the filler retention slowly decreased until the concentration of bentonite in the white water reaches steady state. On the other hand, when the bentonite dosage was decreased in a step-change from 3 to 0 mg/g, filler retention instantly dropped due to the removal of bentonite bridging. The bentonite concentration in the white water slowly decreased, resulting in the removal of any excess bentonite. Consequently, the filler retention slowly increased as a function of time.

Transfer functions for the input variables, the thick stock flow rate (F_1) and the filler slurry flow rate (F_7) are shown in Table 5.2 and 5.3 respectively. Transfer functions for the two input variables share the same type of system (second order systems with one zero) for the headbox consistency, the white water consistency

Table 5.2. Transfer functions for the headbox consistency (C_2), the white water consistency (C_4) and the basis weight (BW) and the ash content (Ash) of paper. Input variable is the thick stock flow rate (F_1).

output	transfer functions
C_2	$C_2(s) = \dfrac{\frac{C_1}{F_2-(1-R)F_5}(\frac{V_{wp}}{F_5+F_6}s+1)}{\frac{F_2}{F_2-(1-R)F_5}(\frac{V_{hb}}{F_2})(\frac{V_{wp}}{F_5+F_6})s^2+\frac{F_2}{F_2-(1-R)F_5}(\frac{V_{hb}}{F_2}+\frac{V_{wp}}{F_5+F_6})s+1}F_1(s)$
C_4	$C_4(s) = \dfrac{\frac{(1-R)C_1}{F_2-(1-R)F_5}(\frac{V_{wp}}{F_5+F_6}s+1)}{\frac{F_2}{F_2-(1-R)F_5}(\frac{V_{hb}}{F_2})(\frac{V_{wp}}{F_5+F_6})s^2+\frac{F_2}{F_2-(1-R)F_5}(\frac{V_{hb}}{F_2}+\frac{V_{wp}}{F_5+F_6})s+1}F_1(s)$
BW	$BW(s) = \dfrac{\frac{R\ F_2C_1}{ms\cdot W\cdot r_s(F_2-(1-R)F_5)}(\frac{V_{wp}}{F_5+F_6}s+1)}{\frac{F_2}{F_2-(1-R)F_5}(\frac{V_{hb}}{F_2})(\frac{V_{wp}}{F_5+F_6})s^2+\frac{F_2}{F_2-(1-R)F_5}(\frac{V_{hb}}{F_2}+\frac{V_{wp}}{F_5+F_6})s+1}F_1(s)$
Ash	$Ash = \frac{K_{ash}(\xi_1 s+1)(\xi_2 s+1)}{(\tau_1 s+1)(\tau_2 s+1)}F_1(s)$ $K_{ash} = \frac{F_2\left[F_3C_{3s,filler}R_{total}C_1(F_2-(1-R_{filler})F_5+R_fC_1^{filler}(F_3C_{3,total,s})(F_2-(1-R_{total})F_5)\right]}{(F_3C_{3,total,s})^2(F_2-(1-R_{filler})F_5)(F_2-(1-R_{total})F_5)}$ $\xi_1 = \frac{V_{wp}}{F_5+F_6},\ \xi_2 = \frac{F_2\left[R_{filler}C_{1,filler}F_3C_{3,total,s}+R_{total}F_3C_{3,filler,s}C_{1,total}\right]}{R_{total}C_{1,total}(F_3C_{3,filler,s})[F_2-(1-R_{filler})F_5]+R_fC_{1,filler}(F_3C_{3,total,s})[F_2-(1-R_{total})F_5]}\left(\frac{V_{wp}}{F_5+F_6}\right)$ $\tau_1 = \frac{F_2}{F_2-(1-R_{filler})F_5}\left(\frac{V_{wp}}{F_5+F_6}\right),\ \tau_2 = \frac{F_2}{F_2-(1-R_{total})F_5}\left(\frac{V_{wp}}{F_5+F_6}\right)$

Table 5.3. Transfer functions for the headbox consistency (C_2), the white water consistency (C_4) and the basis weight (BW) and the ash content (Ash) of paper. Input variable is the flow rate of filler slurry (F_7).

output	transfer functions
C_2	$C_2(s) = \dfrac{\frac{C_7}{F_2-(1-R)F_5}(\frac{V_{wp}}{F_5+F_6}s+1)}{\frac{F_2}{F_2-(1-R)F_5}(\frac{V_{hb}}{F_2})(\frac{V_{wp}}{F_5+F_6})s^2+\frac{F_2}{F_2-(1-R)F_5}(\frac{V_{hb}}{F_2}+\frac{V_{wp}}{F_5+F_6})s+1}F_7(s)$
C_4	$C_2(s) = \dfrac{\frac{(1-R)C_7}{F_2-(1-R)F_5}(\frac{V_{wp}}{F_5+F_6}s+1)}{\frac{F_2}{F_2-(1-R)F_5}(\frac{V_{hb}}{F_2})(\frac{V_{wp}}{F_5+F_6})s^2+\frac{F_2}{F_2-(1-R)F_5}(\frac{V_{hb}}{F_2}+\frac{V_{wp}}{F_5+F_6})s+1}F_7(s)$
BW	$BW(s) = \dfrac{\frac{R\ F_2C_7}{ms\cdot W\cdot r_s(F_2-(1-R_f)F_5)}\ (\frac{V_{wp}}{F_5+F_6}s+1)}{\frac{F_2}{F_2-(1-R)F_5}(\frac{V_{hb}}{F_2})(\frac{V_{wp}}{F_5+F_6})s^2+\frac{F_2}{F_2-(1-R)F_5}(\frac{V_{hb}}{F_2}+\frac{V_{wp}}{F_5+F_6})s+1}F_7(s)$
Ash	$Ash(s) = \dfrac{\frac{R_{filler}F_2C_{7,filler}\left(F_3C_{3,total,s}-F_3C_{3,filler,s}\right)}{(F_3C_{3,total,s})^2[F_2-(1-R_{filler})F_5]}\ (\frac{V_{wp}}{F_5+F_6}s+1)}{\frac{F_2}{F_2-(1-R_{filler})F_5}(\frac{V_{hb}}{F_2})(\frac{V_{wp}}{F_5+F_6})s^2+\frac{F_2}{F_2-(1-R_{filler})F_5}(\frac{V_{hb}}{F_2}+\frac{V_{wp}}{F_5+F_6})s+1}F_7(s)$

and the basis weight. Time constants are identical between the two input variables except for the ash content. The time constants are a function of the volumes of the headbox (V_{hb}) and the wire pit (V_{wp}), the flow rates of the headbox stock (F_2), the recirculating white water (F_5) and the overflowing white water (F_6), which are related to the circulation of white water. Process gains is influenced by the first-pass retention (R), the flow rates of the headbox stock (F_2), the recirculating white water (F_5) and the concentration of the input flows (C_1 for the thick stock flow change and C_7 for the filler flow change). Concerning that the first-pass retention does not change significantly by varying the thick stock mass flow and the filler concentration (Chapter 3), the parameters related to the circulation of white water and the concentrations of the thick stock and the filler slurry are two important factors influencing the dynamics of the paper machine. Unlike the case of changing the dosage of a retention aid, the headbox consistency is affected immediately after step-changing the flow rates of the thick stock and the filler slurry (Figures 5.6 and 5.7). The white water consistency, the basis weight and the ash content initially shows rapid changes due to the sudden changes in the headbox consistency. Then, the white water consistency in the wire pit slowly changes to reach a new steady state, resulting in slow transition in the recirculating white water consistency after the rapid change. Consequently, the basis weight and ash content of paper slowly changes to a new steady state.

Table 5.4 show the transfer functions for the changes in the headbox flow rate (F_2). Again, the parameters related to the white water circulation play a major role in deciding the time constants. Since a change in the headbox flow rate leads to a change in the white water consistency, the differences in the headbox consistency and the white water consistency ($(C_{2,s} - C_{4,s})$ and $(C_{2,s} - C_{5,s})$), which are mainly influenced by the first-pass retention of solids, influence the process gains and the

Table 5.4. Transfer functions for the headbox consistency (C_2), the white water consistency (C_4) and the basis weight (BW) and the ash content (Ash) of paper. Input variable is the headbox flow rate (F_2).

output	transfer functions
C_2	$C_2(s) = \dfrac{-\frac{F_{5,s}(C_{2,s}-C_{4,s})+F_{6,s}(C_{2,s}-C_{5,s})}{(F_{2,s}-F_{5,s}(1-R))(F_{5,s}+F_{6,s})}\left(\frac{(C_{2,s}-C_{5,s})V_{wp}}{F_{5,s}(C_{2,s}-C_{4,s})+F_{6,s}(C_{2,s}-C_{5,s})}s+1\right)}{\frac{F_{2,s}}{F_{2,s}-F_{5,s}(1-R)}\frac{V_{hb}}{F_{2,s}}\frac{V_{wp}}{F_{5,s}+F_{6,s}}s^2+\frac{F_{2,s}}{F_{2,s}-F_{5,s}(1-R)}\left(\frac{V_{hb}}{F_{2,s}}+\frac{V_{wp}}{F_{5,s}+F_{6,s}}\right)s+1}F_2(s)$
C_4	$C_4(s) = \dfrac{-(1-R)\frac{F_{5,s}(C_{2,s}-C_{4,s})+F_{6,s}(C_{2,s}-C_{4,s})}{(F_{2,s}-F_{5,s}(1-R))(F_{5,s}+F_{6,s})}(\frac{(C_{2,s}-C_{5,s})V_{wp}}{F_{5,s}(C_{2,s}-C_{4,s})+F_{6,s}(C_{2,s}-C_{5,s})}s+1)}{\frac{F_{2,s}}{F_{2,s}-F_{5,s}(1-R)}\frac{V_{hb}}{F_{2,s}}\frac{V_{wp}}{F_{5,s}+F_{6,s}}s^2+\frac{F_{2,s}}{F_{2,s}-F_{5,s}(1-R)}\left(\frac{V_{hb}}{F_{2,s}}+\frac{V_{wp}}{F_{5,s}+F_{6,s}}\right)s+1}F_2(s)$
BW	$BW(s) = \frac{K_{bw}(\xi_{bw1}s^2+\xi_{bw2}s+1)}{\tau_{bw1}s^2+\tau_{bw2}s+1}F_2(s)$ $K_{bw} = \frac{R_{total}F_{2,s}[F_{5,s}(C_{4,s}-C_{2,s})+F_{6,s}(C_{5,s}-C_{2,s})]+RC_{2,s}(F_{2,s}-F_{5,s}(1-R_{total}))(F_{5,s}+F_{6,s})}{ms\cdot W\cdot r_s\cdot(F_{2,s}-F_{5,s}(1-R_{total}))(F_{5,s}+F_{6,s})}$ $\xi_{bw1} = \frac{C_{2,s}V_{hb}V_{wp}}{F_{2,s}[F_{5,s}(C_{4,s}-C_{2,s})+F_{6,s}(C_{5,s}-C_{2,s})]+C_{2,s}(F_{2,s}-F_{5,s}(1-R))(F_{5,s}+F_{6,s})}$ $\xi_{bw2} = \frac{C_{2,s}[V_{hb}(F_{5,s}+F_{6,s})+V_{wp}F_{2,s}]-F_2(C_{2,s}-C_{5,s})V_{wp}}{F_2[F_{5,s}(C_{4,s}-C_{2,s})+F_{6,s}(C_{5,s}-C_{2,s})]+C_{2,s}(F_{2,s}-F_{5,s}(1-R))(F_{5,s}+F_{6,s})}$ $\tau_{bw1} = \frac{F_{2,s}}{F_{2,s}-F_{5,s}(1-R)}\left(\frac{V_{hb}}{F_{2,s}}\right)\left(\frac{V_{wp}}{(F_{5,s}+F_{6,s})}\right), \quad \tau_{bw2} = \frac{F_{2,s}}{F_{2,s}-F_{5,s}(1-R)}\left(\frac{V_{hb}}{F_{2,s}}+\frac{V_{wp}}{(F_{5,s}+F_{6,s})}\right)$
Ash	F_2 does not affect ash content significantly. Hence $\frac{Ash(s)}{F_2(s)} = 0$

time constants. It can be noticed that the headbox consistency change at 25 min showed faster response than that at 57 min (Figure 5.8-(A)). That is because the the headbox flow rate at steady state ($F_{2,s}$) affects the time constants: the higher the value of F_2, the lower the time constants. The headbox flow rate was step-changed from 340 L/min to 245 L/min at 25 min and from 245 L/min to 320 L/min at 57 min. Consequently, the first step-change at 25 min showed faster response than the second step-change. Discrepancy is found between the experimental results of the basis weight and the simulated one (Figure 5.8-(C)): the experimental results showed a high peak. This could be explained by a nonuniform mixing at the pipeline between the headbox and the headbox valve and at the headbox, while an ideal mixing was assumed in simulation. The changes in the headbox flow rate influence the headbox consistency while the mass flow rate of headbox stock remained constant. The changes in the white water consistency and the formation is due to the changes in the headbox consistency. On the other hand, the steady state values of the ash content and the basis weight remain unchanged due to the constant headbox mass flow rate of pulp and filler.

From the above discussion, it is clear that, in addition to the flow rate and consistency of the input variables, the two main factors affecting the dynamics of the solids concentration in a paper machine are the first-pass retention of the solids and the parameters related to the circulation of the white water (V_{wp}, F_5 and F_6) under the paper machine.

5.5.2 Implications for the wet end control

The main factors affecting the dynamics of the solid concentration (fibres, fines and fillers) were the first-pass retention of the fines and fillers (R) and the parameters

related to the white water circulation, which include the volume of the wire pit and the residence time at the wire pit (F_5 and F_6). Using different retention aids than the CPAM/bentonite system would mainly affect the first-pass retention. At this point it is difficult to evaluate strictly from first-principles the deposition efficiency of a given retention aid and to predict the first-pass retention of fillers. The safest is still to perform experiments and to obtain an empirical model for first-pass retention. Hermann et. al.'s results support that this approach can be used to include the effect of wet end chemistry, in which they used polyethylene oxide (PEO)-cofactor(CF) retention aid system and simulated white water consistency [116]. A mechanistic attempt to model the polymer bridging behavior as a function of shear and salt concentration was presented by Asselman and Garnier [93,94]. The volume of tanks and the flow rate of white water can be considered as fixed parameters for a given paper machine and paper grade. Flow rates and consistencies of the thick stock and the filler slurry also can be considered as fixed parameters for a given grade. Consequently, the dynamics of filler and fines retention play a fundamental role for process optimization.

The first-pass retention of solids can be controlled by regulating retention aids. When a microparticulate retention aid system is used, the manipulation of polymer and microparticle flow rates has to be careful. The inverse response in Figure 5.4-(B) is quite an uncommon dynamic behaviour in a papermaking system and can create difficulties to control the dynamics. The best solution is to avoid the inverse response by keeping a constant ratio between the mass flow of polymer and microparticle during the retention control. Also, it was suggested that, when formation is concerned, a constant ratio between the mass flow of polymer and bentonite has to be kept : i.e, a constant surface coverage of bentonite on the polymer covered fibre surface (Chapter 4).

During the changes in the thick stock flow rate, which can occur for grade changes, formation was influenced due to the changes in fibre concentration (Figure 5.6-(E)). The variations in formation can be minimized by keeping a constant headbox fibre consistency by regulating the headbox flow rate at the same time during grade changes. However, the headbox valve has to be controlled very carefully, since any sudden changes in the headbox valve will significantly affect the dynamics of basis weight (see Figure 5.8-(C)).

5.6 Chapter summary

Dynamic models of a pilot paper machine for the retention process including headbox total and filler consistencies, white water total and filler consistencies and the basis weight and the ash content of paper were developed from first-principles (mass balances). To describe the wet end chemistry effect, first-pass retention was included in the model as a parameter dependent on operating conditions. In addition, an empirical model for formation was developed as a function of the crowding number, the bridging strength and the filler fraction in headbox stock and implemented into the dynamic simulation models. It was shown that the dynamics of a paper machine can be simulated using mathematical models describing the mass balance of solids in the paper machine coupled with empirical models of the first-pass retention and the paper formation. Transfer functions were derived from the mathematical models. It was discussed that two important factors affecting the dynamics of solid concentrations in the paper machine are the first-pass retention and the parameters related to the white water circulation such as the volume of the wire pit and the residence time at the wire pit for a given paper machine and for a given grade. Considering the piping and tanks configuration as fixed parameters

for a given paper machine, the dynamics of filler retention play a fundamental role for the process optimization.

Chapter 6

Control of the Retention and Formation Processes

6.1 Introduction

The main objective of controlling the retention process is to obtain uniform basis weight and ash content of paper in machine direction (MD). The most frequently used control strategy for the retention process is to control oven dry basis weight by manipulating the flow rates of thick stock, paper ash content by filler flow and white water consistency by retention aid flow. The decentralized single-input, single-output configuration is mostly used, whereby each variable is controlled separately and independently. Basis weight and ash content have been controlled for decades without doubting the efficiency of the control structure. Even though the use of a microparticulate retention aid system has been increasing, it is not clear how to manipulate polymer and microparticle for the white water consistency control. The problem concerning the selection of set-points of white water consistency during grade changes has not been clearly answered yet. Moreover, variations in formation

during the control of the retention process have been neglected.

This chapter focuses on the selection of the control objectives and the control configurations to control the retention process without deteriorating paper formation. Several possibilities of manipulated variables and controlled variables are chosen and tested in the nonlinear model developed in Chapter 5. In pulp and paper mills, most of the control loops currently utilize PI controller, even though the use of advanced control algorithms such as MPC (model predictive control) is increasing. Single-input single-output (SISO) control and multi-input multi-output (MIMO) control are used for this study. The basics of these controllers are discussed in the next Section. In Section 6.3, the control strategies for basis weight and paper ash content are discussed. The white water consistency control with a microparticulate retention aid system is discussed in Section 6.4. The selection of set-points during grade changes is also discussed. Headbox pulp consistency control concerning paper formation is discussed in Section 6.5. Finally, the multivariable control scheme for retention and formation processes are discussed in Section 6.6.

6.2 Controllers

6.2.1 PI controller

PI and PID controllers are the most widely used in paper industry. To avoid overshoot, Lambda-tuning [61, 117, 118], which is a direct synthesis method, was chosen instead of Quarter-Amplitude tuning [119, 120]. In the Lambda-tuning, the closed loop transfer function $G_{SP}(s)$ is typically chosen to be a first order plus deadtime:

$$G_{SP}(s) = \frac{1}{\lambda s + 1} e^{-sT_d} \tag{6.1}$$

where λ is the closed loop time constant and T_d the deadtime. Considering a first order plus deadtime process (i.e., with a process gain K_P, a time constant τ and a deadtime T_d) and using a Taylor approximation ($e^{-sTd} \approx 1 - T_d s$) for a deadtime, a PI controller (in a standard form) is obtained:

$$G_C(s) = K_C\left[1+\frac{1}{T_R s}\right] = \frac{\tau}{K_P(\lambda+T_d)}\left[1+\frac{1}{\tau s}\right] \tag{6.2}$$

with design parameters:

$$T_R = \tau \tag{6.3}$$

$$K_C = \frac{\tau}{K_P(\lambda+T_d)} \tag{6.4}$$

where K_C is the controller gain and T_R is the reset time. The controller reset time is determined from the open loop time constant. The speed of the closed loop response is determined from the controller gain, where λ is chosen to decide the desired response. λ is the only tuning parameter in this tuning method. The time constants of the open and closed loop are the same when $\lambda = \tau$. The closed-loop system responds faster than the open loop system, if $\lambda < \tau$. In practice, it is common to choose λ between 0.5 τ and 5τ [121].

6.2.2 Decoupling control system

The controlled variables of the retention process are severely interacting with each other. When control loop interactions are a problem, we can detune one or more feedback controllers, use a decoupling controller or consider a multivariable control scheme [122]. The term detuning refers to using a conservative choice of controller setting that results in more sluggish closed-loop responses.

Since the dynamic decoupling results in complicated equations, it is rarely used

and the steady state decoupling is generally used. Generalized steady state decoupling was used for this study. The decoupler matrix G_I is calculated by:

$$G_I = K^{-1}K_R \tag{6.5}$$

where K is the matrix of steady state gains, K^{-1} is the inverse matrix of K and K_R is the matrix of the diagonal elements of K.

6.3 Control of basis weight and ash content

Basis weight and paper ash content in machine direction (MD) are traditionally controlled by manipulating the thick stock flow rate and the filler slurry flow rate, respectively. To avoid the interactions between the moisture content and the basis weight of paper, the oven dry basis weight is controlled. Basis weight and ash content have strong cross effects. Both of thick stock flow and filler slurry flow affect both of basis weight and ash content by the equations 5.20 and 5.21. Hence the use of decoupler is required.

The interactions between the basis weight and the ash content control loops could be easily eliminated by choosing the pulp mass and the filler mass in paper as controlled variables instead of basis weight and ash content. The filler mass and the pulp mass in paper can be calculated from the set points of the basis weight (BW, g/m^2) and the ash content (Ash, %):

$$\text{Filler mass (g/m}^2\text{)}, \; M_{filler} = \frac{BW \times Ash}{100} \tag{6.6}$$

$$\text{Pulp mass (g/m}^2\text{)}, \; M_{pulp} = BW - M_{filler} = \frac{BW(100 - Ash)}{100} \; . \tag{6.7}$$

In addition, a simple static feedforward compensation of filler in thick stock helps

to eliminate the disturbances from thick stock [67]. The static feedforward compensation of filler in thick stock is:

$$\Delta F_7 = -k_{ff}\Delta F_1 \tag{6.8}$$

where

$$k_{ff} = \frac{C_{1,filler}}{C_{7,filler}} \tag{6.9}$$

where $C_{1,filler}$ is the filler consistency in the thick stock (g/L) and $C_{7,filler}$ is the concentration of the filler slurry (g/L).

First order plus delay models were developed by performing bump tests on manipulated variables. For the basis weight and ash content control system, the output variables are the dry basis weight and the ash content of paper and the manipulated variables are the thick stock flow rate (F_1) and the filler slurry flow rate (F_7). For the pulp mass and filler mass control system, the output variables are the pulp mass and the filler mass of paper and the manipulated variables are the thick stock flow rate and the filler slurry flow rate. The reference values used for the simulation is shown in Table 6.1. The models for basis weight and ash content control are:

$$\begin{bmatrix} BW(s) \\ Ash(s) \end{bmatrix} = \begin{bmatrix} \frac{1.1533\ e^{-170s}}{108s+1} & \frac{0.1533\ e^{-150s}}{138s+1} \\ \frac{-1.0831\ e^{-170s}}{108s+1} & \frac{0.814\ e^{-150s}}{138s+1} \end{bmatrix} \begin{bmatrix} F_1(s) \\ F_7(s) \end{bmatrix} \tag{6.10}$$

and the transfer functions for the pulp mass and filler mass control are:

$$\begin{bmatrix} M_{pulp}(s) \\ M_{filler}(s) \end{bmatrix} = \begin{bmatrix} \frac{0.8982\ e^{-170s}}{108s+1} & \frac{-0.0005\ e^{-150s}}{138s+1} \\ \frac{0.1449\ e^{-170s}}{108s+1} & \frac{0.7688\ e^{-150s}}{138s+1} \end{bmatrix} \begin{bmatrix} F_1(s) \\ F_7(s) \end{bmatrix}. \tag{6.11}$$

The input variables and the output variables were scaled to be in the range between 0 and 1 by diving by their maximum allowed values for output variables and by the maximum pump speed for input variables.

Table 6.1. Reference values for the simulations.

item	values
Thick stock flow rate F_1(L/min)	60
Thick stock consistency (%)	2.6
Fines content in thick stock (%)	5
Filler content in thick stock (%)	5
Filler slurry flow rate F_7 (L/min)	2
Filler slurry concentration (%)	10
CPAM solution flow rate F_{pol} (L/min)	0.404
CPAM concentration (%)	0.15
Bentonite suspension flow rate F_{mp} (L/min)	1.5
Bentonite concentration (%)	0.3
Headbox flow rate F_2 (L/min)	340

The steady state RGA (relative gain array) analysis confirms that $BW-F_1/Ash-F_7$ pairing and $M_{pulp}-F_1/M_{filler}-F_7$ pairing are the right choices and that choosing the pulp mass and the filler mass in paper as controlled variables instead of basis weight and ash content reduces the cross interactions. The RGA matrix (Λ) for the basis weight and ash content control system is:

$$\Lambda = \begin{bmatrix} 0.8497 & 0.1503 \\ 0.1503 & 0.8497 \end{bmatrix} \tag{6.12}$$

and that for the pulp mass and filler mass control system is:

$$\Lambda = \begin{bmatrix} 0.9999 & 0.0001 \\ 0.0001 & 0.9999 \end{bmatrix} . \tag{6.13}$$

The element of the RGA, λ_{ij}, is a measure of the steady state interaction expected in the ith loop of the multivariable system if output y_i is paired with input u_j and is defined as [61]:

$$\lambda_{ij} = \frac{\left(\frac{\partial y_i}{\partial u_j}\right)_{u_k, j\neq k}}{\left(\frac{\partial y_i}{\partial u_j}\right)_{u_k, i\neq k}} = \frac{\left(\frac{\partial y_i}{\partial u_j}\right)_{\text{all loops open}}}{\left(\frac{\partial y_i}{\partial u_j}\right)_{\text{all loops closed except}j}} \tag{6.14}$$

If $\lambda_{ij} = 1$, u_j affects y_i without interacting with, and/or eliciting interaction from, the other control loops. If $\lambda_{ij} = 0$, u_j has no effect on y_i. The elements of the RGA are obtained from:

$$\lambda_{ij} = K_{ij} r_{ij} \tag{6.15}$$

where K_{ij} are the steady state gains of the transfer function matrix and r_{ij} are the elements of the transpose matrix R of the inverse of the steady state gain matrix, i.e.;

$$R = (K^{-1})^T . \tag{6.16}$$

Three cases were tested: (1) the basis weight and ash content control without a decoupler; (2) the basis weight and ash content control with a decoupler; and

(3) the pulp mass and filler mass control with a static feedforward compensation. In all cases, PI controller was used and for comparison, the same tuning rule was applied: $\lambda = 3\tau$, where τ is the time constant of a process [117].

Figure 6.1 compares the responses of the basis weight, the thick stock flow rate, the paper ash content and the filler slurry flow rate for the three different control schemes when the set-points of basis weight and ash content are step-changed. The PI controller is able to handle the set-point changes for both basis weight and ash content. The pulp mass and filler mass control system (case 3) responds slightly faster than the basis weight and ash content control system with a decoupler (case 2). Interactions still exist when the pulp mass and the filler mass are controlled: when the basis weight set-point is changed, the ash content is varied as well, and *vice versa*. The interactions are due to the dependency of the fines and filler retention on the pulp flow and the filler flow. However, the magnitude of interaction is smaller than the basis weight and ash content control system without a decoupler (case 1).

Figures 6.2 and 6.3 show responses of the three control structures to the introduction of disturbances. Disturbances are introduced in the thick stock total consistency, the filler slurry concentration (Figure 6.2) and the filler retention (Figure 6.3). The pulp mass and filler mass control system (case 3) provides a faster settling time in the basis weight and the paper ash content than the basis weight and ash content control systems with and without decoupling when the thick stock consistency is perturbed at 11000 sec and 15000 sec (Figure 6.2). This is due to the effect of the static feedforward compensation of thick stock filler. When the filler slurry consistency is step-changed at 20000 sec and 25000 sec, the disturbances are eliminated well by the feedback controllers and the response of three cases are almost same.

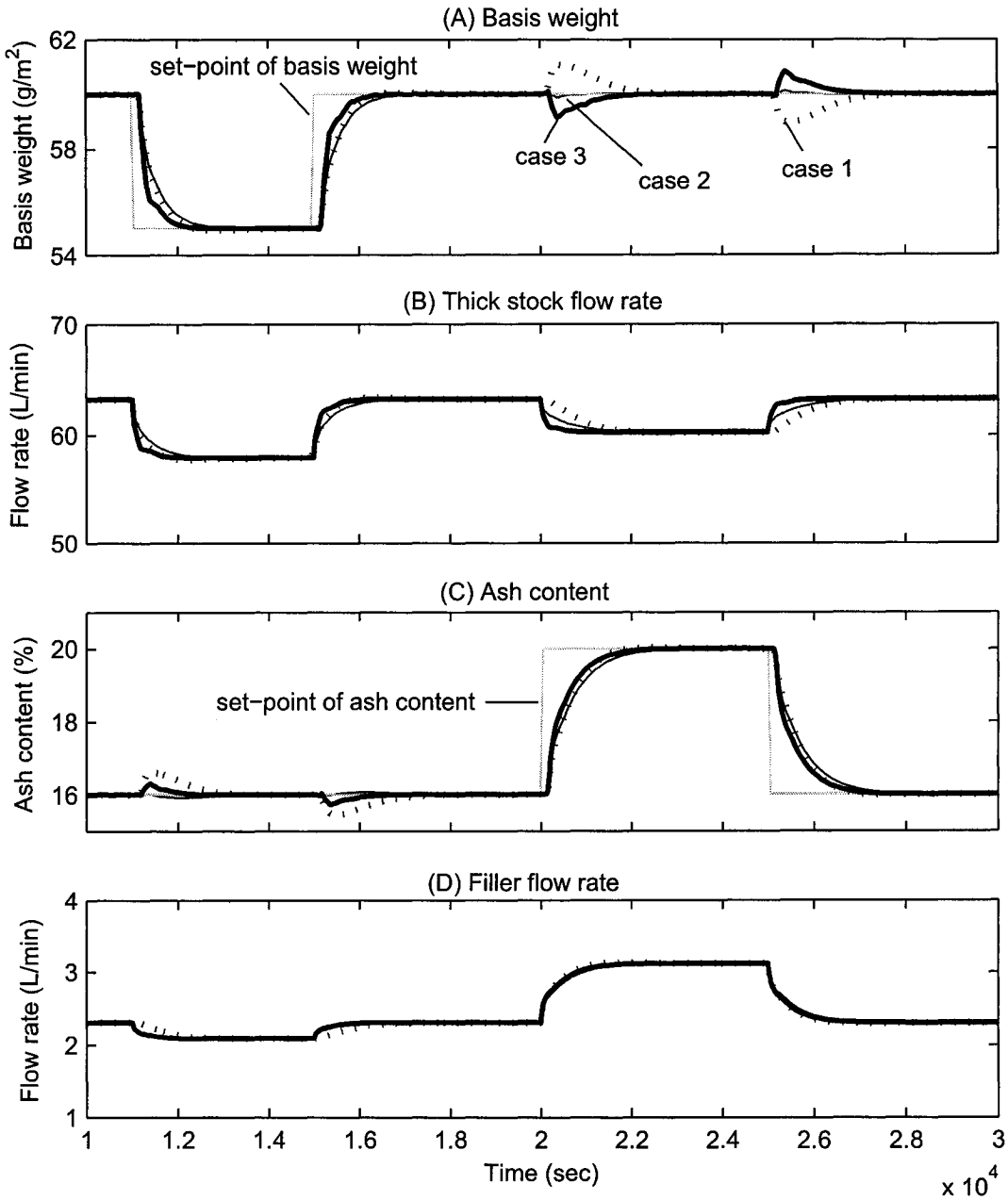

Figure 6.1. Comparison of three control schemes for basis weight and paper ash content when the set-points of the basis weight and the ash content are step-changed. Step changes of the basis weight set-point: 60 to 55 g/m^2 at 11000 sec. and reverse at 15000 sec. Step changes of the ash content set-point: 16 to 20 % at 20000 sec. and reverse at 25000 sec. Case 1 (dotted line): control of basis weight and ash content without decoupling; case 2 (thin solid line): control of basis weight and ash content with decoupling; case 3 (thick solid line): control of pulp mass and filler mass.

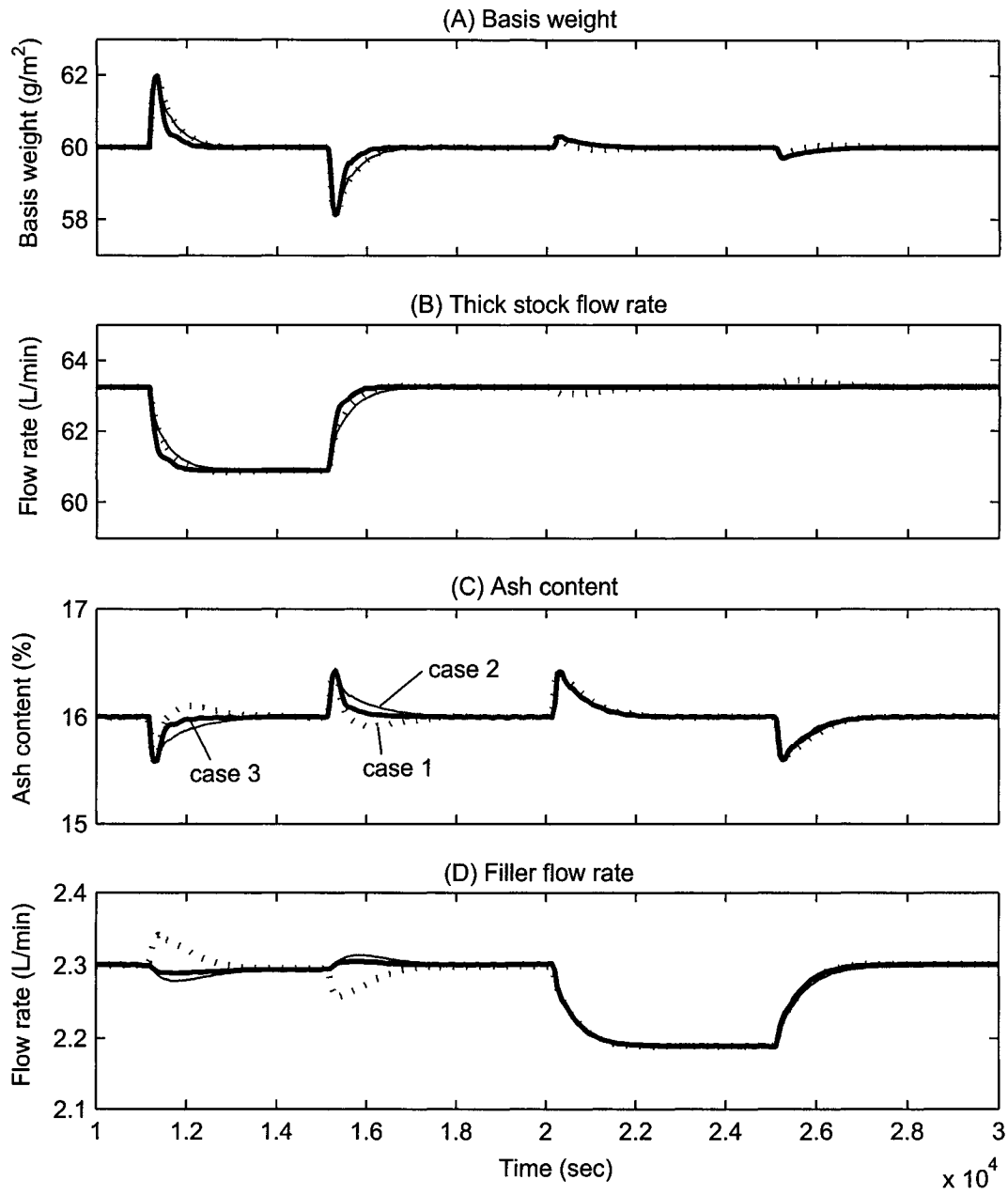

Figure 6.2. Comparison of three control schemes for basis weight and paper ash content when disturbances are introduced into the thick stock total consistency and the filler slurry concentration. Step changes of the thick stock total consistency: 2.6 to 2.7 % at 11000 sec and reverse at 15000 sec. Step changes of the filler slurry concentration: 10 to 10.5 % at 20000 sec and reverse at 25000 sec.
Case 1 (dotted line): control of basis weight and ash content without decoupling; case 2 (thin solid line): control of basis weight and ash content with decoupling; case 3 (thick solid line): control of pulp mass and filler mass.

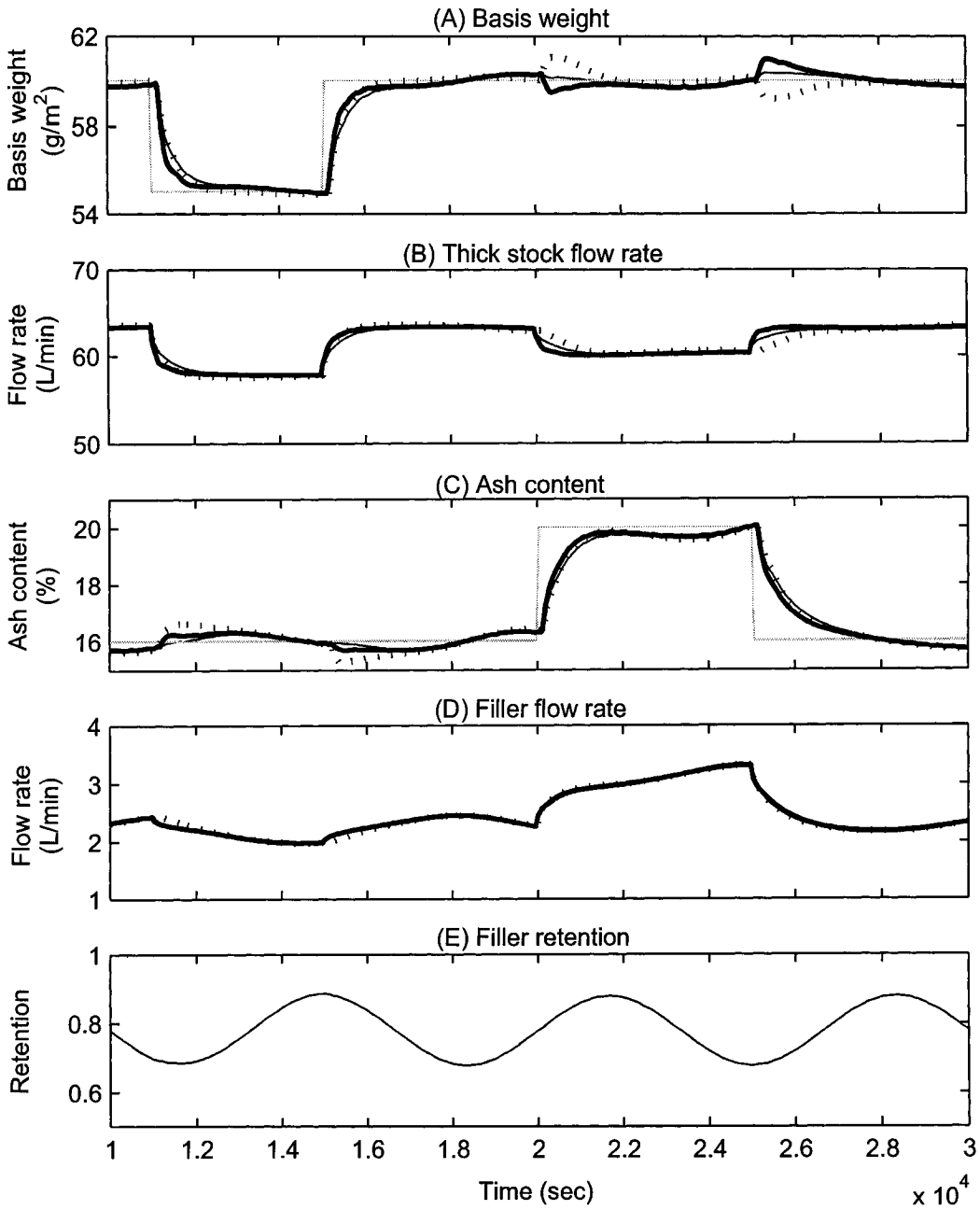

Figure 6.3. Comparison of three control schemes for basis weight and paper ash content when sinusoidal disturbance is introduced into the filler and fines retention during the set-point changes of the basis weight and the ash content. Step changes of the basis weight set-point: 60 to 55 g/m^2 at 11000 sec. and reverse at 15000 sec. Step changes of the ash content set-point: 16 to 20 % at 20000 sec. and reverse at 25000 sec. Case 1 (dotted line): control of basis weight and ash content without decoupling; case 2 (thin solid line): control of basis weight and ash content with decoupling; case 3 (thick solid line): control of pulp mass and filler mass.

Varying the first-pass retention of filler and fines directly results in variations in basis weight and ash content. Sinusoidal disturbance with an amplitude of 0.1 was introduced into the filler and fines retention during the set-point changes of basis weight and ash content. The resulted variation in filler and fines retention is shown in Figure 6.3-(E). All three control systems are able to handle the disturbances in retention during the set-point changes in basis weight and ash content (Figure 6.3-(A) and (C)). However, the responses become a bit oscillatory due to the variation in retention. The responses of the pulp mass and filler mass control system are similar with the basis weight and ash content control system with decoupling. The response of basis weight and ash content control system without decoupling is more oscillatory.

6.4 Control of white water consistency

The idea of white water consistency control is to bring under control the white water consistency by manipulating the flow rate of retention aids through which retention and the whole wet end are stabilized. Typically, the controlled variable is the white water total consistency and the manipulated variable is the flow rate of polymer solution.

Figure 6.4 compares the pulp mass and filler mass control system with and without white water total consistency control system. The white water total consistency control loop was implemented separately (SISO control). Sinusoidal disturbance with an amplitude of 0.1 was introduced into the filler and fines retention during the set-point changes of basis weight and ash content. Without the white water total consistency control, the variations in the white water consistency are high,

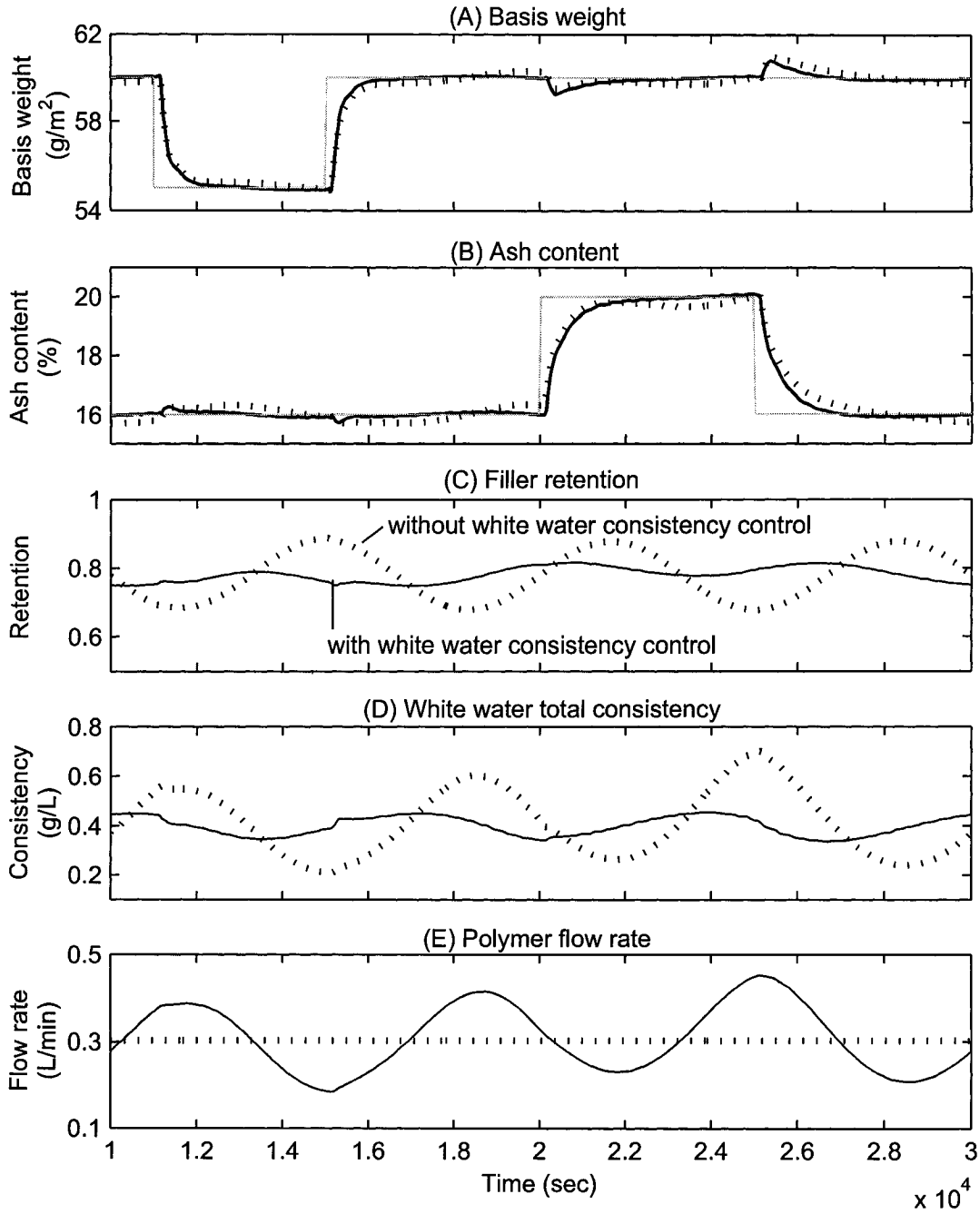

Figure 6.4. Effect of the white water consistency control. The pulp mass and filler mass control systems with (solid line) and without (dotted line) the white water total consistency control are compared. Step changes of the basis weight set-point: 60 to 55 g/m^2 at 11000 sec. and reverse at 15000 sec. Step changes of the ash content set-point: 16 to 20 % at 20000 sec. and reverse at 25000 sec. Sinusoidal disturbance with an amplitude of 0.1 was introduced into the fines and filler retention during the set-point changes of the basis weight and the ash content.

which is influenced by the variations in retention. The varied white water consistency directly affects the basis weight and the ash content of paper. When the white water total consistency is controlled, the variations in retention and consequently in the white water total consistency are reduced, resulting in less oscillatory basis weight and ash content responses.

6.4.1 Comparison between white water total consistency control and white water filler consistency control

Several possibilities exist to choose a controlled variable for the white water consistency control: (1) white water total consistency; (2) white water fibre consistency; (3) white water fines consistency; and (4) white water filler consistency. Kajaani-RMi white water consistency sensor provides white water total consistency and white water filler consistency measurements [20, 47, 81]. White water pulp consistency, which consists of fibre and fines, can be calculated from the two measurements. First-pass retention of fibre does not vary substantially during papermaking and also is not influenced significantly by dosages of retention aids. Hence, white water fibre consistency should not be chosen as a controlled variable. Considering the fibre retention is a constant close to one, white water fines consistency might be calculated. However, reliability of fines measurement has not been substantiated yet. Consequently, the two remaining possibilities are: white water total consistency and white water filler consistency.

White water total consistency control and white water filler consistency control are compared in Figure 6.5. Both control systems handle well the sinusoidal disturbance in retention during the set-point changes of basis weight and ash content. The responses of both control systems are almost identical. These results suggest

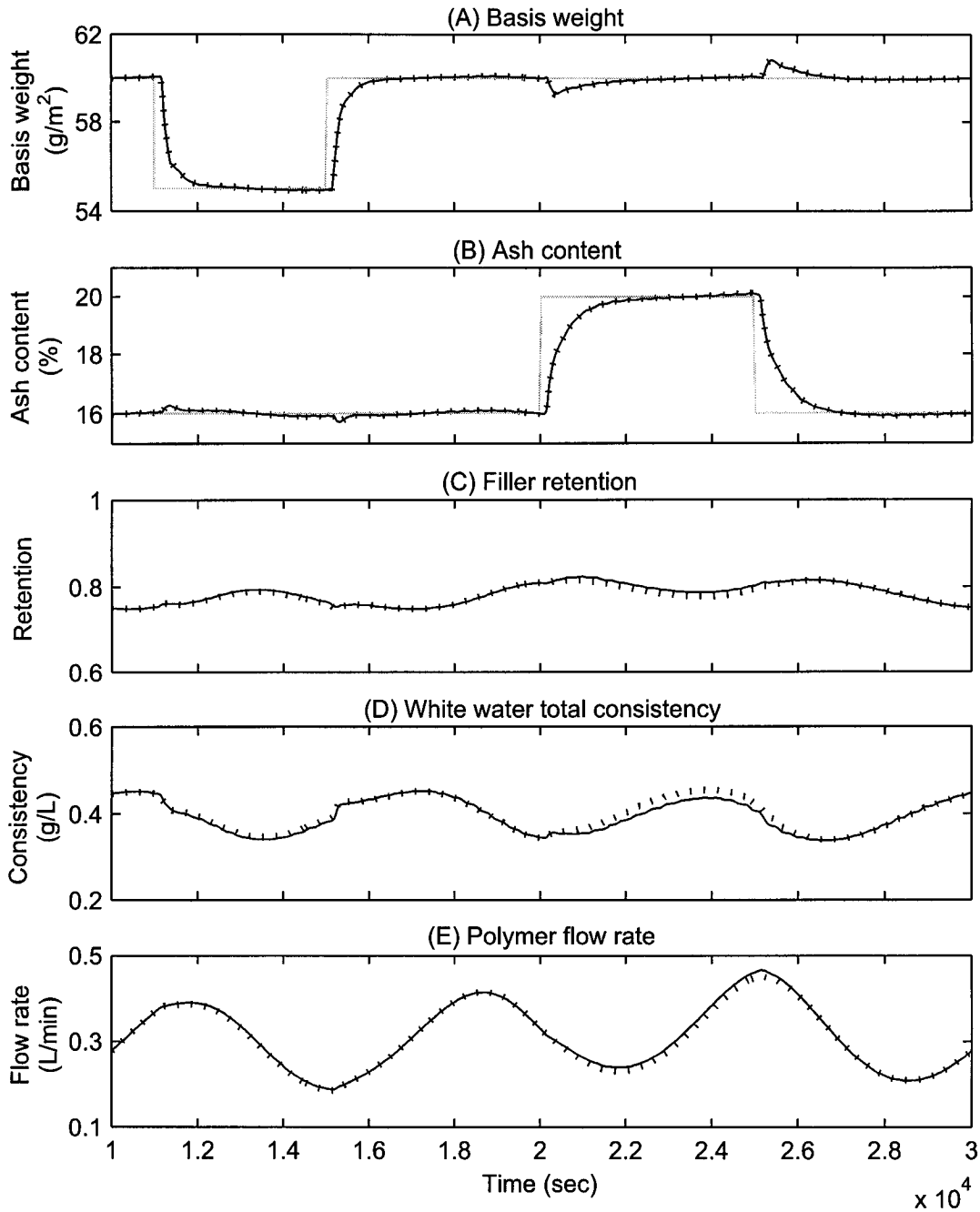

Figure 6.5. Comparison between the white water total consistency control (solid line) and the white water filler consistency control (dotted line). Step changes of the basis weight set-point: 60 to 55 g/m^2 at 11000 sec and reverse at 15000 sec. Step changes of the ash content set-point: 16 to 20 % at 20000 sec and reverse at 25000 sec. Sinusoidal disturbance with an amplitude of 0.1 was introduced into the fines and filler retention during the set-point changes of the basis weight and the ash content.

that either variable between the white water total consistency and the white water filler consistency can be chosen as a controlled variable. In practice, it will depend on the paper grade produced. If a paper machine produces highly filled paper, either white water filler consistency or white water total consistency can be chosen. If a paper machine produces a grade with no or low ash content, white water total consistency has to be chosen as a controlled variable. White water total consistency was chosen for the rest of this study.

6.4.2 Comparison between a constant bentonite flow rate and a ratio controlled bentonite flow rate

There also exist several possibilities to choose a manipulated variable to control white water consistency when a microparticulate retention aid system is used:

1. to regulate a polymer flow, keeping a constant microparticle flow rate;
2. to regulate a polymer flow, keeping a constant ratio between polymer and microparticle flow rates;
3. to regulate a microparticle flow, keeping a constant polymer flow rate; and
4. to regulate a microparticle flow, keeping a constant ratio between polymer and microparticle flow rates.

From the results in Chapter 3, it is clear that the polymer plays a more important role in controlling retention and consequently white water consistency. Hence, it is a more effective strategy to manipulate the flow rate of polymer solution to control the white water consistency than to manipulate the flow rate of bentonite suspension. During the manipulation of polymer flow, bentonite flow can be either

kept constant or manipulated in a certain way. Discussions in Chapters 3 and 4 suggest the ratio control for the bentonite flow. The physical meaning of controlling the ratio between the bentonite flow rate and the polymer flow rate is to control the surface coverage of bentonite onto the polymer covered surface on fibre. A bentonite flow rate can be ratio controlled by:

$$\triangle F_{mp} = K_{mp} \Delta F_{pol} \tag{6.17}$$

where F_{mp} represents the flow rate of microparticle suspension, F_{pol} is the flow rate of polymer solution and K_{mp} can be calculated with:

$$K_{mp} = \frac{\mu_i A_{pol} C_{pol}}{A_{mp} C_{mp}} \tag{6.18}$$

where A_{pol} and A_{mp} are the maximum coverage of polymer and microparticle; C_{pol} and C_{mp} the concentrations of polymer solution and microparticle suspension; and μ_i is the target surface coverage of bentonite on polymer covered surface.

Figures 6.6 and 6.7 compare the responses of a paper machine with a constant bentonite flow to that with a ratio controlled bentonite flow during the white water set-point changes. The responses of basis weight, ash content and white water total consistency during the set-point changes are identical. The only difference is the response of formation. Variations in formation are smaller when the bentonite flow rate is ratio controlled. This can be explained by the bridging strength (Chapter 4). When the polymer flow rate is increased, keeping a constant bentonite flow rate, to reduce the white water consistency at 15000 sec in Figure 6.6, the surface coverage of polymer without bentonite is increased, resulting in the increased interactions between bare fibre and polymer covered fibre surfaces and hence the increased bridging strength. This leads to the increased fibre flocculation and then impaired paper formation. On the other hand, when the polymer flow rate is increased, keeping the ratio between polymer and microparticle flow rates constant,

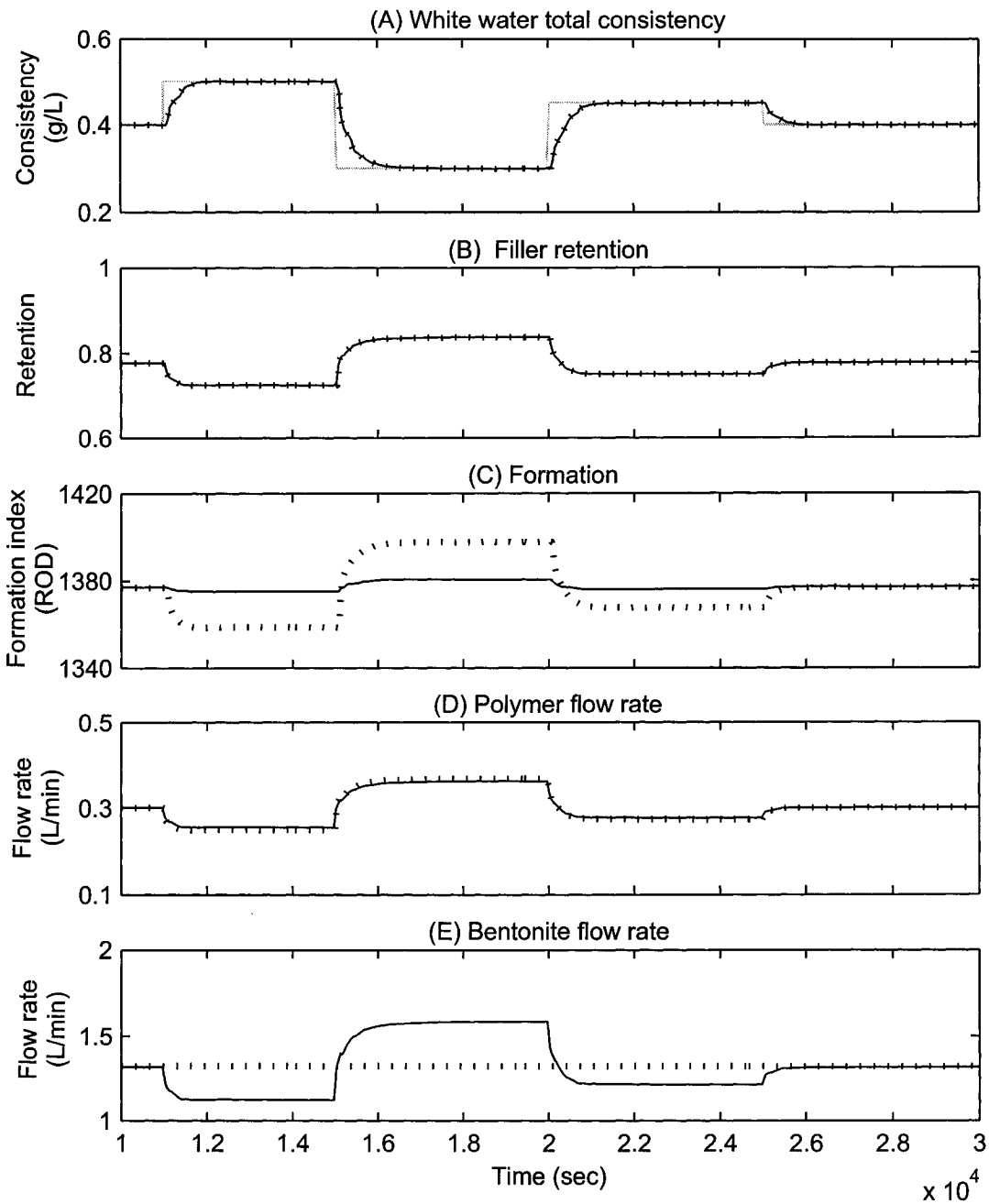

Figure 6.6. Comparison between the white water total consistency control with a ratio controlled bentonite flow (solid line) and that with a constant bentonite flow (dotted line). Responses of white water total consistency, filler retention, formation, polymer flow rate and bentonite flow rate to the set-point changes of the white water total consistency. Step changes of the white water total consistency set-point: 0.4 to 0.5 g/L at 11000 sec, 0.5 to 0.3 g/L at 15000 sec, 0.5 to 0.45 g/L at 20000 sec and 0.45 to 0.5 g/L at 25000 sec.

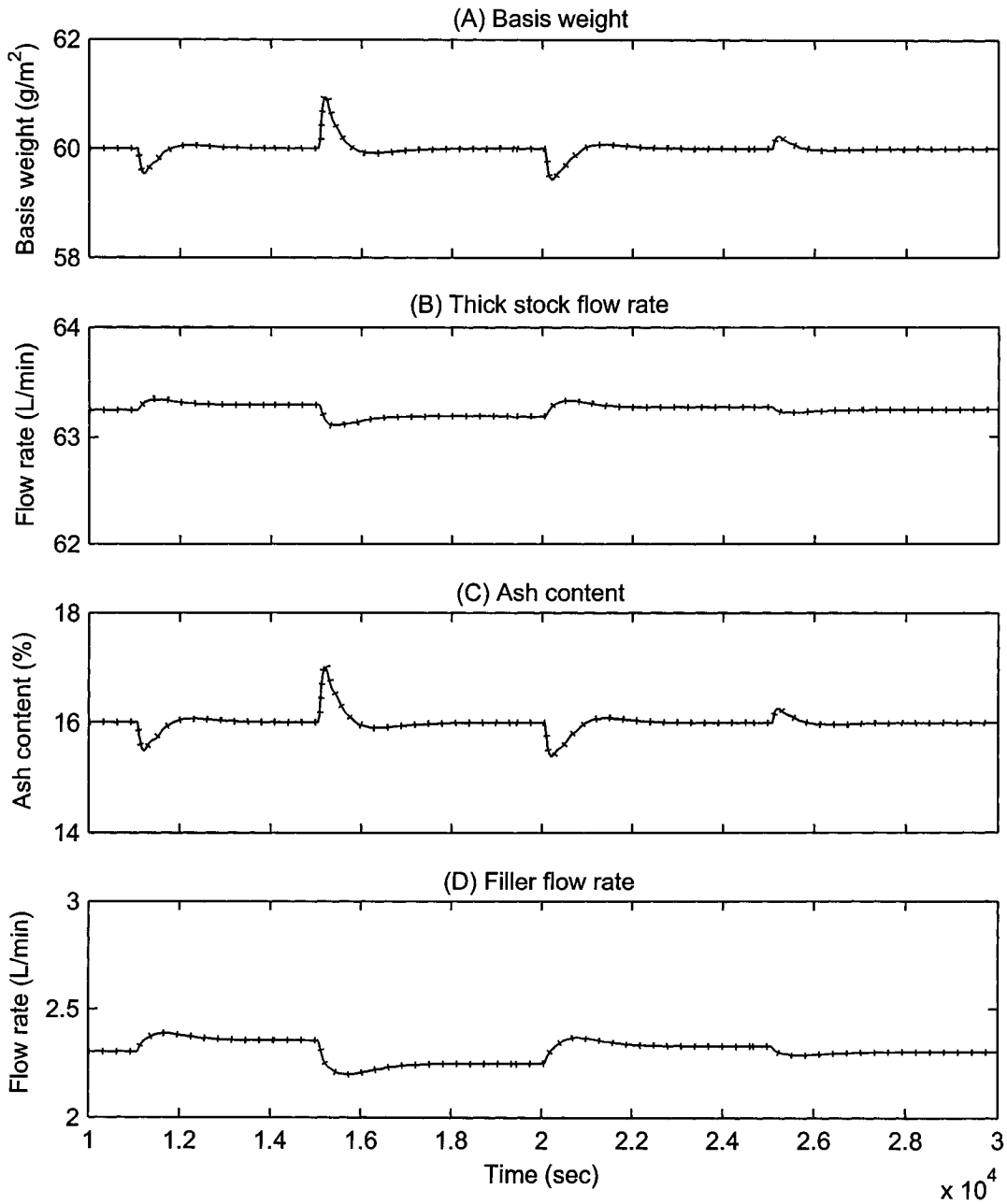

Figure 6.7. Comparison between the white water total consistency control with a ratio controlled bentonite flow (solid line) and that with a constant bentonite flow (dotted line). Responses of basis weight, thick stock flow rate, ash content and filler flow rate to the set-point changes of the white water total consistency. Step changes of the white water total consistency set-point: 0.4 to 0.5 g/L at 11000 sec, 0.5 to 0.3 g/L at 15000 sec, 0.5 to 0.45 g/L at 20000 sec and 0.45 to 0.5 g/L at 25000 sec.

the increase in the polymer covered surface without microparticle is minimized, resulting in smaller variations in the bridging strength and the paper formation. The target surface coverage of bentonite on the polymer covered fibre surface was 0.7.

Figures 6.8 and 6.9 show the responses of a paper machine to the sinusoidal disturbance introduced into the fines and filler retention during the set-point changes of basis weight and ash content. All of the responses of the paper machine are identical for both of the white water consistency control schemes except formation. When the bentonite flow is ratio controlled, it provides constant surface coverage of bentonite on the polymer covered fibre surface and hence less variations in formation. The variations in formation in case of the ratio controlled bentonite in Figure 6.8-(C) are mainly due to the changes in the headbox pulp consistency.

These results confirm that the only difference between the white water consistency control with a constant bentonite flow and with a ratio controlled bentonite is the response of formation. It is recommended that when a microparticulate retention aid system is used and formation is concerned, the ratio of bentonite dosage to polymer dosage has to be controlled while the flow rate of a polymer solution is manipulated based on white water consistency measurements.

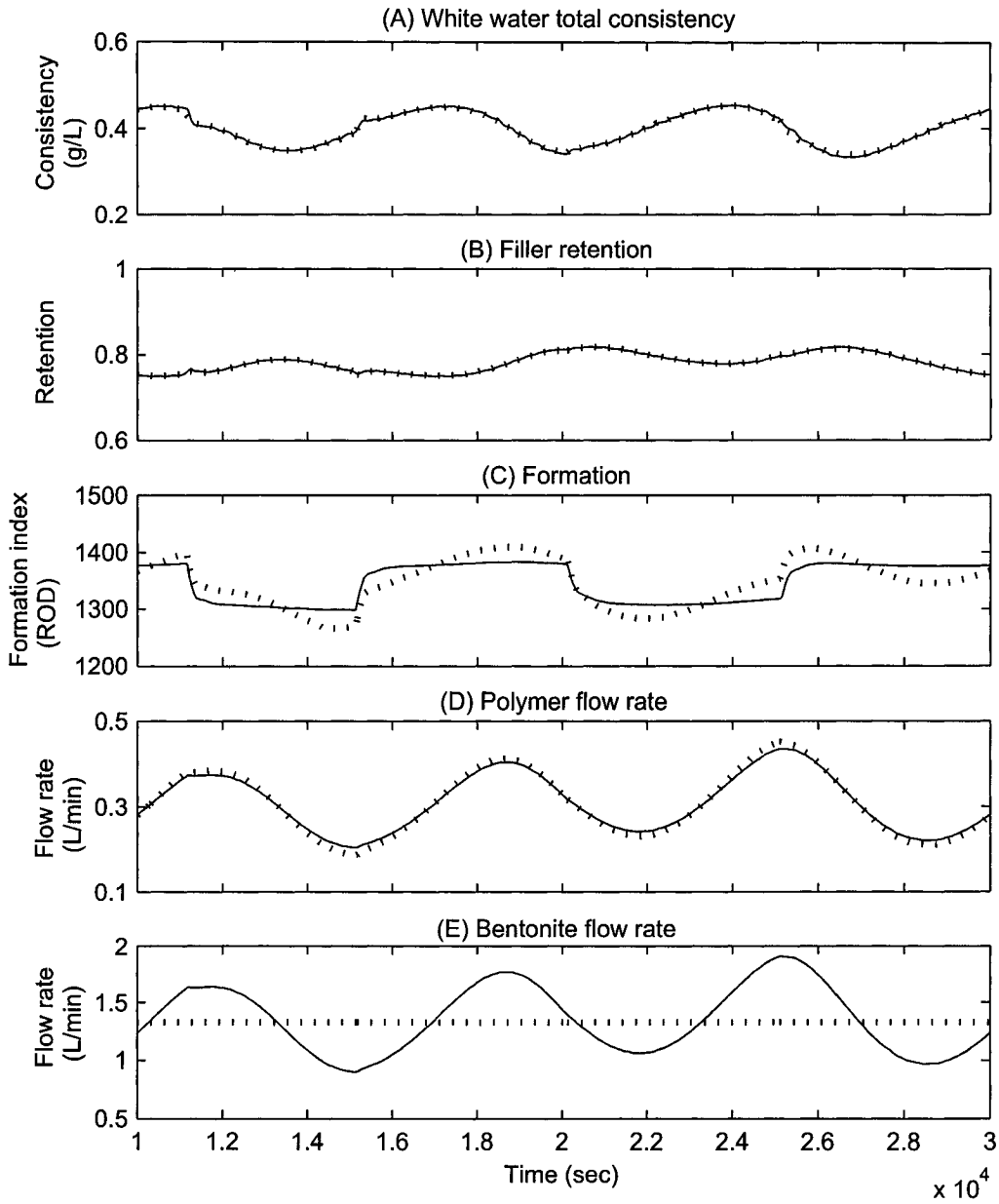

Figure 6.8. Comparison between the white water total consistency control with a ratio controlled bentonite flow (solid line) and that with a constant bentonite flow (dotted line). Responses of white water total consistency, filler retention, formation, polymer flow rate and bentonite flow rate to the set-point changes of the basis weight and the ash content. Step changes of the basis weight set-point: 60 to 55 g/m^2 at 11000 sec and reverse at 15000 sec. Step changes of the ash content set-point: 16 to 20 % at 20000 sec and reverse at 25000 sec. Sinusoidal disturbance with an amplitude of 0.1 was introduced into the fines and filler retention during the set-point changes of the basis weight and the ash content.

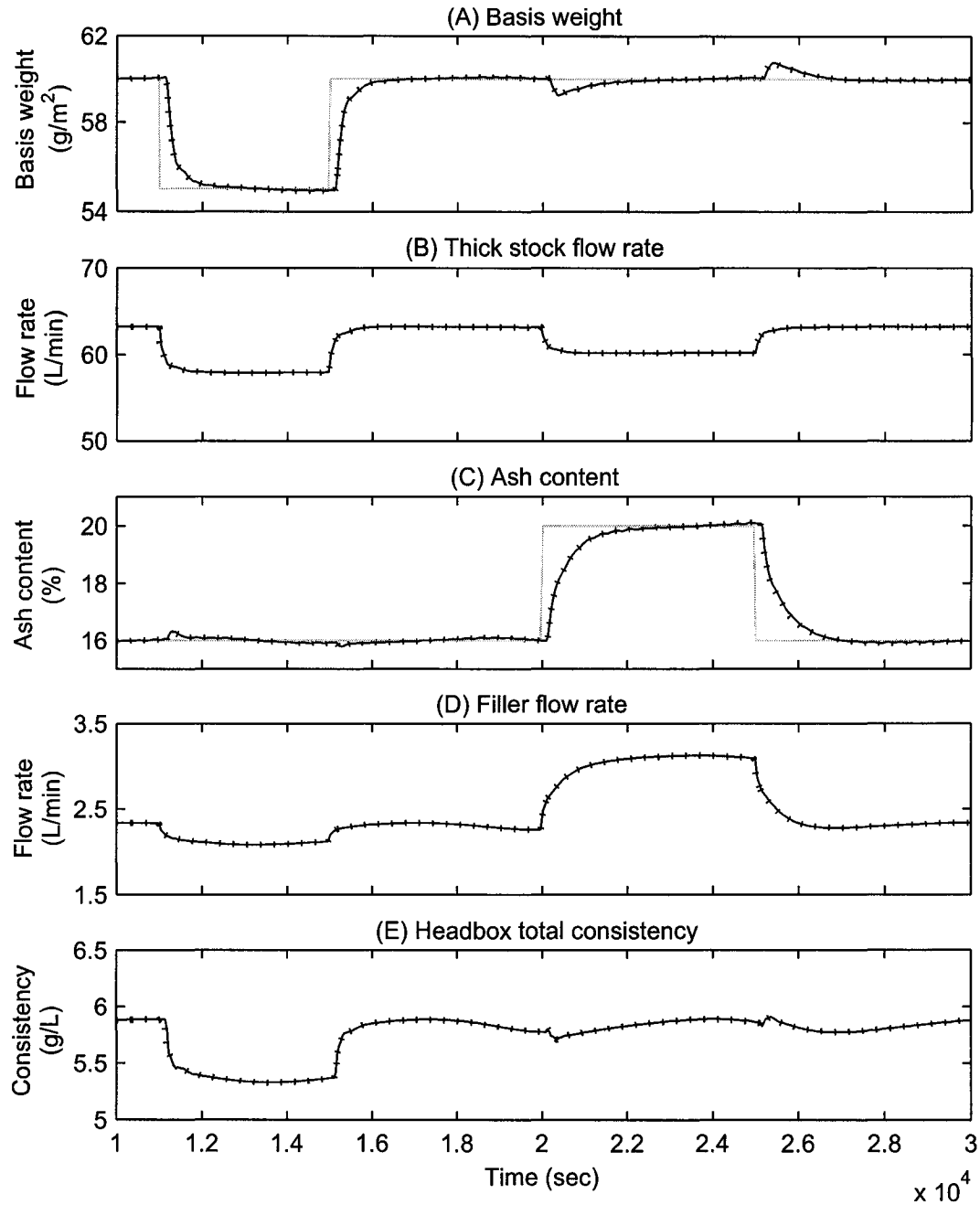

Figure 6.9. Comparison between the white water total consistency control with a ratio controlled bentonite flow (solid line) and that with a constant bentonite flow (dotted line). Responses of basis weight, thick stock flow rate, ash content, filler flow rate and headbox total consistency to the set-point changes of the basis weight and the ash content. Step changes of the basis weight set-point: 60 to 55 g/m^2 at 11000 sec and reverse at 15000 sec. Step changes of the ash content set-point: 16 to 20 % at 20000 sec and reverse at 25000 sec. Sinusoidal disturbance with an amplitude of 0.1 was introduced into the fines and filler retention during the set-point changes of the basis weight and the ash content.

6.4.3 Set-points of white water consistency during grade changes

The determination of set-points of white water consistency is problematic. Generally, the white water consistency measured when the controller is in manual mode is chosen as a set-point. This would work well when a paper machine produces a single grade of paper. However, different white water consistency values might be needed for different grades when several grades of paper are produced in a paper machine.

White water consistency is mainly influenced by the basis weight and the ash content of the paper produced, which decide the flow rates and the consistencies of thick stock and filler slurry, and the first-pass retention of solids. Hence, the problem of different white water consistency set-points can be solved by collecting pairs of basis weight, ash content and white water consistency and developing an empirical model of the white water consistency as a function of basis weight and ash content. Then, the set-points of white water consistency can be calculated from the set-points of basis weight and ash content. To ensure smooth transition in grade changes, the set-points can be configured to follow a first-order model dynamics or a ramp type transition from one value to another. The transition pattern and speed are limited by: the inherent limitations of a paper machine such as dewatering capacity of wire section, steam pressure and machine speed; operator's experience and knowledge; operational procedure; and process dynamic coordination [123].

Two cases are compared in Figures 6.10 and 6.11: (1) grade changes with a constant set-point of white water total consistency; and (2) grade changes with automatic set-point changes of white water total consistency according to the set-points of basis weight and ash content. For the simulation, basis weight and

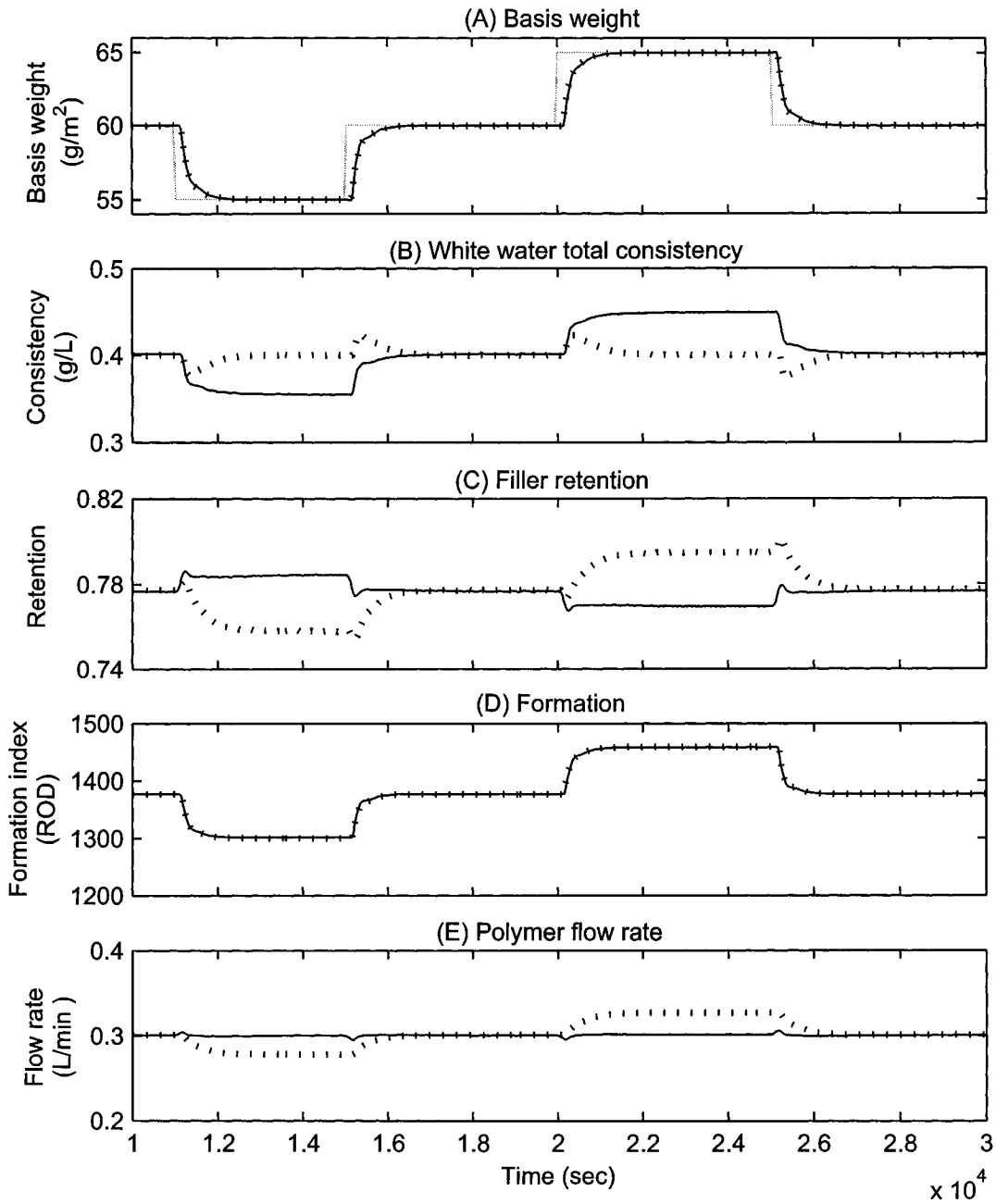

Figure 6.10. Comparison between a constant set-point (dotted line) and automatic set-point changes (solid line) of white water total consistency. Responses of basis weight, white water total consistency, filler retention, formation and polymer flow rate to the set-point changes of the basis weight. Step changes of the basis weight set-point: 60 to 55 g/m^2 at 11000 sec. and reverse at 15000 sec, and 60 to 65 g/m^2 at 20000 sec and reverse at 25000 sec.

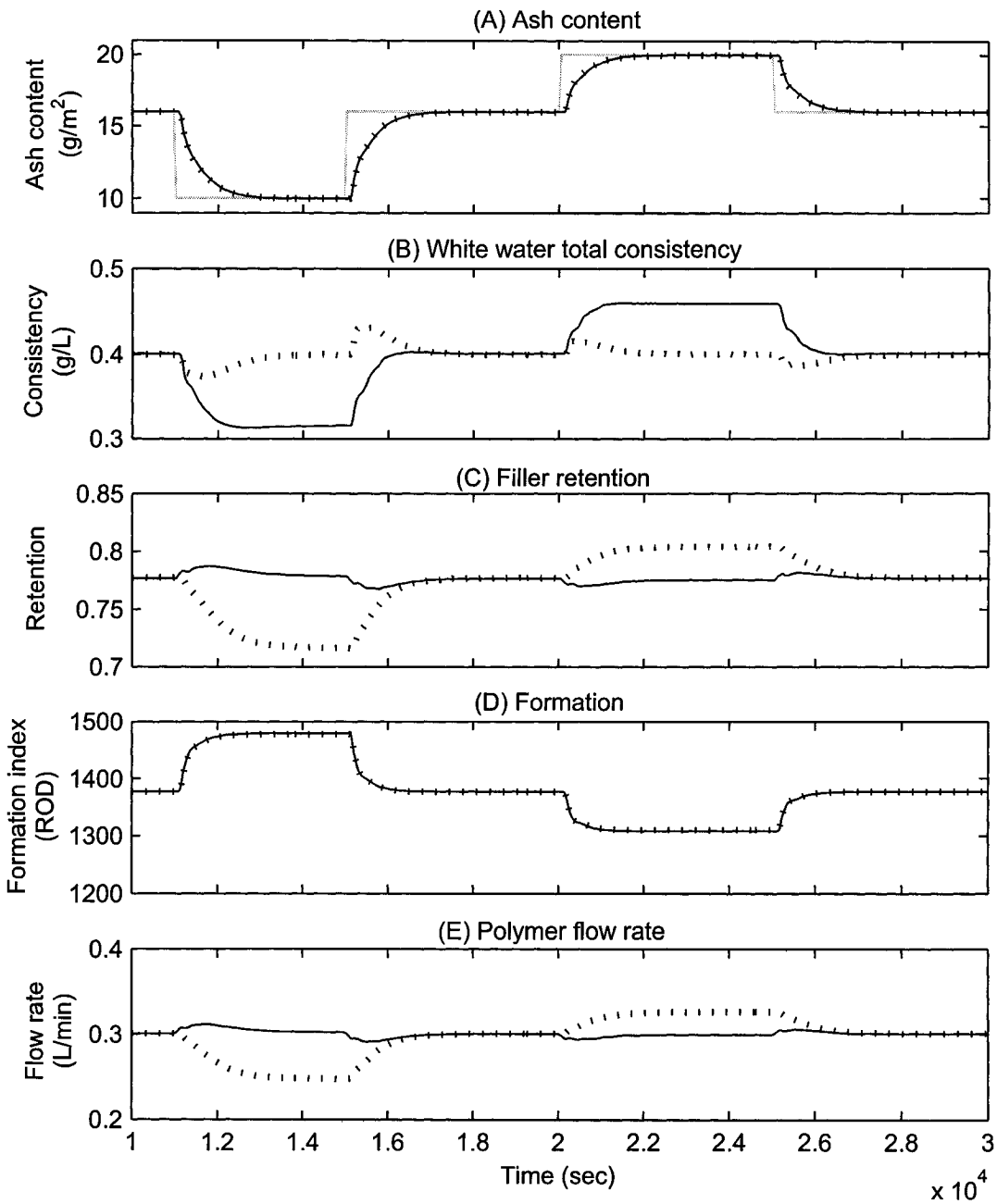

Figure 6.11. Comparison between a constant set-point (dotted line) and automatic set-point changes (solid line) of white water total consistency. Responses of ash content, white water total consistency, filler retention, formation and polymer flow rate to the set-point changes of the ash content. Step changes of the ash content set-point: 16 to 10 % at 11000 sec. and reverse at 15000 sec, and 16 to 20 % at 20000 sec and reverse at 25000 sec.

ash content were controlled by the pulp mass and filler mass control system. The white water total consistency was controlled by manipulating polymer flow. Bentonite flow was ratio controlled. The model for the set-points of white water total consistency was developed from a second order polynomial regression.

The responses of basis weight, ash content and formation are identical between two cases. When a set-point is kept, the variations in the fines and filler retention and the polymer flow rate are higher. When the set-point of basis weight or ash content is decreased, the flow rate of thick stock or filler slurry decreases, resulting in the decrease in the headbox pulp or filler consistency and consequently the white water total consistency. To recover the white water total consistency to the set-point value, the polymer flow rate and the bentonite flow rate are decreased to reduce the fines and filler retention and consequently to increase the white water consistency. On the other hand, when set-points of white water consistency are varied according to the changes in basis weight and ash content, the water water consistency control system let the consistency decrease and there are no significant changes in the polymer and bentonite flow. Variations in retention are also minimized in case of automatic set-point changes of white water total consistency.

6.5 Control of headbox pulp consistency

One of the main factors affecting formation is the number of contacts between fibres, which can be expressed by the crowding number and is mainly influenced by fibre consistency and fibre dimensions by the equation 4.3. Considering that fibre dimension is a fixed factor for a given grade, which is determined by the type of pulp used and the refining degree, fibre consistency is the main factor influencing formation. Variations in headbox pulp consistency, which can occur during grade

changes and can be introduced by disturbances in the thick stock pulp consistency and the thick stock flow rate, can results in variations in paper formation.

The headbox pulp consistency disturbances can be eliminated by either controlling thick stock consistency or directly controlling the headbox pulp consistency. The details of the feedforward control system of thick stock consistency were discussed elsewhere [81]. It manipulates the thick stock valve based on thick stock consistency measurements, which is also connected to the feedback basis weight control loop. The feedforward control system prevents the disturbances in thick stock consistency from reaching the headbox and thus the paper. What is really controlled is the thick stock mass flow rate or the headbox mass flow rate.

During grade changes, the changes in the thick stock flow rate influence both the mass flow rate and the consistency of headbox stock. The variations in the headbox pulp consistency will influence the degree of fibre flocculation and then paper formation. Hence, it is required to keep a constant pulp consistency for a uniform formation while the mass flow rate of headbox stock is varied according to the changes in basis weight. The headbox pulp consistency control strategy could be beneficial especially when grade is changed from a low basis weight to a higher basis weight since the increased headbox pulp consistency can deteriorate paper formation.

Headbox pulp consistency can be controlled by manipulating the flow rates of either the dilution water into the headbox or the recirculating white water. The pilot paper machine used for this study manipulates headbox flow rate to control the headbox consistency. If the headbox flow rate is increased, keeping a constant thick stock flow rate and filler flow rate, the flow rate of the recirculating white water from the wire pit is increased and consequently the headbox consistency is decreased, and *vice versa.*

Headbox pulp consistency control was tested through simulation. In the control system, the headbox valve opening and hence the headbox flow rate is manipulated based on headbox pulp consistency measurements. The headbox consistency sensor provides headbox total consistency and headbox ash consistency measurements. The headbox pulp consistency was calculated from the two measurements. It was assumed that the headbox valve opening is controlled by an automatic control system. The pulp mass and the filler mass in paper and white water total consistency were controlled as well. Figures 6.12 and 6.13 compare responses of a paper machine with a headbox pulp consistency control to that without a headbox pulp consistency control system when disturbances are introduced to the thick stock consistency and the filler slurry consistency. When the filler slurry consistency was disturbed at 20000 and 25000 sec, the responses of the two systems (with and without a headbox pulp consistency control) are identical. When thick stock total consistency was step-changed at 11000 and 15000 sec, paper formation responds faster when headbox pulp consistency is controlled (Figure 6.12-(C)). This is simply due to the faster stabilization of headbox pulp consistency (Figure 6.12-(D)). The headbox pulp consistency control also helps eliminating the effects of thick stock consistency disturbances on headbox total consistency and white water total consistency (Figure 6.13).

Figures 6.14 and 6.15 compare the responses of a paper machine with and without the headbox pulp consistency control during grade changes. The responses of basis weight and ash content are almost identical in both cases (Figures 6.14-(A) and (B)). The variations in formation are considerably reduced when the headbox pulp consistency is controlled (Figures 6.14-(C) and (D)). When the set-point of ash content is increased at 20000 sec, keeping the set-point of basis weight constant, the flow rate of thick stock is reduced while the flow rate of filler slurry is

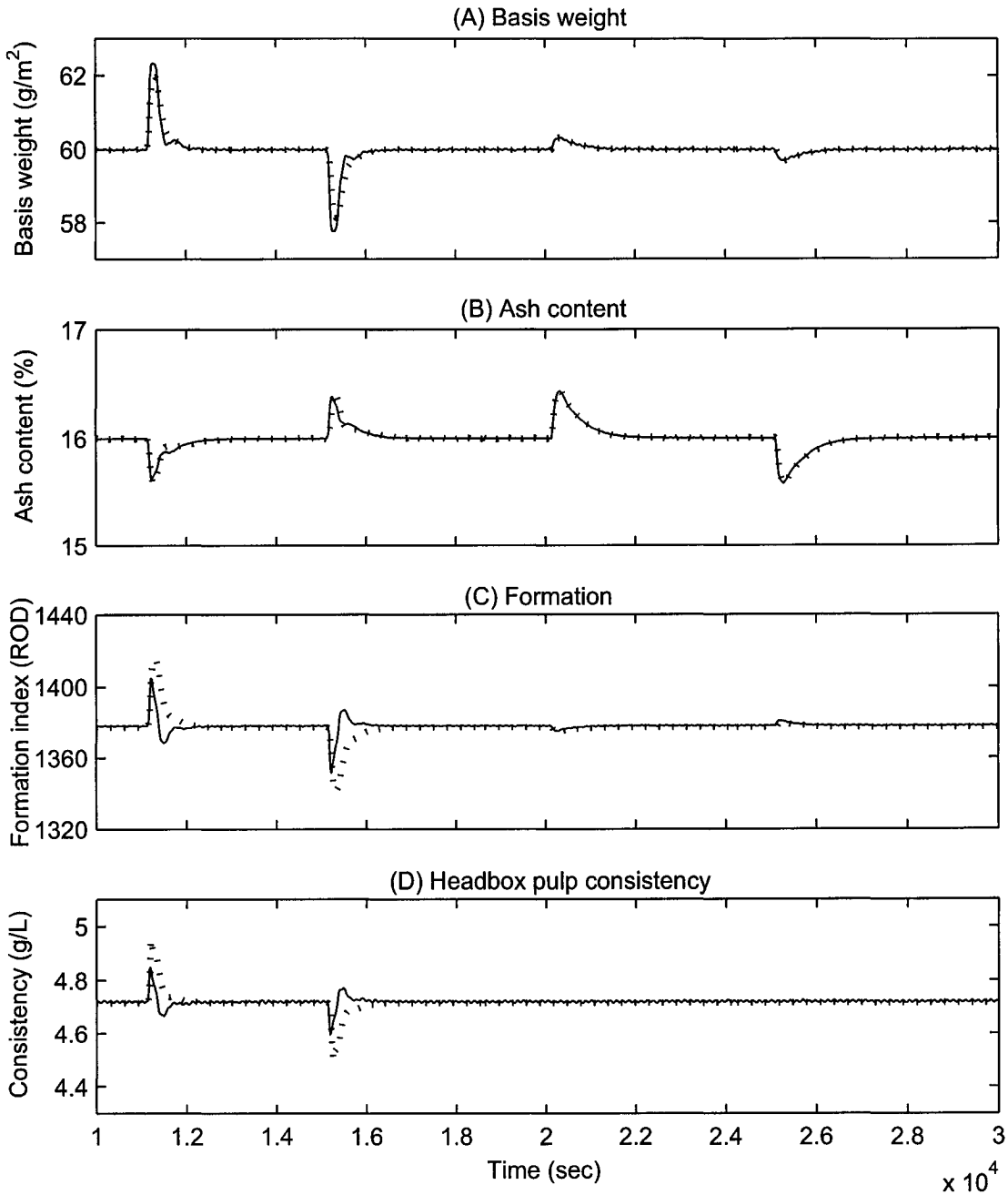

Figure 6.12. Effect of the headbox pulp consistency control. Responses of basis weight, ash content, formation and headbox pulp consistency to perturbations of thick stock total consistency and filler slurry consistency with (solid line) and without (dotted line) headbox consistency control. Step changes of the thick stock total consistency: 2.6 to 2.7 % at 11000 sec and reverse at 15000 sec. Step changes of the filler slurry consistency: 10 to 10.5 % at 20000 sec and reverse at 25000 sec.

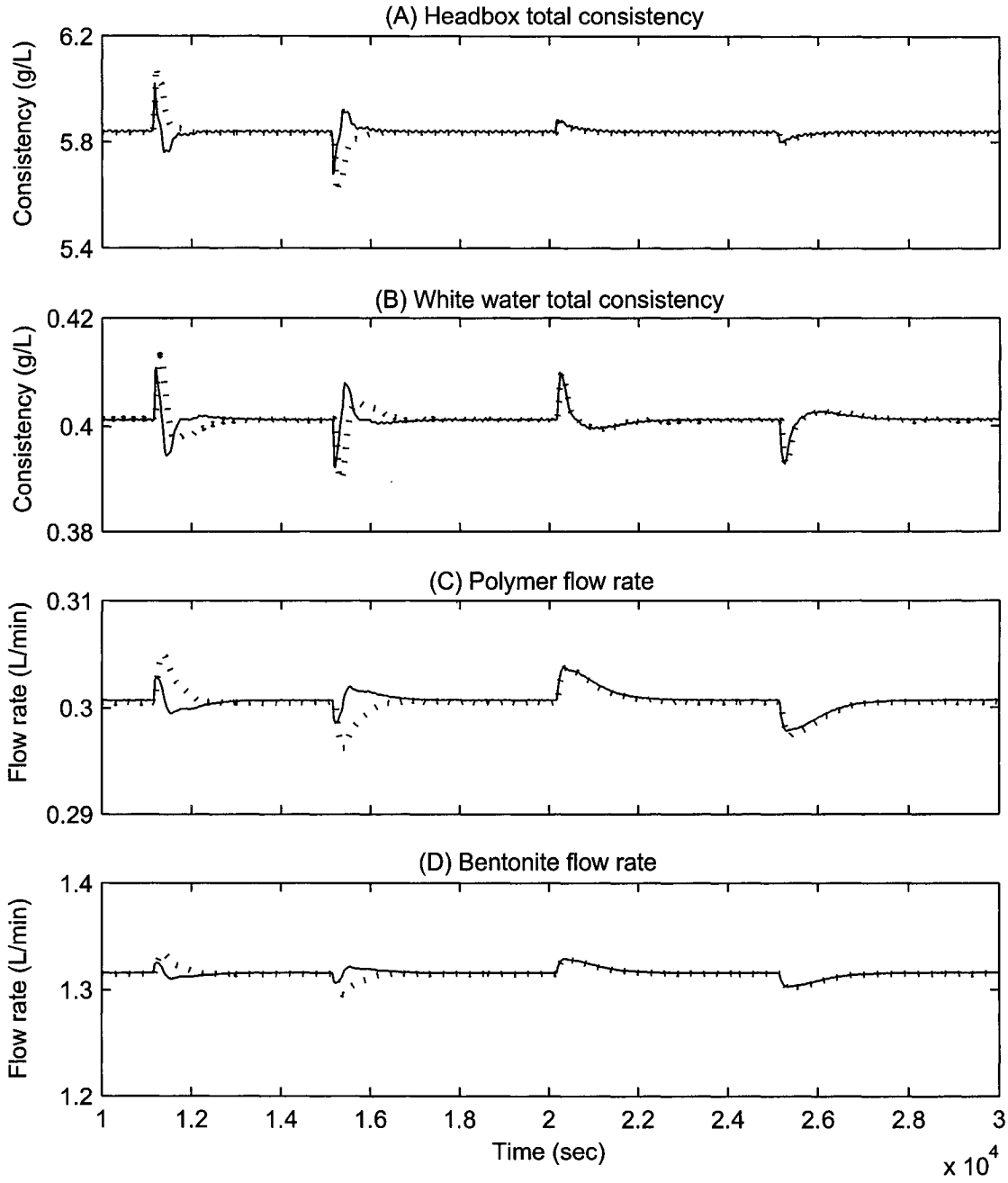

Figure 6.13. Effect of the headbox pulp consistency control. Responses of headbox total consistency, white water total consistency, polymer flow rate and bentonite flow rate to perturbations of thick stock total consistency and filler slurry consistency with (solid line) and without (dotted line) headbox consistency control. Step changes of the thick stock total consistency: 2.6 to 2.7 % at 11000 sec and reverse at 15000 sec. Step changes of the filler slurry consistency: 10 to 10.5 % at 20000 sec and reverse at 25000 sec.

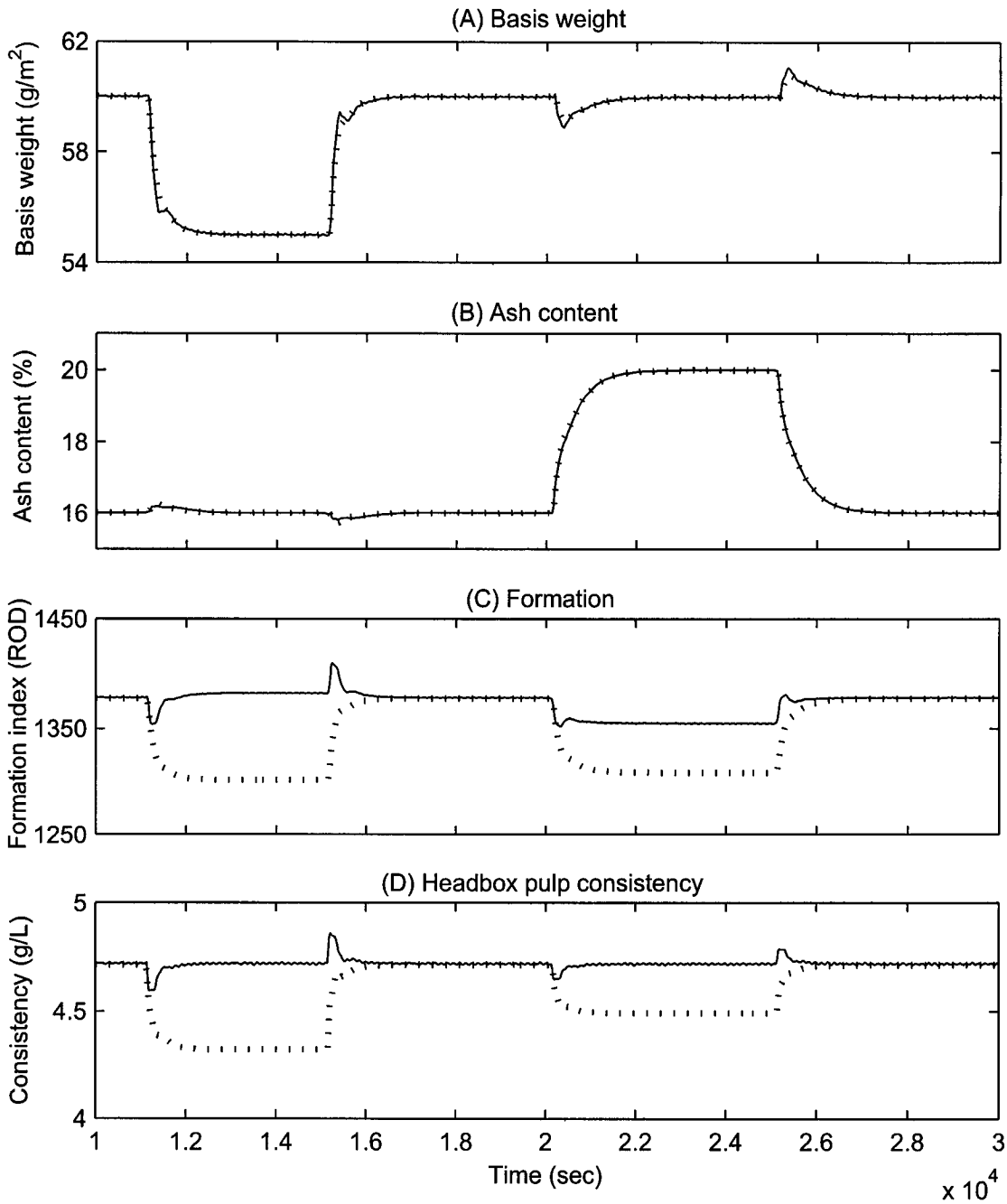

Figure 6.14. Effect of the headbox pulp consistency control. Responses of basis weight, ash content, formation and headbox pulp consistency to the set-point changes of the basis weight and the ash content with (solid line) and without (dotted line) the headbox pulp consistency control. Step changes of the basis weight set-point: 60 to 55 g/m^2 at 11000 sec and reverse at 15000 sec. Step changes of the ash content set-point: 16 to 20 % at 20000 sec and reverse at 25000 sec.

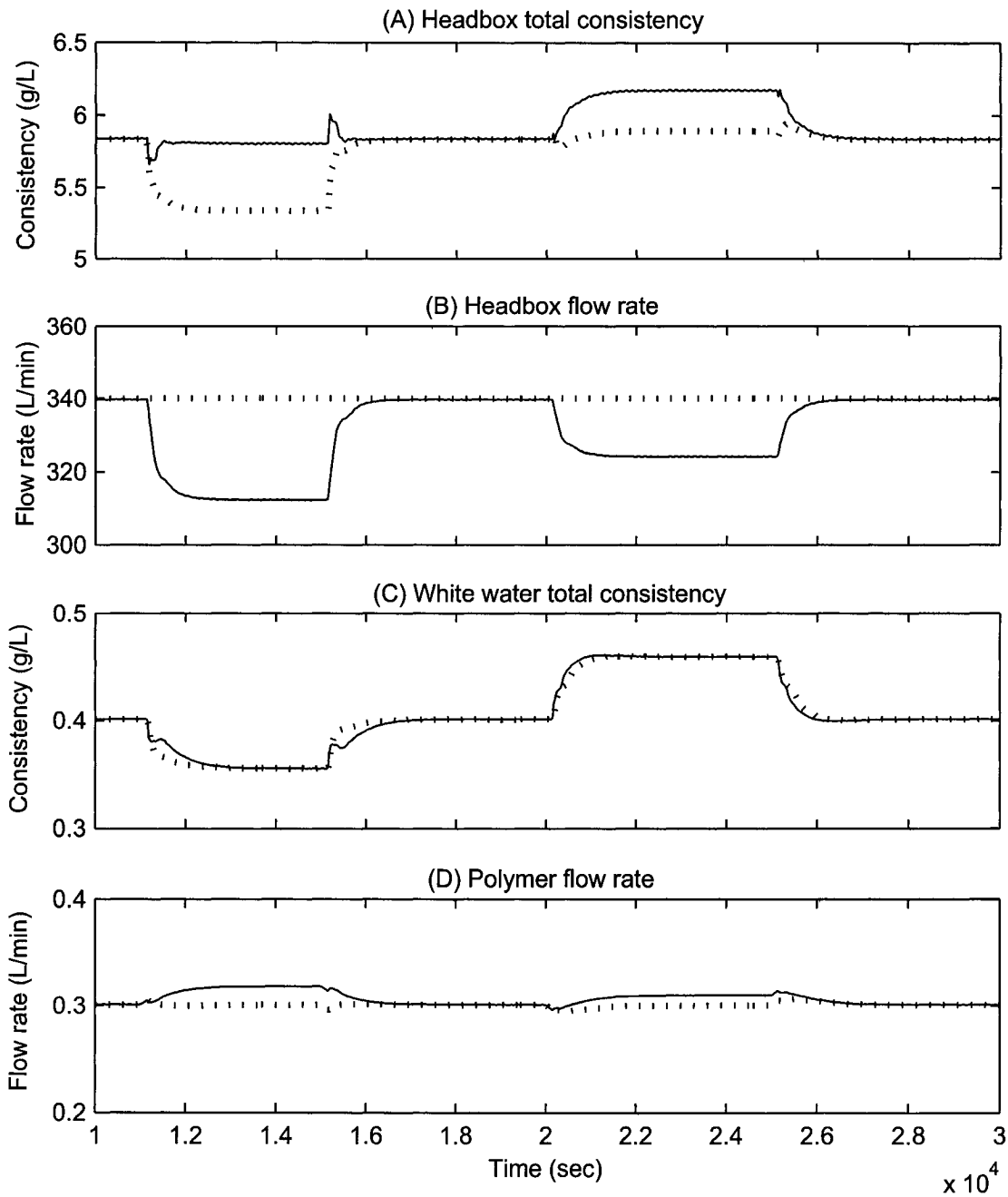

Figure 6.15. Effect of the headbox pulp consistency control. Responses of headbox total consistency, headbox flow rate, white water total consistency and polymer flow rate to the set-point changes of the basis weight and the ash content with (solid line) and without (dotted line) the headbox pulp consistency control. Step changes of the basis weight set-point: 60 to 55 g/m^2 at 11000 sec and reverse at 15000 sec. Step changes of the ash content set-point: 16 to 20 % at 20000 sec and reverse at 25000 sec.

increased. The reduced thick stock flow rate would result in the decreased headbox pulp consistency. To keep the headbox pulp consistency at set-point value, the headbox flow rate is reduced (Figures 6.15-(B)) and as a result the headbox total consistency is increased at 20000 sec (Figures 6.15-(A)). The increased headbox total consistency will influence the white water total consistency. To keep the white water consistency to the set-point, the white water consistency control loop reacts and hence the polymer flow rate is varied.

6.6 Multivariable control

Two types of control strategies are tested through simulation: (1) control of pulp mass and filler mass in paper and white water total consistency; (2) control of pulp mass and filler mass in paper, white water total consistency and headbox pulp consistency. As discussed in previous sections, the pulp mass in paper is controlled by thick stock flow rate, the filler mass in paper by filler flow, the white water total consistency by the polymer flow (with the ratio-controlled bentonite flow) and the headbox pulp consistency by headbox flow rate. For comparisons, same tuning rules are applied for sing-input single-output (SISO) and multi-input multi-output (MIMO) control.

SISO control and MIMO control are compared in Figures 6.16-6.19. In Figures 6.16 and 6.18, sinusoidal disturbances are introduced into the filler and fines retention during the set-point changes of basis weight and ash content. In Figures 6.17 and 6.19, disturbances are introduced into the thick stock consistency and the filler slurry consistency. Both SISO and MIMO control schemes are able to eliminate the disturbances well. In addition, when thick stock consistency and filler consistency were disturbed, the decoupling control is able to eliminate the

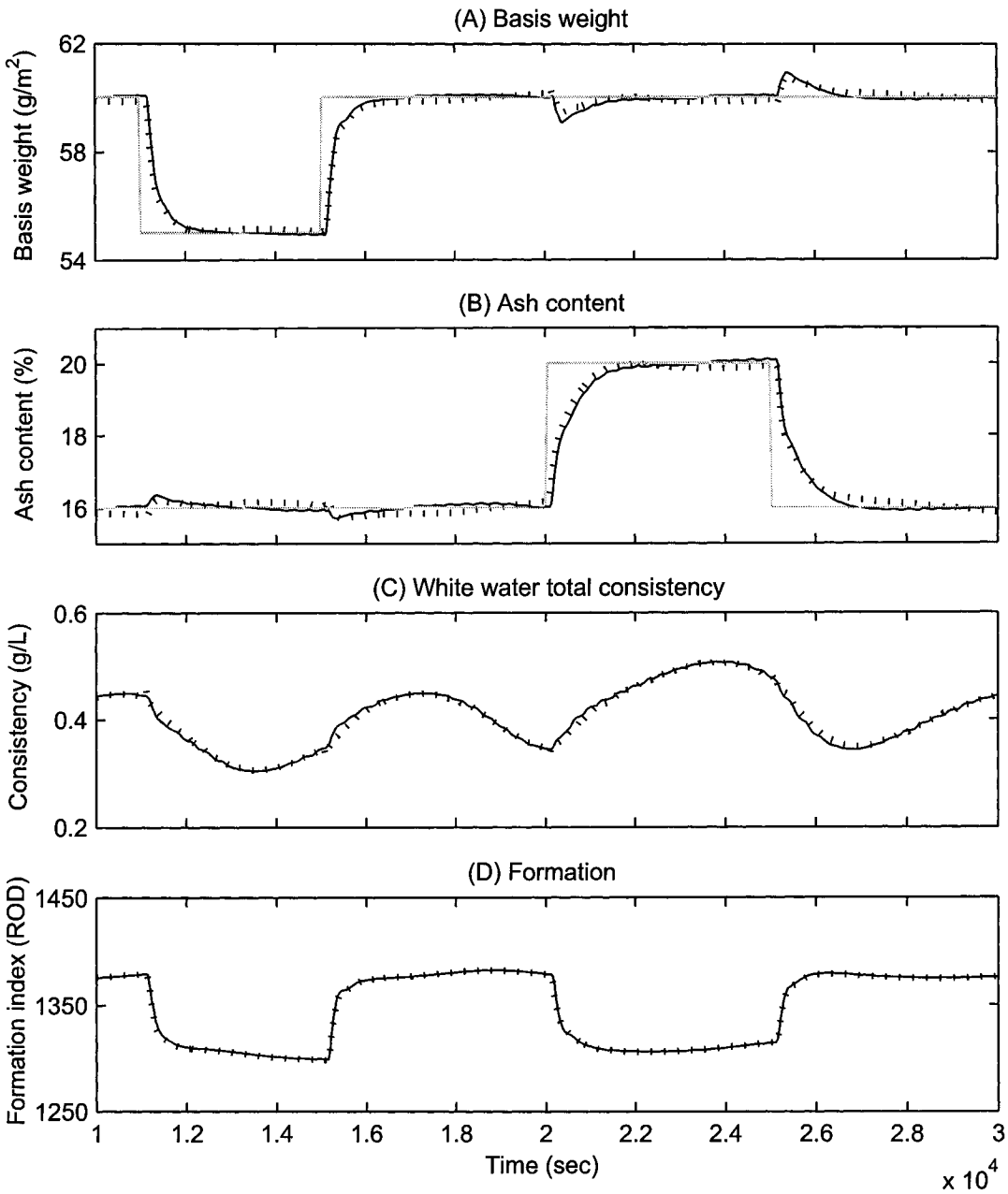

Figure 6.16. Comparison between SISO (solid line) and MIMO (dotted line) control for pulp mass, filler mass and white water total consistency control. Responses of basis weight, ash content, white water total consistency and formation to the set-point changes of the basis weight and the ash content with sinusoidal disturbance in the fines and filler retention. Step changes of the basis weight set-point: 60 to 55 g/m^2 at 11000 sec and reverse at 15000 sec. Step changes of the ash content set-point: 16 to 20 % at 20000 sec and reverse at 25000 sec. Sinusoidal disturbance with an amplitude of 0.1 was introduced into the fines and filler retention during the set-point changes of the basis weight and the ash content.

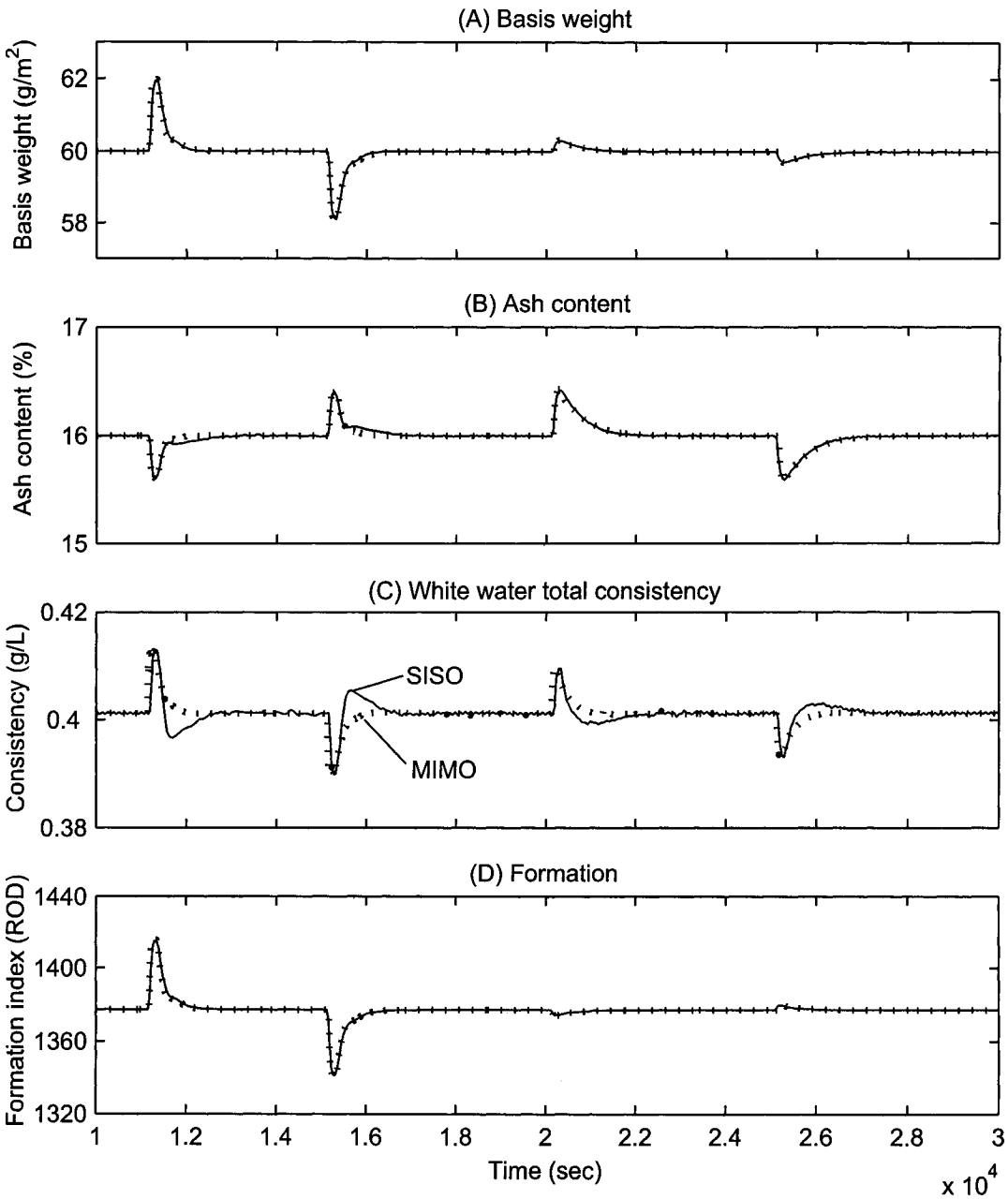

Figure 6.17. Comparison between SISO (solid line) and MIMO (dotted line) control for pulp mass, filler mass and white water total consistency control. Responses of basis weight, ash content, white water total consistency and formation to disturbances in the thick stock consistency and the filler slurry consistency. Step changes of the thick stock total consistency: 2.6 to 2.7 % at 11000 sec and reverse at 15000 sec. Step changes of the filler slurry consistency: 10 to 10.5 % at 20000 sec and reverse at 25000 sec.

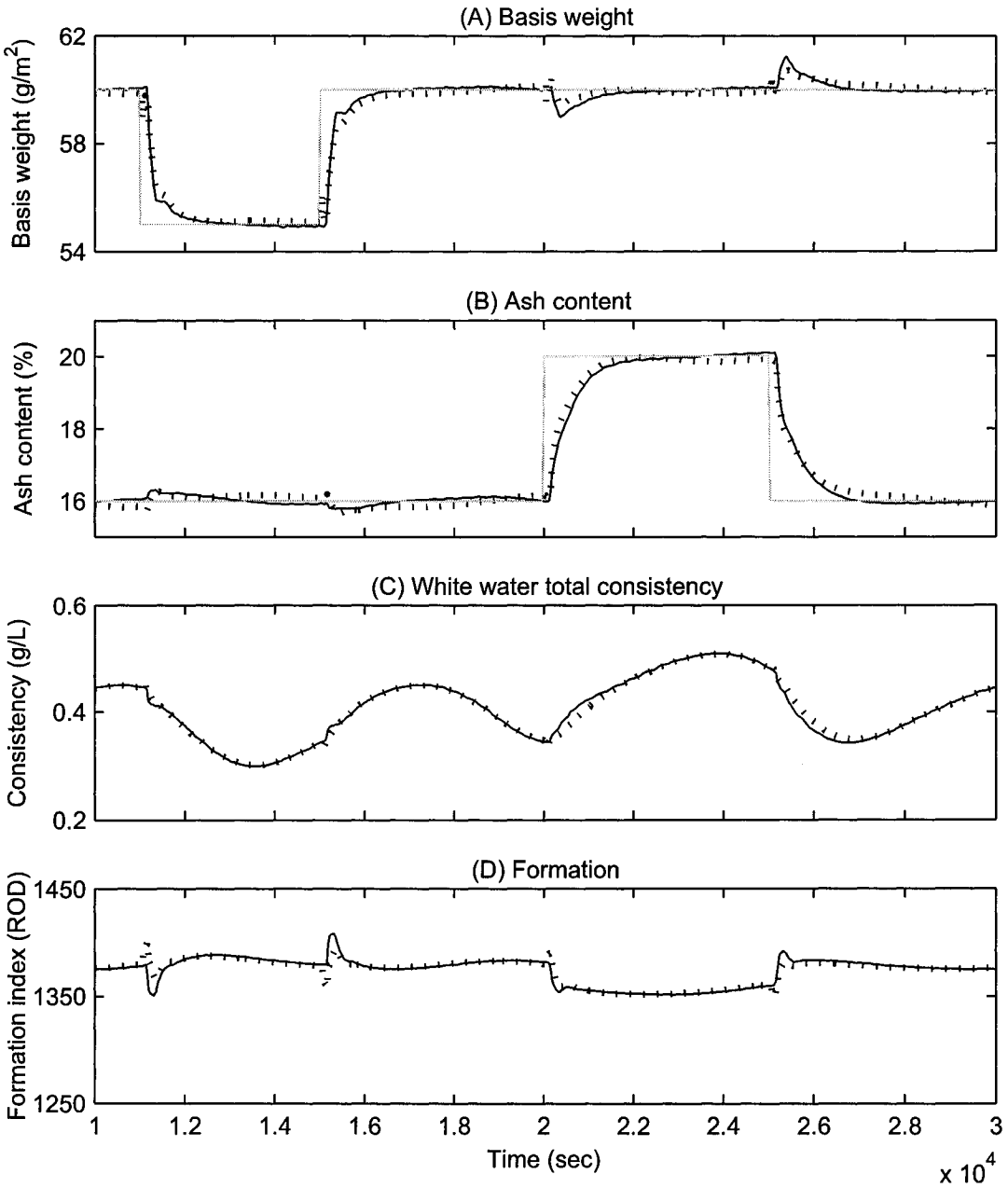

Figure 6.18. Comparison between SISO (solid line) and MIMO (dotted line) control for pulp mass, filler mass, white water total consistency and headbox pulp consistency control. Responses of basis weight, ash content, white water total consistency and formation to the set-point changes of the basis weight and the ash content with sinusoidal disturbance in the fines and filler retention. Step changes of the basis weight set-point: 60 to 55 g/m^2 at 11000 sec and reverse at 15000 sec. Step changes of the ash content set-point: 16 to 20 % at 20000 sec and reverse at 25000 sec. Sinusoidal disturbance with an amplitude of 0.1 was introduced into the fines and filler retention during the set-point changes of the basis weight and the ash content.

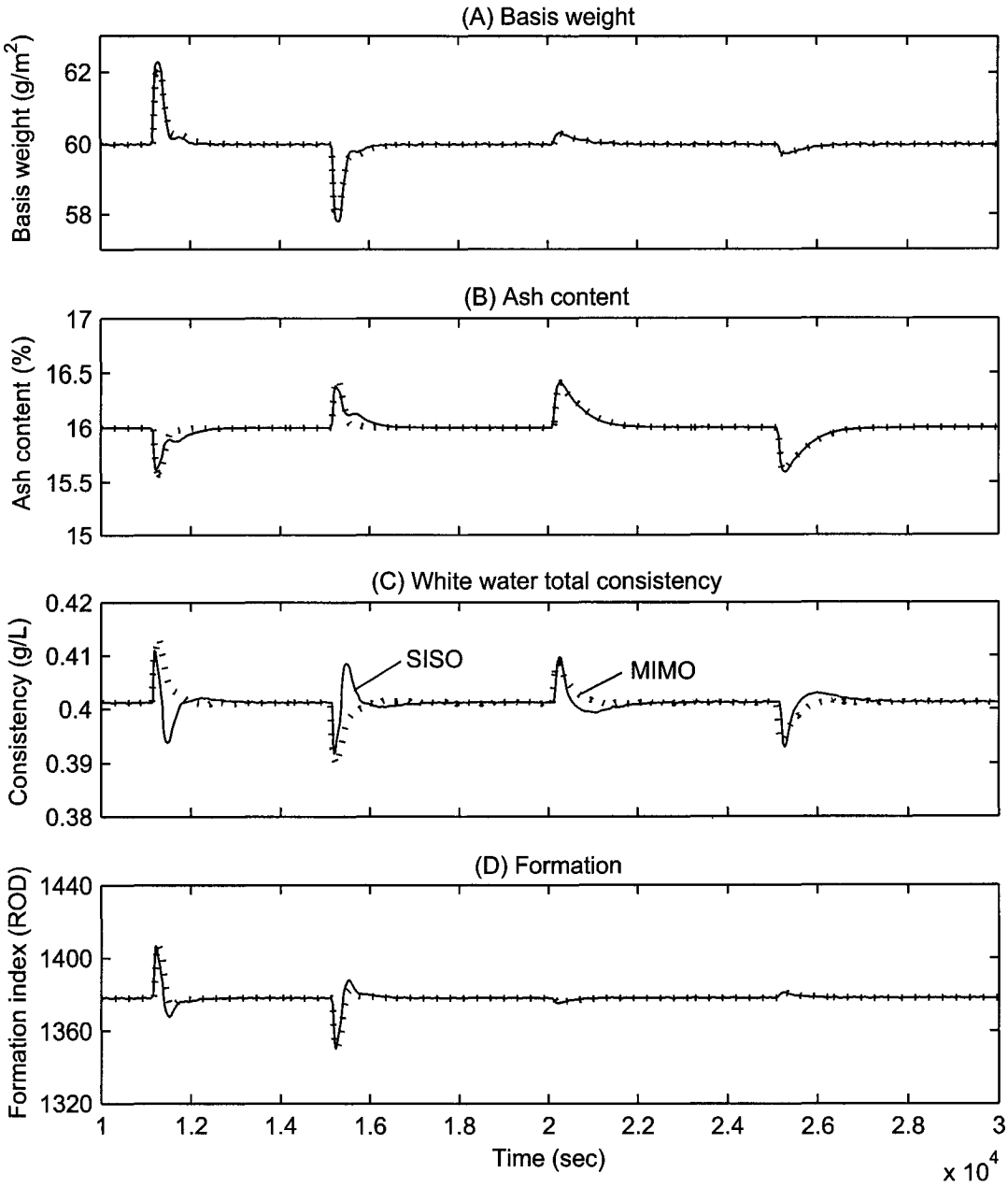

Figure 6.19. Comparison between SISO (solid line) and MIMO (dotted line) control for pulp mass, filler mass, white water total consistency and headbox pulp consistency control. Responses of basis weight, ash content, white water total consistency and formation to disturbances in the thick stock consistency and the filler slurry consistency. Step changes of the thick stock total consistency: 2.6 to 2.7 % at 11000 sec and reverse at 15000 sec. Step changes of the filler slurry consistency: 10 to 10.5 % at 20000 sec and reverse at 25000 sec.

interactions in white water consistency (Figures 6.17-(C) and 6.19-(C)). However, the magnitude is so small that the effect is not detected well in the basis weight and the paper ash content. When sinusoidal disturbance in the filler and fines retention is introduced during the set-point changes of basis weight and ash content, no distinctive advantage in decoupling control scheme is observed compared to SISO control (6.16 and 6.18). The performances of SISO and MIMO control are quite similar. This is also observed in the basis weight and ash content control when the thick stock and the filler slurry consistencies are disturbed (Figures 6.17 and 6.19).

This can be explained by the fact that the diagonal values in the relative disturbance gain (RDG) is close to one (Table 6.2). Considering the following multivariable process:

$$\mathbf{y} = \mathbf{K} \cdot \mathbf{u} + \mathbf{K_L} \cdot \mathbf{d} \tag{6.19}$$

where $\mathbf{K}$ and $\mathbf{K_L}$ are the gain matrix, $\mathbf{y}$ is the output, $\mathbf{u}$ is the manipulated input and $\mathbf{d}$ is the load variable. The relative disturbance gain (RDG), β_i is defined as the changes in the controller output that is required to counteract changes in d and bring u_i back to its set-point. Mathematically the ith element of RDG is defined as [124]:

$$\beta_i = \frac{\left(\frac{\partial u_i}{\partial d_i}\right)_{y_j}}{\left(\frac{\partial u_i}{\partial d_i}\right)_{y_i, u_j, j \neq i}} \tag{6.20}$$

The term in the numerator denotes the changes in the manipulated variable u_i needed for perfect disturbance rejection. The term in the denominator represents the change in a manipulated variable u_i when one of the output y_i is kept perfect. In a matrix form, RDG can be calculated with [125]:

$$\text{RDG} = (\mathbf{K}_{diag} \cdot \mathbf{K}^{-1} \cdot \mathbf{K_L}) \oslash \mathbf{K_L} \tag{6.21}$$

Table 6.2. Relative disturbance gain (RDG) for different control schemes and for several disturbances. M_{pulp} represents the pulp mass flow in paper, M_{filler} is the filler mass flow in paper, WWT is white water total consistency and HBp is headbox pulp consistency. Controlled variables: $y_1 = M_{pulp}$, $y_2 = M_{filler}$, y_3 = WWT and y_4 = HBp. Manipulated variables: $u_1 = F_1$ (thick stock flow rate), $u_2 = F_7$ (filler flow rate), $u_3 = F_{pol}$ (polymer flow rate) and $u_4 = F_2$ (headbox flow rate).

item	β_1	β_2	β_3	β_4
M_{pulp}-M_{filler}-WWT control				
disturbances in				
$C_{1,total}$	1.0	0.41	-0.18	
C_7	-4.86	1.0	0.06	
R_{filler}	0.01	-0.01	1.00	
M_{pulp}-M_{filler}-WWT-HBp control				
disturbances in				
$C_{1,total}$	0.92	0.38	0.22	-0.42
C_7	-4.40	1.00	0.06	-0.82
R_{filler}	0.01	-0.01	1.00	0.00

where $\mathbf{K}_{diag}$ is the diagonal matrix and $\oslash$ denotes element-by-element division. The RDG gives a measure of whether or not the interaction resulting from a particular disturbance is favorable or unfavorable. If $\beta_i > 1$, then larger changes in controller output are required for a classical interacting control system (multiloop) than for a single-input, single-output (SISO) system. A small value of β_i means that the controller output does not have to move very far in the steady state. When $\beta_i = 1$, the performances of SISO control and MIMO control are same, as observed in the study.

6.7 Chapter summary

Control strategies for the retention process without deteriorating formation were investigated through simulation. The pulp mass and filler mass control structure can eliminate the interactions between basis weight and ash content control loops and provides a similar control performance with the basis weight and ash content control scheme with decoupling. The white water consistency control can help eliminating the disturbances related with the fines and filler retention. Ratio control of bentonite flow rate helps reducing the variations in formation, while the white water consistency is controlled by manipulating the polymer flow rate. The white water consistency set-point problem during grade changes was solved by developing a model for white water consistency as a function of basis weight and ash content. Headbox pulp consistency control helps optimizing paper formation. Multi-input multi-out (MIMO) control helps eliminating interactions in the white water consistency control. However, no distinctive advantage is found for the pulp mass and the filler mass control loops.

Chapter 7

Conclusions

7.1 Conclusions

The dynamics and control strategies for retention and formation processes of a paper machine using a microparticulate retention aid system were investigated. The control objective was to obtain a uniform basis weight and ash content of paper without deteriorating formation. The main findings from the study are summarized in the next paragraphs.

7.1.1 Parameters influencing retention and formation

The major parameter affecting first-pass retention is the dosage of cationic polyacrylamide (CPAM) followed by the dosage of bentonite. The pulp mass flow and the filler addition are secondary variables. The effects of the dosages on first-pass retention can be explained by the deposition efficiency model, which includes the effect of bimodal particles and the polymer transfer from fibre to filler. The increase in the deposition efficiency leads to the increase in the filler retention. The decrease in the filler retention with increasing filler addition is likely due to the

increase of polymer transfer from fibre surface to filler surface. The increase in filler retention with increasing thick stock flow is due to the fact that the influence of the increased fibre concentration is more dominant than that of the decreased deposition efficiency.

The two main parameters in the wet end affecting formation are the number of contacts between fibres and the bond strength at the contacts, which influence the fibre floc strength. The effects of the dosages of retention aids on the fibre floc strength and subsequently the formation can be explained by the bridging strength model. The model is based on interactions between a single fibre and neighbouring fibres in a fibre network and is a function of the surface coverage of polymer and microparticles on fibre and relative bond strength of each interactions. Increasing the bridging strength leads to the increase of fibre floc strength and hence a poor formation. Increasing headbox fibre concentration results in the increased contact number between fibres, which can be represented with the crowding number, providing a stronger fibre floc strength and consequently an impaired formation. Filler concentration in the wet end is a more dominant factor than the filler content of paper. It is likely that increasing the filler concentration in the wet end increases polymer transfer from fibre to filler particles and leads to weaker fibre flocs, resulting in an improved formation.

Based on the deposition efficiency and the bridging strength models, best retention with a minimum variation in fibre flocculation and formation, can be achieved by controlling the first-pass retention of solids by manipulating the flow rate of polymer, keeping a constant ratio between the dosages of polymer and microparticle. A best formation can be achieved, at a given polymer dosage, when microparticles cover all of the polymer covered sites on fibre surface.

7.1.2 Dynamics of the retention and formation processes

The dynamics of the retention process of a paper machine can be modeled from first-principles (mass balances). The effect of wet end chemistry on the retention process dynamics can be described by developing an empirical model for first-pass retention and including it as a parameter dependent on operating conditions. In addition, it was attempted to simulate the dynamics of formation by developing an empirical model for formation as a function of the crowding number, the bridging strength and the filler addition and combining with the dynamic models for the retention process. The two major factors affecting the dynamics of the retention process are the first-pass retention of solids and the parameters related to the white water circulation such as the volume of the wire pit and the residence time at the wire pit. Considering the piping and tanks configuration as fixed parameters for a given paper machine, the dynamics of fines and filler retention play a fundamental role for the process optimization.

7.1.3 Control strategies for the retention and formation processes

The control structure that controls the pulp mass and the filler mass in paper instead of basis weight and paper ash content can significantly reduce the inherent interactions between basis weight and ash content control loops. In addition, it provides similar control performance to the conventional control scheme, which control basis weight and ash content with decoupling. The white water consistency control can help eliminating the disturbances related with the fines and filler retention. Keeping a constant ratio between polymer flow rate and bentonite flow rate helps reducing the variations in formation, while the polymer flow rate is manipulated

to control the white water consistency. The problem concerning the determination of the white water consistency set-point during grade changes can be solved by developing an empirical model for the white water consistency as a function of basis weight and ash content. Headbox pulp consistency control helps optimizing paper formation during grade changes. Multi-input multi-out (MIMO) control helps eliminating interactions in the white water consistency control. However, no distinctive advantage is found for the pulp mass and the filler mass control loops.

7.2 Contributions

The main contributions to knowledge are:

1. The deposition efficiency model is developed to explain the effects of the dosages of microparticulate retention aids on the first-pass retention of fines and filler. The model includes the effect of bimodal particles and the polymer transfer from fibre surface to filler surface.

2. The bridging strength model is developed to explain the effects of the dosages of microparticulate retention aids on fibre flocculation and paper formation, based on interactions between a single fibre and neighbouring fibres in a fibre network.

3. Dynamic models for the concentrations of solids (fibre, fines and filler) are developed from first principles. To include the effect of wet end chemistry variables into the dynamic models, a simple approach is proposed: an empirical model for the first-pass retention of solids was developed and included as a parameter dependent on operating conditions.

4. A method to simulate the dynamics of formation is proposed: an empirical model was developed as a function of the crowding number, the bridging strength and the filler addition and coupled with the dynamic models for the concentrations of solids.

5. The problem of different white water consistency set-points during grade changes is solved by collecting pairs of basis weight, ash content and white water consistency and developing an empirical model of the white water consistency as a function of the basis weight and the ash content.

6. Control strategies to optimize paper formation during the control of the retention process are proposed: the headbox pulp consistency control and the ratio control of bentonite flow to polymer flow.

References

[1] D. L. Dauplaise, "A balancing act: Defining the varables of wet end chemistry," *PIMA*, vol. Oct., pp. 28–30, 1985.

[2] W. E. Scott, *Principles of wet end chemistry.* Atlanta: TAPPI Press, 1996.

[3] W. E. Scott, "Fines management and control in wet-end chemistry," *Tappi J.*, vol. 69(11), pp. 30–34, 1986.

[4] F. Onabe, "Measurement and control," in *Paper chemistry* (J. C. Roberts, ed.), ch. 11, pp. 198–216, 1991.

[5] S. Renaud and B. Olsson, "Improvements in boardmaking applications through better wet-end control and understanding," *Pulp & Paper Canada*, vol. 104(6), pp. T158–162, 2003.

[6] J. Nokelainen, R. Piirainen, and B. N. Ramsey, "Practical experiences with white water consistency control of a paper machine wet end," in *Process Control Conference*, pp. 3–13, 1993.

[7] D. Lang, M. Kosonen, and R. Kuusisto, "Coordinating wet end and dry end controls on a fine paper machine," *Pulp & Paper Canada*, vol. 102(8), pp. T214–218, 2001.

[8] M. Kosonen, R. Kuusisto, J. Shakespeare, and T. Huhtelin, "Multivariable MD-controls with adaptive process models," in *Preprints of 88th PAPTAC Annual Meeting*, Book B, (Montreal, Canada), pp. 105–109, 2002.

[9] T. A. Hauge, R. Slora, and B. Lie, "Model predictive control of a Norske Skog Saugbrugs paper machine: preliminary study," in *Control Systems 2002*, (Stockholm, Sweden), pp. 85–79, 2002.

[10] M. S. Laurikkala, M. T. Vuoti, T. J. Huhtelin, and H. N. Koivo, "Paper quality control by utilizing new consistency measurement capabilities," *Pulp & Paper Canada*, vol. 99(7), pp. T224–227, 1998.

[11] T. Rantala, P. Tarhonen, and H. N. Koivo, "Control of paper machine wire retention," *Tappi J.*, vol. 77(12), pp. 125–132, 1994.

[12] N. Harnois, "Control of the wet end of a pilot scale paper machine," Master's thesis, École Polytechnique, Montréal, Canada, 2001.

[13] P. Austin, J. Mack, D. Lovett, M. Wright, and M. Terry, "Improved wet end stability of a paper machine using model predictive control," in *Control Systems 2002*, (Stockholm, Sweden), pp. 80–84, 2002.

[14] M. Kosonen, C. Fu, S. Nuyan, R. Kuusisto, and T. Huhtelin, "Narrowing the gap between theory and practive: mill experiences with multivariable predictive control," in *Control Systems 2002*, (Stockholm, Sweden), pp. 54–59, 2002.

[15] M. Williamson, "Madison paper stabilizes wet end, quality with model predictive control," *Pulp & Paper*, vol. 78(4), pp. 30–33, 2004.

[16] T. Rantala, T. Ojala, J. Nokelainen, H. Kumpulainen, and K. Vanpembrook, "Wet end management concept: key measuremts for control solutions in one analyser platform," *Pulp & Paper Canada*, vol. 103(4), pp. T84–87, 2002.

[17] B. A. Nazir and J. Carnegie-Jones, "Optimizing wet-end chemistry - the practicalities," *Paper Technology*, vol. Dec, pp. 37–41, 1991.

[18] TAPPI Standard Test Methods, *T240 om-02 Consistency (concentration) of pulp suspensions.*

[19] PAPTAC Standard Testing Methods, *D.16 Consistency of stocks.*

[20] H. Kortelainen, J. Nokelainen, and J. Huttunen, "Mill application of a new system that simulataneously monitor fiber retention and filler retention," *Tappi J.*, vol. 72(8), pp. 113–119, 1989.

[21] R. Proulx and S. Renaud, "Implementation and results of white water consistency control at the wet end," in *2000 TAPPI PCE & I Conference & ISA-PUPID 39th Annual Symposium*, pp. 85–95, 2000.

[22] B. Olsson and S. Renaud, "Wet-end control improvements in boardmaking applications," in *2000 Tappi Papermakers Conference and Trade Fair*, pp. 757–765, 2000.

[23] J. M. Gess, *Retention of fines and fillers during papermaking.* Atlanta: TAPPI Press, 1998.

[24] R. W. Davison, "Mechanism of fine particle retention in paper," in *Proc. TAPPI Papermakers Conference*, pp. 153–164, 1996.

[25] T. G. M. van de Ven, "Theoretical aspects of drainage and retention of small particles on the fourdrinier," *J. Pulp Paper Sci.*, vol. 10(3), pp. J57–63, 1984.

[26] H. Wei, P. Kumar, B. V. Ramarao, and C. Tien, "Drainage and fine particle retention in a forming incompressible fibrous mat," *J. Pulp Paper Sci.*, vol. 22(11), pp. J446–451, 1996.

[27] D. Solberg and L. Wågberg, "On the mechanism of GCC filler retention during dewatering - new techniques and initial findings," *J. Pulp Paper Sci.*, vol. 28(6), pp. 183–186, 2002.

[28] B. Norman, "The formation of paper sheets," in *Paper Structure and Properties* (J. Bristow and P. Kolseth, eds.), pp. 123–150, New York: Marcel Dekker, 1986.

[29] K. Moberg, "Optimizing wet end chemistry in fine paper manufacture," *PIMA*, vol. 67(9), pp. 24–30, 1985.

[30] A. Swerin and L. Ödberg, "Some aspect of retention aids," in *Fundamentals of Papermaking Materials, Trans. 11th Fun. Res. Symp.*, (Cambridge), pp. 265–350, Mech. Eng. Publ. Ltd., London, 1997.

[31] B. Nordström and B. Norman, "Effects of grammage on paper properties for twin-wire roll forming of TMP," *J. Pulp Paper Sci.*, vol. 21(12), pp. J427–431, 1995.

[32] U. W. Winters, G. G. Duffy, and R. P. Kibblewhite, "Effects of grammage and concentration on paper sheet formation of pinus radiata kraft pulps," in *Proc. 54th Appita Annual Conf.*, vol. 2, (Melbourne, Australia), pp. 671–678, 2000.

[33] W. L. Freeman, "Chemical related factors influencing the balance of formation, drainage and retention," in *Proc. TAPPI Papermakers Conference*, pp. 247–253, 1996.

[34] S. G. Mason, "Fiber motions and flocculation," *Pulp Paper Mag. Can.*, vol. 87(13), pp. 96–102, 1954.

[35] R. J. Kerekes, R. M. Sosaynski, and P. A. Tam Doo, "The flocculation of pulp fibres," in *Papermaking Raw Materials, Trans. 8th Fund. Res. Symp*, (Oxford, England), pp. 265–310, Mech. Eng. Publ. Ltd., London, 1985.

[36] B. Nordström and B. Norman, "Influence of headbox nozzle contraction ratio on sheet formation and anisotropy," in *Proc. TAPPI Engineering Conf. book 1*, pp. 225–228, 1994.

[37] B. Carré, "Starch and alumina/silica based compounds as a microparticulate retention aid system," *Nordic Pulp Paper Res. J.*, vol. 8(1), pp. 21–26, 1993.

[38] T. Lindström, H. Hallgren, and F. Hedborg, "Aluminum based microparticulate retention aid systems," *Nordic Pulp Paper Res. J.*, vol. 4(2), pp. 99–103, 1989.

[39] K. Andersson and E. Lindgren, "Important properties of colloidal silica in microparticulate systems," *Nordic Pulp Paper Res. J.*, vol. 11(1), pp. 15–21, 1996.

[40] T. Lindström, "Some fundamental chemical aspects on paper forming," in *Trans. 9th Fundamental Research Symposium*, (Cambridge), pp. 311–412, Mech. Eng. Publ. Ltd., London, September 1989.

[41] J.-F. Bernier and B. Begin, "Experience of a microparticulate retention aid system," *Tappi J.*, vol. 77(11), pp. 217–224, 1994.

[42] B. Alince, F. Bednar, and T. G. M. van de Ven, "Deposition of calcium carbonate particles on fiber surfaces induced by cationic polyelectrolyte and bentonite," *Colloids and Surfaces A*, vol. 190, pp. 71–80, 2001.

[43] T. Asselman and G. Garnier, "The flocculation mechanism of microparticle retention aid systems," *J. Pulp Paper Sci.*, vol. 27(8), pp. 273–278, 2001.

[44] T. Asselman, B. Alince, G. Garnier, and T. G. M. van de Ven, "Mechanism of polyacrylamide-bentonite microparticlulate retention aids," *Nordic Pulp Paper Res. J.*, vol. 15(5), pp. 515–519, 2000.

[45] W. E. Scott, "A review of wet-end chemistry process control instrumentation," *Tappi J.*, vol. 67(11), pp. 72–76, 1984.

[46] H. Kortelainen, "Tools for successful wet-end chemistry control," *Tappi J.*, vol. 75(12), pp. 112–117, 1992.

[47] T. Sopenlehto, "On-line monitoring and control in the wet-end," in *Application of wet end paper chemistry* (C. O. Au and I. Thorn, eds.), pp. 172–182, Blackie Academie and Professional, 1995.

[48] T. Sopenlehto, "Experiences of new microwave consistency transmitter in papermaking process," in *An International Conference Papermaking & Paper Machine Technology*, (Helsinki, Finland), pp. 13–20, 1995.

[49] A. Kaunonen and C. White, "Integrating advanced consistency measurements and controls with MD paper quality controls," in *1997 Tappi Engineering & Papermakers Conference*, pp. 599–604, 1997.

[50] J. R. Lavigne, *An introduction to paper industry instrumentation.* San Francisco, USA: Miller Freeman Publications Inc., 1977.

[51] J. G. Penniman and C. W. Neal, "On-line monitoring of zeta potential and drainage can optimize papermaking," *Wochenblatt Für Papierfabrikation*, vol. 122(15), pp. 598–602, 1994.

[52] S. Thomas and M. Latva, "The robotic laboratory - a wet end information centre," *Paper Technology*, vol. 40(7), pp. 57–60 and 62–66, 1999.

[53] A. Kaunonen, "On-line retention and cationic demand measurements and their utilization on a paper machine," *Paperi ja Puu*, vol. 68(1), pp. 46–52, 1986.

[54] B. Bley, "Latest experiences of on-line charge measurement: a process control concept," *Pulp & Paper Canada*, vol. 99(5), pp. T165–169, 1998.

[55] H. Sirén, R. Kokkonen, T. Hiissa, T. Säme, O. Rimpinen, and R. Laitinen, "Determination of soluble anions and cations from water of pulp and paper mills with on-line coupled capillary electrophoresis," *J. Chromatography A*, vol. 895, pp. 189–196, 2000.

[56] K. H. Boegh, T. M. Garver, D. Henry, H. Yuan, and G. S. Hill, "New methods for on-line analysis of dissolved substances in white water," *Pulp & Paper Canada*, vol. 101(3), pp. T1–8, 2000.

[57] T. M. Garver, H. Yuan, K. H. Boegh, and J. Allen, "On-line analysis of dissolved substances in deinking and papermaking applications," *Pulp & Paper Canada*, vol. 104(9), pp. T230–234, 2003.

[58] D. B. Brewster and M. J. Kocurek, eds., *Mill-wide process control & information systems*, vol. 10 of *Pulp and Paper Manufacture*, ch. 12, pp. 179–236. TAPPI and CPPA, 1993.

[59] J. F. Waterhouse, "On-line formaion measurements and paper quality," in *TAPPI 1996 Papermakers Conference*, pp. 275–288, 1996.

[60] D. Söderberg, "SOFA-STFI on-line forming analyzer," in *Proc. Control Systems 2002*, pp. 288–292, 2002.

[61] B. A. Ogunnaike and W. H. Ray, *Process Dynamics, Modeling and Control.* Oxford University Press, 1994.

[62] M. Piirto and H. Koivo, "Advanced control of a paper machine wet end," in *IFAC Advanced Control of Chemical Processes*, (Toulouse, France), pp. 47–52, 1991.

[63] T. Rantala, P. Tarhonen, and H. N. Koivo, "Retention modeling and control in the paper machine wet end," in *12th IFAC World Congress*, vol. 6, (Sydney, Australia), pp. 61–66, 1993.

[64] T. Rantala, P. Tarhonen, and H. N. Koivo, "Adaptive retention control in a paper machine," *Pulp & Paper Canada*, vol. 95(8), pp. T299–302, 1994.

[65] A. Isaksson, M. Hagberg, and L. E. Jönsson, "Benchmarking for paper machine MD-control: simulation results," *Control Eng. Practice*, vol. 3(10), pp. 1459–1498, 1995.

[66] A. Makkonen, R. Rantanen, A. Kaukovirta, H. Koivisto, J. Lieslehto, T. Jussila, H. N. Koivo, and T. Huhtelin, "Three control schemes for paper machine MD-control," *Control Eng. Practice*, vol. 3(10), pp. 1471–1474, 1995.

[67] J. Piipponen and R. Ritala, "Basis weight and filler content: decoupled smith predictor approach," *Control Eng. Practice*, vol. 3(10), pp. 1463–1466, 1995.

[68] A. E. Beecher, "Dynamic modeling techniques in the paper industry," *Tappi J.*, vol. 46(2), pp. 117–120, 1963.

[69] M. St. Jacques, "Computerized dynamic material balance of a paper machine wet end," in *Proc. Tappi Eng. Conf. Book 1*, (San Francisco, USA), pp. 97–110, 1982.

[70] T. Miyanishi, K. Iida, and T. Iwatsu, "Dynamic simulation for efficient paper machine grade change," *Tappi J.*, vol. 71(1), pp. 49–56, 1988.

[71] S. Bussière, A. Roche, and J. Paris, "Analysis and control of white water network perturbations in an integrated newsprint mill," *Pulp & Paper Canada*, vol. 93(4), pp. 41–44, 1992.

[72] J. A. Orccotoma, J. Paris, M. Perrier, and A. A. Roche, "Dynamics of white water networks during web breaks," *Tappi J.*, vol. 80(12), pp. 101–110, 1997.

[73] J. A. Orccotoma, D. Stiée, J. Paris, and M. Perrier, "Dynamics of fines distribution in a white water network," *Pulp & Paper Canada*, vol. 98(9), pp. T336–339, 1997.

[74] R. W. Shirt, *Modeling and Identification of Paper Machine Wet End Chemistry.* PhD thesis, The University of British Columbia, Vancouver, Canada, 1997.

[75] R. Shirt and M. Manness, "Dynamic simulation of retention chemistry effects using a material attribte array structure," in *Tappi Eng./Process and Product Quality Conf. & Trade Fair, Book 1*, pp. 185–195, 1999.

[76] T. G. M. van de Ven, "Particle deposition on pulp fibers," *Nordic Pulp Paper Res. J.*, vol. 8(1), pp. 130–134 and 147, 1993.

[77] T. A. Hauge and B. Lie, "Paper machine modeling at Norske Skog Saugbrugs: a mechanistic approach," *Modeling, Identification and Control*, vol. 23(1), pp. 27–52, 2002.

[78] B. Kessler, K. Magee, and K. VanPembrook, "Optimizing papermachine retention through tray consistency closed loop control and trend analysis," in *Proc. 2000 TAPPI Papermakers Conference and Trade Fair*, pp. 539–543, 2000.

[79] J. Nokelainen and R. Piirainen, "Wet end control - results and new possibilities," in *Proc. An International Conference on Papermaking and Paper Machine Technology*, (Helsinki, Finland), pp. 21–30, 1995.

[80] R. L. Yeager, "Retention analysis gives Avenor a window into the wet end," *Pulp & Paper*, pp. 73–78, 1997.

[81] T. Rantala, M. Artama, J. Nokwlainen, and T. Sopenlehto, "Wet end management based on on-line measurements and control solutions," in *Proc. Presymposium of the 10th ISWPC*, (Seoul, Korea), pp. 130–139, 1999.

[82] T. Tomney, P. E. Proszynski, J. R. Armstrong, and R. Jurley, "Controlling filler retention in mechnaincal grades," *Pulp & Paper Canada*, vol. 99(8), pp. T274–277, 1998.

[83] M. A. Blanco, B. van der Heijden, P. Barbadillo, and J. Tijero, "El control de la floculación en la fabricación del papel," *Inv. Téc. Papel*, vol. 120, pp. 232–245, 1994.

[84] H. Yue, E. Brown, J. Jiao, and H. Wang, "On-line web formation control using stochastic distribution methods," in *Control Systems 2002*, (Stockholm, Sweden), pp. 318–322, 2002.

[85] R. Hogg, "Collision efficiency factors for polymer flocculation," *J. Colloid Interface Sci.*, vol. 102(1), pp. 232–236, 1984.

[86] B. M. Moudgil, B. D. Shah, and H. S. Soto, "Collision efficiency factors in polymer flocculation of fine particles," *J. Colloid Interface Sci.*, vol. 119(2), pp. 466–473, 1987.

[87] A. Molski, "On the collision efficiency approach to flocculation," *Colloid Polym. Sci.*, vol. 267, pp. 371–375, 1989.

[88] S. Behl, B. M. Moudgil, and T. S. Prakash, "Control of active sites in selective flocculation: I. mathematical model," *J. Colloid Interface Sci.*, vol. 161(2), pp. 414–421, 1993.

[89] A. Swerin, L. Ödberg, and L. Wågberg, "An extended model for the estimation of flocculation efficiency factors in multicomponent flocculant systems," *Colloids and Surfaces A*, vol. 113, pp. 25–38, 1996.

[90] R. H. Smellie, Jr and V. K. La Mer, "Flocculation, subsidence and filtration of phosphate slimes," *J. Colloid Sci.*, vol. 13, pp. 589–599, 1958.

[91] T. W. Healy and V. K. La Mer, "The adsorption - flocculation reactions of a polymer with an aqueous colloidal dispersion," *J. Phys. Chem.*, vol. 66(10), pp. 1835–1838, 1962.

[92] H. Tanaka, A. Swerin, and L. Ödberg, "Cleavage of polymer chains during transfer of cationic polyacrylamide from cellulose fibers to polystyrene latex," *J. Colloid Interface Sci.*, vol. 153(1), pp. 13–20, 1992.

[93] T. Asselman and G. Garnier, "Mechanism of polyelectrolyte transfer during heteroflocculation," *Langmuir*, vol. 16(11), pp. 4871–4876, 2000.

[94] T. Asselman and G. Garnier, "The role of anionic microparticles in a poly(acrylamide)-montmorillonite flocculation aid system," *Colloids and Surfaces A*, vol. 170(1), pp. 79–90, 2000.

[95] E. Dickinson and L. Eriksson, "Particle flocculation by adsorbing polymers," *Adv. Colloid Interface Sci.*, vol. 34, pp. 1–29, 1991.

[96] M. Smoluchowski, "Versuch einer mathematischen theorie der koagulationaskinetik kolloider lösungen," *Z. Phys. Chem.*, vol. 92, pp. 129–168, 1917.

[97] P. A. Tam Doo, R. J. Kerekes, and R. H. Pelton, "Estimates of maximum hydrodynamic shear stresses on fiber surfaces in papermaking," *J. Pulp Paper Sci.*, vol. 10(4), pp. J80–88, 1984.

[98] A. Vanerek, *Filler Retention in Papermaking by Polymeric and Microparticulate Retention Aid System.* PhD thesis, McGill University, Montreal, Canada, 2004.

[99] H. Tanaka, A. Swerin, and L. Ödberg, "Transfer of cationic retention aid from fibers to fines particles and clevage of polymer chains under wet-end papermaking conditions," *Tappi J.*, vol. 76(5), pp. 157–163, 1993.

[100] P. G. Saffman and J. S. Turner, "On the collision of drops in turbulent clouds," *J. Fluid Mech.*, vol. 1, p. 16, 1956.

[101] A. Swerin and L. Ödberg, "Flocculation and floc strength in suspension flocculated by retention aids," *Nordic Pulp Paper Res. J.*, vol. 8(1), pp. 141–147, 1993.

[102] A. Swerin, G. Rinsinger, and L. Ödberg, "Shear strength in papermaking suspensions flocculated by retention aid systems," *Nordic Pulp Paper Res. J.*, vol. 11(1), pp. 30–35, 1996.

[103] S. Zauscher and D. J. Klingenberg, "Normal forces between cellulose surfaces measured with colloidal probe microscopy," *J. Colloid Interf. Sci.*, vol. 229, pp. 497–510, 2000.

[104] C. F. Schmid and D. J. Klingenberg, "Properties of fiber flocs with frictional and attractive interfiber forces," *J. Colloid Interface Sci.*, vol. 226, pp. 136–144, 2000.

[105] S. Zauscher and D. J. Klingenberg, "Surface and friction forces between cellulose surfaces measured with colloidal probe microscopy," *Nordic Pulp Paper Res. J.*, vol. 15(5), pp. 459–468, 2000.

[106] A. Swerin, U. Sjödin, and L. Ödberg, "Flocculation of cellulosic fibre suspensions by model microparticulate retention aid systems," *Nordic Pulp Paper Res. J.*, vol. 8(4), pp. 389–398, 1993.

[107] W. W. Sampson, J. McAlpin, H. W. Kropholler, and C. T. J. Dodson, "Hydrodynamic smoothing in the sheet forming process," *J. Pulp Paper Sci.*, vol. 21(12), pp. J422–428, 1995.

[108] R. J. Kerekes and C. J. Schell, "Characterization of fibre flocculation regimes by a crowding factor," *J. Pulp Paper Sci.*, vol. 18(1), pp. J32–38, 1992.

[109] R. J. Kerekes and C. J. Schell, "Effect of fibre length and coarseness on pulp flocculation," *Tappi J.*, vol. 78(2), pp. 133–139, 1995.

[110] B. Cho, G. Garnier, J. Paradis, and M. Perrier, "Filler retention with a CPAM/bentonite retention system - effect of collision efficiency," *Nordic Pulp Paper Res. J.*, vol. 16(3), pp. 188–194, 2001.

[111] H. Tanaka and L. Ödberg, "Transfer of cationic polymer from cellulose fibers to polystyrene latex," *J. Colloid Interface Sci.*, vol. 149(1), pp. 40–48, 1992.

[112] T. Asselman and G. Garnier, "Dynamics of polymer-induced heteroflocculation of wood fibers and fines," *Colloids and Surfaces A*, vol. 174(3), pp. 297–301, 2000.

[113] B. Cho, G. Garnier, J. Paradis, and M. Perrier, "The process dynamics of filler retention in paper using a CPAM/bentonite retention aid system," *Canadian J. Chem. Eng.*, vol. 79(6), pp. 923–930, 2001.

[114] B. Cho, G. Garnier, and M. Perrier, "Dynamic modeling of retention and formation processes," in *Control Systems 2002*, pp. 200–204, 2002.

[115] B. Cho, G. Garnier, T. G. M. van de Ven, and M. Perrier, "Parameters affecting paper formation on a pilot fourdrinier using CPAM/bentonite retention aids," in *5th International Paper and Coating Chemistry Symposium*, pp. 193–200, 2003.

[116] A. Hermann, F. Bednár, M. Perrier, J. Paradis, and J. Paris, "Dynamics of whitewater consistency of a pilot paper machine using a PEO/cofactor retention aid system," *to appear.*

[117] B. Janvier and B. Bialkowski, "On lambda tuning - the how and why," in *PAPTAC 91st Annual Meeting*, pp. D291–296, 2005.

[118] E. B. Dahlin, "Designing and tuning digital controllers," *Instruments and Control Systems*, vol. 42, pp. 77–83, 1968.

[119] J. G. Ziegler and N. B. Nichols, "Optimum settings for automatic controllers," *Trans. ASME*, vol. 64, pp. 753–768, 1942.

[120] G. H. Cohen and G. A. Coon, "Theoretical considerations of retarded control," *Trans. ASME*, vol. 75, pp. 827–834, 1953.

[121] K. J. Åström and T. Hägglund, *PID controllers: Theory, Design, and Tuning.* NC, USA: Instrument Society of America, 1995.

[122] D. Seborg, T. F. Edgar, and D. A. Mellichamp, *Process Dynamics and Control.* John Wiley & Sons, Inc., 1989.

[123] R. F. Murphy and S.-C. Chen, "Transition control of papermaking processes: Paper grade change," in *Proc. the IEEE International Conference on Control Applications*, vol. 2, (Hawai'i, USA), pp. 1278–1283, 1999.

[124] G. Stanley, M. Marino-Galarraga, and T. J. McAvoy, "Shortcut operability analysis. 1. the relative disturbance gain," *Ing. Eng. Chem. Process Des. Dev.*, vol. 24, pp. 1181–1188, 1985.

[125] J.-W. Chang and C.-C. Yu, "Relative disturbance gain array," *AIChE Journal*, vol. 38(4), pp. 521–534, 1992.

Appendix A

SIMULINK model of the paper machine

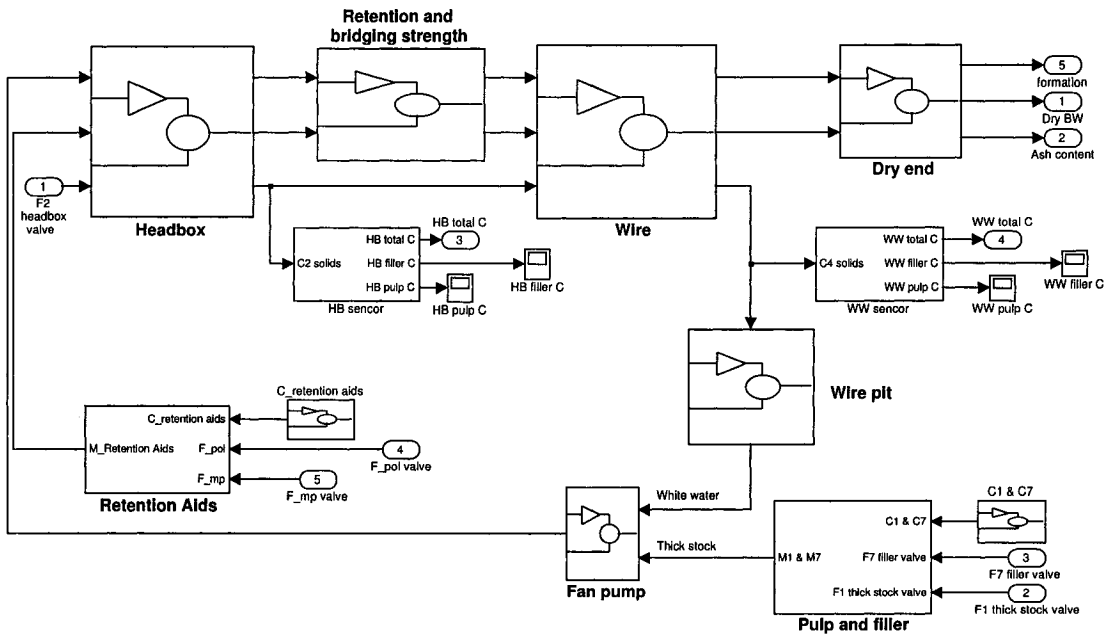

Figure A.1. SIMULINK model of the paper machine. HB = headbox; WW = white water; BW = basis weight; F = flow rate; C = consistency; pol = polymer; and mp = microparticle.

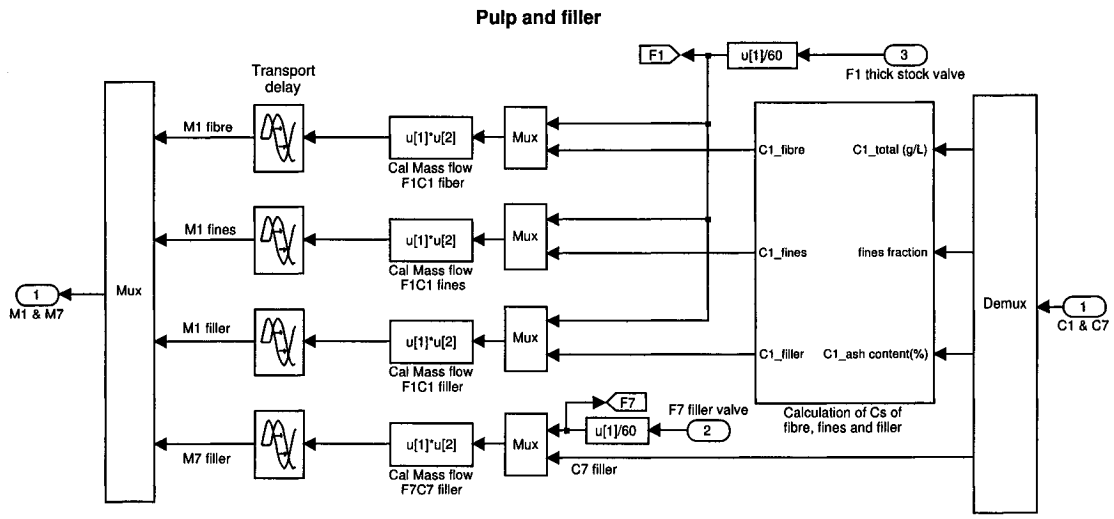

Figure A.2. Calculation of the mass flow rates of fibre, fines and filler in the thick stock flow and in the filler slurry flow. M = mass flow rate.

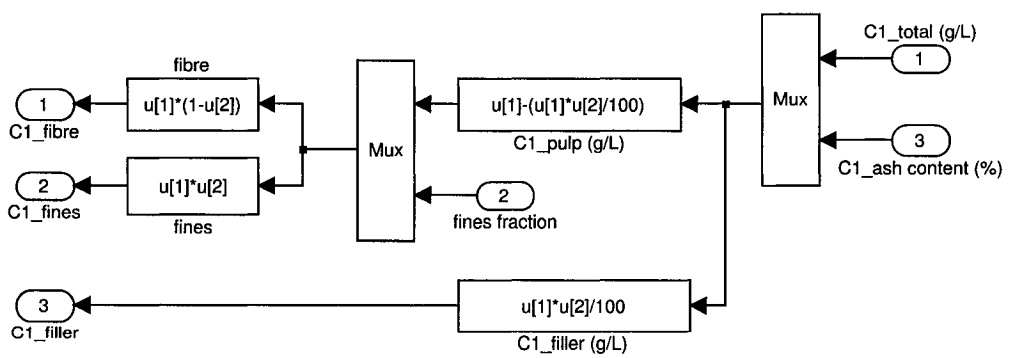

Figure A.3. Calculation of the consistencies of fibre, fines and filler in the thick stock.

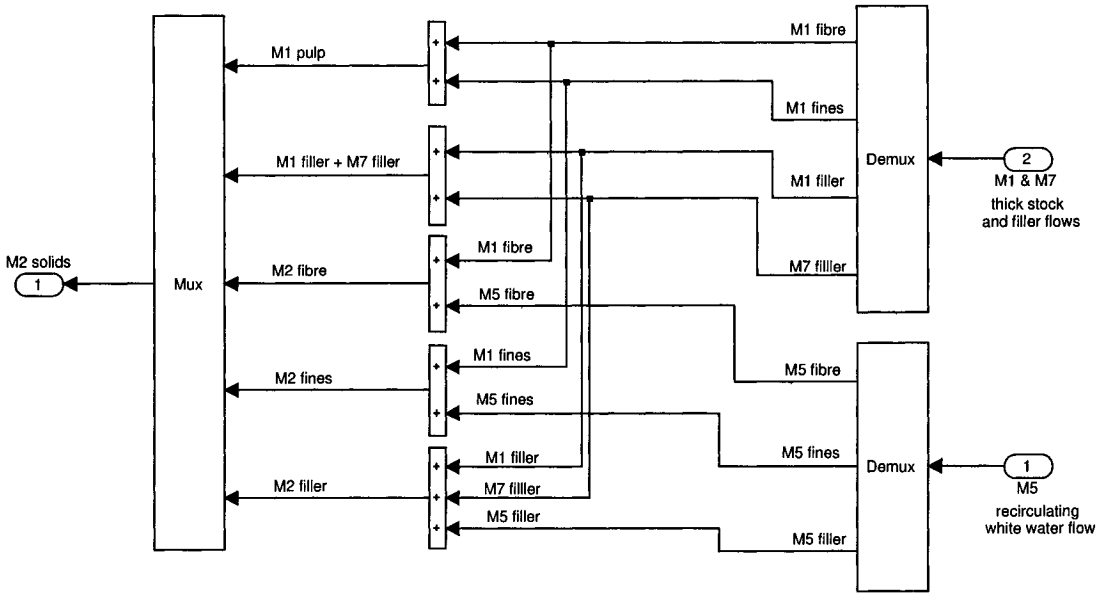

Figure A.4. Fan pump. The recirculating white water flow, the thick stock flow and the filler slurry flow are combined at the fan pump.

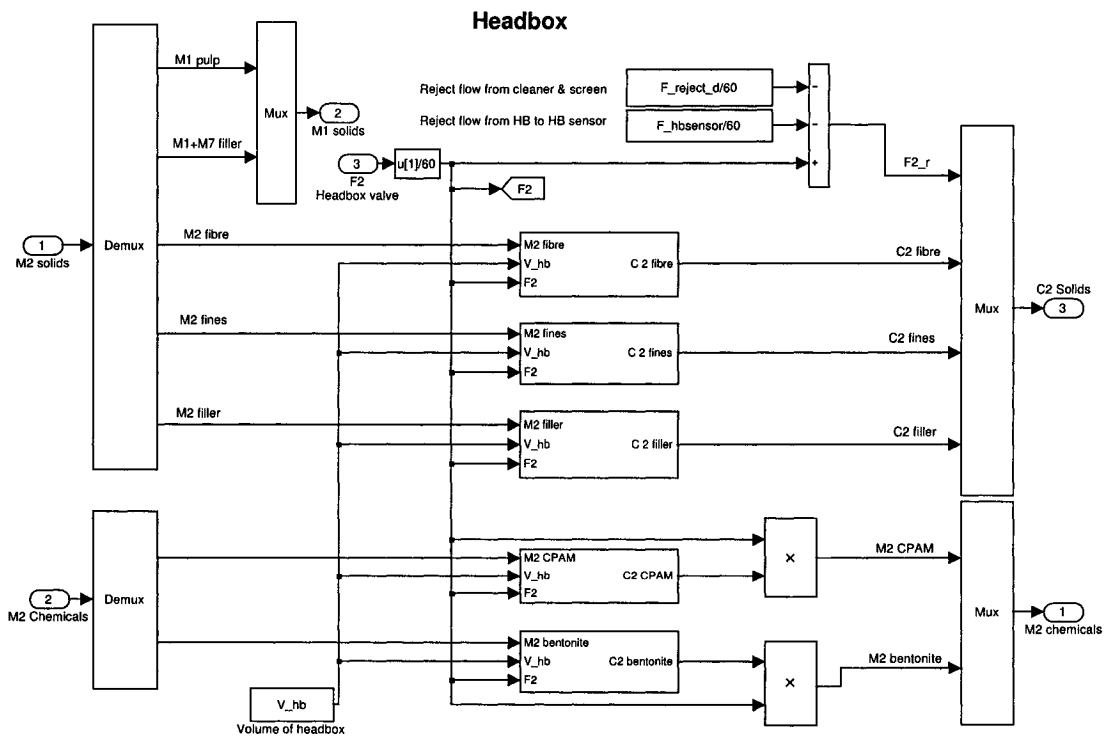

Figure A.5. Headbox.

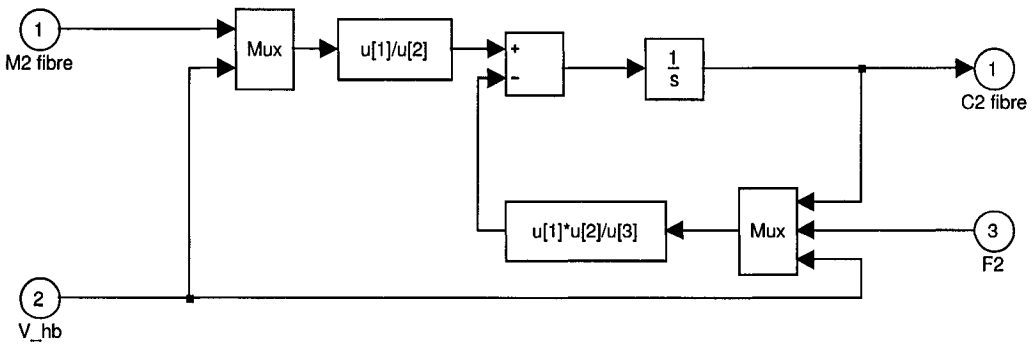

Figure A.6. Calculation of the headbox fibre consistency. The equation 5.4 is solved. The SIMULINK models for the headbox consistencies of fines, filler, polymer and microparticle have the same format.

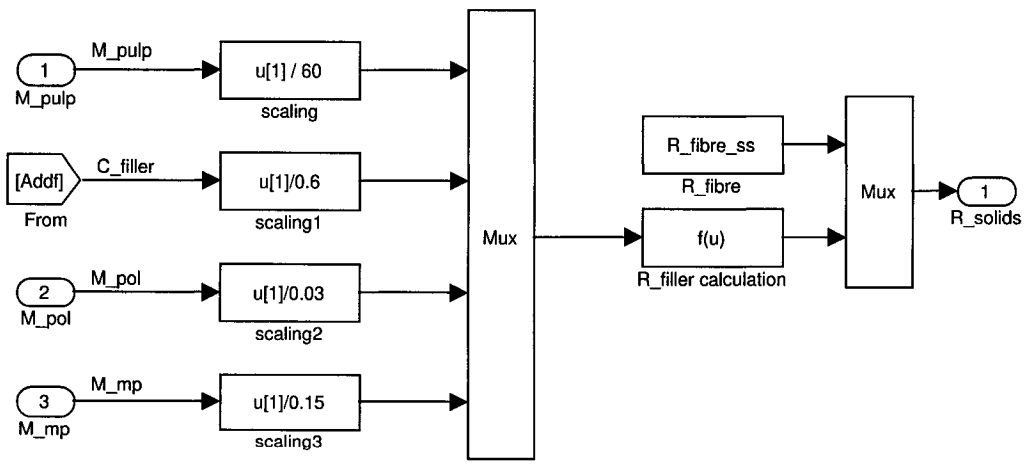

Figure A.7. Calculation of the first-pass retention of solids. R = first-pass retention.

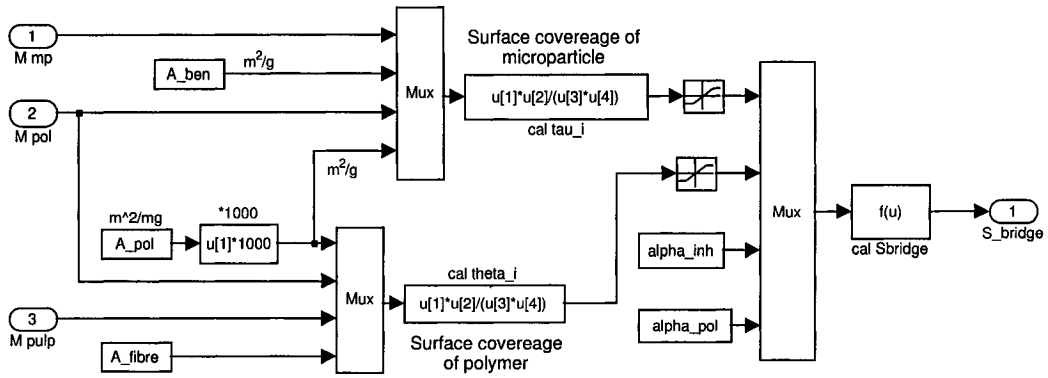

Figure A.8. Calculation of the bridging strength.

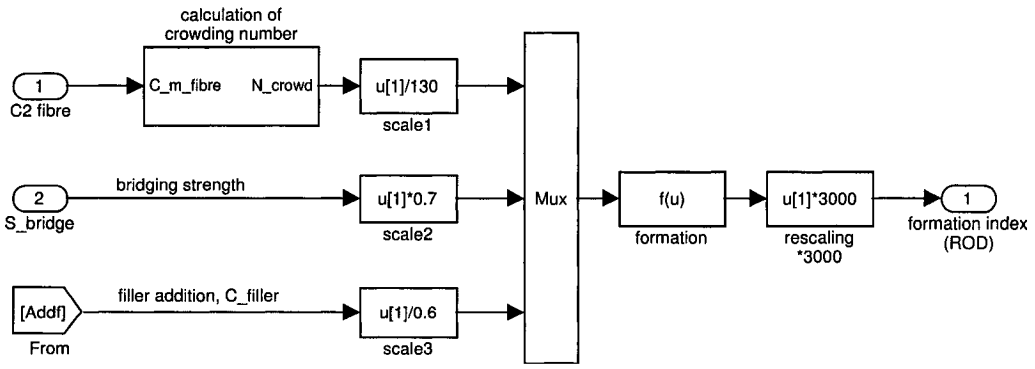

Figure A.9. Calculation of the formation index.

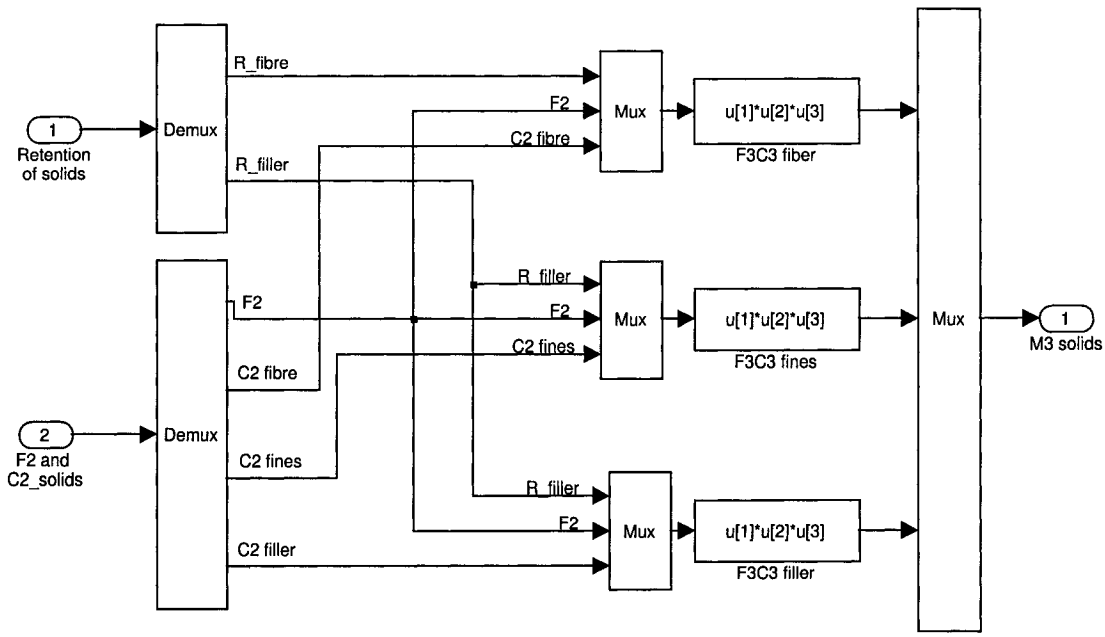

Figure A.10. Calculation of the mass flow rates of fibre, fines and filler retained on the web.

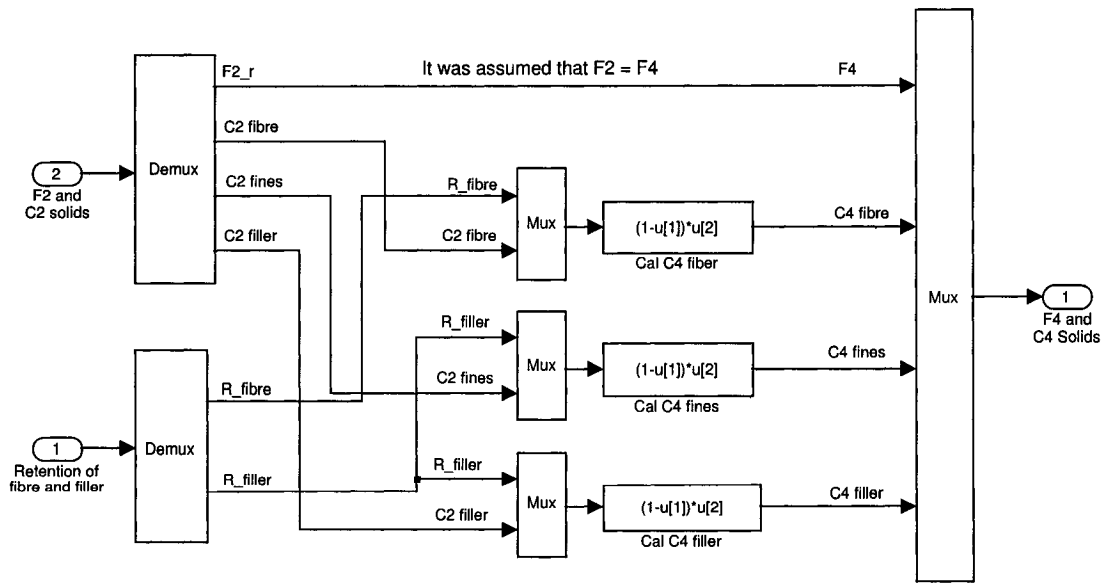

Figure A.11. Calculation of the consistencies of fibre, fines and filler in the white water from the white water tray under the wire to the wire pit.

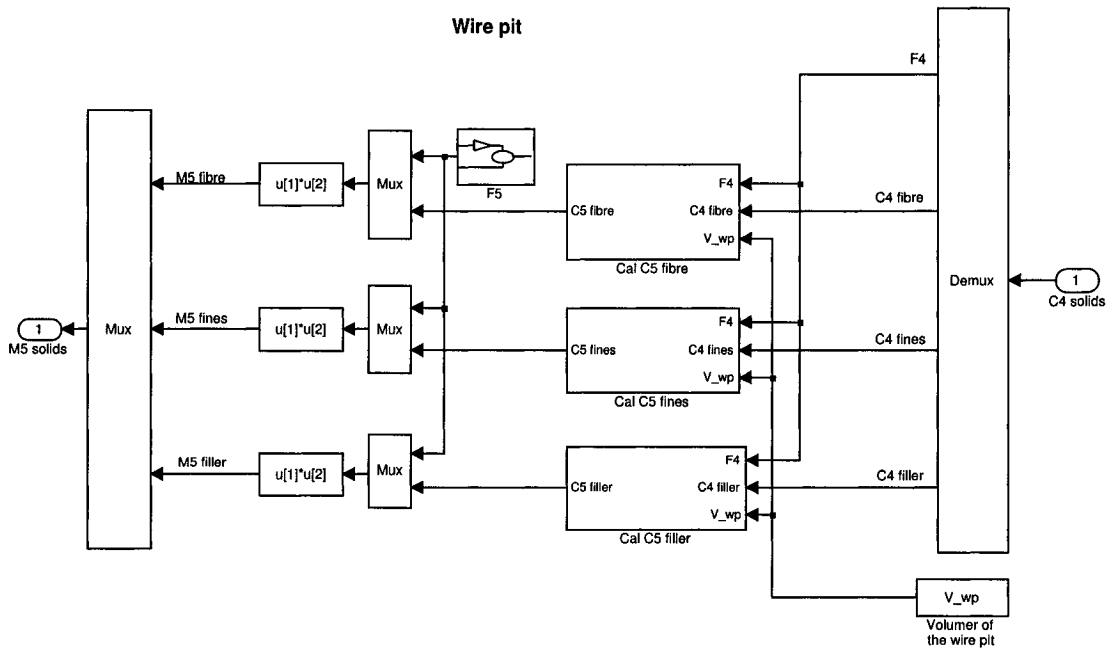

Figure A.12. Wire pit. Consistencies and mass flow rates of fibre, fines and filler in the recirculating white water are calculated.

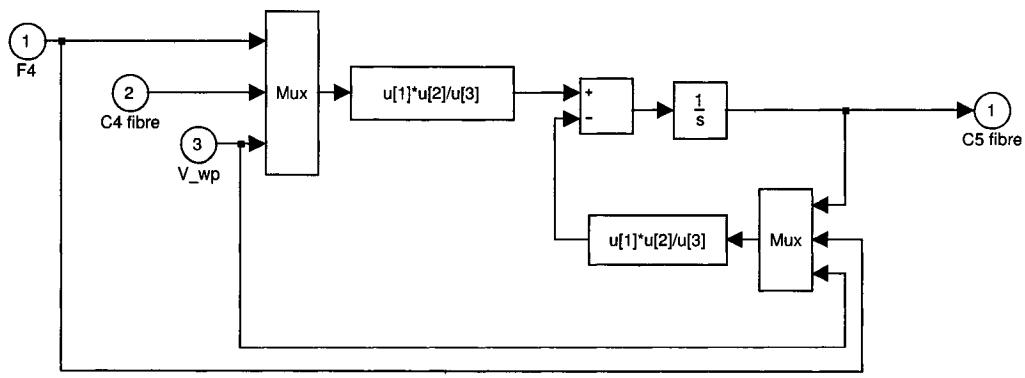

Figure A.13. Calculation of the white water fibre consistency. The equation 5.16 is solved. The SIMULINK models for the headbox consistencies of fines and filler have the same format.

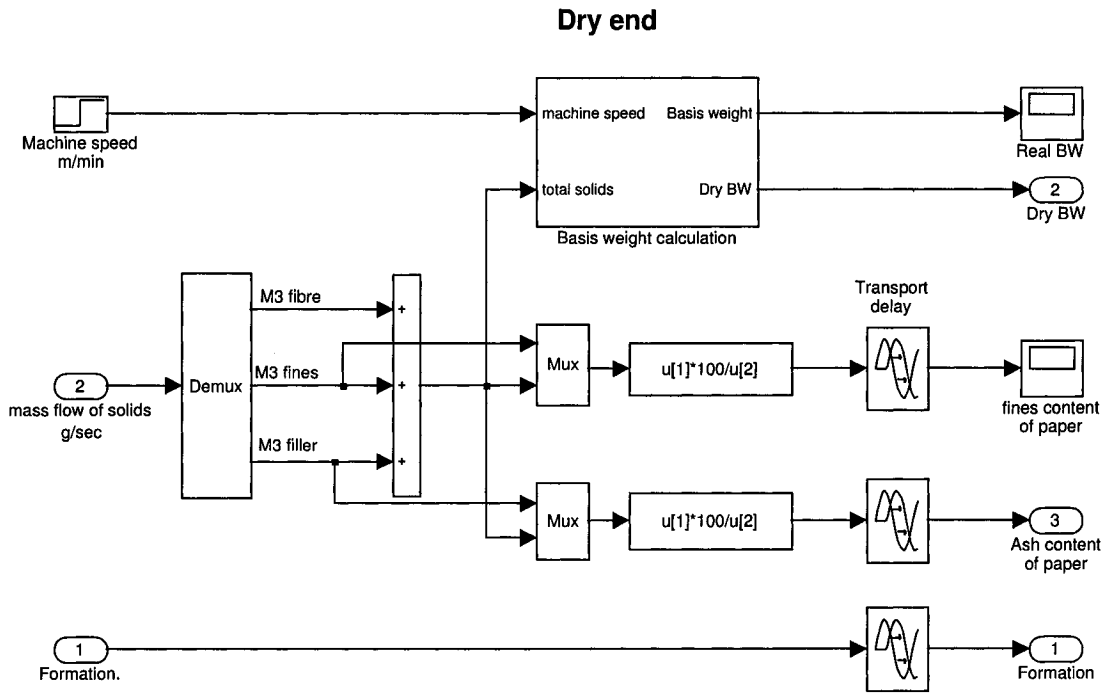

Figure A.14. Dry end of the paper machine. Basis weight, ash content and fines content in paper are calculated.

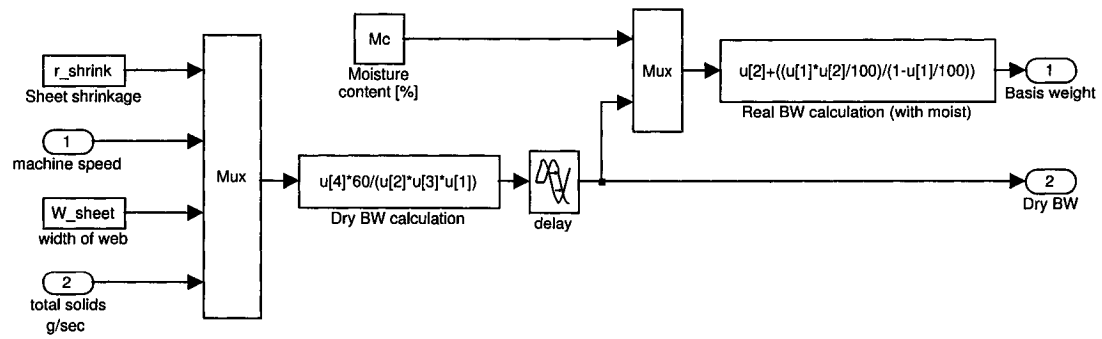

Figure A.15. Calculation of basis weight. A constant moisture content of paper is assumed.

Appendix B

Derivation of transfer functions

The headbox consistency is calculated with (Chapter 5):

$$\frac{dC_2}{dt} = \frac{1}{V_{hb}}(F_1C_1 + F_7C_7 + F_5C_5) - \frac{F_2}{V_{hb}}C_2 \tag{B.1}$$

By defining the deviation variables, $C_2' = C_2 - C_{2,s}$ and $C_5' = C_5 - C_{5,s}$ and taking the Laplace transform results in:

$$C_2(s) = \frac{\frac{F_5}{F_2}}{\frac{V_{hb}}{F_2}s + 1}C_5(s) \tag{B.2}$$

By defining $R = au^2 + bu + c$ (u = the dosage of CPAM or Bentonite), the white water consistency C_4 is:

$$C_4 = (1 - au^2 - bu - c)C_2. \tag{B.3}$$

Carrying out a Taylor series expansion and neglecting quadratic and higher terms for linear approximation [61], the equation B.3 becomes a function of C_2 and u.

$$C_4 = f(C_2, u) \cong f(C_{2,s}, u_s) + \left(\frac{\partial f}{\partial C_2}\right)_{(C_{2,s},u_s)}(C_2 - C_{2,s}) + \left(\frac{\partial f}{\partial u}\right)_{(C_{2,s},u_s)}(u - u_s) \tag{B.4}$$

The reference point for linearization is the normal steady-state operating point $(C_{2,s}, u_s)$. By defining the deviation variables, $C_2' = C_2 - C_{2,s}$ and $u' = u - u_s$.

$$C_4' = \left(\frac{\partial f}{\partial C_2}\right)_{(C_{2,s},u_s)}C_2' + \left.\frac{\partial f}{\partial u}\right|_s u' \tag{B.5}$$

$$C_4' = (1 - R_s)C_2' - (2au_s + b)C_{2,s}u' \tag{B.6}$$

The subscript s stands for steady state. Taking Laplace transform yields:

$$C_4(s) = (1 - R_s)C_2(s) - (2au_s + b)C_{2,s}U(s) \tag{B.7}$$

The recirculating white water consistency is (Chapter 5):

$$\frac{dC_5}{dt} = \frac{F_4}{V_{wp}}C_4 - \frac{F_5}{V_{wp}}C_5 - \frac{F_6}{V_{wp}}C_5 \tag{B.8}$$

Linearizing by taking Taylor series expansion and taking Laplace transform results in:

$$C_5(s) = \frac{1}{\frac{V_{wp}}{F_5+F_6}s + 1}C_4(s) \tag{B.9}$$

Combining equations B.2, B.7 and B.9 yields:

$$C_5(s) = \frac{-\frac{(2au_s+b)F_2C_{2,s}}{F_2-(1-R_s)F_5}\left(\frac{V_{hb}}{F_2}s + 1\right)}{\frac{F_2}{F_2-(1-R_s)F_5}\left(\frac{V_{hb}}{F_2}\right)\left(\frac{V_{wp}}{F_5+F_6}\right)s^2 + \frac{F_2}{F_2-(1-R_s)F_5}\left(\frac{V_{hb}}{F_2} + \frac{V_{wp}}{F_5+F_6}\right)s + 1}U(s) \tag{B.10}$$

Combining equations B.2 and B.10 results in the transfer function of the headbox consistency:

$$C_2(s) = \frac{-\frac{(2au_s+b)F_5C_{2,s}}{F_2-(1-R_s)F_5}}{\frac{F_2}{F_2-(1-R_s)F_5}\left(\frac{V_{hb}}{F_2}\right)\left(\frac{V_{wp}}{F_5+F_6}\right)s^2 + \frac{F_2}{F_2-(1-R_s)F_5}\left(\frac{V_{hb}}{F_2} + \frac{V_{wp}}{F_5+F_6}\right)s + 1}U(s) \tag{B.11}$$

The transfer function for the white water consistency is obtained by combining equations B.7 and B.11:

$$C_4(s) = \frac{-\frac{(2au_s+b)F_2C_{2,s}}{F_2-(1-R_s)F_5}\left(\frac{V_{hb}}{F_2}s + 1\right)\left(\frac{V_{wp}}{F_5+F_6}s + 1\right)}{\frac{F_2}{F_2-(1-R_s)F_5}\left(\frac{V_{hb}}{F_2}\right)\left(\frac{V_{wp}}{F_5+F_6}\right)s^2 + \frac{F_2}{F_2-(1-R_s)F_5}\left(\frac{V_{hb}}{F_2} + \frac{V_{wp}}{F_5+F_6}\right)s + 1}U(s) \tag{B.12}$$

The mass flow of solids leaving wire section is calculated from (Chapter 5):

$$F_3C_3 = (au^2 + bu + c)F_2C_2 \tag{B.13}$$

Linearizing by taking Taylor series expansion and taking Laplace transform results in:

$$F_3C_3(s) = (2au_s + b)F_2C_{2,s}U(s) + R_sF_2C_2(s) \tag{B.14}$$

Combining this with the equation B.11 yields the transfer function for the mass flow of solids leaving the wire section:

$$F_3C_3(s) = \frac{\frac{(2au_s+b)(F_2C_{2,s})(F_2-F_5)}{[F_2-(1-R_s)F_5]}\left[\frac{F_2}{(F_2-F_5)}\left(\frac{V_{hb}}{F_2}\right)\left(\frac{V_{wp}}{F_5+F_6}\right)s^2 + \frac{F_2}{(F_2-F_5)}\left(\frac{V_{hb}}{F_2} + \frac{V_{wp}}{F_5+F_6}\right)s + 1\right]}{\frac{F_2}{F_2-(1-R_s)F_5}\left(\frac{V_{hb}}{F_2}\right)\left(\frac{V_{wp}}{F_5+F_6}\right)s^2 + \frac{F_2}{F_2-(1-R_s)F_5}\left(\frac{V_{hb}}{F_2} + \frac{V_{wp}}{F_5+F_6}\right)s + 1}U(s) \tag{B.15}$$

The basis weight of paper is calculated with:

$$BW(g/m^2) = \frac{F_3C_{3,total}}{ms \cdot W \cdot r_s} \tag{B.16}$$

Then the transfer function function for the basis weight is obtained by combining equations B.15 and B.16

$$BW(s) = \frac{\frac{(2au_s+b)(F_2C_{2,s})(F_2-F_5)}{ms\cdot W\cdot r_s[F_2-(1-R_s)F_5]}\left[\frac{F_2}{(F_2-F_5)}\left(\frac{V_{hb}}{F_2}\right)\left(\frac{V_{wp}}{F_5+F_6}\right)s^2 + \frac{F_2}{(F_2-F_5)}\left(\frac{V_{hb}}{F_2} + \frac{V_{wp}}{F_5+F_6}\right)s + 1\right]}{\frac{F_2}{F_2-(1-R_s)F_5}\left(\frac{V_{hb}}{F_2}\right)\left(\frac{V_{wp}}{F_5+F_6}\right)s^2 + \frac{F_2}{F_2-(1-R_s)F_5}\left(\frac{V_{hb}}{F_2} + \frac{V_{wp}}{F_5+F_6}\right)s + 1}U(s) \tag{B.17}$$

From the equation 5.20, the ash content of paper can be calculated with:

$$Ash = \frac{F_3C_{3,filler}}{F_3C_{3,total}} \tag{B.18}$$

Linearizing by taking Taylor series expansion and taking Laplace transform results in:

$$Ash(s) = \frac{1}{F_3C_{3s,total}}F_3C_{3,filler}(s) - \frac{F_3C_{3s,filler}}{(F_3C_{3s,total})^2}F_3C_{3,total}(s) \tag{B.19}$$

Combining equations B.15 and B.19 and assuming that $\frac{V_{hb}}{F_2} = 0$, since the headbox does not affect the dynamics of ash content significantly, yields the transfer function for the ash content of paper:

$$Ash(s) = \frac{K_{ash}(\xi_1 s + 1)\left(\xi_2 s + 1\right)}{(\tau_1 s + 1)(\tau_2 s + 1)} \tag{B.20}$$

where

$$\begin{aligned} K_{ash} &= \frac{(F_2 - F_5)}{(F_3 C_{3s,total})^2 [F_2 - (1 - R_{s,filler})F_5][F_2 - (1 - R_{s,total})F_5]} \\ &\times \Big\{(2au_{s,filler} + b)F_2 C_{2,s,filler} F_3 C_{3s,total}[F_2 - (1 - R_{s,total})F_5] \\ &- (2au_{s,total} + b)F_2 C_{2,s,total} F_3 C_{3s,filler}[F_2 - (1 - R_{s,filler})F_5]\Big\} \end{aligned} \quad \text{(B.21)}$$

$$\tau_1 = \frac{F_2}{F_2 - (1 - R_{filler,s})F_5}\left(\frac{V_{wp}}{F_5 + F_6}\right) \quad \text{(B.22)}$$

$$\tau_2 = \frac{F_2}{F_2 - (1 - R_{total,s})F_5}\left(\frac{V_{wp}}{F_5 + F_6}\right) \quad \text{(B.23)}$$

$$\xi_1 = \frac{F_2}{F_2 - F_5}\left(\frac{V_{wp}}{F_5 + F_6}\right) \quad \text{(B.24)}$$

and

$$\xi_2 = \frac{\alpha_1 - \alpha_2}{\beta_1 - \beta_2}\left(\frac{V_{wp}}{F_5 + F_6}\right) \quad \text{(B.25)}$$

where

$$\begin{aligned} \alpha_1 &= F_2(2au_{filler,s} + b)(F_2 C_{2,filler,s})(F_3 C_{3,total,s}) \\ \alpha_2 &= F_2(2au_{total,s} + b)(F_2 C_{2,total,s})(F_3 C_{3,filler,s}) \\ \beta_1 &= (2au_{filler,s} + b)(F_2 C_{2,filler,s})(F_3 C_{3,total,s})[F_2 - (1 - R_{total,s})F_5] \\ \beta_2 &= (2au_{total,s} + b)(F_2 C_{2,total,s})(F_3 C_{3,filler,s})[F_2 - (1 - R_{filler,s})F_5]. \end{aligned}$$